Analysis of three dimensional culture mechanisms to induce de-differentiation and reprogramming in human multipotent stromal cells

Rebecca R. Mason

Thesis submitted for the degree of Doctor of Philosophy (PhD)

University of York

Department of Biology

April 2014

Abstract

Cells undergo reprogramming/de-differentiation through nuclear and cytoplasmic remodelling. Autophagy is a physiological stress response, in which cytoplasmic contents including mitochondria are recycled to aid cell survival in response to nutrient starvation. It has recently been demonstrated that a functional autophagy response is required for factor-based reprogramming to pluripotency, but there is little work explicitly linking the stimulation of autophagy with the mechanism of cytoplasmic clearance and metabolic remodelling. Human multipotent stromal cells/mesenchymal stem cells (MSCs) are cells of mesenchymal origin, which are cultured as adherent monolayers *in vitro.* MSCs can also be cultured as 3D cell aggregates or spheroids. Variations in spheroid size should result in variations in nutrient availability. I hypothesised that in 3D spheroids, controlled autophagy, stimulated by nutrient deprivation, and balanced in favour of its pro-survival/anti-apoptotic effects, would be sufficient to drive cytoplasmic remodelling and de-differentiation towards a more primitive state. When MSCs were cultured under optimal conditions, they had a multi-lobed irregular nuclear morphology, and reduced staining for the heterochromatin marker H3K9me3. 3D spheroids increased expression of Oct4, Nanog, Sox2 and telomerase. Under optimal conditions markers of increased autophagy were observed along with indicators of a shift to anaerobic metabolism. Mitochondria underwent remodelling to a small, rounded morphology, highly similar to mitochondria observed in pluripotent cells. Furthermore, oxygen consumption rate reduced significantly in 3D culture, and genes associated with oxidative metabolism were down-regulated. 3D MSCs increased expression of early mesendoderm markers including Brachyury (T), Goosecoid, KDR, Mixl1 and CXCR4. *In vitro* haematopoietic induction stimulated disaggregated 3D MSCs to form blast-like colonies, whilst 2D MSCs were unresponsive to haematopoietic stimulation. On implantation into nude mice, 3D MSCs formed organised mesodermal tissues, indicating enhanced lineage-restricted regenerative capacity, but did not form teratomas, so avoiding associated risks. Strikingly optimal 3D culture restored proliferative capacity and reversed senescence-associated hypertrophy in culture-aged MSCs, suggestive of cellular rejuvenation. Together these results suggest that a scaled autophagy response could play a fundamental role in reprogramming/de-differentiation and tissue regeneration in human cells.

Table of contents

List of Tables

List of figures

Acknowledgements

I would like to thank my supervisors Paul Genever and Drew Burdon for all their help, guidance and support throughout this project. Thanks in particular to Paul, whose open office door policy I have taken full advantage of over the last 3 years with a constant stream of good/not so good ideas! I would also like to thank Paul Pryor and Sally James in York, and Roger Sturmey and Paul McKeegan at HYMS for their assistance, advice and guidance. My TAP panel, Dawn Coverley and Louise Jones have provided support and suggestions throughout the project, so I wish to thank them for their continued contribution. Thank you to the staff of the Technology Facility in the Department of Biology, for all the help I have received. In particular I must thank Meg Stark for all the TEM work, and Pete O'Toole, Karen Hogg and Graeme Park for assistance with imaging and flow cytometry. Especially thanks to Graeme, who must have lost count of the times he has 'rescued' me from disaster on the 510 over the years! I would like to thank all members, past and present, of the Genever group. I am most grateful for all the support I have received from everyone both in and out of the lab. In particular I must mention Dave Cook and Sally Clough. Dave is the calmest, most reassuring person any new PhD student could wish to work alongside and particularly important for me, a technological expert as well. Sally, with her encyclopaedic knowledge of anything and everything related to lab management, has been a friend, a mentor and a constant support during and after my PhD. Quite frankly, Sally, I don't think I could have done it without you! It has been fantastic to be part of such a friendly, fun, supportive research group, so thanks to everyone for a super few years. Outside of work I wish to thank all my family and friends, for their help over the last three and a half years. Particular thanks to my dad and brothers, who have supported me throughout. A huge thank you to my partner Richard, for helping me to put this write up into perspective, and for still managing to keep me smiling, even when I could have quite happily thrown the laptop, and the lab books, out of the nearest window! Rich, without your love and support, I very much doubt this thesis would ever actually have got finished, so thank you for getting me through the last few months! Lastly I need to thank my mum, who sadly did not get the chance to see most of this work being done, but whom I know would have been indescribably proud to have seen my thesis in print. In acknowledgement of the unending help, support and encouragement I've received

over the years, I dedicate this thesis to the memory of my mum, the late Hazel Mason.

Declaration

The work presented in this thesis was performed by the author between October 2010 and December 2013, in the laboratory of Dr. Paul Genever, in the Biology Department of The University of York. All experiments were performed by the author, with the exception of preparation of cells for teratoma assays, and teratoma staining, which was performed by Elen Bray, and teratoma assays, which were performed by Reinervate Ltd. Teratoma slides were re-imaged and analysed by the author. Dr. Sally James performed the promoter search using MatInspector software and the Agilent array preparation and analysis. TEM preparation and imaging were performed by the staff of the Technology Facility at The University of York. Metabolic measurements and analysis (OCR and lactate production) were performed by Paul McKeegan and the author at Hull York Medical School (The University of Hull). Cell culture and cell counting prior to senescence assays was performed by Lihong Cheng, Julia Marshall performed the analysis of Brachyury+ cell distribution using Volocity software and Dr. Fatima Saleh cultured H9 ESCs prior to RNA analysis.

Chapter 1: Introduction

1.1 An introduction to the field of pluripotent stem cell research

Stem cells are undifferentiated cells, which have the capacity for self-renewal and can give rise to a number of different cells types through differentiation. Embryonic stem cells (ESCs) can be isolated from early embryos, and can give rise to all cells in the fully developed organism, so are termed pluripotent. Adult stem cells can be isolated from various tissues of the body, and can give rise to some but not all tissues of the organism, so are termed multipotent (Wagers and Weissman, 2004). Due to their capacity to generate different tissues, stem cells are of significant interest to the fields of regenerative medicine and cell-based therapies.

In 2006 Takahashi and Yamanaka demonstrated the generation of pluripotent cells similar to embryonic stem cells (ESCs) from mouse fibroblasts by forced expression of four transcription factors – Oct4, Sox2, Klf4 and c-Myc. The cells generated from these experiments were referred to as induced pluripotent stem cells (iPSCs) (Takahashi and Yamanaka, 2006). One year later this group generated iPSCs from human fibroblasts using the same four factor approach (Takahashi et al., 2007), whilst at the same time the Thomson laboratory demonstrated the induction of iPSCs from human fibroblasts using a different four factor combination - Oct4, Sox2, Nanog and Lin28 (Yu et al., 2007). The generation of iPSCs represented a major advancement in stem cell research, with the possibilities it opened up for the generation of patient-specific cells. It could also be said to have redefined the way development and differentiation are viewed, demonstrating that differentiation is not an irreversible procedure, and that fully differentiated cells maintain the capacity for pluripotency if stimulated to undergo de-differentiation/reprogramming (Figure 1.1). The generation of iPSCs has contributed greatly to our understanding of pluripotency and differentiation, although in turn, the many years of research into embryonic development and pluripotency regulation prior to 2006 provided the basis on which iPSC generation was first established.

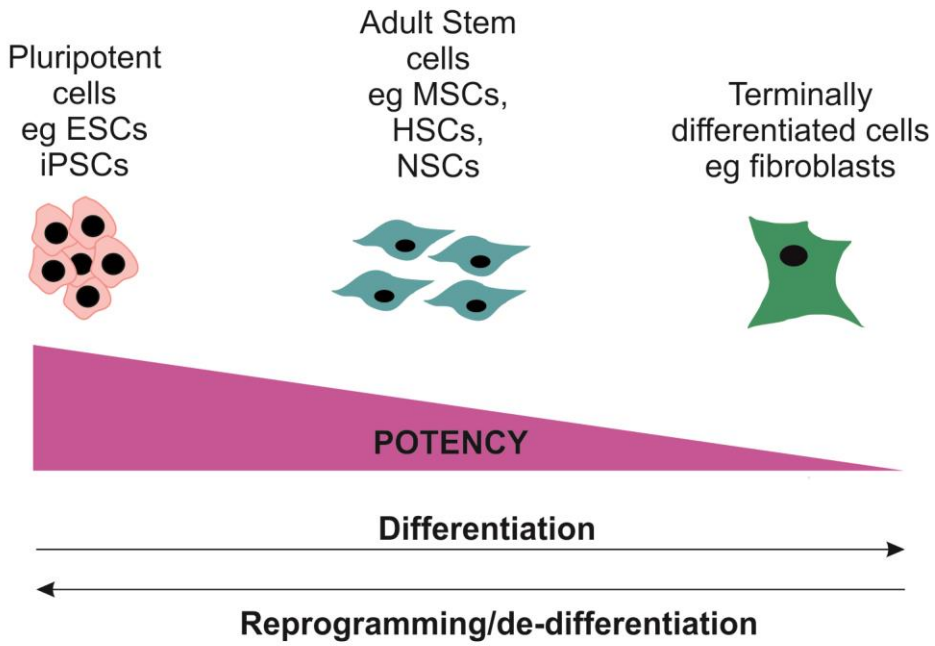

Figure 1.1. Schematic showing the effects of differentiation and reprogramming/de-differentiation on cell potency

Differentiation of ESCs results in a progressive loss of potency. Differentiated cells can reacquire pluripotent characteristics through forced de-differentiation (reprogramming to pluripotency). Adult stem cells are multipotent, maintaining self-renewal and the potential to differentiate into some but not all cell types. Adult stem cells occupy a position between pluripotent ESCs and terminally differentiated cells in terms of potency.

1.2 Embryonic development and cell fate specification in vivo

During mammalian development, fertilisation is followed by early cleavage, which gives rise to a solid mass of cells, known as the morula. The first cell specification events occur at around day 3.5 after fertilisation in the mouse embryo, with the formation of the blastocyst, and the specification of two distinct cell populations, the trophectoderm and the inner cell mass (ICM). The trophectoderm, which will give rise to the placenta and other extra-embryonic tissue, is positioned to the outer edges of the blastocyst, whereas the ICM is located towards one end of the blastocyst. Following blastocyst formation, at around 4.5 days post-fertilisation, the ICM divides into two regions; the outer cells become primitive endoderm, which will contribute to extra-embryonic tissues, whilst the inner layer of cells will go on to form the epiblast, which will generate the foetus (Figure 1.2). The blastocyst then implants into the uterine wall and the extra-embryonic tissues form the placenta, whilst the epiblast forms a cup shape, following formation of the proamniotic cavity. At around day 6.5 after fertilisation, gastrulation marks the beginning of morphological patterning within the embryo and the specification of the 3 germ layers (Beddington and Robertson, 1999).

1.3 Isolation and culture of pluripotent cells in vitro

1.3.1 Mouse embryonic stem cells

Control of embryonic development in these early developmental stages is regulated by a complex transcriptional network of both maternal and zygotic factors. Prior to the derivation of ESCs, researchers utilised embryonal carcinoma (EC) stem cells which can be isolated from teratocarcinomas and differentiated via embryoid body formation *in vitro*, as a model for development and cell fate determination in the early embryo (Martin and Evans, 1975). Teratocarcinomas are malignant germ cell tumours containing both somatic tissue and undifferentiated stem cells (the EC cells). Teratomas are distinguishable from teratocarcinomas, as they contain only somatic tissue. Teratocarcinomas continue to form tumours on serial transplantation, whilst teratomas are benign on re-transplantation because they do not contain EC cells (Andrews, 2002).

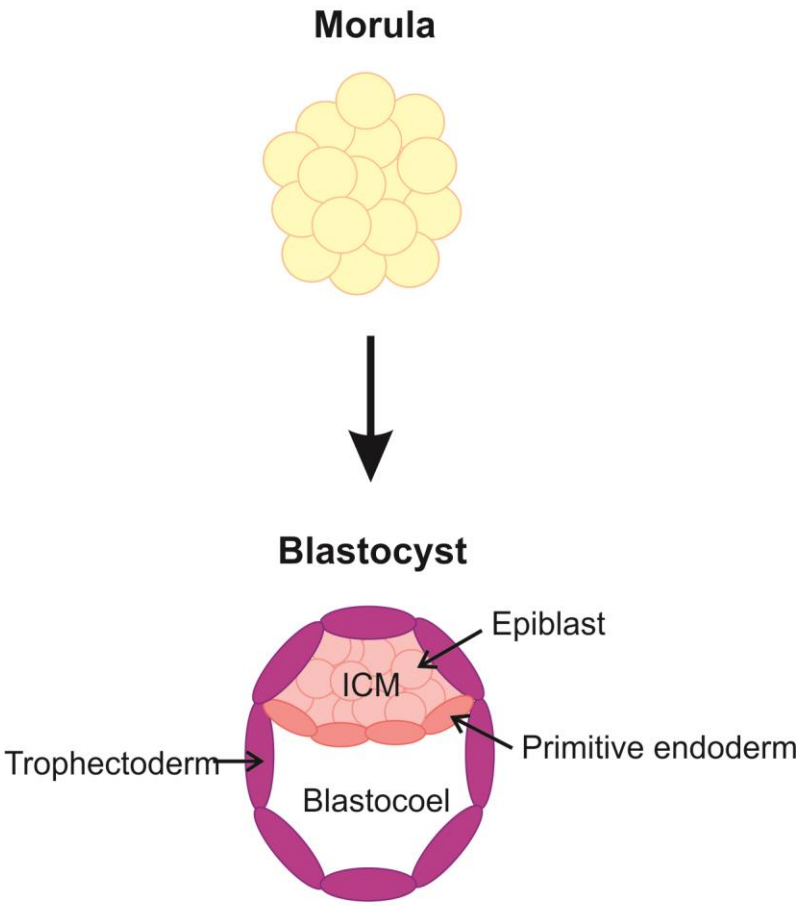

Figure 1.2. Schematic showing the first specification events in embryonic development during blastocyst formation

Following cleavage in the early embryo, the blastocyst forms from the morula. At this point, two distinct cell populations are specified. The trophectoderm, localised to the outside of the blastocyst, will form extra-embryonic tissue (the placenta), whilst the inner cells, localised at one end of the blastocyst form the inner cell mass (ICM). The ICM will generate both primitive endoderm, from its outer layer, which forms extra-embryonic tissue, and epiblast, from the central ICM, which will give rise to the foetus.

Mouse ESCs were first isolated in the laboratory from pre-implantation embryos isolated and separated *in vitro.* Prior to this it had not been possible to maintain pluripotent cells isolated from early embryos in culture. However in 1981, cells from the ICM of diapause (Evans and Kaufman, 1981) or normal pre-implantation (Martin, 1981) embryos were isolated and passaged repeatedly on inactivated fibroblast feeder layers, either in serum-supplemented medium (Evans and Kaufman, 1981), or EC cell-conditioned medium (Martin, 1981). The colonies formed by these cultured cells resembled the domed, tightly packed colonies observed in EC cell cultures. It was possible to generate embryoid bodies with the cultured cells *in vitro*, and they formed teratocarcinomas on subcutaneous implantation in mice. These early experiments defined the characteristics of ESCs, as cells which can be maintained as undifferentiated pluripotent cultures *in vitro*, and which can differentiate into tissues from all 3 germ layers both *in vitro* and *in vivo* (Evans and Kaufman, 1981; Martin, 1981).

In early experiments to generate mouse ESCs in the laboratory, culture on mouse embryonic fibroblast (MEF) feeder cells was required to maintain the undifferentiated state. However in the mid-1980s a factor was identified which could maintain pluripotency in mouse ESCs in the absence of a feeder layer. A single chain glycoprotein was identified in media conditioned with Buffalo rat liver cells. When cultured in media containing this factor, mouse ESCs maintained an undifferentiated morphology, and expressed the pluripotency cell surface marker SSEA1, with no need for a feeder layer. On removal of the factor, ESCs underwent spontaneous differentiation, so it was termed ‘differentiation inhibitory activity’ or DIA. The protein sequence of DIA was found to be identical to leukaemia inhibitory factor (LIF), the term by which it is now referred to when used in mouse ESC culture media (Smith et al., 1988) Notably it was demonstrated that established mouse ESC lines cultured with LIF in the absence of feeders were capable of both chimera contribution and germline transmission. Furthermore it was shown that in the presence of LIF, it was possible to establish cultures of freshly-isolated mouse ESCs from blastocysts, and that feeder cells were not required for this process if LIF was added to the media. It was possible to passage ESCs isolated in the absence of feeders. These cells maintained a typical pluripotent morphology and character in culture in LIF-supplemented media, whilst LIF withdrawal stimulated

differentiation. ESCs isolated in the presence of LIF (without feeders) were also capable of chimera contribution and germline transmission (Nichols et al., 1990). Taken together this demonstrated that it was possible to isolate and maintain mouse ESCs, in LIF-supplemented media without feeder cells, and that these cells were developmentally equivalent to mouse ESCs isolated and maintained in traditional feeder based cultures.

1.3.2 Human and non-human primate embryonic stem cells

Human EC cells have variable cell line-dependent capacity to form tissues from all 3 germ layers and are usually karyotypically abnormal. This means they are less useful as a model of pluripotent cells from the early embryo. Non-human primate (Rhesus monkey) ESCs were first isolated from *in vitro*-separated ICM in 1995. These cells expressed similar cell surface markers to human ECs – SSEA3, SSEA4, Tra-1-60 and Tra-1-81 and had alkaline phosphatase activity (Thomson et al., 1995). The colony morphology of primate ESCs was much flatter than observed in mouse ESC colonies, with individual cells clearly visible. Primate ESCs could be maintained undifferentiated in culture for many passages on inactivated mouse feeder cells, and notably this state was LIF-independent, which distinguished these pluripotent cells from mouse ESCs. Unlike human EC cells, isolated primate ESCs were karyotypically normal. Implantation into SCID mice resulted in teratomas containing tissues from all 3 germ layers, which confirmed the pluripotency of primate ESCs (Thomson et al., 1995).

Following on from this work with non-human primates, in 1998 Thomson derived the first human ESCs from embryos generated by *in vitro* fertilisation (IVF). Cells isolated from blastocyst stage embryos resembled ESCs previously isolated from non-human primates, characterised by high nuclear to cytoplasmic ratio and prominent nucleoli. Human ESCs expressed the cell surface markers SSEA3, SSEA4, Tra-1-60 and Tra-1-81, and had high levels of telomerase activity. Their colony morphology was similar to that of non-human primates, but distinct from the domed colonies formed by mouse ESCs. Human ESCs could proliferate for many passages *in vitro* when maintained on MEFs and this was LIF-independent, highlighting the differing requirements for pluripotency maintenance in primate

versus mouse ESCs. The pluripotency of human ESCs was confirmed by teratoma assays (Thomson, 1998). Another group also demonstrated the LIF-independent nature of undifferentiated human ESC cultures. Flat colonies resembling human ECs and primate ESCs, which expressed the cell surface markers Tra-1-60 and SSEA4, along with the pluripotency factor Oct4, could be maintained undifferentiated in culture for many passages in the absence of LIF (Reubinoff et al., 2000).

Whilst mouse ESCs require LIF for pluripotency maintenance, human ESCs require signalling through the transforming growth factor β (TGFβ)/Nodal/Activin pathways to maintain an undifferentiated state. Signalling through these pathways results in phosphorylation and nuclear localisation of Smad2/3. Inhibition of Smad2/3 phosphorylation resulted in loss of Oct4 and Nanog expression in human ESCs, with colony morphology changes indicative of differentiation (James et al., 2005). Inhibition of activin binding was also sufficient to induce loss of pluripotency markers such as the cell surface marker Tra-1-60 in human ESCs. However this effect was diminished in cells over-expressing Nodal, indicating that Nodal could compensate for activin inhibition. It was also noted that in Nodal over-expressing cells, spontaneous differentiation was uncommon (Vallier et al., 2005). Taken together these results suggest that TGFβ/Nodal/Activin signalling, rather than LIF, is required for pluripotency maintenance in human ESCs.

Recently it has been demonstrated that specific blockade of signalling pathways that induce differentiation can be used to maintain ESCs in an undifferentiated state. Autocrine fibroblast growth factor 4 (FGF4) stimulates the mitogen-activated protein kinase/extracellular signal-regulated kinase (MAPK/ERK) pathway, and differentiation is induced by ERK activation. Whilst LIF can maintain mouse ESCs in their undifferentiated state, this does not occur by inhibition of ERK activation. In contrast a combination of inhibitors of MAPK/ERK signalling can prevent intrinsic stimulation of differentiation from within the ESC population itself (Ying et al., 2008). ESCs cultured in the presence of an FGF receptor tyrosine kinase inhibitor, in combination with an ERK cascade inhibitor could be maintained undifferentiated for many cultures, although cell death at a reasonably high frequency was observed. The addition of a glycogen synthase kinase 3β (GSK3β) inhibitor, which acts to stimulate canonical Wnt signalling, improved viability in these cultures. The use of these three

inhibitors (3i) allowed highly efficient expansion of ESCs over many passages. ESCs cultured in these conditions maintained expression of pluripotency factors, and there was little/no expression of genes associated with differentiation. Expansion of ESCs in 3i conditions was comparable to expansion in LIF-supplemented media, and ESC clonogenicity was actually improved in 3i versus LIF-supplemented media. Combinations of 3i media comprising the FGF receptor inhibitor PD184352, the MEK (MAPK kinase) inhibitor PD0325901 and the GSK3β inhibitor CHIR99021 (Ying et al., 2008), or the more simplistic 2i comprising PD0325901 and CHIR99021 (Silva et al., 2008) are now commonly used for the long-term maintenance of undifferentiated ESC cultures.

1.3.3 Epiblast stem cells

Mouse ESCs are derived from the ICM of the pre-implantation embryo, but it is possible to isolate pluripotent cells from the epiblast of post-implantation mouse embryos. Cells isolated from post-implantation epiblasts (EpiSCs) expressed the pluripotency markers Oct4, Nanog and Sox2. Furthermore, like mouse ESCs, EpiSCs could differentiate to form tissues from all 3 germ layers in embryoid bodies and formed teratomas on transplantation to nude mice. However, there are a number of defining characteristics which distinguish EpiSCs from mouse ESCs. EpiSCs are pluripotent because they have the ability to form teratomas, but unlike mouse ESCs, they are unable to contribute to chimeras when implanted in blastocyst stage embryos (Brons et al., 2007; Tesar et al., 2007). Passaging mouse ESCs using disaggregation to single cells is common practice, but in EpiSCs this results in increased cell death. Rather, EpiSCs require dissociation to small cell clumps (Brons et al., 2007). Expression of epiblast marker genes was observed in EpiSCs (Brons et al., 2007; Tesar et al., 2007), whilst the ICM –specific marker Rex1 was only expressed in mouse ESCs and not in EpiSCs (Brons et al., 2007). In the pluripotent ICM and in mouse ESCs, Oct4 expression is driven by the activity of its distal enhancer. In contrast, the proximal enhancer drives Oct4 expression in both the epiblast and EpiSCs (Tesar et al., 2007). In culture, EpiSCs form large flat colonies, distinct from the smaller domed colonies observed in mouse ESCs. In fact the colonies formed by EpiSCs much more closely resemble those of human ESCs (Bernemann et al., 2011; Brons et al., 2007; Tesar et al., 2007). Interestingly EpiSCs

and human ESCs also share regulatory signalling pathways. Whilst mouse ESCs are dependent on LIF/BMP signalling to maintain pluripotency, human ESCs rely on Activin/Nodal signalling. Reliance on Activin/Nodal signalling for pluripotency maintenance is also a characteristic of EpiSCs (Brons et al., 2007; Tesar et al., 2007). Blocking Activin/Nodal signalling with an Alk inhibitor induced differentiation in EpiSCs and human ESCs but not in mouse ESCs, demonstrating that in morphology and signalling pathway dependency, EpiSCs resemble human ESCs more closely than mouse ESCs. Dax1 is a key pluripotency regulator in mouse ESCs, but is not expressed in either EpiSCs or in human ESCs. Furthermore, gene expression analyses revealed that different EpiSC lines cluster together and distinct from mouse ESCs (Tesar et al., 2007). Although cells isolated from the post-implantation epiblast appear to represent a distinct pluripotent cell type, it has been demonstrated that some EpiSCs can be reprogrammed to an ESC-like state using the stringent culture conditions required for maintenance of mouse ESCs. It was observed that when isolated epiblasts were dissociated to single cells and maintained in culture in standard ESC media (supplemented with LIF), there was gradual appearance at relatively high frequency of ESC-like cells. With continued passaging, these cells reactivated a GFP reporter driven by the ICM/ESC-specific distal enhancer of Oct4. Furthermore, these colonies had strong alkaline phosphatase activity, which is not associated with EpiSCs, and were capable of chimera contribution on blastocyst injection. The authors suggested therefore that it was possible to reprogramme some EpiSCs to a mouse ESC-like state, capable of chimera contribution, through continued culture in mouse ESC media (Bao et al., 2009). It has recently been confirmed by another group that such culture conditions are sufficient to drive reprogramming of some EpiSCs to a mouse ESC-like state. However it was noted that variations between EpiSC lines can affect this reprogramming process. EpiSC lines expressing mesendodermal markers such as Brachyury (also known as T), Goosecoid and Mixl1 were refractory to reprogramming using mouse ESC culture conditions, and displayed reduced capacity to differentiate down neural lineages *in vitro*. In contrast, a number of EpiSCs which did not express these mesendodermal markers were easily reprogrammed to a mouse ESC-like state by culture conditions alone. It was suggested that EpiSCs expressing markers of mesendoderm may represent a different developmental state, with a reduced capacity for reprogramming *in vitro*. However it should be noted that all the EpiSC lines in this study were

capable of teratoma formation, so displayed pluripotency in the *in vivo* environment (Bernemann et al., 2011). The differing characteristics of ESCs from mouse and human have previously been explained by species variation. The identification of EpiSCs from mouse has highlighted the possibility that even amongst pluripotent cells, there exists different subsets with subtle variations in developmental potential. Further analysis and comparison of such cells may give important insights into early events in embryonic developmental which occur after ICM specification but before the loss of pluripotency and germ layer commitment.

1.4 Transcriptional, epigenetic and metabolic signature of pluripotency

1.4.1 The master transcriptional regulators of pluripotency

Pluripotency is established and maintained by a transcriptional network, regulated by the pluripotency factors Oct4, Nanog and Sox2 (Boyer et al., 2005). Oct4 (also referred to as Oct3 and POU5F1) is a homeo-domain containing transcription factor expressed by pluripotent, undifferentiated EC cells and ESCs; expression of Oct4 is lost upon differentiation (Okamoto et al., 1990; Rosner et al., 1990). In situ hybridisation on mouse embryos detected Oct4 in a number of cell populations prior to implantation, but following implantation it was only present in the epiblast (Rosner et al., 1990). Oct4 is essential for correct ICM development in early embryos. $Oct4^{-/-}$ embryos develop to the blastocyst stage, but the cells which should form the pluripotent ICM form a trophoblast- restricted cell population instead, which cannot maintain proliferation (Nichols et al., 1998). Precise control of Oct4 expression levels is required to maintain pluripotency and self-renewal in ESCs. A 2-fold increase of Oct4 expression resulted in differentiation towards extra-embryonic endoderm and mesoderm, evidenced by expression of Gata4 and Brachyury respectively. In contrast, ESCs formed trophectoderm, indicating a loss of pluripotency through de-differentiation, when Oct4 expression was repressed (Niwa et al., 2000).

Nanog is another homeo-domain transcription factor, which is only expressed in pluripotent cells and is required for maintenance of pluripotency. Nanog overexpression could sustain self-renewal in murine ESCs in the absence of LIF,

which under normal culture conditions is required to prevent differentiation. However in the absence of LIF, endogenous Nanog was not sufficient to maintain ESC self-renewal. Loss of Nanog expression resulted in differentiation to extra-embryonic endoderm (Chambers et al., 2003; Mitsui et al., 2003).

The transcription factor Sox2 is an SRY-related HMG box gene family member. Sox2 is expressed in the ICM of blastocyst stage embryos and throughout the epiblast. When homozygous Sox2 mutants were generated, there was loss of the epiblast, and instead populations of trophectoderm and extra-embryonic endoderm were formed. Furthermore it was not possible to isolate ESCs from homozygous mutant embryos, demonstrating a role for Sox2 in epiblast maintenance and in ESCs (Avilion et al., 2003).

Genome-wide chromatin immunoprecipitation studies revealed that Oct4, Sox2 and Nanog co-occupy a high number of genes, acting as both transcriptional activators and repressors. They form an auto-regulatory loop to regulate their own expression, and also activate the expression of other pluripotency related genes, along with components of the Wnt and TGF-β signalling pathways, which have been linked to the maintenance of pluripotency and self-renewal. Many key genes associated with lineage specification and development are co-bound and repressed by Oct4, Sox2 and Nanog (Boyer et al., 2005).

1.4.2 Chromatin organisation and regulation in pluripotency

As well as these transcriptional hallmarks, pluripotent cells also have a characteristic chromatin conformation, which is distinct from that of differentiated cells. Within the interphase nucleus, DNA is packaged as chromatin, a complex of DNA and the histone proteins. The nucleosome is the functional unit of chromatin, consisting of 146bp of DNA wound approximately one and a half times around a histone octamer of the four core histones (H2A, H2B, H3 and H4), (Kouzarides, 2007). Histone modifications most strongly associated with the establishment of chromatin domains are methylation and acetylation. Broadly speaking, there are two different chromatin conformations, heterochromatin and euchromatin, which are marked by characteristic histone modification profiles. Heterochromatin is transcriptionally

repressive, and is marked by tri-methylation of a number of lysine residues on histones 3 and 4 (H3K9me3, H3K27me3 and H4K20me3). Euchromatin can be marked by both histone acetylation and tri-methylation of histone 3 (H3K4me3, H3K36me3 and H3K79me3), and is transcriptionally permissive (Figure 1.3), although not all genes marked by euchromatin marks are being actively transcribed, rather they have a conformation which is permissive to transcription (Kouzarides, 2007).

It has recently been reported that the global profile of chromatin modifications is altered as cells progress though differentiation. In pluripotent ESCs there is an enrichment of histone modifications which mark euchromatic regions of the genome, as well as the transcriptional elongation-associated mark H3K36me2. Levels of the heterochromatin marker H3K9me3 are low in ESCs, and pluripotent cells show an increase in global transcription compared to differentiated cells. An interesting observation is that ESCs express some tissue-specific genes, albeit at extremely low levels (Efroni et al., 2008). This suggests that ESCs express many genes which one would expect to be repressed (i.e. those associated with tissue-specific differentiation). It is hypothesised that low level transcription of lineage-specific genes is necessary to maintain pluripotency and upon differentiation these genes are either up-regulated or silenced depending on their tissue specificity (Efroni et al., 2008). Key developmental genes such as the Hox gene cluster are marked by bivalent domains in pluripotent cells. Bivalent domains are genome regions which are modified with both activating (H3K4me3) and repressive (H3K27me3) histone marks, and frequently overlap the transcriptional start sites of developmental transcription factors which are involved in lineage specification and are expressed at very low levels in ESCs. This is thought to maintain them in a 'poised' state. As cells differentiate, relevant lineage-specific genes are then either fully activated or repressed when cell fate is specified, by the addition/removal of the appropriate histone modification (Azuara et al., 2006; Bernstein et al., 2006). As differentiation proceeds, only genes related to a specific cell fate are expressed, whilst others become repressed, either by repressive histone marks and/or DNA methylation.

Recent studies have linked the master transcriptional regulators of pluripotency with chromatin regulatory mechanisms, demonstrating how Oct4, Nanog and Sox2 can

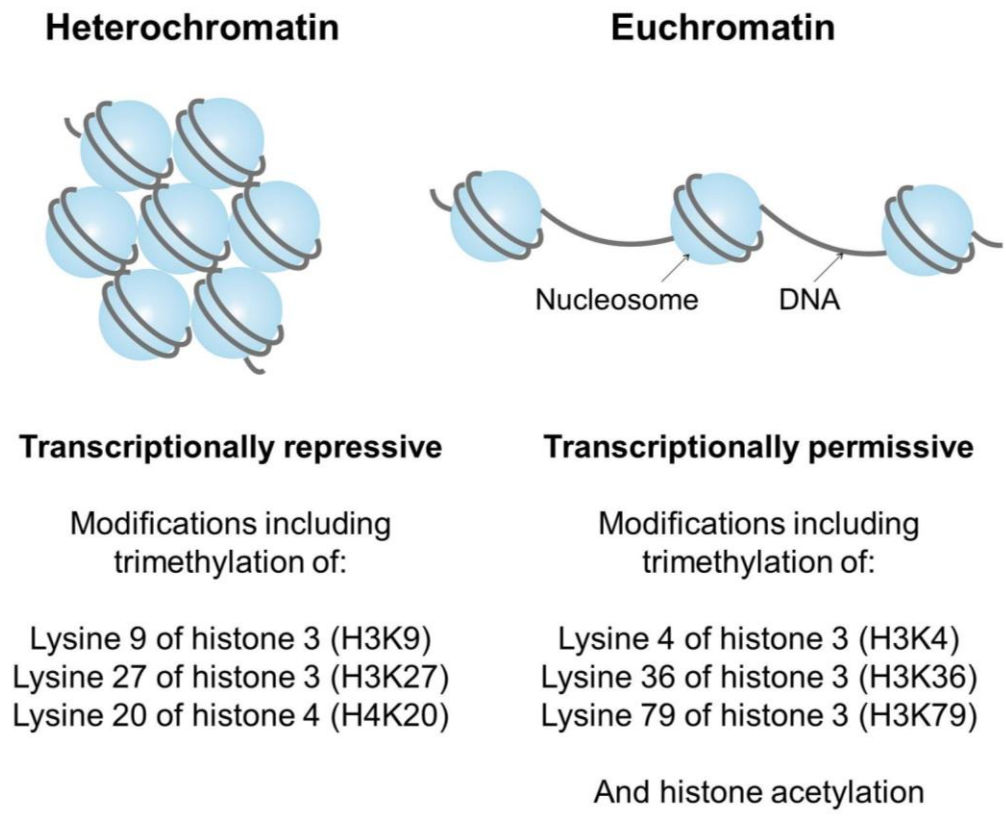

Figure 1.3. Schematic showing the organisation and characteristic modifications of heterochromatin and euchromatin

Chromatin can be organised into two conformations. Heterochromatin is repressive to transcription, with tightly packed nucleosomes, denying access of the transcriptional machinery to DNA. Characteristic modifications include tri-methylation of specific lysine residues on histones 3 and 4. Euchromatin is transcriptionally permissive, with more widely spaced nucleosomes allowing access of the transcriptional machinery to DNA. Characteristic modifications include tri-methylation of specific lysine residues on histone 3, and histone acetylation.

cooperate with chromatin re-modellers to achieve the precise control of gene expression required for maintenance of pluripotency and self-renewal.

1.4.3 Pluripotency regulation by chromatin remodelling factors

Brg1 is the core catalytic subunit of an ATP-dependent chromatin remodelling complex. Brg1 binds both active and repressed genes in ESCs, and co-occupies many genes with Oct4, Nanog and Sox2 (Kidder et al., 2009). Reduction of Brg1 in mouse ESCs resulted in colony morphology changes indicative of differentiation and a reduction in alkaline phosphatase activity. Furthermore, decreased expression of pluripotency-related genes including Oct4 and Sox2, and increased expression of lineage specific genes was observed. Notably Brg1 regulated the expression of the polycomb group (PcG) proteins, which are known to co-bind with Oct4, Nanog and Sox2 at many repressed genes in ESCs. Reduction of Brg1 resulted in decreased expression of some PcG proteins (Kidder et al., 2009).

The PcG proteins form complexes known as the polycomb repressive complexes (PRC) which act to repress gene expression through histone modification and chromatin condensation which prevents transcription of target genes. PRC2 catalyses the methylation of H3K27 and this histone modification (H3K27me3) is required for the association of PRC1, which alters chromatin to a condensed, non-permissive conformation (Boyer et al., 2006; Lee et al., 2006). Eed is a PRC2 component, and $Eed^{-/-}$ ESCs failed to maintain pluripotency, so were prone to spontaneous differentiation. In $Eed^{-/-}$ ESCs, there was an increase in expression of genes bound by the PcG proteins, so clearly a functional PRC complex acts to repress the expression of these genes in wild type ESCs (Boyer et al., 2006). Targets of the PRCs are key developmental regulators including the Hox, Pax, Sox, Fox and Tbx gene families, and many of these genes are co-occupied and repressed by Oct4, Nanog and Sox2 in pluripotent cells. The master regulators of pluripotency appear to act alongside PcG complexes to silence genes associated with lineage specification in ESCs and indeed many of these genes were up-regulated upon differentiation (Boyer et al., 2006; Lee et al., 2006).

As previously discussed, other histone modifications are associated with transcriptional repression. Jmjd1a and Jmjd2c are histone demethylases which act to demethylate H3K9me2 and H3K9me3 respectively. When Jmjd1a and Jmjd2c were knocked down using short hairpin RNAs (shRNAs), there were widespread effects on ESCs indicative of a loss of pluripotency. ESC morphology was altered to a more fibroblast-like state, with reduced alkaline phosphatase activity. There was a decrease in expression of Oct4, Nanog and Sox2 along with an increase in the expression of lineage specific genes. Furthermore, global levels of H3K9me2 and H3K9me3 increased, indicative of a shift to a more differentiated state (Loh et al., 2007). The expression of Jmjd1a and Jmjd2c is linked to the master regulators of pluripotency. Oct4 binds both genes and depletion of Oct4 by RNA interference (RNAi) resulted in down-regulation of their expression. Furthermore Jmjd2c has been linked to the regulation of Nanog, as it binds Nanog, and Jmjd2c depletion resulted in reduced expression of Nanog due to an increase in the repressive modification H3K9me3 in the Nanog promoter (Loh et al., 2007).

A number of chromatin modifying proteins and complexes act in the co-binding of pluripotency factor target genes, and in the regulation of expression of both other chromatin modifiers and the pluripotency factors themselves. This clearly highlights the complex transcriptional networks required in pluripotent cells to precisely control gene expression and maintain the capacity for pluripotency and self-renewal.

1.4.4 Metabolic hallmarks of pluripotency

Along with a characteristic chromatin conformation, the mitochondrial network of pluripotent cells is distinct from that of differentiated cells. GFP-labelling of a component of the pyruvate dehydrogenase (PDH) complex, which localises to the mitochondrial matrix, revealed significant differences in mitochondrial morphology and positioning in pluripotent human ESCs and differentiated fibroblasts. Human ESCs contain small, rounded perinuclear mitochondria, which under TEM microscopy were shown to contain few cristae. In contrast, fibroblasts have complex mitochondrial networks, localised to the cytoplasm, and made up of elongated, tubular, cristae-rich mitochondria (Varum et al., 2011). Pluripotent and differentiated cells also rely on different mechanisms for energy generation. Differentiated cells

undergo oxidative phosphorylation under normal oxygen conditions, which can produce up to 38 molecules of ATP per molecule of glucose. Pluripotent ESCs have a glycolytic metabolism, which produces only 2 molecules of ATP per molecule of glucose. Glycolysis is usually adopted under hypoxic conditions, and low oxygen conditions have been used for ESC culture. Strikingly though, ESCs are glycolytic even under normoxic conditions, and rely on a high glycolytic flux to meet their energy requirements. When ESCs are induced to differentiate, mitochondria develop to more complex tubular, cristae-rich morphologies, and a cytoplasmic mitochondrial network is established. There is also a metabolic shift from glycolysis to oxidative phosphorylation (Zhang et al., 2012). The events of *in vitro* differentiation mimic those observed in embryogenesis. Immediately following fertilisation, embryos have an oxidative metabolism due to the inheritance of maternal mitochondria. However as early cleavage occurs, the metabolism in the morula becomes glycolytic. Prior to implantation, the embryo exists in a hypoxic environment, and in the ICM, there are few immature, perinuclear mitochondria. The mitochondria observed in ESCs very closely resemble mitochondria of the early embryo (Varum et al., 2011). As observed in *in vitro* differentiation, there is a shift to oxidative phosphorylation *in vivo*, following implantation, as differentiation to the three germ layers progresses (Zhang et al., 2012).

Taken together, these studies highlight the complex characteristic profile of pluripotent stem cells, with both transcriptional control and metabolic capacity playing a role in the establishment and maintenance of the pluripotent state.

1.5 Generation of pluripotent cells by cloning and cell fusion

In 1962 John Gurdon demonstrated the generation of pluripotential cells from differentiated epithelial cells. Labelled nuclei from Xenopus laevis intestinal epithelia were transferred into enucleated oocytes. The experiment generated a small number of viable tadpoles, which had arisen from the labelled transplanted nuclei. This suggests that oocytes can initiate the conversion of a differentiated nucleus to a pluripotent nucleus, which is then capable of development into a viable organism, demonstrating that differentiation is not an irreversible developmental progression. Differentiated cells must possess the genetic capacity to regain pluripotency, and

oocytes must contain factors which can initiate this process (Gurdon, 1962). Decades later this was followed by the generation of live mammals by somatic cell nuclear transfer (SCNT). It was first possible to generate lambs by this method from nuclei from an embryo-derived cell population and from foetal fibroblasts. Most significantly, this study produced 'Dolly the Sheep', the first mammal generated from adult cells by SCNT. This demonstrated that fully differentiated adult mammalian cells (in this case mammary epithelial cells from a six year old ewe) could be converted to pluripotency, and could generate viable organisms on transplantation into enucleated oocytes (Wilmut et al., 1997). The results of this study supported the work of John Gurdon and provided further evidence to demonstrate the plasticity of differentiated nuclei when exposed to factors contained in enucleated oocytes.

It is also possible to generate pluripotent cells by cell fusion of ESCs with adult cells. Cells resulting from the fusion of mouse ESCs with Oct4-GFP reporter thymocytes expressed GFP in a pattern highly similar to endogenous Oct4 expression in ESCs. Furthermore the thymocytes used for fusion experiments were XX female, with an inactive X-chromosome and stable expression of the long non-coding RNA Xist. Following fusion the hybrid cells reactivated the inactive X-chromosome derived from the female thymocytes and expression of Xist was unstable, similar to undifferentiated cells. On injection into normal blastocysts, hybrid cells were capable of some chimera contribution, demonstrating pluripotency (Tada et al., 2001). Cowan and colleagues demonstrated that this technique could also be applied to reprogramme human cells, when cells with characteristics similar to ESCs were generated from fusion of ESCs with fibroblasts. Cells produced from these fusions had an ESC-like morphology and expressed ESC surface markers SSEA4, Tra-1-60 and Tra-1-81. They also reactivated expression of pluripotency-associated genes Oct4, Nanog and Rex1. Telomerase activity was detectable in hybrid cells, which could be maintained in culture for many passages. Hybrid cells had a highly similar global gene expression pattern to ESCs. They formed embryoid bodies *in vitro*, and teratomas when transplanted into nude mice, confirming the pluripotential of hybrid cells (Cowan et al., 2005). These studies demonstrated that cell fusion with pluripotent cells is sufficient to convert differentiated cells to the

pluripotent state, and that ESCs possess the factors required to initiate this conversion.

1.6 Induction of pluripotency by forced expression of transcription factors

1.6.1 Induction of pluripotency in mouse somatic cells

In 2006 Takahashi and Yamanaka demonstrated that the forced expression of just four factors could convert mouse embryonic fibroblasts (MEFs) and adult mouse fibroblasts to ESC-like pluripotent cells. 24 candidate genes were selected for screening due to their expression in ESCs and/or roles in pluripotency maintenance. These genes were introduced into Fbx15- reporter MEFs by retroviral transduction. Expression of Fbx15, which is downstream of Oct4 and is expressed specifically in mouse ESCs and the early mouse embryo, lead to activation of the promoter reporter and conferred antibiotic resistance on MEFs, indicative of successful reprogramming. The combination of Oct4, Sox2, Klf4 and c-Myc (OKSM) generated ESC-like cells which could be maintained undifferentiated in culture, termed induced pluripotent stem cells (iPSCs). These cells formed embryoid bodies *in vitro* and teratomas when transplanted into nude mice (Takahashi and Yamanaka, 2006). Although morphologically similar to ESCs, expression of endogenous Oct4 and Sox2 was variable between clones in Fbx15-selected iPSCs, due to partially maintained methylation in the promoter regions of these genes. Furthermore, these iPSCs were unable to form viable adult chimeras, and subsequently were unable to contribute to germline transmission when injected into blastocyst stage embryos. The cells generated in this study represented a pluripotent cell type, generated from somatic cells, which were quite distinct from mouse ESCs (Takahashi and Yamanaka, 2006). A schematic of iPSC generation is shown in Figure 1.4.

Whilst Fbx15 is expressed in mouse ESCs and the early embryo, it is not essential for the establishment or maintenance of pluripotency. As previously discussed, Oct4 and Nanog are key pluripotency regulators, and so the use of Oct4 (Wernig et al., 2007) or Nanog-reporter MEFs (Okita et al., 2007; Wernig et al., 2007) provides more stringent evidence of reprogramming to pluripotency. Oct4-and Nanog-selected iPSCs could be stably cultured for many passages *in vitro*. Unlike Fbx15-

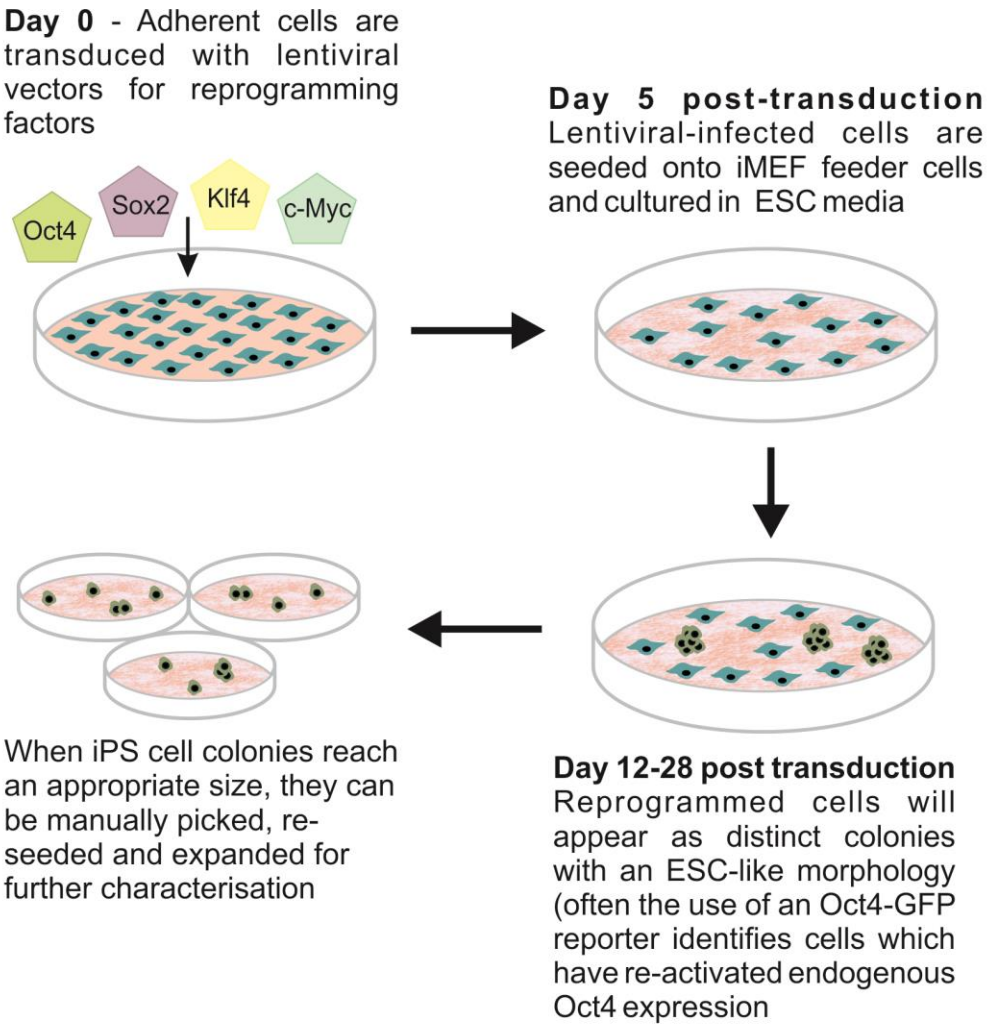

Figure 1.4. Schematic showing a typical time line for the generation of pluripotent iPSCs from differentiated cells using lentiviral vectors

Differentiated cells can be reprogrammed to pluripotency by forced expression of transcription factors. These factors are commonly transduced into cells using lentiviral vectors. Following treatment with lentiviruses, differentiated cells are typically counted, and re-seeded onto irradiated MEF feeder cells around 5 days after transduction. The differentiated cells are then maintained in ESC media. ESC-like colonies will begin to appear, this can take less than two weeks, or up to a month after transduction. Oct4-GFP reporter cells are commonly used, as GFP fluorescence can be used to identify colonies which have reactivated endogenous Oct4 expression. iPSC colonies will proliferate in culture in a similar manner to ESCs, and should be expanded for full characterisation.

selected iPSCs, Oct4 and Nanog promoters were largely unmethylated in Oct4 and Nanog-selected cells. The cells formed teratomas containing tissues from all three germ layers, but unlike Fbx15-selected cells, were also capable of both chimera contribution and germline transmission (Okita et al., 2007; Wernig et al., 2007). There were many more colonies in Fbx15-selected cultures than in Nanog-selected cultures, demonstrating that activation of the Fbx-15 gene reporter was much more efficient than Nanog-reporter activation. However, Nanog-selected iPSCs were capable of sustained pluripotency factor expression *in vitro*, whilst this was lost with passaging of Fbx15-selected cells. It was also possible to propagate Nanog-selected iPSCs in the absence of feeder cells in LIF-supplemented media. In contrast Fbx15-selected colonies were feeder-dependent and underwent spontaneous differentiation in the absence of feeder cells, even in the presence of LIF (Okita et al., 2007). Although Wernig and colleagues could generate iPSCs highly similar to ESCs from both Oct4 and Nanog-reporter MEFs, the authors noted that there was variation in the colonies generated, depending upon the selection genes used, even within their own system. Whilst Nanog-selection gave rise to more colonies overall, Oct4-selection produced more colonies which were morphologically similar to ESCs, and generated a higher number of stable, homogeneous iPSC colonies. Reprogramming to pluripotency using Oct4-reporter MEFs was a gradual process. SSEA1 expression and alkaline phosphatase activity were observed some time prior to the expression of detectable levels of Nanog protein. Although Nanog-reporter MEFs generated more GFP-positive colonies, fewer of these were typical ESC colonies which could go on to establish stable iPSC lines, than those generated using Oct4-reporter MEFs. This suggested that the Nanog locus was more easily activated by exogenous pluripotency factor expression and highlights issues with the use of Nanog expression as a marker of reprogramming to pluripotency. Certainly this side by side comparison identified endogenous Oct4 activation as the most stringent marker of reprogramming to pluripotency that had been tested up to this point (Wernig et al., 2007).

1.6.2 Reprogramming to pluripotency in the presence and absence of the oncogene c-Myc

During experiments to test germline transmission of Nanog-selected iPSCs, tumours in which retroviral c-Myc was reactivated were observed in a number of F1

offspring. However in normal tissues, expression of exogenous factors including c-Myc remained silenced. Attempts to generate iPSCs without c-Myc yielded no GFP-positive colonies, so this raised serious concerns about the production of iPSCs using oncogenic factors (Okita et al., 2007). A number of later studies would demonstrate that exogenous c-Myc is in fact dispensable for reprogramming to pluripotency, however the onset of reprogramming occurs much later in the absence of c-Myc, and the process is less efficient (Nakagawa et al., 2008; Wernig et al., 2008). Indeed it was observed that some colonies generated from 3 factor reprogramming using Oct4, Klf4 and Sox2 (OKS) only acquired ESC-like morphology and endogenous pluripotency factor expression after repeated passaging (Wernig et al., 2008). Using the same Nanog-GFP reporter as Okita and colleagues, it was necessary to delay antibiotic selection until 14 days after infection with OKS, compared to the 7 days after infection which yielded reprogrammed colonies from OKSM-infected MEFs. Whilst induction of pluripotency was slower and less efficient in the absence of c-Myc, it appeared that OKS-reprogramming resulted in a more specific induction of iPSC colonies. The number of non-typical GFP-negative colonies observed in the absence of c-Myc was much lower (Nakagawa et al., 2008). The GFP-positive colonies induced by three factor reprogramming were highly similar to ESCs. Endogenous expression of ESC marker genes was equivalent to levels in ESCs, and these cells contributed to adult chimeras when injected into blastocyst stage embryos, so pluripotency was not compromised by c-Myc omission (Nakagawa et al., 2008; Wernig et al., 2008). Notably, removal of c-Myc from the reprogramming cocktail resulted in the generation of iPSCs highly similar to ESCs using Fbx15 selection. As previously discussed, iPSCs selected using Fbx15 selection are similar, but not identical to ESCs. They express lower levels of the endogenous pluripotency factors and cannot contribute to adult chimeras (Takahashi and Yamanaka, 2006). In contrast, in the absence of c-Myc, iPSCs selected for expression of Fbx15 expressed pluripotency factors at levels highly similar to ESCs and were capable of producing adult chimeras when injected into blastocyst stage embryos. Although this is again a very inefficient process, with few colonies produced, it demonstrates a more specific induction of true ESC-like cells in the absence of c-Myc. Furthermore based on ESC-morphology and retroviral silencing (evidenced by silencing of retroviral GFP), it was possible to generate OKS-reprogrammed iPSCs, which were capable of chimera contribution, in the absence of any form of antibiotic selection. None of the

chimeras generated from OKS-reprogrammed iPSCs were affected by tumours during early life (100 days), whilst a number of chimeras from OKSM-reprogrammed iPSCs died from tumours during this period. This suggests that omission of c-Myc results in a reduction in tumorigenicity, at least in early life, although tumour formation in later life was not investigated (Nakagawa et al., 2008).

1.6.3 Induction of pluripotency in human somatic cells

In 2007 the Yamanaka group demonstrated the generation of human iPSCs from adult dermal fibroblasts (HDFs) using the same four factor approach they had applied to MEFs and mouse adult fibroblasts (Takahashi et al., 2007). At the same time, the laboratory of James Thompson demonstrated the generation of human iPSCs using a different four factor approach, comprising of Oct4, Sox2, Nanog and Lin28 (OSNL). These factors could induce pluripotency in foetally-derived IMR90 fibroblasts and also in postnatal foreskin fibroblasts (Yu et al., 2007). Both groups demonstrated that their respective four factor combinations produced ESC-like cells which expressed the cell surface markers SSEA3, SSEA4, Tra-1-60 and Tra-1-81. iPSCs derived from both combinations expressed high telomerase activity and could be passaged repeatedly in culture. Both OKSM- and OSNL-derived iPSCs were pluripotent, evidenced by generation of tissues from all three germ layers in embryoid bodies and teratoma formation (Takahashi et al., 2007; Yu et al., 2007).

As demonstrated in mice, it is also possible to generate human iPSCs in the absence of c-Myc at extremely low efficiency. OKSM-reprogramming produced a small number of ESC-like colonies, but these were difficult to isolate, as very high numbers of non-typical colonies were also generated in these experiments. In contrast a few ESC-like colonies were generated from OKS-reprogramming, but in the absence of c-Myc there was a notable absence of non-typical colonies, only a few of these cells were observed. This suggests that similar to OKS-reprogramming in mouse cells, omission of c-Myc results in a more specific induction of true iPSCs from human fibroblasts (Nakagawa et al., 2008). The iPSCs generated from 3 factor reprogramming could be expanded in culture and were highly similar to ESCs. Expression of ESC cell surface markers SSEA3, SSEA4, TRA-1-60 and Tra-1-81 was observed, along with endogenous expression of Oct4, Nanog and Sox2 at levels

comparable with those in H9 ESCs. These cells could form differentiating embryoid bodies *in vitro*, which expressed markers of tissues derived from all three germ layers, demonstrating the pluripotency of three factor iPSCs. The authors did note however, that the efficiency of the process was extremely low (Nakagawa et al., 2008). Therefore, whilst c-Myc omission appears to induce the generation of pluripotent cells highly similar to ESCs, with reduced concerns over tumorigenicity, issues regarding the generation of viable numbers of iPSCs in the absence of c-Myc remain.

1.7 Methods to enhance the efficiency of reprogramming to pluripotency

1.7.1 The tumour suppressor p53 as a barrier to reprogramming to pluripotency

The omission of c-Myc from the reprogramming cocktail generates iPSCs at extremely low efficiency, and even in the presence of c-Myc the vast majority of cells exposed to reprogramming factors fail to undergo the full transition to pluripotency. Maximum reprogramming efficiencies of around 1% are typically observed, so whilst reprogramming technologies are reproducible, the inefficiency of the procedure means it is difficult to generate high numbers of iPSC clones, unless extremely high starting numbers of cells are transduced (Yamanaka, 2012). The p53 pathway is stimulated in response to stress signals including over-expression of oncogenes and DNA damage. This stimulation results in cell cycle arrest and apoptosis in affected cells (Kawamura et al., 2009). Infection of cells with retroviral vectors in the reprogramming process results in DNA integration events and increased expression of the oncogenes c-Myc and Klf4. Following retroviral infection increased expression of p53 (Kawamura et al., 2009; Marion et al., 2009a) and its downstream target p21 (Hong et al., 2009) were observed, along with an increase in apoptosis (Marion et al., 2009a). There was a significant increase in reprogramming efficiency in p53-null MEFs compared to wild type cells and a similar result was observed in human fibroblasts treated with a short hairpin RNA (shRNA) to knockdown p53 (Hong et al., 2009; Kawamura et al., 2009; Marion et al., 2009a). Furthermore, it was possible to derive iPSCs from p53-null terminally differentiated T lymphocytes, whilst no colonies were observed in wild type cells

(Kawamura et al., 2009). Knockdown of the p53 downstream target p21, a cyclin dependent kinase inhibitor which halts cell cycle progression, also resulted in enhanced reprogramming efficiency in MEFs (Kawamura et al., 2009). Taken together this suggests that p53 acts as a barrier to reprogramming, probably through inhibition of proliferation and apoptosis induction in response to forced expression of reprogramming factors. Clearly p53 reduction or knockout acts to increase reprogramming efficiency. However such approaches should be used with caution, as p53 acts to detect and remove cells with genomic instabilities. In wild type cells, it was not possible to generate iPSCs from MEFs with critically short telomeres, however colonies were derived from such cells in a p53-null background (Marion et al., 2009a). Whilst p53 reduction can be used to increase reprogramming efficiency it also allows the propagation of genomic instabilities to resultant iPSCs, which would be a major concern for therapeutic applications.

1.7.2 Small molecule chromatin modifiers as enhancers of reprogramming to pluripotency

As previously discussed, pluripotent cells have a characteristic epigenetic profile distinct from lineage committed cells. Resetting of both histone modifications and DNA methylation to an ESC-like pattern occurs during reprogramming to pluripotency (Maherali et al., 2007). However even in some fully reprogrammed cell lines there are reports of 'epigenetic memory', where somatic cell DNA methylation patterns are observed at some sites in iPSCs (Kim et al., 2010; Lister et al., 2011). Frequently cells undergo partial reprogramming, adopting some but not all characteristics of pluripotency. Incomplete epigenetic remodelling in these cells is considered a significant barrier to complete reprogramming. It was observed that in a number of partially reprogrammed cells, pluripotency-related genes remained hypermethylated, and that in these cells there was little or no detectable expression of these endogenous pluripotency factors (Mikkelsen et al., 2008). Treatment of partially reprogrammed cells with the DNA methyltransferase inhibitor 5-azacytidine (5-AZA) resulted in transition to full pluripotency. The fully reprogrammed cells showed decreased DNA methylation in pluripotency related genes. Furthermore the cells formed teratomas on implantation in nude mice, whilst partially reprogrammed cells did not form teratomas under identical experimental conditions. It was noted

that correct timing of 5-AZA addition was required. Treatment early in the reprogramming procedure had no effect on reprogramming efficiency, and actually resulted in significant cell death. It was suggested that in these early stages, cells are still susceptible to the effects of DNA hypomethylation, which in somatic cells induces apoptosis. However 5-AZA added later in the reprogramming process (8 days after induction of reprogramming through addition of doxycycline) could increase reprogramming efficiency, suggesting that DNA de-methylation occurs at a later stage when cells have begun the transition towards pluripotency and are not therefore adversely affected by a hypomethylated state (Mikkelsen et al., 2008).

Other small molecule epigenetic modifiers have also been demonstrated to increase reprogramming efficiency. Addition of the histone deacetylase (HDAC) inhibitor valproic acid (VPA) enhanced three factor (OKS) reprogramming of MEFs by 50-fold compared to untreated OKS-reprogramming. The addition of VPA also enhanced efficiency of generation of iPSCs from human fibroblasts with OKS, producing colonies with morphology and marker expression similar to human ESCs (Huangfu et al., 2008a; Huangfu et al., 2008b). Notably the efficiency of MEFs reprogrammed with OKS with VPA treatment was higher than the efficiency of MEFs reprogrammed with OKSM, demonstrating that VPA treatment could replace c-Myc transduction. iPSCs generated by OKS reprogramming with VPA treatment were similar to ESCs in morphology and global gene expression profile. They were pluripotent, evidenced by embryoid body differentiation to tissues from all germ layers, teratoma formation and chimera contribution (Huangfu et al., 2008a). Furthermore, when human fibroblasts were treated with VPA during reprogramming it was possible to derive iPSC colonies after infection with Oct4 and Sox2 (OS) alone. The colonies could be repeatedly passaged in culture and maintained ESC-like morphology with no further need for VPA treatment. These colonies expressed ESC markers, and had reactivated endogenous Oct4 and Sox2. Furthermore, the Oct4 and Nanog promoters had undergone DNA de-methylation, resulting in DNA methylation profiles similar to those observed in ESCs. iPSCs derived with OS and VPA treatment were confirmed pluripotent *in vitro* and by teratoma formation *in vivo* (Huangfu et al., 2008b). In contrast to the late treatment of MEFs with 5-AZA, in both MEFs and human fibroblasts, VPA was applied 1 day following lentiviral transduction, and maintained for up to 2 weeks, for optimal reprogramming

enhancement (Huangfu et al., 2008a; Huangfu et al., 2008b). This suggests that the alteration of histone modifications early in the reprogramming process does not have the same detrimental effects as those observed by Mikkleson and colleagues when using compounds which drive DNA demethylation (Mikkelsen et al., 2008).

Further small molecule chromatin modifiers have been demonstrated to improve reprogramming to pluripotency with fewer factors. Transduction of MEFs with Oct4 and Klf4 (OK) alone yielded few non-typical colonies which were difficult to expand and stained weakly for alkaline phosphatase (Shi et al., 2008). However addition of a small molecule, the G9a histone methyltransferase inhibitor BIX01294, which acts to inhibit dimethylation at lysine 9 of histone 3 (H3K9me2), resulted in typical ESC-like colonies with strong alkaline phosphatase activity. These cells were also positive for Oct4, Nanog and SSEA1. Furthermore, transduction with OK, along with the combined treatment of MEFs with both BIX01294 and another small molecule, BayK, increased the number of colonies observed. Cells transduced with OK and treated with BIX01294 and BayK produced greater numbers of colonies which stained strongly for alkaline phosphatase, and were positive for Oct4, Nanog, Sox2 and SSEA1. These colonies could be maintained for many passages *in vitro* and had a highly similar gene expression pattern to ESCs. Interestingly, BayK is an L-type calcium channel agonist, with no known epigenetic effects, and treatment with BayK alone did not yield ESC-like colonies from OK-transduced cells. The mode of action of BayK is unclear, but it was suggested that BayK may act to impact signalling pathways involved in reprogramming to pluripotency (Shi et al., 2008).

1.7.3 Inhibition of chromatin remodelling complexes in reprogramming to pluripotency

A recent breakthrough has provided the strongest evidence yet that epigenetic factors can act as a major barrier for reprogramming to pluripotency. MBD3 is a component of the nucleosome remodelling and histone deacetylation (NuRD) complex. Depletion of MBD3 in MEFs resulted in almost 100% reprogramming efficiency, whilst only around one fifth of wild type cells were reprogrammed to pluripotency with four factor (OKSM) methods (Rais et al., 2013). Although typically in four factor reprogramming experiments a maximum efficiency of around 1% reprogramming is observed (Yamanaka, 2012). It was noted that the effects of

MDB3 depletion could be reversed if MEFs were infected with MBD3-expressing lentivirus in the first 5 days of reprogramming, but that after this point, lentiviral infection with MBD3 had a reduced effect on reprogramming efficiency. This suggested that MBD3 must act early in the reprogramming process, but could not significantly inhibit the final stages of conversion to pluripotency, or affect pluripotency maintenance in reprogrammed MEFs (Rais et al., 2013). A similar effect was observed when human fibroblasts with a mutation in MDB3 were reprogrammed to pluripotency with near 100% efficiency. Notably MDB3 inhibition alone was not sufficient to drive reprogramming to pluripotency in the absence of OKSM. However inhibition of MDB3 using short interfering RNA (siRNA) could induce partially reprogrammed cells to convert to full pluripotency, and activate endogenous Oct4 and Nanog expression. Interestingly, it was demonstrated that MDB3 only binds pluripotency factor target genes after induction of reprogramming, and that MBD3 recruitment increases at this point. OKSM co-immunoprecipitate with MBD3, and MBD3 co-binds many genes which are required for reprogramming to pluripotency. It would appear that upon the induction of reprogramming, the pluripotency factors co-bind with MBD3 at a number of genes, and that MBD3 is able to repress these genes even in the presence of pluripotency factors that would activate their expression. The role of MBD3 seems to be to restrain expression of factors required for the establishment of the pluripotent state, which would explain why MBD3 depletion enhances reprogramming efficiency so effectively. Clearly the chromatin modification and gene repression mediated by MBD3 is a major barrier to reprogramming, and in its absence, the pluripotency factors can freely activate genes which would normally be repressed by MBD3, so easily establishing pluripotency in the vast majority of cells exposed to reprogramming stimuli (Rais et al., 2013).

1.7.4 Other small molecules which can enhance reprograming efficiency

Whilst Shi and colleagues (Shi et al., 2008) noted that the small molecule BayK could not reprogramme MEFs to pluripotency in the absence of an epigenetic modifier, other groups have identified compounds with no known epigenetic effects which can act alone to enhance reprogramming efficiency or replace reprogramming factors.

A small molecule inhibitor of TGFβ signalling has been shown to either enhance reprogramming efficiency and/or replace the need for some exogenous reprogramming factors. E-616452, a TGFβ receptor 1 inhibitor acted to enhance the reprogramming efficiency of OKSM-transduced MEFs when treatment was applied at the same time as doxycycline (dox) in a dox-inducible system, but had no effect on reprogramming efficiency when administered prior to dox treatment (Maherali and Hochedlinger, 2009). In contrast another group used the same inhibitor, but found less than a 2-fold increase in colony numbers over control samples, so suggested that this inhibitor acted to replace exogenous factors rather than enhance reprogramming efficiency (Ichida et al., 2009). The inhibitor could act to functionally replace c-Myc in the reprogramming cocktail (Ichida et al., 2009; Maherali and Hochedlinger, 2009). Ichida and colleagues suggested that this occurred via the stimulation of endogenous L-Myc expression. L-Myc is a homologue of c-Myc previously shown to replace it in reprogramming to pluripotency (Ichida et al., 2009). Both groups also demonstrated that E-616452 could replace Sox2 (Ichida et al., 2009; Maherali and Hochedlinger, 2009), however only one group found that E-616452 could replace both Sox2 and c-Myc simultaneously (Ichida et al., 2009). There were also striking differences in the optimal timing of inhibitor treatment. One group found that E-616452 was optimally applied with the start of dox addition, so it was concluded that the inhibitor acted early in the reprogramming process (Maherali and Hochedlinger, 2009). In contrast, the other group found that in their system, E-616452 acted on partially reprogrammed cells. These cells formed colonies which resembled iPSCs, and could be maintained for several passages, but failed to activate the endogenous Oct4-GFP reporter, a robust marker of full reprogramming to pluripotency. Activation of Oct4-GFP was observed in a number of these colonies after addition of E-61642. Furthermore within 24-48 hours of inhibitor treatment, cells which were responsive to the inhibitor (i.e. those that activated Oct4-GFP following treatment) had up-regulated endogenous Nanog expression by up to 10-fold. Notably in this period endogenous Sox2 expression did not significantly increase, so it would appear that whilst E-616452 can replace exogenous Sox2, it does this by activating endogenous expression of Nanog rather than Sox2 (Ichida et al., 2009). Despite the differences observed with the use of E-616452 in different laboratories, inhibition of TGFβ signalling appears to positively benefit reprogramming to pluripotency. Indeed the

addition of TGFβ1 or TGFβ2 lead to a dramatic reduction in the number of colonies observed in OKSM-transduced MEFs compared to control samples, suggesting that TGFβ signalling is a barrier to reprogramming. During development, cells undergo an epithelial to mesenchymal transition, which is driven by TGFβ signalling, whilst reprogramming to pluripotency requires a mesenchymal to epithelial transition (Maherali and Hochedlinger, 2009). As reprogramming to pluripotency can be considered as the reversal of development, it would make sense that signalling which drives developmental progression may need to be suppressed in order to allow a regression to the pluripotent state.

Lin and colleagues showed inhibition of TGFβ signalling, this time in combination with an inhibitor of the MAPK/ERK cascade, could improve the efficiency of reprogramming to pluripotency in human fibroblasts using a four factor (OKSM) approach. The authors observed that treatment 7 days after infection with the Alk inhibitor SB431542 in combination with the MEK inhibitor PD0325901 resulted in the generation of ESC-like colonies with increased mRNA levels of endogenous pluripotency factors compared to untreated control samples. Furthermore Nanog-positive colonies were observed in treated samples, whilst there were no Nanog-positive colonies from control experiments. This suggested that the combination of TGFβ and MAPK/ERK inhibition resulted in an increase in colonies which expressed endogenous markers of pluripotency (Lin et al., 2009)

The MEK inhibitor PD0325901 is one part of the 2i combination of inhibitors commonly used in the maintenance of undifferentiated ESCs in culture. PD0325901 combined with the GSK3β inhibitor CHIR99021 (2i) and LIF, acted to push partially reprogrammed neural stem cells (NSCs) to full pluripotency. In four factor (OKSM) transduced NSCs, early but unstable activation of Oct4-GFP was observed, which was not maintained on passaging, suggesting incomplete reprogramming to pluripotency. GFP-positive colonies first appeared at around day 5 following infection, so at this point NSCs were trypsinised and replated in media supplemented with 2i/LIF. This resulted in the growth of multiple colonies, of which around two thirds expressed Oct4-GFP. A similar effect was seen without the need for replating. Exchange of medium on days 3/5 to serum-free medium supplemented with 2i/LIF yielded many colonies of which over half had reactivated Oct4-GFP. These iPSCs

expressed endogenous pluripotency factors at levels equivalent to ESCs, and like ESCs were LIF-dependent in culture, differentiating on LIF withdrawal. They were also capable of chimera contribution on blastocyst injection, confirming the pluripotency of colonies treated with 2i/LIF (Silva et al., 2008). Reactivation of Oct4-GFP in partially reprogrammed cells following 2i/LIF treatment demonstrates that signalling mechanisms involved in the maintenance of the undifferentiated state in ESCs also play a role in reprogramming somatic cells to pluripotency.

1.8 Metabolic restructuring during reprogramming to pluripotency

As previously discussed, the metabolic profile of differentiated cells is quite distinct from that of pluripotent cells. A number of recent studies have focused on and highlighted the need for metabolic remodelling, along with transcriptional and epigenetic alterations, to achieve reprogramming to pluripotency. Folmes and colleagues (Folmes et al., 2011) demonstrated that during four factor (OKSM)-based reprogramming, MEFs undergo remodelling in which many tubular cristae-rich mitochondria are remodelled to a small number of perinuclear mitochondria, a cytotype highly similar to that seen in ESCs. iPSCs showed increased cellular levels and increased production of lactate compared to MEFs, along with lower oxygen consumption, indicative of a shift to a glycolytic metabolism. Lactate production and oxygen consumption rates (OCR) in iPSCs were highly similar to those observed in ESCs. The reprogramming factor c-Myc has previously been shown to affect glycolysis and mitochondrial biogenesis, so to investigate if c-Myc transduction was driving the observed metabolic changes, MEFs were reprogrammed to pluripotency using three factors (OKS). In the absence of c-Myc, iPSCs increased glycolysis, evidenced by accumulation of glycolytic end products, and had a limited capacity for oxidative metabolism. This demonstrated that the reprogramming process itself, and not c-Myc transduction, was driving metabolic remodelling in MEFs (Folmes et al., 2011). The glycolysis inhibitor 2-deoxy-glucose (2DG) impaired induction of the pluripotency marker alkaline phosphatase (Folmes et al., 2011), and reduced the number of GFP-positive colonies generated (Panopoulos et al., 2012), suggesting that inhibition of glycolysis inhibits reprogramming to pluripotency. Conversely, treatment with D-fructose-6-phosphate (F6P), a glycolytic stimulator, was able to enhance reprogramming efficiency. Metabolomic analyses showed that iPSCs

clustered with ESCs and distinct from their parental cells. It was also demonstrated that whilst early passage (p16) iPSCs were similar to ESCs in their metabolic profile, late passage (>p41) iPSCs were much more similar (Panopoulos et al., 2012). This increased similarity to ESCs with time in culture echoes that observed with so called 'epigenetic memory,' in which parental cell epigenetic characteristics are maintained at some points in the genome following iPSC derivation, but which are then altered to an ESC-like state with repeated passaging in culture. Analysis of DNA methylation patterns in genes related to metabolism also showed iPSCs clustering with ESCs, and distinct from parental cells. iPSCs up-regulated glycolytic genes and down-regulated expression of genes related to oxidative phosphorylation compared to their parental cells of origin. Notably the metabolic status of somatic cells has been linked to reprogramming efficiency. The authors observed that somatic cells have a higher oxidative:glycolytic ratio compared to pluripotent cells, which are highly glycolytic. Keratinocytes and human umbilical vein endothelial cells (HUVECs) reprogrammed with much greater efficiency than fibroblasts, and it was demonstrated that both these cell types had a lower oxidative:glycolytic ratio than fibroblasts. This meant that the starting metabolism in these cells was more similar to that in pluripotent cells, so it was suggested that cells with a low oxidative:glycolytic ratio could be reprogrammed to pluripotency with higher efficiency (Panopoulos et al., 2012). A schematic summary of metabolic differences between pluripotent and differentiated cells is given in Figure 1.5.

1.9 Cellular remodelling during a cell stress-triggered autophagy response

Autophagy is a physiological stress response which allows the recycling of cytoplasmic contents, as a survival mechanism under conditions of nutrient deprivation/starvation. Autophagy is induced by the action of nutrient sensors, which can act to detect fluctuations in nutrient availability. Following autophagy induction, there is formation of a double-membrane vesicle, which can sequester cytoplasmic contents, including organelles such as mitochondria. The double-membrane vesicle encloses cytoplasmic contents, and is then referred to as an autophagosome. The degradation and recycling of the autophagosome contents occurs on fusion with a lysosome, forming an autolysosome. This structure consists of a fusion of the

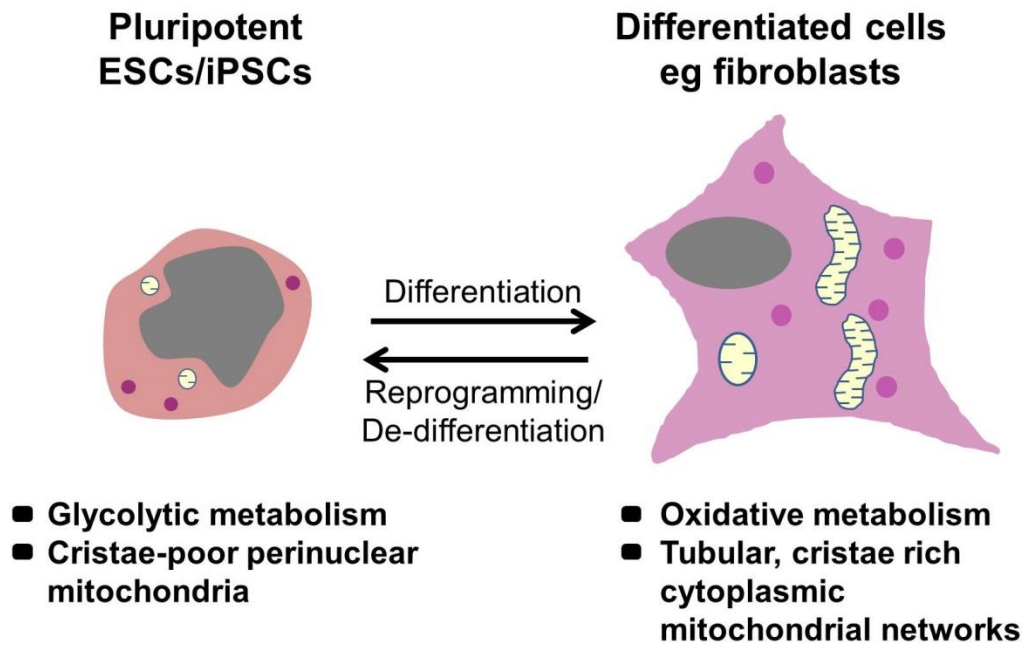

Figure 1.5. Schematic showing the distinct metabolic profiles of pluripotent and differentiated cell types

Pluripotent ESCs have a characteristic simple cytotype, with few small, rounded, cristae poor perinuclear mitochondria. They rely on glycolysis (anaerobic metabolism) even in normoxic conditions. In contrast, differentiated cells have an oxidative metabolism, and a more complex cytotype, with a cytoplasmic network of tubular, cristae-rich mitochondria. Increased metabolic complexity develops during differentiation, and cells undergo a metabolic switch from glycolysis to oxidative metabolism. During reprogramming to pluripotency, the cytotype of differentiated cells must be remodelled to an ESC-like state, and iPSCs adopt the characteristic pluripotent cytotype and glycolytic metabolic profile.

lysosome and outer autophagosome membranes, whilst the autophagosome inner membrane is broken down, to release its contents for breakdown by lysosomal enzymes (Klionsky and Emr, 2000).

Mammalian target of rapamycin (mTOR) is one such nutrient sensor, which inhibits autophagy in nutrient rich conditions. The compound rapamycin stimulates autophagy by inhibiting the action of mTOR. Rapamycin and other mTOR inhibitors have also been shown to promote longevity in a number of experimental organisms. It was demonstrated that rapamycin could act in a dose-dependent manor to increase the efficiency of iPSC generation from four factor (OKSM) transduced MEFs. It was also noted that this action of rapamycin was most effective early (1-3 days) in the reprogramming process (Chen et al., 2011). This result was also observed by another group, although they found that even earlier application (day 1) was required, and that rapamycin treatment started 3 days after infection could not improve reprogramming efficiency (Wang et al., 2013). PP242 is another mTOR inhibitor and longevity enhancing drug, which like rapamycin improved reprogramming efficiency in OKSM-transduced MEFs. The authors suggested that this could mean that longevity enhancing drugs positively benefitted reprogramming to pluripotency. They also demonstrated that a similar enhancement of reprogramming efficiency was observed on treatment with spermidine, a known autophagy stimulator (Chen et al., 2011). So it is possible that rapamycin and PP242 may have been acting through their role in autophagy stimulation, to increase reprogramming efficiency. Recent work has highlighted that a functional autophagic response is required for reprogramming to pluripotency. Depletion of factors required for autophagosome formation resulted in an absence of iPSC colonies from MEFs, whilst numerous colonies were observed in control samples. Furthermore, in control samples, autophagosome formation was observed early (day 1) after initiation of reprogramming. This timing coincides with an early requirement for rapamycin treatment, and may suggest that autophagy induction is required early in the reprogramming process, and could act as a driver for later events. It was observed that ectopic expression of Sox2, actually resulted in a dramatic reduction in mTOR mRNA, and promoter studies revealed binding of Sox2 in a repressive region of the mTOR promoter. This work demonstrates how ectopic expression of reprogramming factors can stimulate autophagy, and highlights the requirement of a functional

autophagic response in reprogramming to pluripotency. Strikingly in cells depleted for key autophagy genes, there was a noticeable failure to reduce mitochondrial numbers, and an absence of iPSC colonies (Wang et al., 2013). As previously discussed, remodelling of the mitochondrial network and a metabolic shift to glycolysis are key features of successful reprogramming. Taken together these results suggest that a functional autophagic response is required for successful metabolic remodelling, and that this remodelling to immature, limited mitochondria may drive the metabolic shift to glycolysis.

1.10 Enhanced expression of pluripotency factors in mesenchymal stem cells/multipotent stromal cells cultured as 3D spheroids

It was previously observed in our laboratory that culturing mesenchymal stem cells/multipotent stromal cells (MSCs) in 3D conditions resulted in up-regulation of pluripotent transcription factors compared to expression in 2D MSCs (Elen Bray, unpublished observations). Primary human MSCs can be isolated from human bone marrow, and selected based on plastic-adherent growth in serum-supplemented media. Using appropriate induction protocols, MSCs are multipotent, and can be induced to differentiate down osteogeneic, adipogenic and chondrogenic lineages. However their potency is restricted to tissues of mesenchymal origin (Pittenger, 1999). The laboratory in York has utilised a number of dynamic methods for 3D culture, including the use of spinner flasks and a rotating wall vessel bioreactor designed to enhance MSC stem cell properties and therapeutic potential (Frith et al., 2010). The laboratory also uses a static 3D methyl cellulose media-based system, in which MSCs are seeded into non-adherent U-bottomed 96-well plates, in media supplemented with methyl cellulose. Due to the viscosity of this media, MSCs are maintained in suspension, and adhere together to form cell aggregates, referred to hereafter as spheroids. Spheroid size is dependent on initial seeding cell number and also time in culture, as it was previously demonstrated that MSCs do not proliferate under these conditions, and spheroid size actually decreases with time in 3D culture. Along with increased expression of pluripotency markers, 3D MSCs showed a much greater increase in expression of cardiac markers than that observed in 2D MSCs, when stimulated to undergo cardiomyogenic differentiation following 3D culture in optimal conditions (Elen Bray, unpublished observations). In summary, it was

previously established that 3D MSCs can be cultured in 3D conditions and that during 3D culture, spheroids reduced in size. During 3D culture, 3D MSCs displayed characteristics of enhanced potency, including pluripotency marker expression, compared to 2D MSCs. However, the mechanism driving enhanced potency in 3D MSCs was not established.

Recent work in iPSC research has highlighted a role for autophagy and metabolic remodelling in reprogramming to pluripotency, although the processes of autophagy and mitochondrial/cytoplasmic remodelling have not been explicitly linked. It is interesting that autophagy, a physiological response to cell stress, particularly nutrient deprivation, has been demonstrated as a key early step in reprogramming to pluripotency. Given that 3D MSCs will be exposed to varying nutrient availability due to variations in spheroid size, and that 3D MSCs increase expression of pluripotency factors, as well as reducing in size during 3D culture, I hypothesised that controlled autophagy, stimulated by nutrient deprivation, may be the mechanism driving enhanced potency in 3D MSCs. In my hypothesis MSCs transferred to 3D culture would be exposed to varying nutrient deprivation, depending on spheroid size and time in 3D culture. In optimal conditions, autophagy, scaled in favour of cell survival, would result in cytoplasmic and metabolic remodelling, driving de-differentiation towards a more primitive state, in 3D MSCs.

Project aims

The aim of this work was to investigate whether a scaled autophagic response, induced by nutrient deprivation in 3D culture, was sufficient to drive de-differentiation towards a more primitive state. Initially this project focused on establishing 3D culture conditions in which enhanced pluripotency factor expression was observed in human MSCs. Following the establishment of such conditions the project then aimed to:

- establish the extent of de-differentiation in 3D MSCs
- examine MSCs cultured under 3D conditions for evidence of cytoplasmic and metabolic remodelling
- establish if autophagy was the driving mechanism for enhanced pluripotency factor expression in 3D MSCs by looking for evidence of increased autophagy during 3D culture

Chapter 2: Materials and methods

2.1 Materials

All cell culture media, supplements and reagents were purchased from Invitrogen (Carlsbad, CA, USA) unless otherwise stated. Foetal bovine serum (FBS) was batch tested for MSC proliferation and differentiation down osteogenic and adipogenic lineages, and the best performing sera were purchased from Invitrogen and Biosera (Labtech, Uckfield, East Sussex, UK). Cell culture flasks and plates were purchased from Corning Life Sciences (Corning, NY, USA) and all chemicals were purchased from Sigma Aldrich (St. Louis, MO, USA) unless otherwise stated.

2.2 General methods

2.2.1 Cell culture methods

2.2.1.1 Isolation of MSCs from femoral heads

Bone marrow was manually isolated from femoral heads from hip replacement surgery following full informed consent under approval of the York Local Research Ethical Committee. Marrow was added to 10ml Dulbecco's modified Eagle's medium (DMEM, high glucose) supplemented with 100 units/ml penicillin and 100µg/ml streptomycin. Bone marrow fragments were then minced with scissors, allowed to settle, and media was transferred to a collection tube. 10ml of medium was added to bone marrow fragments, and the mincing procedure was performed twice more. 10ml of fresh medium was then added, before vortexing. After the fragments had settled, the medium was transferred to the collection tube. The collection tube containing the cell suspension was centrifuged for 450g, 5 minutes, before the cell pellet was re-suspended in fresh medium, and passed through a 70µm cell strainer. The cell suspension was then layered over 12ml Ficoll-Paque Plus, and centrifuged at 350g for 30 minutes with low braking. The white mononuclear cell layer was isolated, and washed by centrifugation (450g, 5 minutes) in wash buffer (5 mM EDTA, 0.2% BSA in PBS). Finally, the cell pellet was re-suspended in 2D MSC medium (for composition please see 2.2.1.3), and seeded into a T75 tissue culture flask. After 3-4 day, the medium was refreshed, removing non-adherent cells from the culture.

2.2.1.2 Isolation of MSCs from knee samples

Bone samples from knee replacement surgery were dissected into small pieces and placed in cell culture 100mm dishes (BD Falcon, San Jose, CA, USA). 20ml 2D MSC medium (for composition please see 2.2.1.3) was added to dishes, which were maintained in culture (37ºC, 5% CO_2) for 7 days, after which point bone pieces were removed and medium replenished. Samples were then cultured as described in 2.2.1.3.

2.2.1.3 MSC expansion conditions

Following isolation, MSCs were cultured as adherent monolayers in 2D MSC medium - DMEM (high glucose) supplemented with 15% FBS and 100 units/ml penicillin and 100µg/ml streptomycin at 37ºC, 5% CO_2. Samples were cultured to approximately 90% confluence, before passaging at a ratio of 1:3 or 1:4. Briefly, cultures were washed with PBS, before treatment with 0.25% Trypsin/EDTA. Following detachment, 2D MSC medium was added, and cells were re-plated into the appropriate number of tissue culture flasks. For the experiments performed here, primary MSCs from 26 donors, both male and female, with an age range from 51 – 87 years were used. For ease of reading the donors for a particular experiment used were simply identified as Donors 1, 2 and 3. However this identity applies only to each particular experiment. 2-3 donors from the 26 were selected at random for each experiment, then for the purpose of this thesis identified as Donor 1, 2 or 3.

2.2.1.4 Human dermal fibroblast (HDF) expansion conditions

For 2D HDF culture, HDFs were maintained as described for 2D MSCs in 2.2.1.3, but 2D HDF medium was supplemented with 10% FBS and the passaging ratio for HDFs was 1:4.

2.2.1.5 3D culture conditions

For 3D culture, 2D MSCs were grown to approximately 90% confluence and trypsinised as described in 2.2.1.3. Cells were counted using a haemocytometer and light microscopy, and then re-suspended in 3D medium; DMEM (high glucose), supplemented with 15% FBS, 100 units/ml penicillin, 100µg/ml streptomycin and

0.25% methyl cellulose (2% stock solution made up in DMEM high glucose). For 3D HDF culture, HDFs were cultured as described for MSCs above, but 3D HDF medium was supplemented with 10% FBS.

2.2.1.6 ESC culture conditions

H9 human ESCs were maintained on irradiated MEF (iMEF) feeder layers, with daily medium changes. ESC medium consisted of KO DMEM, supplemented with 20% KO serum replacement, 100 units/ml penicillin, 100µg/ml streptomycin, 2mM L-glutamine, 100µM non-essential amino acids (NEAA), 100µM β-mercaptoethanol and 4ng/ml basic fibroblast growth factor (bFGF). ESCs were passaged every 3 days at a ratio of 1:6.

2.2.1.7 2102Ep embryonal carcinoma cell culture conditions

2102Ep cells were cultured as adherent monolayers in DMEM (high glucose) supplemented with 10% FBS and 100 units/ml penicillin and 100µg/ml streptomycin. Samples were cultured to approximately 80% confluence, before passaging at a ratio of 1:4, or harvesting by trypsinisation for further analysis.

2.2.2 Disaggregation of spheroids for return to 2D culture

2.2.2.1 Disaggregation and re-seeding

At the appropriate time point, spheroids were collected, washed in PBS and then re-suspended in Liberase TL working solution (32 µl Liberase TL (Roche, Basel, Switzerland) mixed with 318µl sterile PBS). Spheroids were incubated on an orbital shaker for 20 minutes at 37°C and then disaggregated to a single cell suspension by pipetting. Disaggregated 3D (d-3D) MSCs were then either collected in suspension for further analysis or re-seeded onto tissue culture plastic in 2D MSC medium. Following this process, d-3D MSCs were cultured as 2D MSCs (described in 2.2.1.3) and were treated as 2D MSCs for RNA and protein extraction.

2.2.2.2 Crystal violet staining

To observe the morphology of 3D MSCs following disaggregation (d-3D MSCs), samples were fixed in 95% ethanol for 5 minutes, followed by incubation in 0.5% Crystal Violet (in 95% ethanol) for 30 minutes. Samples were then washed in tap water and air dried. Imaging was performed using a Leica IRB inverted microscope.

2.2.3 3D MSC snap freezing and sectioning

3D MSCs were transferred to the caps of 500µl Eppendorf tubes, and then washed with PBS (2/3 spheroids per cap). Samples were then embedded in OCT Tissue Tek and snap-frozen by submersing in liquid nitrogen. Samples were stored at -80ºC, and when required were cryosectioned at 5-7µm, before mounting on Superfrost Plus microscope slides (Thermo Scientific, Waltham, MA, USA). Slides were either freshly stained or stored at -20ºC.

2.2.4 Transmission electron microscopy

2.2.4.1 Sample preparation and fixation

2D MSCs were cultured on Thermanox cover slips (Thermo Scientific), to enable sectioning. 3D MSCs were collected in Eppendorf tubes. Samples were fixed in 8% formaldehyde, 5% glutaraldehyde in 100mM phosphate buffer mixed 50/50 with 3D MSC medium for 10 minutes followed by fixing with 4% formaldehyde, 2.5% glutaraldehyde in 100mM phosphate buffer, pH7.2 for 30 minutes at room temperature. Samples were then washed in 100mM phosphate buffer, 2 x 20 minutes.

2.2.4.2 Preparation for imaging

Following fixation, samples were treated as described in Table 2.2.1

Table 2.2.1 TEM sample preparation

Procedure/Reagent	**Time**
1% OsO4 in 100mM buffer on ice	60 minutes
Wash in 100mM phosphate buffer	2 x 10 minutes
25% Ethanol	20 minutes
50% Ethanol	20 minutes

70% Ethanol	20 minutes
90% Ethanol	20 minutes
100% Ethanol	2 x 20 minutes
Epoxy propane	15 minutes
25% epon araldite, 75% epoxy propane	30 minutes
50% epon araldite, 50% epoxy propane	30 minutes
75% epon araldite, 25% epoxy propane	30 minutes
100% epon araldite	

2.2.4.3 Preparation for imaging (enhanced contrast)

Following fixation, for enhanced contrast TEM used in Chapter 5, samples were prepared as described in Table 2.2.2

Table 2.2.2 TEM sample preparation (enhanced contrast)

Procedure	**Time**
1% tannic acid in 100mM phosphate	10 minutes
100mM phosphate buffer	2 x 20 minutes
0.5% OsO4 on ice	60 minutes
Water	2 x 20 minutes
1% uranyl acetate in water (in dark)	60 minutes
Water	20 minutes
Water (at 4ºC)	overnight
25% acetone	20 minutes
50% acetone	20 minutes
70% acetone	20 minutes
90% acetone	20 minutes
100% acetone	2 x 25 minutes
25% Spurr (R) : 75% acetone	30 minutes
50% Spurr (R) : 50% acetone	30 minutes
75% Spurr (R) : 25% acetone	30 minutes
100% Spurr (R)	2 hours
100% Spurr (R)	2 x 30 minutes

2.2.4.4 Sectioning and imaging

Polymerised sample blocks and 2D samples were then sectioned at 70nm using a Leica RM2165 rotary microtome and imaged on a FEI Tecnai G transmission electron microscope.

2.2.5 RNA techniques

2.2.5.1 Cell lysis

2D MSCs/HDFs were trypsinised, centrifuged at 400g for 5 minutes, and then re-suspended in 350 µl RA1 lysis buffer (Nucleospin RNA II kit) with 3.5µl β-mercaptoethanol. 3D MSC/HDF spheroids were collected in Eppendorf tubes, washed with PBS, re-suspended in lysis buffer as above, before homogenisation with a hand-held tissue micro-homogeniser for 5 seconds. H9 ESC colonies were trypsinised using recombinant trypsin (TrypLE) and resuspended in lysis buffer as above.

2.2.5.2 RNA extraction

Following cell lysis, RNA was extracted using Nucleospin RNA II columns (Macherey Nagel, Duren, Germany) following manufacturer's instructions. Briefly, lysates were cleared by passing through the filter column, before being mixed with 350µl 70% ethanol. Samples were then bound to the extraction column by centrifugation. Membrane desalting buffer (MBD) was added to desalt the silica membrane. Buffer was removed by centrifuging and samples were treated with 95µl DNase reaction mixture for 15 minutes at room temperature. Columns were washed by centrifugation with RA2 buffer, followed by 2 washes with RA3 buffer. To ensure columns were free of buffer, they were centrifuged at 11,000g for 30 seconds in a dry collection tube. RNA was then eluted in 30-40µl RNase-free H_2O. For maximal RNA recovery, the total volume of RNase-free H_2O was centrifuged through the column twice. Samples were kept on ice throughout and all centrifugation steps were performed at 4ºC, 11,000g for 1 minute unless otherwise stated. RNA samples were then quantified using the Nanodrop spectrophotometer (Thermo Scientific).

2.2.5.3 cDNA synthesis

cDNA was synthesised from 1µg mRNA, all reagents were from Invitrogen unless otherwise stated. Briefly, mRNA was mixed with 1µl Oligo dT primer, 1µl 10mM dNTPs and RNase-free H_2O, to a total volume of 12µl. Samples were then incubated at 65ºC for 5 minutes. After 2 minutes cooling on ice, a master mix (consisting of

4µl First Strand Buffer, 2µl 0.1mM DTT and 1µl RNase-free H_2O), was added to samples, before incubation at 42ºC for 2 minutes. Samples were then mixed with 1µl Superscript II reverse transcriptase (or 1µl RNase-free H_2O for No RT controls). cDNA synthesis consisted of incubation at 42ºC for 1 hour, followed by 15 minutes at 70ºC (to inactivate the reverse transcriptase). All samples were then diluted to a total volume of 100µl.

2.2.5.4 qPCR

Samples were prepared for qPCR by mixing with Power SYBR Green PCR Master Mix (Applied Biosystems, Carlsbad, CA, USA). Briefly, 5 µl of cDNA was added to a master mix consisting of 12.5µl Power SYBR Green, 5.5µl RNase-free H_2O, and 1µl each of 20µM forward and reverse primer, in triplicate wells for all genes of interest. QPCR was performed using the Applied Biosystems 7300 Real Time PCR System, (50°C for 2 minutes, 95°C for 10 minutes followed by 40 cycles of 95°C for 15 seconds, 60°C for 1 minute). Primer sequences are listed in each chapter. Fold changes were calculated as follows: Delta (D) C_t values were calculated by normalising C_t values for target genes to average C_t values for GAPDH, which was selected as an appropriate housekeeping gene from three others (βactin, B2M, RPS27a, GAPDH primer sequences are given in Table 2.2.3). DDC_t values were then calculated between control conditions and experimental conditions. Fold changes were calculated as $2^{(-DDCt)}$. Statistical analyses were performed using Sigmaplot software. Data were analyzed using Kruskal Wallis One Way Analysis of variance on ranks (with Tukey test for pairwise multiple comparison procedures).

Table 2.2.3 Primer sequence for GAPDH (housekeeping gene for all qPCR)

Gene	**Forward primer sequence (5'-3')**	**Reverse primer sequence (5'-3')**
GAPDH	TGCACCACCAACTGCTTAGC	GGCATGGACTGTGGTCATGAG

2.2.6 Immunocytochemistry

For 2D samples, MSCs were seeded on coverslips in 24-well plates at a density of 10,000 cells per cm^2 in MSC expansion medium and allowed to adhere overnight.

3D MSCs were snap-frozen and sectioned as described in 2.2.3.1. Sections and coverslips were fixed in 4% paraformaldehyde for 10 minutes at room temperature, followed by washing in PBS. Samples were blocked in 10% serum from the animal in which the secondary antibody was raised. For intracellular proteins, blocking sera contained 0.3% Triton X-100. Primary antibody incubations were overnight at 4ºC (in PBS, also containing 0.3% Triton X-100 for intracellular proteins). Samples were then washed 3 times for 5 minutes in 1 x PBS, before incubation with fluorescently-conjugated secondary antibodies for 1 hour at room temperature in the dark. Washing was repeated, before nuclear counterstaining with 4',6-diamidino-2-phenylindole (DAPI). Samples were mounted in Vectashield Mounting Medium for Fluorescence (Vector Labs, Peterborough, UK). Slides were imaged using the LSM510 confocal imaging system (Zeiss). Antibody details are given in each chapter.

Chapter 3: Culture of human MSCs as 3D spheroids

3.1 Introduction

Human MSCs adopt an adherent fibroblastic morphology when seeded as 2D monolayers onto tissue culture plastic, and this morphology is maintained through repeated passage in culture (Pittenger, 1999). As previously discussed, the laboratory at York has developed a number of methods of 3D MSC culture, in which MSCs form spheroids. Up-regulation of transcription factors expressed exclusively by pluripotent cells was observed when 3D MSCs were cultured using the static methyl cellulose-based method (Elen Bray, unpublished observations).

Pluripotency marker expression characterises pluripotent ESCs, which are morphologically and transcriptionally distinct from MSCs. In contrast to the fibroblastic form of MSCs, human ESCs grow as colonies of rounded cells, with a high nuclear:cytoplasmic ratio (Thomson, 1998). This distinct pluripotent morphology is also re-adopted by somatic cells when they undergo factor-based reprogramming to pluripotency (Yu et al., 2007). High nuclear physical plasticity is observed in pluripotent ESCs, and it is thought that this may reflect the requirement for migration of undifferentiated cells through established tissue blocks during embryogenesis *in vivo*. Certainly, nuclear plasticity is associated with the pluripotent state, and nuclear rigidity increases during differentiation. It is thought that the high nuclear envelope flexibility in ESCs can be attributed to its unique composition in pluripotent cells (Pajerowski et al., 2007). Pluripotent cells do not express the nuclear lamina component Lamin A/C. In cultured human ESCs Lamin A/C was first detected after down-regulation of the cell surface markers Tra-1-60, Tra-1-81 and SSEA-4, but before down-regulation of the transcription factor Oct4. However this differed in a mouse *in vivo* model, where Oct4 was down-regulated before detectable expression of Lamin A/C was observed (Constantinescu et al., 2006). Despite differences in the precise timing of Lamin A/C up-regulation, its expression can act as a differentiation marker, and may be required for the differentiation process. Indeed a recent study has demonstrated that Lamin A/C haploinsufficiency or knockdown in mouse ESCs affects differentiation. Whilst there was no observed defects in undifferentiated Lamin $A/C^{+/-}$ ESCs or those expressing a short hairpin

RNA (shRNA) to Lamin A/C, upon differentiation there were defects in the formation of a number of tissues, linking the expression of Lamin A/C to lineage specification during development (Sehgal et al., 2013). In contrast, the nuclear lamina components Lamin B1 and Lamin B2 are expressed in both pluripotent and differentiated cells. It is though that increased nuclear rigidity during differentiation may reflect the establishment of a defined cell fate, without the need for cellular or chromatin plasticity, as nuclear lamina-chromatin interactions are known to regulate gene expression. The absence of Lamin A/C is considered a key requirement for high flexibility in the pluripotent nuclear envelope (Pajerowski et al., 2007).

As described in Chapter 1, ESCs and other pluripotent cells also have a characteristic chromatin organisation, with reduced abundance of heterochromatin markers, and the presence of bivalent domains. It is considered that the nuclear lamina plays a role in the organisation of chromatin, and the determination of chromosome positioning, and through these roles can influence gene expression. In particular, heterochromatin can be linked to the nuclear lamina, and this interaction assists transcriptional repression. Loss of heterochromatin marks is observed in cells with Lamin A/C deficiencies, or those cells which produce mutant truncated forms of the Lamin A/C protein (Dechat et al., 2008).

During the reprogramming to pluripotency of human somatic cells, one of the first observed events is the emergence of ESC-like colonies, which are morphologically distinct from the originating parental population (Yu et al., 2007). The work presented in this chapter will investigate how 3D spheroid size can be regulated by initial cell seeding number and time in culture. It will also examine nuclear morphology, envelope composition and chromatin organisation, to observe any changes, which could act as markers of de-differentiation/reprogramming in 3D MSCs.

3.2 Aims

The general aims of the work presented in this chapter are to investigate how 3D culture affects MSC cellular and nuclear morphology, viability and chromatin organisation, and to observe changes which could indicate de-differentiation towards the pluripotent state.

Specific objectives are to:

- Observe changes in size of 3D MSC with time in culture.
- Assess cellular and nuclear morphology changes of MSCs cultured as 3D spheroids.
- Identify the effects of 3D culture on MSC viability after spheroid disaggregation.
- Determine how nuclear morphology changes may affect chromatin organisation in 3D MSCs.

3.3 Methods

3.3.1 Analysis of 3D spheroid size

3D MSCs were seeded with initiating cell numbers of 30-, 60-, and 120,000 MSCs and cultured as described in section 2.2.1.5. On days 1, 3, 5 and 7 of culture, 6 replicate spheroids for each initial seeding density were imaged using light microscopy and analysed using Image J software to measure spheroid diameters. Briefly, image files were uploaded to Image J, and the diameter of each spheroid was measured. Unit values in Image J were equated to µm (77.364 units = 100µm), which allowed the calculation of spheroid diameters in µm.

3.3.2 Observation of nuclear morphology by TEM

3D spheroids were seeded with initiating cell numbers of 60,000 MSCs and cultured as described in 2.2.1.5 for up to 5 days. On days 1 and 5 of culture, 3D spheroids were fixed and prepared as described in 2.2.4.1 and 2.2.4.2, before imaging using TEM as described in 2.2.4.4.

3.3.3 Quantitative real time polymerase chain reaction

2D MSCs were cultured as described in 2.2.1.3. 3D spheroids were seeded with initiating cell numbers of 30-, 60-, and 120,000 MSCs and cultured for up to 6 days as described in 2.2.1.5. Samples were isolated on days 1,3,4,5 and 6 of 3D culture. RNA was isolated from 2D and 3D samples before cDNA was generated and analysed by qPCR as described in 2.2.5. Primer sequences are shown in Table 3.3.1.

Table 3.3.1 Nuclear lamina genes primer sequences

Gene	Forward primer sequence (5'-3')	Reverse primer sequence (5'-3')
Lamin A/C	GATCAAGCGCCAGAATGGA	CCCAGCCTTCAGGGTGAAC
Lamin B	AAGGCGAAGAAGAGAGGTTGAAG	GCGGRRTGAGAGATGCTAACACT

3.3.4 Immunocytochemistry

2D monolayers were cultured as described in 2.2.1.3. 3D spheroids were seeded with initiating cell numbers of 60,000 MSCs, cultured for 5 days, then snap-frozen and sectioned as described in 2.2.1.5 and 2.2.3.2. 2D and 3D samples were then fixed and stained as described in 2.2.6. Antibody details are given in Table 3.3.2. Samples were imaged using a Zeiss LSM 510 upright confocal microscope.

Table 3.3.2 Nuclear antibodies

Antibody	**Host**	**Dilution**	**Supplier**	**Cat. no.**
Anti-Lamin B1	Goat	1:400	Santa Cruz	sc-6217
Anti-H3K4me3	Rabbit	1:200	Cell Signalling	#9751
Anti-H3K9me3	Rabbit	1:800	Abcam	ab8898
Anti-Goat IgG (Cy3 congugate)	Rabbit	1:400	Sigma	c-2821
Anti-Rabbit IgG (Cy3 congugate)	Sheep	1:400	Sigma	c-2306

3.3.5 Assay of MSC plastic-adherent growth following 3D culture

2D MSCs were cultured to 90% confluence as described in 2.2.1.3 in 35mm dishes. 3D spheroids were seeded with initiating cell numbers of 60,000 MSCs as described in 2.2.1.5. On day 5 of 3D culture 3D spheroids were disaggregated to single cells and then d-3D MSCs were seeded in 35mm culture dishes and cultured as described in 2.2.2.1. At 5, 24 and 48 hours post-disaggregation, d-3D MSC samples were fixed and stained with Crystal Violet as described in 2.2.2.2. All samples were then imaged using light microscopy.

3.4 Results

3.4.1 3D MSC spheroid size is dependent on cell number and decreases with time in culture

MSCs are traditionally cultured as adherent 2D monolayers on tissue culture plastic. However this method of culture means that nutrients are readily available to all cells in the population, and that cells are not susceptible to mechanical cell stress. In order to test the hypothesis that culturing MSCs as 3D spheroids would induce a physiological stress response and stimulate cytoplasmic clearance to a rejuvenated state, it was first necessary to examine the behaviour of MSCs cultured as 3D spheroids. MSCs were removed from 2D culture, seeded as spheroids containing different initiating numbers of cells (30-, 60-, or 120,000 cells per spheroid), and maintained in culture for 7 days. On days 1, 3, 5 and 7 of 3D culture, spheroids were imaged by light microscopy. Initial spheroid size was dependent on cell number, the higher the cell number, the larger the spheroid. 3D spheroids reduced in size with time in culture, with the greatest reduction in size seen between days 1 and 3 of culture (Figure 3.4.1. A). On average, spheroids seeded from 30,000 MSCs reduced in size from 741µm - 438µm diameter over 7 days in culture, and on day 7 the average spheroid diameter was 41% smaller than the average diameter on day 1. Spheroids seeded from 60,000 MSCs reduced in size from 1017µm - 609µm diameter over 7 days in culture, and on day 7 the average spheroid diameter was 40% smaller than the average diameter on day 1. Spheroids seeded from 120,000 MSCs reduced in size from 1474µm - 793µm diameter over 7 days in culture, and on day 7 the average spheroid diameter was 46% smaller than the average diameter on day 1 (Figure 3.4.1. B). Nutrient availability/deprivation in 3D MSCs will be dependent on spheroid size, and this static 3D culture method generates a wide repertoire of spheroid sizes by varying initial seeding number and culture time. This method should therefore have also resulted in varying levels of nutrient deprivation in the different sized spheroids.

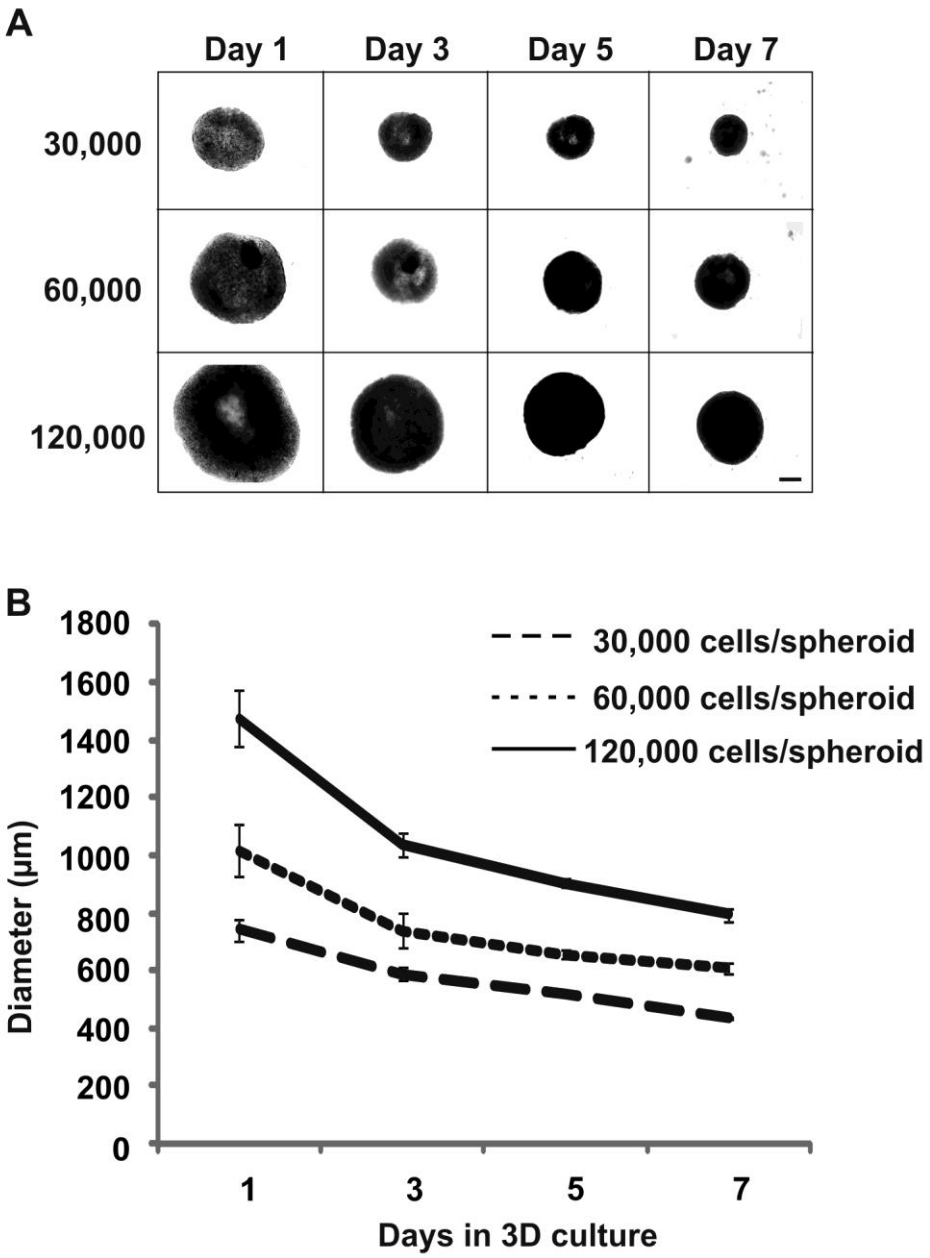

Figure 3.4.1. Analysis of changes in MSC spheroid size over time in 3D culture

MSCs were cultured as 3D spheroids with initiating cell numbers of 30-, 60-, or 120,000 cells for up to 7 days in culture. On days 1, 3, 5 and 7, 3D spheroids were imaged using light microscopy. Images were then subject to analysis using Image J to measure spheroid diameters. A) Example images of 3D MSC spheroids over time in culture. B) Changes in spheroid size with time in 3D culture (mean diameters are shown ± SEM, n = 1, 6 replicates, scale bar = 250µm).

3.4.2 Nuclear morphology and envelope composition changes in MSCs cultured as 3D spheroids

3.4.2.1 Nuclei of MSCs cultured in 3D have a multi-lobed, distorted morphology

In order to examine changes in 3D MSC nuclear morphology, TEM was used to examine sections from 3D MSCs isolated at different times during 3D culture. 2D MSC nuclei had a rounded regular shape, reflecting the fibroblastic morphology of MSCs when cultured as adherent monolayers on tissue culture plastic (Figure 3.4.2, left panel). In contrast, in spheroids initiated from 60,000 cells, 3D MSCs had multi-lobed nuclei, with irregular morphologies, throughout 3D culture (Figure 3.4.2, centre and right panels), possibly suggestive of increased nuclear envelope flexibility in 3D MSCs (Only spheroids initiated from 60,000 MSCs were examined in this way, as this was established as the optimal 3D culture condition for markers of de-differentiation, please see 4.4.1).

3.4.2.2 Reduced expression of the nuclear lamina component Lamin A/C early in 3D culture

The observed changes in nuclear morphology in 3D MSCs may have reflected changes in the composition of the nuclear lamina. Lamin A/C is a nuclear lamina component expressed in most cell types. Only pluripotent cells do not express Lamin A/C, so Lamin A/C expression acts as a marker of non-pluripotent cells. In order to examine the expression of Lamin A/C in 3D MSCs, spheroids initiated from 30-, 60- or 120,000 cells were cultured for up to 6 days. In the two primary MSC donors examined expression of Lamin A/C was initially reduced in 3D culture. mRNA expression of Lamin A/C in all spheroid sizes fell below levels in 2D MSCs on day 1, with expression levels similar across all spheroid sizes. By day 3, mRNA expression of Lamin A/C had started to recover in donor 1, in 30,000 and 60,000 MSCs spheroids, although this recovery occurred slightly later (day 4) in Donor 2. Recovery of Lamin A/C levels towards those observed in 2D MSCs continued with time in 3D culture for both these spheroid sizes; by days 5 and 6 of culture, 3D levels were similar to those in 2D MSCs. In contrast Lamin A/C levels in 120,000 MSC spheroids remained much lower than 2D MSC levels throughout 3D culture (Figure 3.4.3)

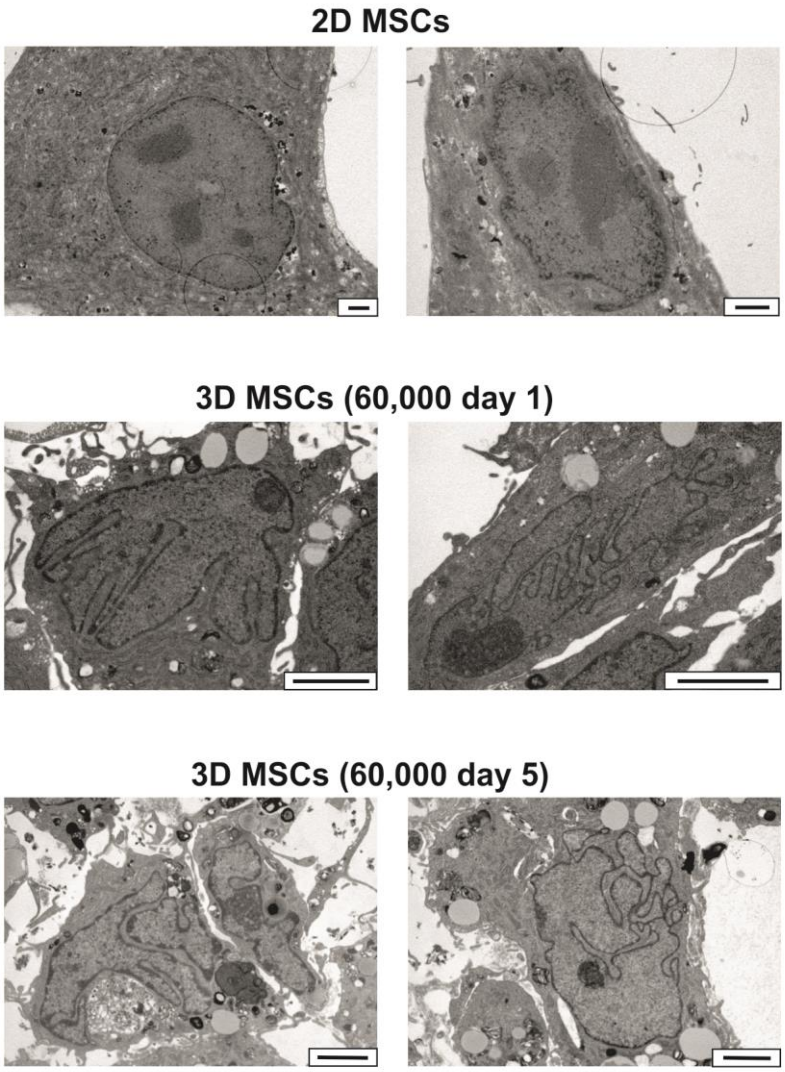

Figure 3.4.2. Analysis of nuclear morphology changes in MSCs cultured as 3D spheroids

MSCs were cultured as 2D monolayers or 3D spheroids with initiating cell numbers of 60,000 cells for up to 5 days in culture. 2D MSCs were cultured on Thermanox coverslips (to allow monolayer sectioning). 3D spheroids were removed from culture at days 1 and 5, and sectioned. Samples were examined by transmission electron microscopy (TEM). Example images of nuclei are shown (scale bars = 2µm)

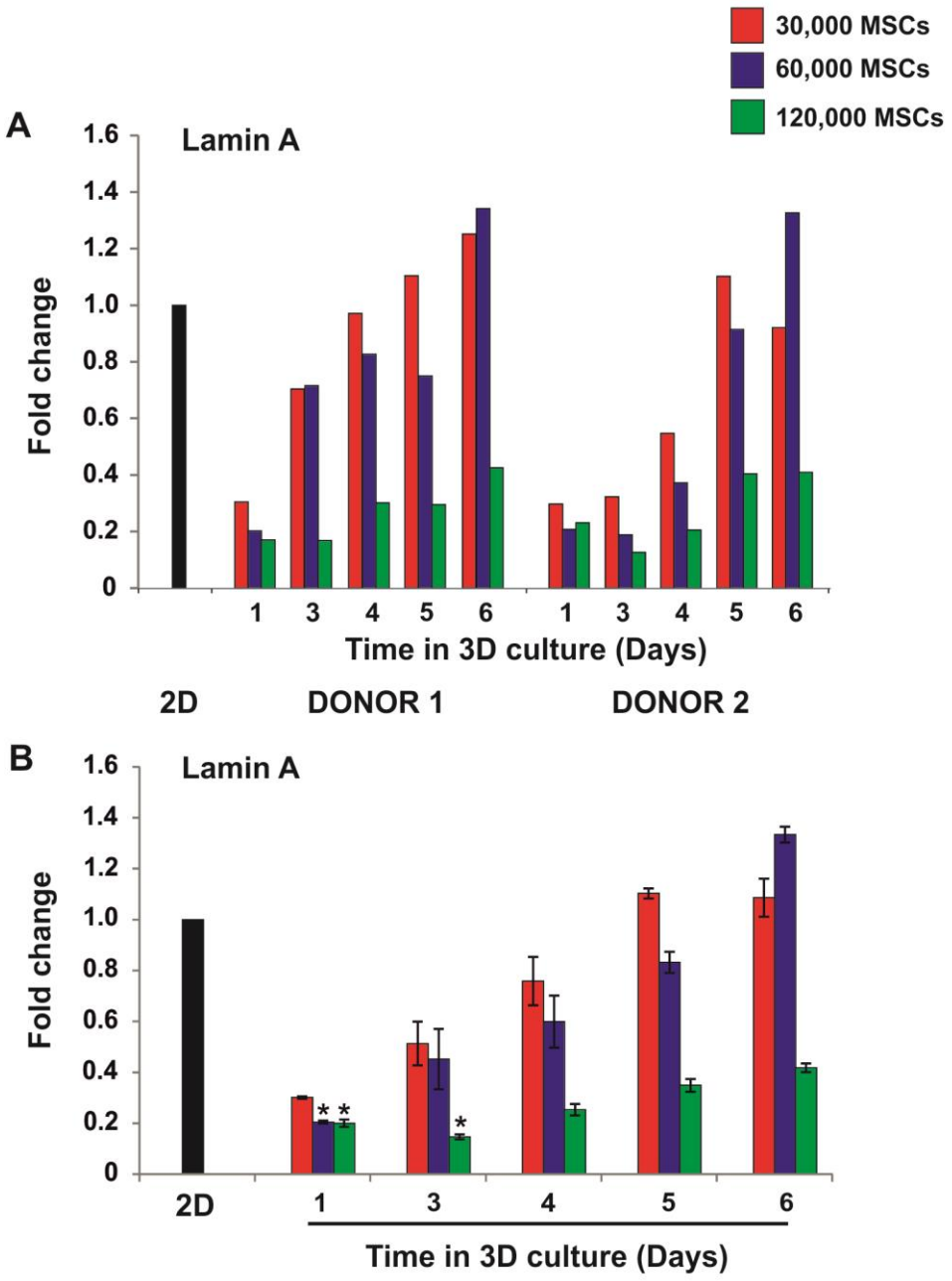

Figure 3.4.3. qPCR analysis of expression of the nuclear lamina component Lamin A in MSCs over time in 3D culture

MSCs from 2 donors were cultured as 2D monolayers and 3D spheroids with initiating cell numbers of 30-, 60-, or 120,000 cells for up to 6 days in culture. cDNA samples were generated and then analysed by qPCR. A) Expression of Lamin A for each donor was normalised to expression of the housekeeping gene GAPDH and made relative to expression levels in the donor matched 2D sample. Fold changes were calculated as 2^{-ddCt}. B) Data from both donors was pooled and subject to statistical analysis, mean fold changes are shown ± SEM, * $p < 0.05$. Statistical significance is relative to expression in 2D MSCs (by Kruskal Wallis test, n = 2).

3.4.2.3 Sustained loss of the nuclear lamina component Lamin B in 3D MSCs

Lamin B is a nuclear lamina component expressed in all cell types. To analyse expression of Lamin B in 3D MSCs, spheroids initiated from 30-, 60-, or 120,000 cells were cultured for up to 6 days. In the two primary MSC donors examined, expression of Lamin B mRNA remained below levels in 2D MSCs throughout 3D culture. In donor 1, expression of Lamin B was variable and low in 60,000 and 120,000 MSC spheroids. This pattern was also observed for donor 2 in spheroids initiated from 120,000 cells, although in this donor, the expression of Lamin B in 60,000 MSC spheroids increased slightly with time in 3D culture, as did expression in 30,000 MSC spheroids. In contrast, an increase in Lamin B expression with time in 3D culture was only observed in donor 1 in spheroids initiated from 30,000 MSCs. Notably, whilst there was a small increase in expression of Lamin B in some samples, the recovery of expression was not comparable to that observed for Lamin A/C, and expression remained well below 2D MSC levels in all 3D samples (Figure 3.4.4).

To examine if reduced Lamin B transcript resulted in a reduction in Lamin B protein, 3D MSC spheroids were initiated from 60,000 cells, as this was established as the optimal 3D culture model for markers of enhanced potency (please see 4.4.1). 3D MSCs were maintained in culture for 5 days, then snap-frozen, sectioned and stained for Lamin B. Immunocytochemistry revealed clear strong Lamin B staining at the nuclear periphery in 2D MSCs. In contrast, there was no detectable Lamin B protein expression in 3D MSCs. Although no Lamin B protein was observed by immunocytochemistry, DAPI counter-staining highlighted the multi-lobed irregular nuclear morphology of 3D MSCs, previously shown by TEM microscopy (Figure 3.4.5).

There was a substantial loss of Lamin B transcript expression within one day of the initiation of spheroid culture. In order to examine how soon MSCs down-regulated expression of Lamin B, spheroids initiated from 60,000 MSCs were cultured for up to 24 hours. At 4 hours and 24 hours after spheroid seeding, samples were isolated and analysed by qPCR for expression of Lamin B. In the two primary MSC donors examined, there was already a prominent reduction in Lamin B expression within 4

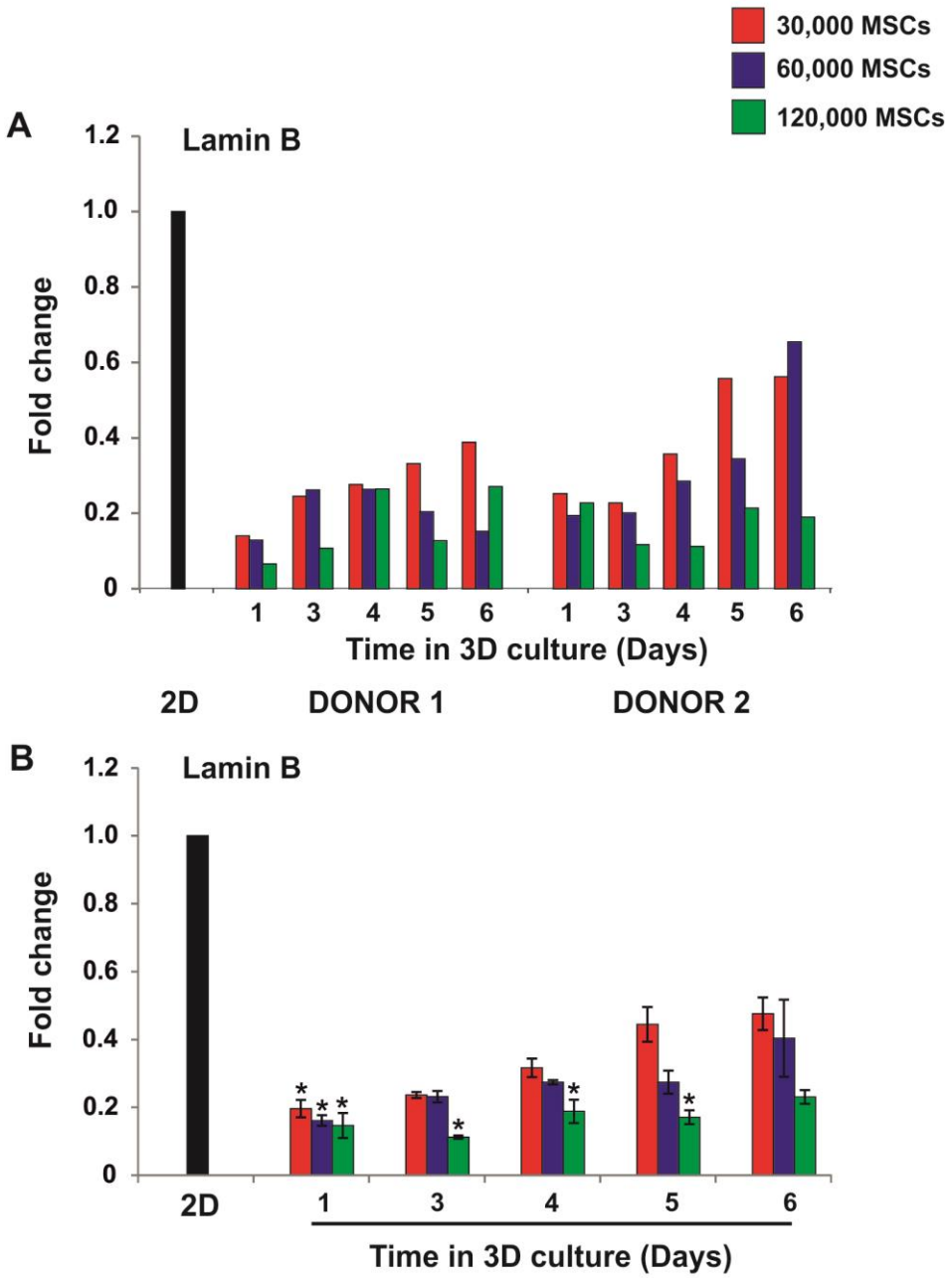

Figure 3.4.4. qPCR analysis of expression of the nuclear lamina component Lamin B in MSCs over time in 3D culture

MSCs from 2 donors were cultured as 2D monolayers and 3D spheroids with initiating cell numbers of 30-, 60-, or 120,000 cells for up to 6 days in culture. cDNA samples were generated and then analysed by qPCR. A) Expression of Lamin B for each donor was normalised to expression of the housekeeping gene GAPDH and made relative to expression levels in the donor matched 2D sample. Fold changes were calculated as 2^{-ddCt}. B) Data from both donors was pooled and subject to statistical analysis, mean fold changes are shown ± SEM, * $p < 0.05$. Statistical significance is relative to expression in 2D MSCs (by Kruskal Wallis test, n = 2).

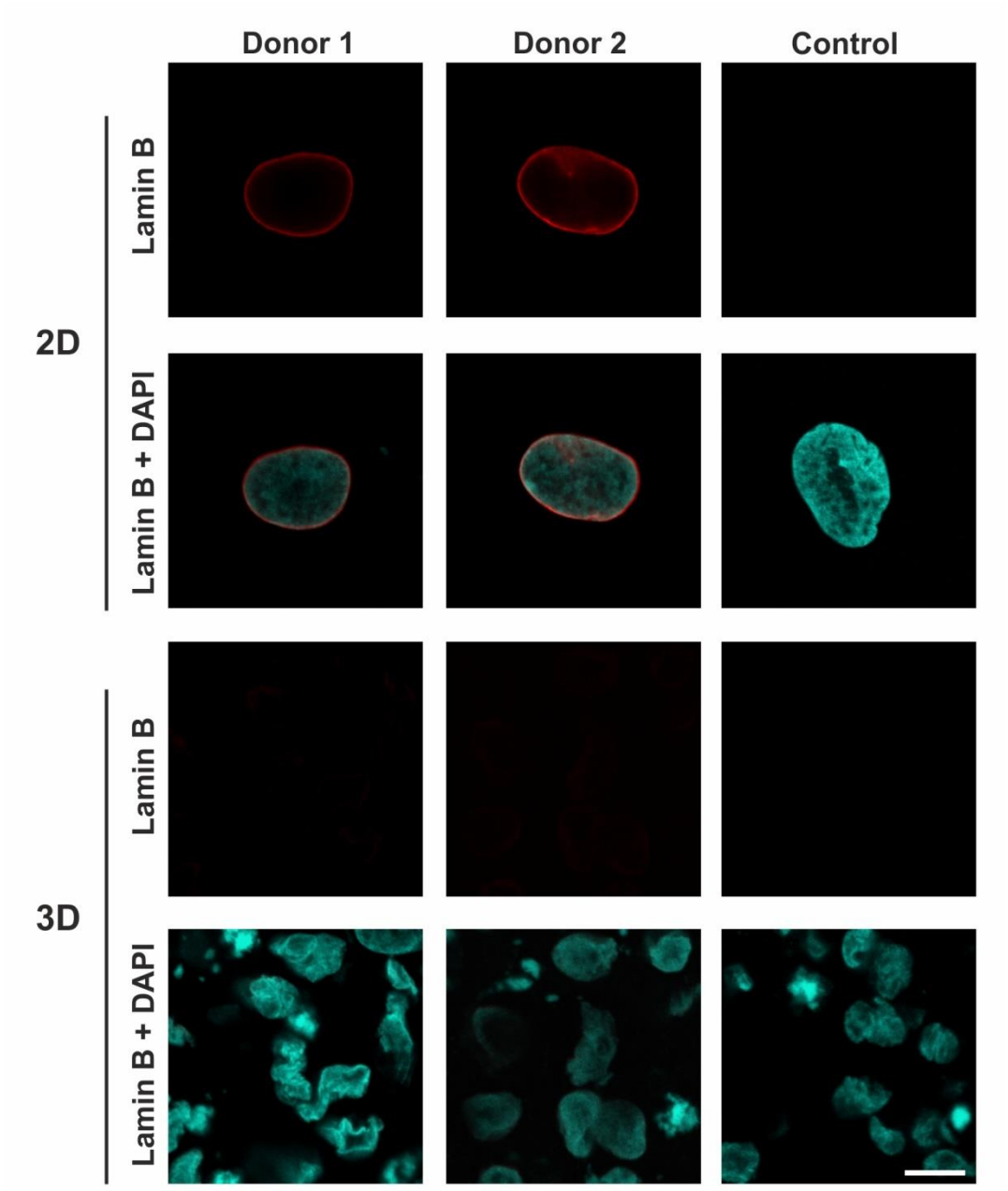

Figure 3.4.5. Staining of 2D MSCs and 3D MSC spheroid sections for the nuclear lamina component Lamin B

2D MSCs were cultured as monolayers on coverslips. 3D spheroids were initiated from 60,000 MSCs and cultured for 5 days. Spheroids were then snap-frozen and sectioned. All samples were fixed and stained for Lamin B (red) and DAPI (cyan), 2º antibody only controls were also performed; these showed no positive red staining. Imaging was performed using confocal microscopy under identical conditions (example images from 2 donors shown, scale bars = 10µm).

hours of spheroid initiation, which continued to decrease up to 24 hours in culture (Figure 3.4.6). Four hours after spheroid initiation, the spheroid structure has only just started to aggregate together, with individual rounded cells remaining visible by light microscopy.

3.4.3 MSCs can be returned to plastic-adherent culture following disaggregation of spheroids

Nuclear lamina composition was altered and nuclei underwent major morphological changes in MSCs cultured as 3D spheroids. To examine if these nuclear structural alterations affected the capacity of 3D MSCs to return to 2D culture conditions, MSCs were cultured as 3D spheroids (initiating cell number = 60,000 MSCs) for 5 days. On day 5 of 3D culture, spheroids were disaggregated to a single cells suspension using enzymatic digestion (d-3D MSCs). The resulting cell suspension was re-seeded onto plastic, and cultured as 2D MSCs. At 5, 24 and 48 hours after re-seeding d-3D MSCs were fixed and stained with crystal violet solution. A sample of the originating 2D MSC population was also stained. 2D MSCs had a typically flat, fibroblastic morphology. At 5 hours after re-seeding, d-3D MSCs were small and rounded, but had adhered to plastic, so remained viable immediately after spheroid disaggregation. 24 hours after seeding, there appeared to be slightly fewer cells remaining, although there was a clear change in morphology, with d-3D MSCs adopting a more fibroblastic morphology. This morphology change continued to 48 hours after re-seeding, where d-3D MSCs had continued to spread into a flatter more typical MSC morphology. At this point there also appeared to be a small increase in cell numbers, suggesting that d-3D MSCs retain proliferative capacity after spheroid disaggregation (Figure 3.4.7).

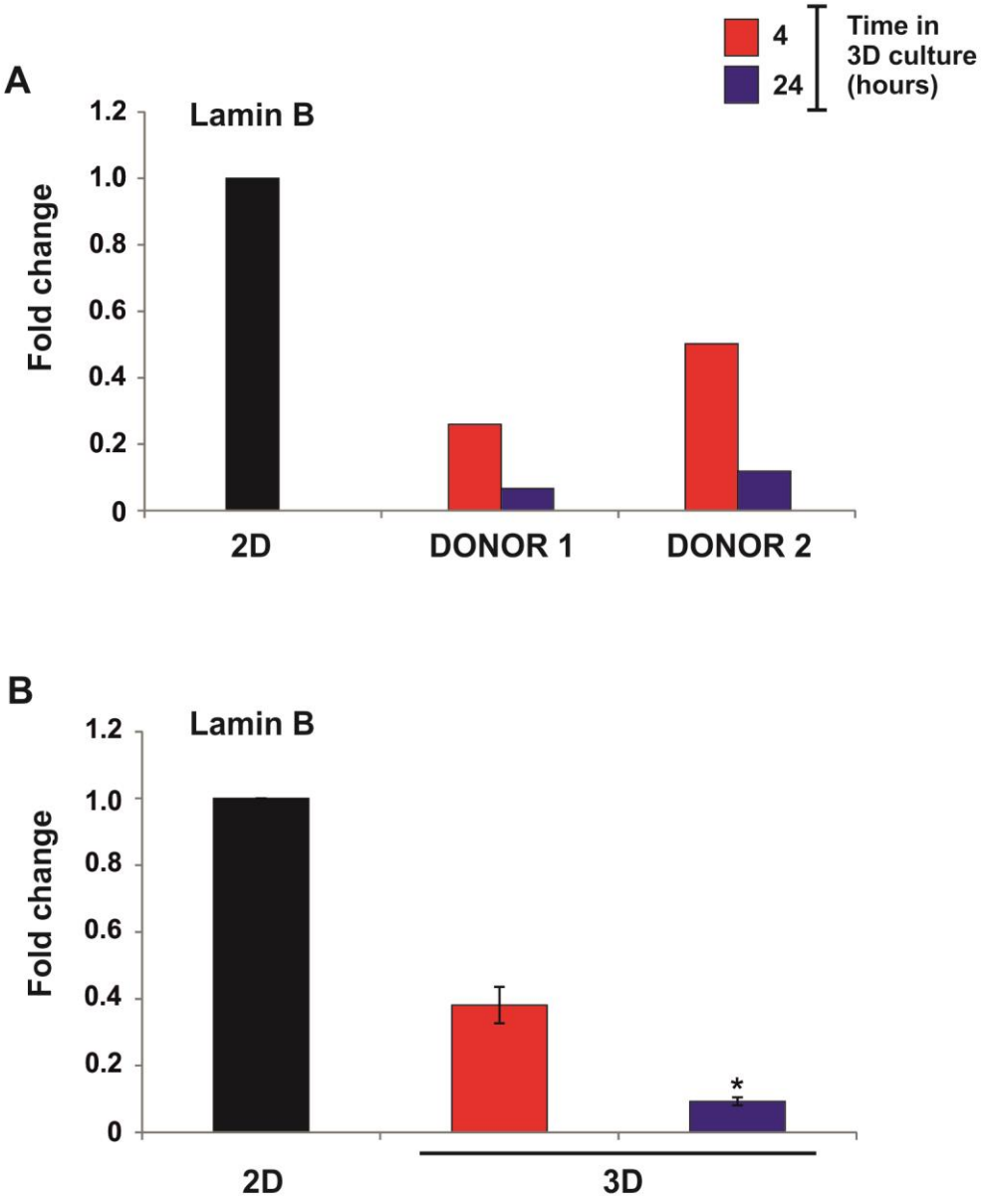

Figure 3.4.6. qPCR analysis of expression of the nuclear lamina component Lamin B in MSCs following 3D spheroid seeding

MSCs from 2 donors were cultured as 2D monolayers and 3D spheroids with initiating cell numbers of 60, 000 cells for up to 24 hours in 3D culture. cDNA samples were generated and then analysed by qPCR. A) Expression of Lamin B for each donor was normalised to expression of the housekeeping gene GAPDH and made relative to expression levels in the donor matched 2D sample. Fold changes were calculated as 2^{-ddCt}. B) Data from both donors was pooled and subject to statistical analysis, mean fold changes are shown ± SEM, * $p< 0.05$. Statistical significance is relative to expression in 2D MSCs (by Kruskal Wallis test, n = 2).

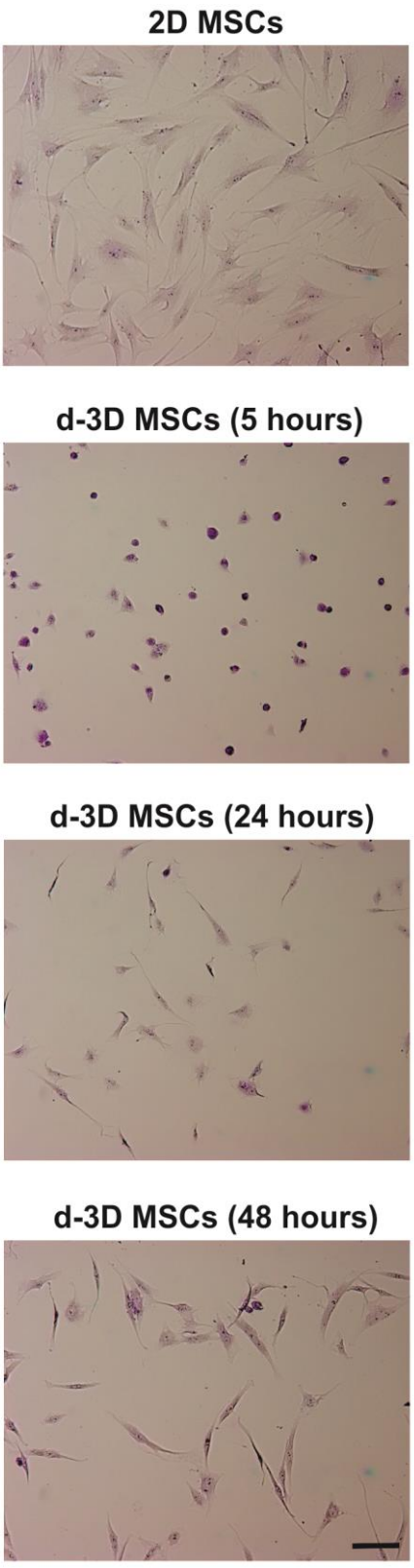

Figure 3.4.7. Analysis of MSC behaviour following disaggregation of 3D spheroids and return to 2D culture

MSCs were cultured as 2D monolayers and 3D spheroids with initiating cell numbers of 60,000 cells for 5 days in culture. On day 5 of 3D culture, 3D spheroids were disaggregated to a single cell suspension (d-3D MSCs) using enzymatic digestion and re-seeded onto tissue culture plastic. Samples were isolated at 5, 24 and 48 hours following spheroid disaggregation. 2D MSC and d-3D MSC samples were fixed and stained with crystal violet staining solution, and then imaged using light microscopy. (Example images shown, scale bar = 100µm).

3.4.4 Reduced staining for the heterochromatin marker H3K9me3 in 3D MSCs

3D MSCs underwent major nuclear morphology changes during 3D culture, but remained viable after spheroid disaggregation. Linking of chromatin to the nuclear lamina can regulate gene expression, so changes in nuclear lamina composition and morphology may lead to changes in chromatin organisation. To examine this, MSC spheroids initiated from 60,000 cells were cultured for 5 days. On day 5, spheroids were snap-frozen, sectioned and stained for histone markers. Euchromatin is permissive to transcription and is marked by the presence of the histone modification H3K4me3 (histone 3 trimethylated at lysine 4). Comparative staining of 2D MSCs and 3D MSC sections showed little difference in H3K4me3 staining, with relatively bright staining seen throughout nuclei of MSCs cultured in both conditions (Figure 3.4.8). A more notable difference was observed when MSCs were stained for H3K9me3 (histone 3 trimethylated at lysine 9). H3K9me3 is a marker of heterochromatin, which has a conformation that is repressive to transcription. Reduction in H3K9me3 has been reported in pluripotent cells. Whilst 2D MSCs stained strongly for H3K9me3, with a typical punctate staining pattern, the staining of 3D MSC sections was much fainter at identical imaging conditions (Figure 3.4.9). This may suggest a reduction in detectable H3K9me3 when MSCs are cultured as 3D spheroids.

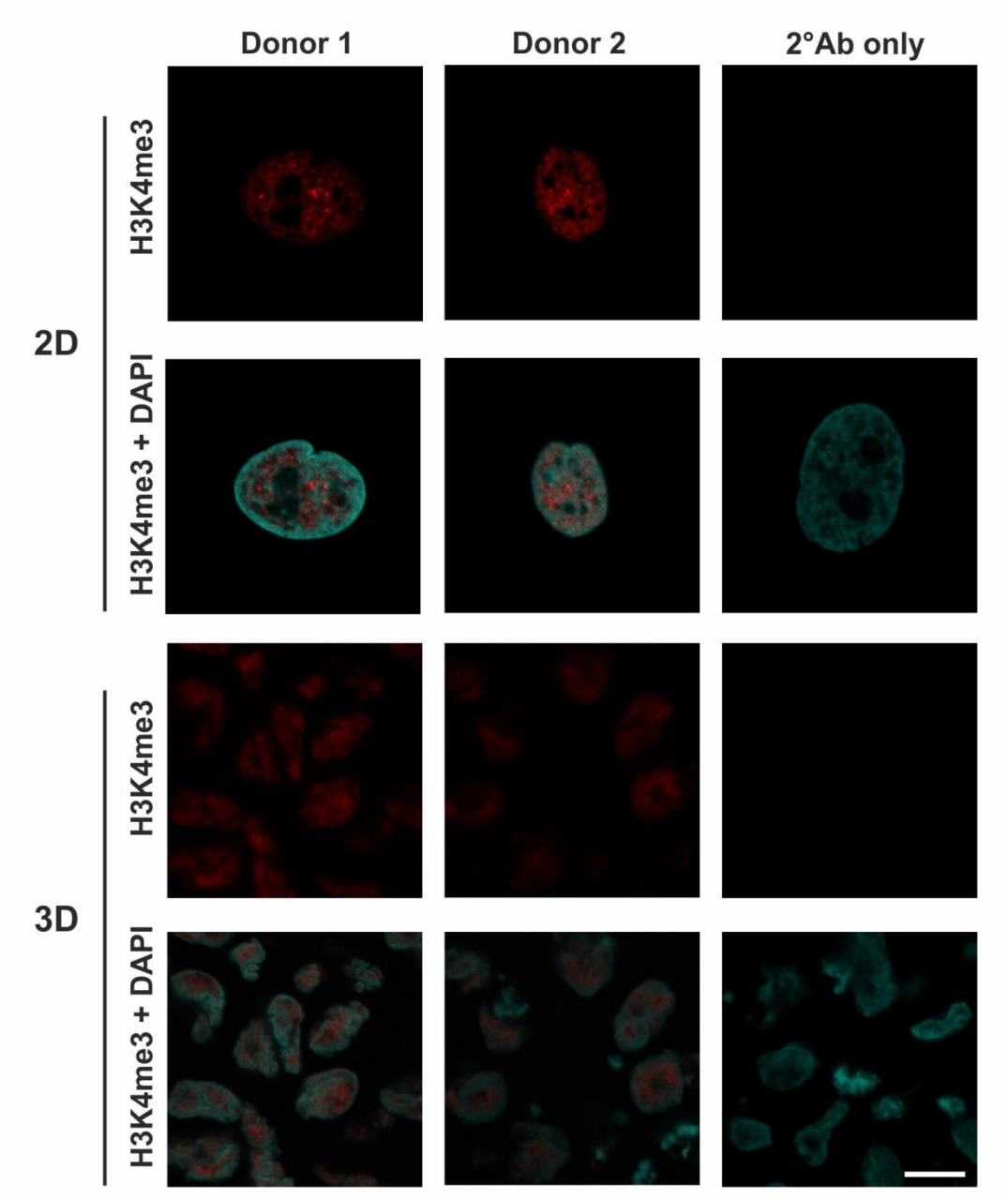

Figure 3.4.8. Staining of 2D MSCs and 3D MSC spheroid sections for the euchromatin marker H3K4me3

2D MSCs were cultured as monolayers on coverslips. 3D spheroids were initiated from 60,000 MSCs and cultured for 5 days. Spheroids were then snap-frozen and sectioned. All samples were fixed and stained for H3K4me3 (red) and DAPI (cyan), 2º antibody only controls were also performed; these showed no positive red staining. Imaging was performed using confocal microscopy under identical conditions (example images from 2 donors shown, scale bars = 10µm).

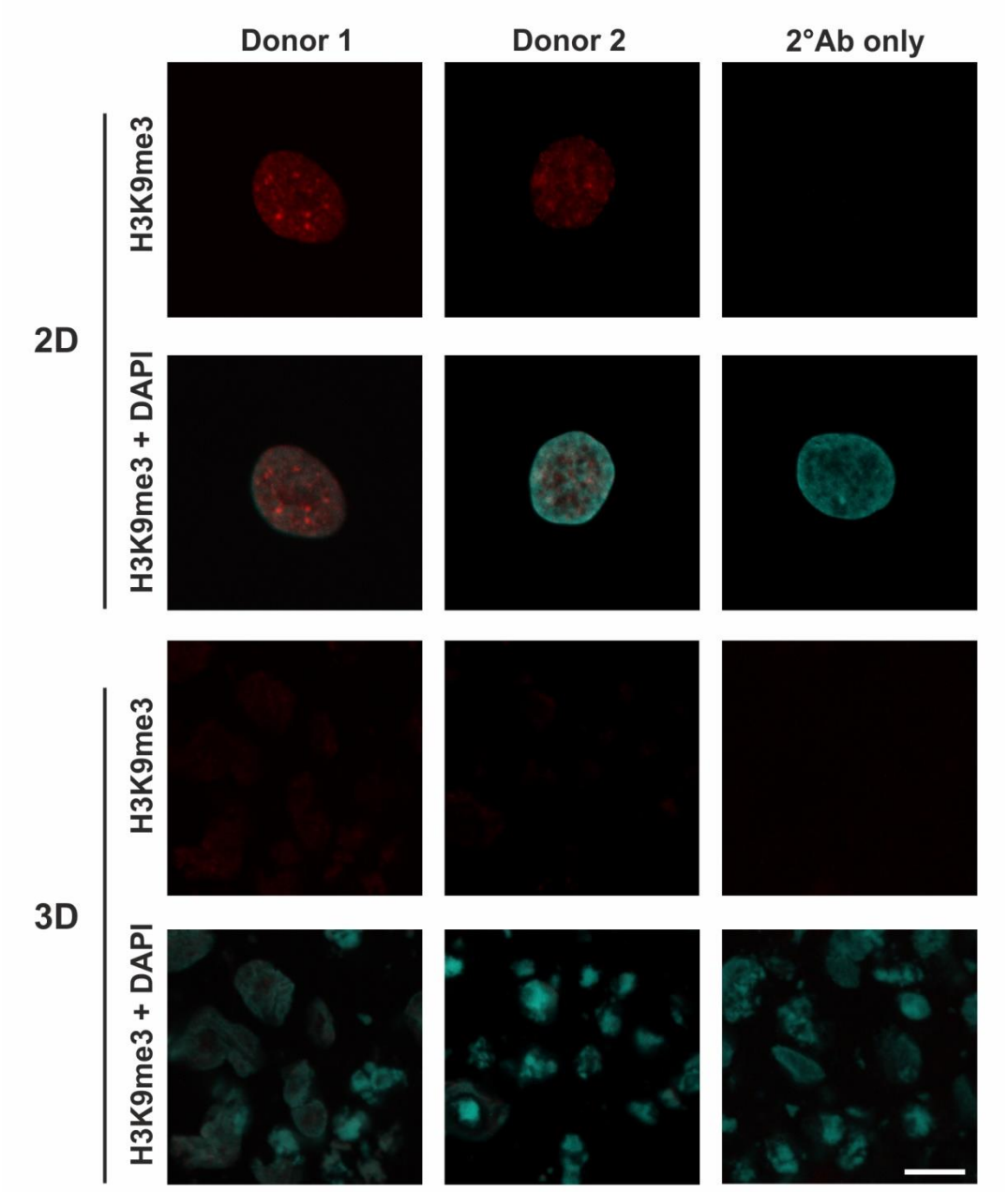

Figure 3.4.9. Staining of 2D MSCs and 3D MSC spheroid sections for the heterochromatin marker H3K9me3

2D MSCs were cultured as monolayers on coverslips. 3D spheroids were initiated from 60,000 MSCs and cultured for 5 days. Spheroids were then snap-frozen and sectioned. All samples were fixed and stained for H3K9me3 (red) and DAPI (cyan), 2º antibody only controls were also performed; these showed no positive red staining. Imaging was performed using confocal microscopy under identical conditions (example images from 2 donors shown, scale bars = 10µm).

3.5 Discussion

MSCs are traditionally cultured as monolayers on tissue culture plastic. In these conditions nutrients and oxygen are readily available, and sufficient space for cell growth is maintained through repeated passaging in culture. In contrast, when MSCs are cultured as 3D spheroids, they are subject to mechanical forces and enhanced cell-cell contacts by growing as a cell aggregate. As well as this, there will be a gradient of nutrient availability across the spheroid structure. Previous work in this laboratory demonstrated that 3D MSCs do not express the proliferation marker Ki67 whilst in 3D culture, so appeared to have adopted a quiescent state, and MSC spheroids did not increase in size with time in culture (Elen Bray, unpublished results). It was demonstrated here that MSC spheroid size is understandably dependent on initial cell seeding density, with more cells resulting in a bigger spheroid. Furthermore, MSC spheroids reduced in size over time in 3D culture, with between 40 – 46% reductions in spheroid diameter over 7 days. This change in size with time in culture meant that not only would MSCs in 3D be exposed to nutrient gradients, but that these gradients would vary, as spheroid size changed with time in culture. Consequently, this screen, varying both initial cell number and time in culture, generated a large repertoire of spheroid sizes, which I hypothesised would induce varying degrees of cell stress due to nutrient deprivation. Although MSCs in 3D culture would be experiencing varying nutrient availability across the spheroid structure, there was no evidence to suggest that spheroids had a necrotic core caused by nutrient deprivation. Spheroids generated from 60,000 MSCs cultured for 5 days were not cystic, samples for both TEM and immunocytochemistry consisted of complete sections with no obvious internal cyst, which would have suggested a necrotic core. Lack of cell death in the centre of spheroids suggested that the magnitude of stress imposed on MSCs by 3D culture was sub-lethal.

Using TEM microscopy, it was revealed that nuclei in 3D MSCs had undergone major morphological changes. Whilst the nuclei of 2D MSCs were regular and rounded, nuclei observed in 3D MSCs were multi-lobed and irregular in shape. This distorted nuclear morphology was observed throughout 3D culture in 60,000 MSC spheroids. 3D MSCs showed a prominent reduction of Lamin A/C transcript early in 3D culture, however in both 30-, and 60,000 MSC spheroids, levels of Lamin A/C

transcript increased with time in 3D culture. By day 5/6, levels had returned to those observed in 2D MSCs. Very low level/absence of Lamin A/C expression can act as a marker of pluripotency (Constantinescu et al., 2006). However, Lamin A/C down-regulation was transient in 3D MSCs, so did not indicate a sustained shift to a pluripotent state. Given that reprogramming somatic cells to a reprogrammed state occurs over a period of days to weeks, rather than hours, it is also unlikely that very low levels of Lamin A/C early in 3D culture represented a transient passage through a pluripotent state. Early loss of Lamin A/C is more likely to reflect the major structural alterations MSCs undergo on entry to 3D culture, and reduced Lamin A/C in our model may allow for increased nuclear envelope flexibility early in 3D culture. Absence of Lamin A/C is considered an important factor in the high level of flexibility of the pluripotent nuclear envelope (Pajerowski et al., 2007).

In contrast there was sustained down-regulation of the expression of Lamin B, another nuclear lamina component, during 3D culture. Lamin B transcript was significantly down-regulated, and Lamin B protein was undetectable by immunocytochemistry in 3D MSCs. Recently, loss of Lamin B has been identified as a both a biomarker (Dreesen et al., 2013; Freund et al., 2012; Shimi et al., 2011) and a trigger (Shimi et al., 2011) of cellular senescence. However these findings have proved contradictory, as another study demonstrated that in mutant mice with skin keratinocyte knockouts for both Lamin B1 and Lamin B2, the cells proliferated normally, and the skin and hair development in knockout mice was equivalent to wild type (Yang et al., 2011). So the absence of Lamin B does not affect cellular proliferation or trigger senescence in some cell types. Indeed it was demonstrated in mouse ESCs that both Lamins B1 and B2 are dispensable for self-renewal and pluripotency. ESCs maintained normal marker expression, colony morphology, and karyotype even in the absence of any Lamin B proteins. The nuclear envelopes of $Lmnb1^{-/-}$ $Lmnb2^{-/-}$ ESCs were also normal and indistinguishable from wild type ESCs (Kim et al., 2011). As previously mentioned, ESCs do not express Lamin A/C, so pluripotent cells can maintain self-renewal and pluripotency in the absence of any Lamins. It was demonstrated here that within 4 hours of spheroid seeding, Lamin B transcript levels had fallen substantially. It is unlikely that transfer to 3D culture had triggered such an immediate onset of senescence. Furthermore it was possible to disaggregate MSC spheroids to a single cell suspension (d-3D MSCs) which could

be re-seeded on tissue culture plastic. Five hours after re-seeding, d-3D MSCs appeared as small rounded cells, which maintained plastic adherence. After 24 hours there was a small reduction in adherent MSCs, indicating that some cells were unable to survive the disaggregation process. However the remaining cells had begun to adopt a more typical MSC fibroblast-like morphology. This morphology change continued to 48 hours, and by this point there appeared to be a small increase in cell numbers, indicating that d-3D MSCs retained proliferative capacity. Taken together these results indicate that down-regulation of Lamin B in our 3D model does not mark or trigger the onset of cellar senescence. Rather 3D MSCs are quiescent, and retain their ability to proliferate when re-seeded onto plastic. In 3D MSCs, down-regulation of both nuclear lamina components early in 3D culture may provide increased nuclear envelope flexibility and permit the major structural changes which are initiated by removal from plastic and seeding in 3D culture.

Whilst nuclear envelope morphology and composition in MSCs had been changed by 3D culture, there was no evidence from these changes to suggest that 3D MSCs had undergone de-differentiation or reprogramming towards pluripotency. However, as previously discussed, pluripotent cells have a distinct chromatin state, characterised by an increase in histone modifications which mark euchromatin, and a decrease in histone markers of repressive heterochromatin, which can also be used to track reprogramming to pluripotency. Immunocytochemistry was used to analyse the expression of two different histone modifications, H3K4me3 (a euchromatin marker) and H3K9me3 (a heterochromatin marker which is expressed at low levels in pluripotent cells). There was little detectable difference in H3K4me3 staining between 2D and 3D MSCs. Relatively strong staining was observed throughout nuclei of both 2D and 3D MSCs, indicative of transcriptionally permissive genome regions in both conditions. There was a greater difference observed when staining for H3K9me3. Whilst 2D MSCs showed relatively strong nuclear staining, this was much fainter in 3D MSCs, which could indicate changes in abundance or organisation of the H3K9me3 modification. 2D MSCs showed a staining pattern typical of a more differentiated cell type, with H3K9me3 foci (observed by strong punctate staining) marking repressed genomic regions. Low levels of global H3K9me3 are observed in pluripotent ESCs, and they lack the distinct H3K9me3 foci observed in more differentiated cells. Rather, H3K9me3 staining appears in a

more diffuse pattern, which is suggested to indicate a less organised, more dynamic chromatin organisation. It is proposed that as differentiation progresses and genes become modified by repressive histone marks, chromatin becomes organised into distinct genomic regions, marked by the presence of H3K9me3 foci (Meshorer et al., 2006). Although immunocytochemistry suggested a reduction in H3K9me3 levels in 3D MSCs, the staining pattern was dissimilar to that generally observed in pluripotent cells. The data presented here is therefore not sufficient to confirm wide scale chromatin alterations in 3D MSCs. Further quantitative analysis, and gene targeted approaches may provide evidence for significant chromatin remodelling which has been driven by transfer to 3D culture.

In conclusion, the work presented in this chapter demonstrates that MSCs can be cultured in a self-assembling 3D structure, known as a spheroid. 3D spheroid size is dependent on initiating seeding number of cells, and reduces with time in culture, indicating that MSCs do not proliferate in 3D. 3D MSCs undergo nuclear structural changes, including alterations to the composition of the nuclear lamina, and may also have reduced abundance/altered distribution of H3K9me3, a histone modification associated with heterochromatin. It is possible that altered distribution may be due to the nuclear morphology and lamina composition changes already described, as the nuclear lamina is known to interact with and regulate heterochromatin organisation within the nucleus (Dechat et al., 2008). Loss of Lamin B can be a marker of senescence onset, although in our 3D system, MSCs down-regulate Lamin B expression, whilst maintaining viability and proliferative capacity. It was noted in one study that Lamin B1 depletion in fibroblasts resulted in reduced proliferation, but not in increased cellular senescence. Strikingly in Lamin B1-depleted fibroblasts, senescence associated biomarkers were only observed when cells were exposed to cell stress by culture at low seeding density (Dreesen et al., 2013). When considered in the light of these findings, the results presented here could highlight Lamin B reduction as a marker of the onset of cell stress, which if not countered by pro-survival mechanisms, would lead to senescence and apoptotic cell death. However if cell stress remained at a sub-lethal rather than lethal level, cells may be able to overcome the onset of stress-induced cell death by triggering survival mechanisms. This could also explain why Lamin B expression appeared to stabilise or rise slightly with time in 3D culture. During 3D culture, MSC spheroids reduce in size, possibly

by recycling of cytoplasmic contents via a pro-survival response stimulated by cell stress. Taken together, the work presented in this chapter demonstrates that 3D MSCs undergo some changes to nuclear morphology, envelope composition and chromatin organisation, but none of these changes provide conclusive evidence of de-differentiation or reprogramming towards pluripotency. Work presented in the later chapters of this thesis will analyse 3D MSCs further, to investigate markers of de-differentiation, and look for evidence of autophagy as the mechanism driving this process.

Chapter 4: Assessment of the potency of MSCs cultured as 3D spheroids

4.1 Introduction

As previously described, a complex network of transcription factors and chromatin remodelling complexes, work together to maintain ESCs in an undifferentiated, self-renewing state (Boyer et al., 2005). Factors involved in pluripotency regulation are also amongst those capable of inducing reprogramming of fibroblasts to the pluripotent state (Takahashi et al., 2007; Takahashi and Yamanaka, 2006; Yu et al., 2007). Reprogramming cocktails, including the oncogene c-Myc, can result in the occurrence of tumours, at relatively high frequency, in offspring produced by blastocyst injection of iPSCs (Okita et al., 2007). However, whilst c-Myc is dispensable for reprogramming of both mouse and human fibroblasts, the efficiency of iPSC generation is much lower in the absence of c-Myc (Nakagawa et al., 2008; Wernig et al., 2008). Whilst some groups have explored the use of small molecules which regulate chromatin organisation and cell signalling, others have attempted to identify optimal cell types for reprogramming to pluripotency. Although the expression of reprogramming factors in fibroblasts is undetectable/extremely low, neural stem cells (NSCs) already express c-Myc, Klf4 and Sox2 at levels equivalent to those in pluripotent stem cells, making them ideal candidates for reprogramming to pluripotency (Kim et al., 2008). Endogenous expression of these genes means that it is possible to reprogramme NSCs using fewer exogenous factors. It was possible to generate iPSCs from mouse NSCs using just two factors, Oct4 in combination with either c-Myc (OM) or Klf4 (OK). Sox2 was dispensable for reprogramming of NSCs, most likely because endogenous expression of Sox2 was around 2-fold higher than expression in mouse ESCs. Both OM- and OK-derived iPSCs had similar endogenous expression of ESC markers to mouse ESCs. Furthermore, the pluripotency of both was confirmed by teratoma formation. As previously described, c-Myc can enhance tumourigenesis in offspring, so OK-derived iPSCs were selected for further analysis. They were capable of chimera contribution, and similar to three factor-derived iPSCs (without c-Myc), showed no tumour formation in early stage F1 progeny (Kim et al., 2008). One year later, the same group demonstrated the generation of iPSCs from mouse NSCs with a single factor, Oct4. One factor-derived

iPSCs had highly similar gene expression profiles to ESCs, and were pluripotent, evidenced by *in vitro* differentiation studies, teratoma formation and chimera contribution (Kim et al., 2009b). Following on from the work in mice, this group next demonstrated that human fetal NSCs can also be reprogrammed to pluripotency by both two-factor (OK) reprogramming and by Oct4 (O) alone. Global gene expression profiling revealed that both OK- and O-derived iPSCs clustered closely with human ESC lines, and separate from parental NSCs. Pluripotency of OK- and O-derived iPSCs was confirmed *in vitro* and *in vivo* (Kim et al., 2009a). The work of Kim and colleagues highlighted the possibilities of using fewer factors for reprogramming to pluripotency, by utilising cell types which already express some of the factors required for this process. Whilst this represented a major technological advance, the accessibility of human NSCs means that they are not the most viable option for use in cell-based therapies. Dermal papilla cells are cells of mesenchymal origin located in the hair follicle, which can be isolated with relative ease. Similar to NSCs, these cells also express endogenous Klf4, c-Myc and Sox2. It was possible to reprogramme mouse dermal papilla cells to pluripotency using two factor OK and single factor O reprogramming. iPSCs derived from both OK and O reprogramming of dermal papilla cells are pluripotent, evidenced by teratoma formation and germline contribution (Tsai et al., 2011; Tsai et al., 2010). Notably, Oct4 alone was also sufficient to reprogramme human adult keratinocytes to pluripotency, when used in combination with a small molecule cocktail. Keratinocytes are also accessible cells isolated from the skin or hair follicle, and endogenously express Klf4 and c-Myc. When infected with exogenous Oct4, and exposed to a cocktail of small molecules regulating cell signalling pathways, chromatin organisation and metabolism, iPSCs colonies were generated. These cells expressed endogenous pluripotency factors, and had an ESC-like DNA methylation profile. Furthermore, they were capable of embryoid body and teratoma formation, evidence of their pluripotential (Zhu et al., 2010). These studies demonstrate that it is possible to apply the principles of fewer-factor reprogramming to a more accessible cell type, which may improve the clinical relevance of iPSC technology. It has also recently been demonstrated that the same type of factor-based approach can be used for direct differentiation – the differentiation of one somatic cell type to another, by exogenous expression of relevant transcription factors, so the principles of factor-based reprogramming can also be applied when a transition to full pluripotency is not

desired or required (Huang et al., 2011; Ieda et al., 2010; Szabo et al., 2010; Vierbuchen et al., 2010).

The work presented in this chapter will investigate optimal 3D culture conditions for the induction of de-differentiation towards pluripotency in human MSCs, through assays and marker analysis commonly used to confirm pluripotency in human cells. It will also examine the suitability of MSCs 'primed' by optimal 3D culture, for traditional factor-based reprogramming techniques. Finally it will seek to examine the extent of de-differentiation driven by optimal 3D culture conditions, and identify markers to confirm the developmental position of MSCs cultured in 3D.

4.2 Aims

The aims of the work presented in this chapter are to assess the extent to which 3D culture is driving de-differentiation of MSCs, to examine the effects of 3D culture on the efficiency of factor-based reprogramming in human MSCs, and to use marker expression to establish the developmental position of 3D MSCs.

More specifically, the objectives are to:

- Determine the effects of 3D culture on the expression of pluripotency-related factors in MSCs
- Assess 3D MSC pluripotency by *in vivo* teratoma assays
- Identify expression of reprogramming factors in MSCs and other cell types used in factor-based reprogramming to pluripotency
- Derive iPSCs by factor-based methods from both 2D and 3D MSCs to allow comparison of the efficiency of iPSC derivation
- Establish suspension culture methods for 3D MSCs, aimed at maintaining pluripotency factor expression and stimulating proliferation
- Assess the expression of known early mesoderm markers during 3D culture
- Examine mesodermal potency of MSCs *in vitro* and *in vivo*
- Investigate the effects of 3D culture on culture-aged senescent MSCs

4.3 Methods

4.3.1 Quantitative real time polymerase chain reaction (qPCR)

2D MSCs were cultured as described in 2.2.1.3. 3D spheroids were seeded with initiating cell numbers of 30-, 60-, and 120,000 MSCs and cultured for up to 6 days as described in 2.2.1.5. Samples were isolated for RNA extraction on days 1,3,4,5 and 6 of 3D culture. For qPCR using disaggregated 3D MSCs (d-3D MSCs, re-plated on plastic), 3D spheroids were initiated from 60,000 MSCs, and maintained in culture for 5 days as described in 2.2.1.5. On day 5, 3D MSCs were disaggregated to single cells and re-seeded onto tissue culture plastic as described in 2.2.2.1. d-3D MSCs were maintained as described for 2D MSCs in 2.2.1.3, and samples were isolated at 5, 24 and 48 hours after re-seeding. HDF monolayers were cultured as described in 2.2.1.4, and samples were analysed at 90% confluence. H9 human ESCs were cultured as described in 2.2.1.6. For early mesoderm markers 3D spheroids were seeded with 60,000 MSCs and cultured for up to 5 days as described in 2.2.1.5. Samples were isolated for RNA extraction on days 1, 3, and 5 of 3D culture. RNA was extracted from all 2D, 3D and d-3D samples before cDNA was generated and analysed by qPCR as described in 2.2.5. Primer sequences are shown in Table 4.3.1. For comparison of expression levels in MSCs versus ESCs (Figure 4.4.10), following calculation of $2^{(-DDCt)}$, fold changes were then converted to positive and negative numbers using the formula: IF(X>=1,(X),(-1/X)), where $X = 2^{(-DDCt)}$, in order to more easily visualise expression differences in the different samples.

Table 4.3.1 Pluripotency and reprogramming factor primer sequences

Gene	Forward primer sequence (5'-3')	Reverse primer sequence (5'-3')
Oct4	CCCACACTGCAGCAGATCAG	CACACTCGGACCACATCCTTCT
Nanog	CCTCCATGGATCTGCTTATTCAG	TGCGACACTATTCTCTGCAGAAG
Sox2	GAGAACCCCAAGATGCACAAC	CGCTTAGCCTCGTCGATGA
Telomerase	CATTTTTCCTGCGCGTCAT	GCGTTCTTGGCTTTCAGGAT
Klf4	CGCCACCCACACTTGTGAT	GTGCCTTGAGATGGGAACTCTT
c-Myc	CGTCTCCACACATCAGCACAA	TCTTGGCAGCAGGATAGTCCTT
Brachyury	GGGTCCACAGCGCATGAT	TGATAAGCAGTCACCGCTATGAA
Goosecoid	GATGCTGCCCTACATGAACGT	GACAGTGCAGCTGGTTGAGAAG
KDR	TGATGCCAGCAAATGGGAAT	CCACGCGCCAAGAGGCTTA
MIXL1	AAGCCCCAGCTGCCTGTT	CCCTCCAACCCCGTTTG
CXCR4	CGCCTGTTGGCTGCCTTA	ACCCTTGCTTGATGATTTCCA

4.3.2 Immunocytochemistry

3D spheroids were seeded with initiating cell numbers of 60,000 MSCs, cultured for 5 days, then snap-frozen and sectioned as described in 2.2.1.5 and 2.2.3. 3D samples were then fixed and stained as described in 2.2.6. Antibody details are given in Table 4.3.2. Samples were imaged using a Zen 510 upright confocal microscope.

Table 4.3.2 Antibodies used in immunocytochemistry

Antibody	Host	Dilution	Supplier	Cat. no.
Anti-Oct4A	Rabbit	1:100	Cell Signalling	#2840
Anti-Nanog	Rabbit	1:40	Cell Signalling	#3580
Anti-Brachyury	Goat	1:15	R and D Systems	AF2085
Anti-KDR	Mouse	1:25	R and D Systems	MAB3571
Anti-CXCR4	Rabbit	1:100	Chemicon (Millipore)	AB1846
Anti-Rabbit IgG (Alexa 594 conjugate)	Rabbit	1:500	Life Technologies	A-11012
Anti-Goat IgG (Cy3 congugate)	Rabbit	1:400	Sigma	c-2821
Anti-Rabbit IgG (Cy3 congugate)	Sheep	1:400	Sigma	c-2306
Anti-Mouse IgG (Alexa488 congugate)	Goat	1:500	Life Technologies	A-11001

4.3.3 Flow cytometry

2D MSCs were cultured as described in 2.2.1.3. 3D spheroids were seeded with initiating cell numbers of 60,000 MSCs and cultured for 5 days as described in 2.2.1.5. 2102Ep embryonal carcinoma cells were cultured as described in 2.2.1.7. 2D MSCs and 2102Ep cells were harvested by trypsinisation as described in 2.2.1.3. 3D MSCs were disaggregated to single cells (d-3D MSCs) as described in 2.2.2.1, and pipetted through a 25 gauge needle to remove any residual cell clumps. To enable intracellular staining, all samples were fixed in 4% PFA for 10 minutes at room temperature. Samples were chilled for 1 minute, and then permeabilised by incubation in 90% methanol for 30 minutes on ice. Samples were then washed twice in incubation buffer (0.5% BSA in PBS), before 10 minutes blocking in incubation buffer at room temperature. Samples were incubated on ice with primary antibodies for 45 minutes. See Table 4.3.3 for antibody details. Samples were then washed in

incubation buffer followed by centrifugation, before incubation on ice in the dark with secondary antibodies for 45 minutes. Finally, samples were washed with incubation buffer, and re-suspended in 500µl incubation buffer before being analysed on a Beckman Coulter CyAn ADP analyser. Secondary antibody only controls were also performed for all samples.

Table 4.3.3 Antibodies for flow cytometry

Antibody	Host	Dilution	Supplier	Cat. no.
Anti-Oct4A	Rabbit	1:100	Cell Signalling	#2840
Anti-Nanog	Rabbit	1:100	Cell Signalling	#3580
Anti-Sox2	Rabbit	1:100	Cell Signalling	#3579
Anti-Rabbit IgG (Alexa 488 conjugate)	Rabbit	1:200	Life Technologies	A-11034

4.3.4 Teratoma assay

For the teratoma assay, 2D MSCs were cultured as described in 2.2.1.3. 3D spheroids were seeded with initiating cell numbers of 60,000 MSCs and cultured for 5 days as described in 2.2.1.5. The assay was performed by Reinnervate Ltd, who cultured and prepared mouse ESC controls prior to implantation. All work was carried out in accordance with ethical guidelines under the Home Office project licence of Reinnervate Ltd. 2D MSCs and mouse ESCs were trypsinised, and counted before $5x10^5$ cells were injected. 50 MSC spheroids were injected for 3D samples. Injections were performed subcutaneously on adult male nude mice. After 12 weeks, mice were sacrificed, and samples were immediately dissected and fixed, before sectioning on a Leica RM2165 rotary microtome at 5µm. Sections were oven dried at 40ºC prior to histological staining with haematoxylin and eosin and Massons Trichrome.

4.3.4.1 Haematoxylin and eosin staining

After sectioning samples were stained as described in Table 4.3.4. Samples were then mounted in DPX mounting media.

Table 4.3.4 Haematoxylin and eosin staining of tissue sections

Procedure/Reagent	**Time**
Histoclear	5 minutes
Absolute alcohol	2 minutes
95% alcohol	1 minutes
70% alcohol	1 minutes
Distilled Water	1 minutes
Mayers Haematoxylin	5 minutes
Distilled water	30 seconds
Alkaline Alcohol	30 seconds
70% Alcohol	30 seconds
95% Alcohol	30 seconds
Eosin	30 seconds
95% Alcohol	10 seconds
95% Alcohol	10 seconds
Absolute Alcohol	15 seconds
Absolute Alcohol	30 Seconds
Histoclear	3 minutes
Histoclear	3 minutes

4.3.4.2 Massons Trichrome staining

After sectioning samples were stained as described in Table 4.3.5. Samples were then mounted in DPX mounting media.

Table 4.3.5 Massons Trichrome staining of tissue sections

Procedure/Reagent	**Time**
Histoclear	5 minutes
Rehydrate: 100% ethanol	2 minutes
95% ethanol	1 minutes
70% ethanol	1 minutes
Distilled water	1 minutes
Weigerts Iron Haematoxylin	25 minutes
Rinse in running tap water	10 minutes
Rinse in distilled water	
Biebrich Scarlet	10 minutes
Rinse in distilled water	
Phosphomolybdic/phosphotungstic acid	15 minutes

Aniline Blue	7 minutes
Rinse distilled water	
1% acetic acid	3 minutes
Rinse distilled water	
Dehydrate 95% ethanol	10 seconds
100% ethanol	10 seconds
Histoclear	3 minutes

4.3.5 Generation of iPSCs

2D MSCs were cultured as described in 2.2.1.3. 3D spheroids were seeded with initiating cell numbers of 60,000 MSCs and cultured for 5 days as described in 2.2.1.5. 2D MSCs were trypsinised and re-seeded in 6-well plates, 10,500 cells per cm^2. 3D MSCs were disaggregated to single cells as described in 2.2.2.1, before counting and seeding as above for 2D MSCs. Duplicate wells were seeded for each sample. 2 wells for each sample were also seeded for GFP transduction controls. 5 hours after seeding, medium was removed and replaced with transduction media (DMEM high glucose supplemented with 10% FBS, 100 units/ml penicillin and 100µg/ml streptomycin and 6ug/ml polybrene) containing lentiviral vectors for OKSM (Stemgent Lentivirus set:hOKSM ST00044) or GFP (Life Technologies, A1357701). Samples were incubated with lentivirus for 22 hours, and medium was refreshed every other day. For GFP-transduced cells, wells were washed with PBS, then imaged using both brightfield and fluorescence microscopy. 10 images per sample were taken, before GFP images were inverted. Samples were counted for total cells, and GFP+ cells, and these values were used to calculate transduction efficiencies as detailed below:

Transduction efficiency = (No. of GFP+ cells/Total cell no.) x 100

For OKSM-transduced cells, 5 days after transduction, infected cells were removed from plastic with TrypLE, counted and 10,500 cells per cm^2 re-seeded in 6-well plates onto irradiated MEF feeder cells in ESC media (see 2.2.1.6). Duplicate wells were seeded for each sample. Media changes were performed daily until day 18 (Donor 1) and day 27 (Donor 2) after transduction, when samples were fixed and stained as described in 2.2.6. Antibody details are given in Table 4.3.2. Samples were imaged using a Zeiss LSM 710 inverted microscope. This involved a tile

scanning method, which then generated a composite image of the whole well. For each sample, Oct4A+ colonies were manually counted. This number was then used to calculate a reprogramming efficiency, using previously calculated transduction efficiencies as detailed below:

No. of transduced cells per sample =

(transduction efficiency (in %)/100) x total cells (which is 20,000 for all samples)

Reprogramming efficiency = (No. of Oct4A+ colonies/No. of transduced cells) x 100

OKSM-transduced wells were also imaged conventionally using the Zeiss LSM 710 inverted microscope for higher magnification images of individual colonies.

4.3.6 Semi-solid culture of MSCs

For semi-solid expansion studies, MSCs were cultured as 60,000 cell spheroids for 5 days as described in 2.2.1.5, before disaggregation to very small cell clumps/single cells as described in 2.2.2.1, although here incubation time was reduced to 15 minutes to ensure maximum cell viability. d-3D MSCs were then re-suspended in 100µl DMEM high glucose before mixing with semi-solid media (either DMEM high glucose supplemented with 5% FBS and 1% methyl cellulose or ESC media supplemented with 1% methyl cellulose.) d-3D MSCs were cultured in non-adherent 50mm dishes (Sterilin) at 37°C, 5% CO_2 for 7 days, with no media change or refreshment. Samples were imaged by light microscopy. For RNA extraction, d-3D MSCs were isolated by washing with PBS, then pelleted by centrifugation, before RNA extraction was performed using Trizol. Briefly, 500µl Trizol was added to each sample, before samples were frozen overnight at -80ºC. Samples were then brought to room temperature and 100µl chloroform was added, before samples were vortexed, then incubated for 5 minutes at room temperature. Samples were next centrifuged at 12000g for 20 minutes at 4ºC, before the upper aqueous phase was transferred to a new tube, and mixed with 500µl 100% isopropanol by vortexing. Following 30 minutes incubation at 4ºC, samples were centrifuged at 12000g, 4ºC for 15 minutes. After isopropanol removal, 1ml of 75% ethanol was added and samples were centrifuged for 5 minutes at 12000g. Ethanol was removed, and

samples were air dried briefly before re-suspension in 12µl RNase-free H_2O. cDNA samples were generated and analysed by qPCR as described in 2.2.5.3 and 2.2.5.4. Primers are listed in Table 4.3.1.

4.3.7 Analysis of Brachyury+ cell percentage and position using Volocity

A fluorescent image of a single section stained with DAPI and Brachyury as described above was analysed using Volocity software. Due to the nuclear location of Brachyury staining, it was possible to establish thresholds by which the software identified individual nuclei. The number of Brachyury+ cells was calculated as a percentage of the total cells (DAPI+). The software was then used to identify and highlight the highest- and lowest-intensity Brachyury+ cells, to track their distribution throughout the spheroid structure.

4.3.8 Haematopoietic induction of MSCs

2D MSCs were cultured as described in 2.2.1.3. 3D spheroids were seeded with initiating cell numbers of 60,000 MSCs and cultured for 5 days as described in 2.2.1.5. On day 5 2D MSCs were trypsinised to a single cell suspension, and 3D MSCs were disaggregated to a single cell suspension (d-3D MSCs) as described in 2.2.2.1. 2D and d-3D MSCs were counted and seeded in MethoCult Enriched (Stem Cell Technologies, H4435), according to manufacturer's instructions. Briefly cells were seeded at 2100 cells per cm^2 in 50mm dishes (Sterilin) in complete MethoCult Enriched medium. Samples were maintained at 37ºC, 5% CO_2, for 16 days. At this point samples were imaged using bright field microscopy, to assess the formation of haematopoietic-like colonies. Dishes were performed in duplicate for each sample from 2 different primary MSC donors.

4.3.9 Assessment of the effect of 3D culture on mitotically inactive MSCs

2D MSCs were cultured as described in 2.2.1.3, with repeated passaging, until they ceased to actively proliferate. Cells were counted at each passage until a stable, non-proliferative point was reached, but before cells began to undergo apoptosis. 3D spheroids were seeded with initiating cell numbers of 60,000 MSCs and cultured for 5 days as described in 2.2.1.5. 3D MSCs were disaggregated to a single cell

suspension and re-seeded onto plastic as described in 2.2.2.1. Samples of cells immediately before 3D culture and 48 hours following disaggregation and re-seeding were fixed and stained with stained with Crystal Violet as described in 2.2.2.2. Samples were then imaged using light microscopy. Example grayscale images of crystal violet stained cells are shown. Following re-seeding onto plastic, d-3D MSCs were counted at each passage for a further 14 days.

4.4 Results

4.4.1 Enhanced expression of pluripotency-related transcription factors in MSCs cultured as 3D spheroids

Pluripotency is established and maintained by the expression of a network of transcription factors which activate the expression of factors required for self – renewal and repress expression of factors required for differentiation (Boyer et al., 2005). The transcription factors Oct4, Nanog and Sox2 act together to maintain pluripotency. To test the hypothesis that culturing MSCs as 3D spheroids would induce a cellular stress response and stimulate cytoplasmic clearance to a rejuvenated state, MSCs were removed from 2D culture and seeded as spheroids, containing different initiating numbers of cells. As spheroids shrink with time in culture, this method established spheroids with a range of sizes, in which cell stress from nutrient/oxygen availability and mechanical forces would vary.

3D MSC spheroids initiated from 30-, 60-, or 120,000 cells were cultured for up to 6 days. RNA samples were isolated and analysed for expression of Oct4, Nanog and Sox2. Across the three different primary MSC donors tested there was an increase in expression of all three pluripotency factors across different sized spheroids from day 3 of culture onwards.

The expression of Oct4 was up-regulated to a maximum of around 5-fold compared to the donor-matched 2D sample in Donor 3 when 30,000 MSCs were cultured in 3D for 6 days. Donor 1 also showed the highest up-regulation of Oct4 under these conditions, whilst in Donor 2, culturing 60,000 MSCs in 3D for 5 days achieved the highest up-regulation of Oct4 expression compared to the donor matched 2D sample. In both Donors 1 and 3 a considerable up-regulation of Oct4 was also seen when 60,000 MSCs were cultured in 3D for 5 days (Figure 4.4.1. A).

An approximate 15 fold up-regulation of Nanog expression was observed in Donor 1 when 120,000 MSCs were cultured in 3D for 5 days. However for both Donors 2 and 3, maximal Nanog up-regulation was observed when 60,000 MSCs were cultured in 3D for 5 days, and in these donors, expression in 120,000 MSC spheroids remained close to monolayer levels at day 5. In Donor 1, expression of Nanog at day

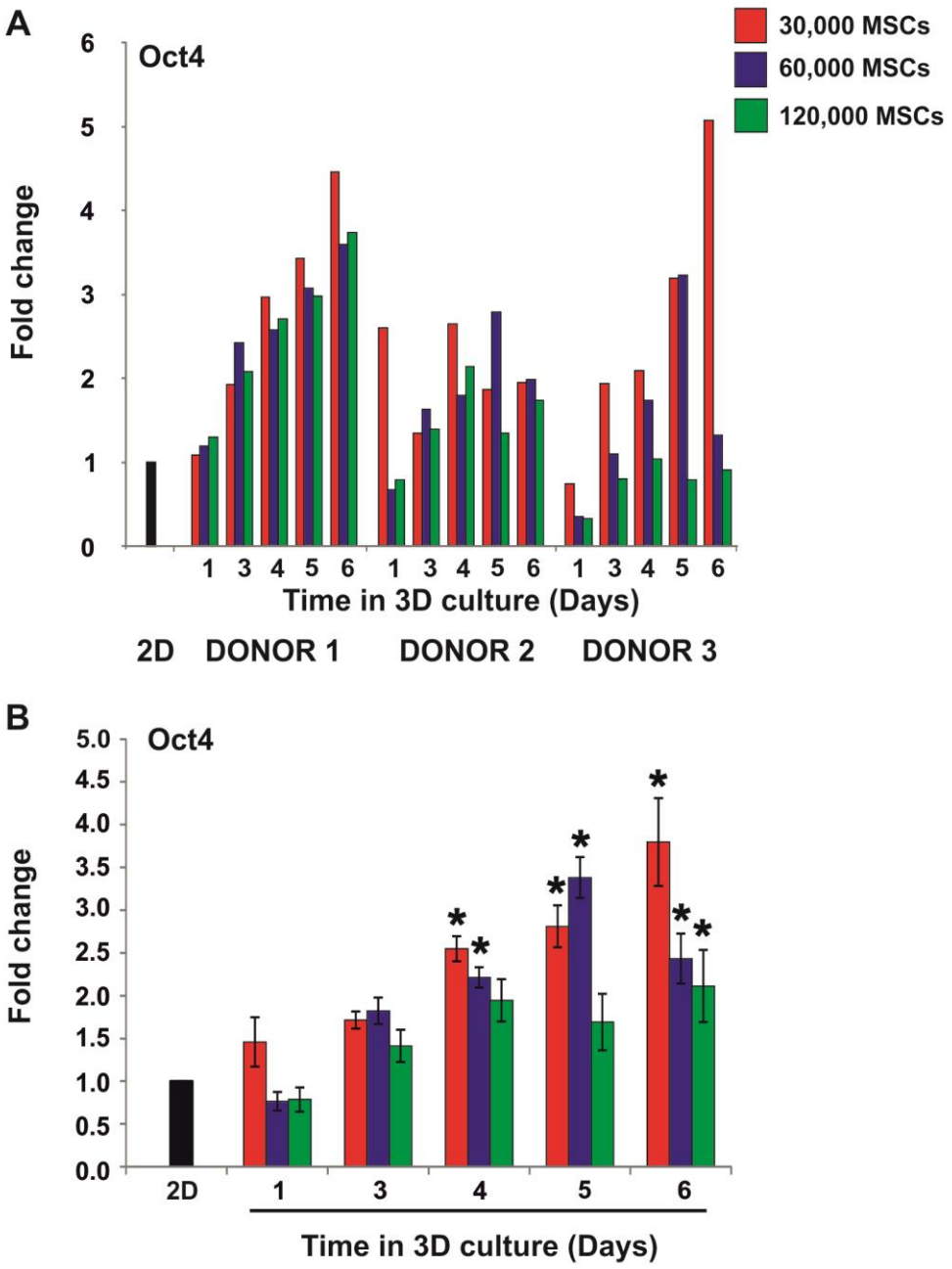

Figure 4.4.1. qPCR analysis of expression of the pluripotency factor Oct4 in MSCs over time in 3D culture

MSCs from 3 donors were cultured as 2D monolayers and 3D spheroids with initiating cell numbers of 30-, 60-, or 120,000 cells for up to 6 days in culture. cDNA samples were generated and then analysed by qPCR. A) Expression of Oct4 for each donor was normalised to expression of the housekeeping gene GAPDH and made relative to expression levels in the donor matched 2D sample. Fold changes were calculated as 2^{-ddCt}. B) Data from all 3 donors was pooled and subject to statistical analysis, mean fold changes are shown ± SEM, * $p < 0.05$. Statistical significance is relative to expression in 2D MSCs (by Kruskal Wallis test, n = 3).

5 in 60,000 MSC spheroids was enhanced around 10 fold compared to 2D MSCs, and other than 120,000 day 5, no other conditions in this donor resulted in a greater increase in Nanog expression (Figure 4.4.2. A).

Notably in both Donors 2 and 3 maximal up-regulation of expression of Sox2 was again observed when 60,000 MSCs were cultured as a spheroid for 5 days, whilst in Donor 1 120,000 MSCs cultured for 5 days again saw the highest expression of Sox2 relative to the donor matched 2D sample, with a prominent increase in expression also observed in 60,000 MSCs at day 5 of 3D culture (Figure 4.4.3. A).

Across the three primary donors used in this experiment, there was a notable similarity in the expression pattern of pluripotent transcription factors in 3D culture. Whilst there was some variation in observed fold changes between donors, the pattern of up-regulation of expression was highly similar, across donors and genes. The variability of MSCs from different primary donors means that normally pooling of data from different donors may be inappropriate. However in this case, given the similarity of response across donors, sample data was pooled, in order to identify patterns in expression, and to help in the choice of optimal conditions to use in further study. When pooled, the highest up-regulation of Oct4 expression was in 120,000 MSC spheroids at day 6, whilst the second highest level of up-regulation was observed in day 5 60,000 MSCs spheroids (Figure 4.4.1. B). Pooled data for both Nanog (Figure 4.4.2. B) and Sox2 (Figure 4.4.3. B) showed that across donors, up-regulation of expression of both genes was substantially higher in 60,000 MSC spheroids at day 5 than under any other conditions tested. For this reason further study was focused on MSC spheroids initiated from 60,000 cells and cultured for 5 days was selected as the optimal culture condition.

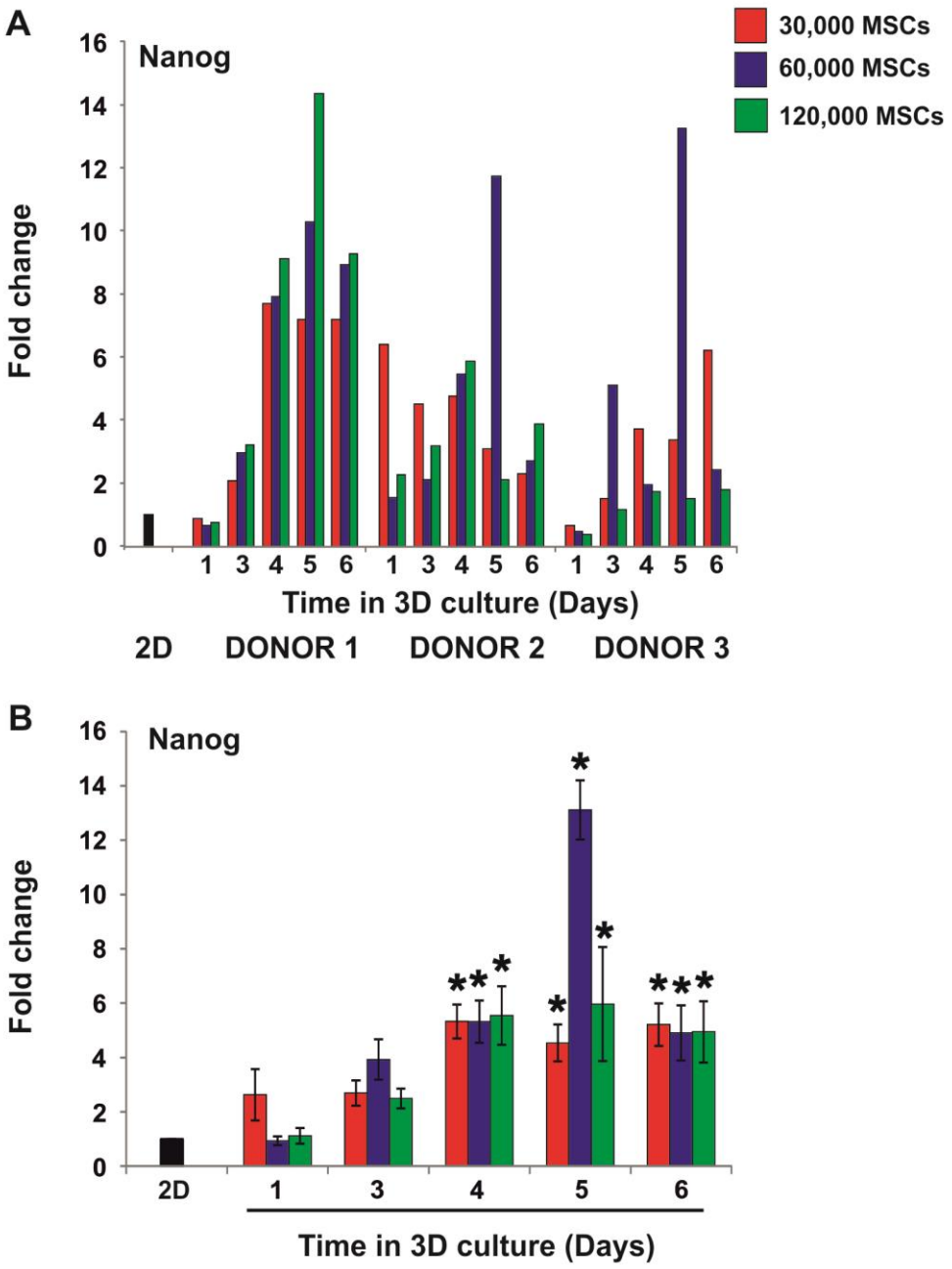

Figure 4.4.2. qPCR analysis of expression of the pluripotency factor Nanog in MSCs over time in 3D culture

MSCs from 3 donors were cultured as 2D monolayers and 3D spheroids with initiating cell numbers of 30-, 60-, or 120,000 cells for up to 6 days in culture. cDNA samples were generated and then analysed by qPCR. A) Expression of Nanog for each donor was normalised to expression of the housekeeping gene GAPDH and made relative to expression levels in the donor matched 2D sample. Fold changes were calculated as 2^{-ddCt}. B) Data from all 3 donors was pooled and subject to statistical analysis, mean fold changes are shown ± SEM, * $p < 0.05$. Statistical significance is relative to expression in 2D MSCs (by Kruskal Wallis test, n = 3).

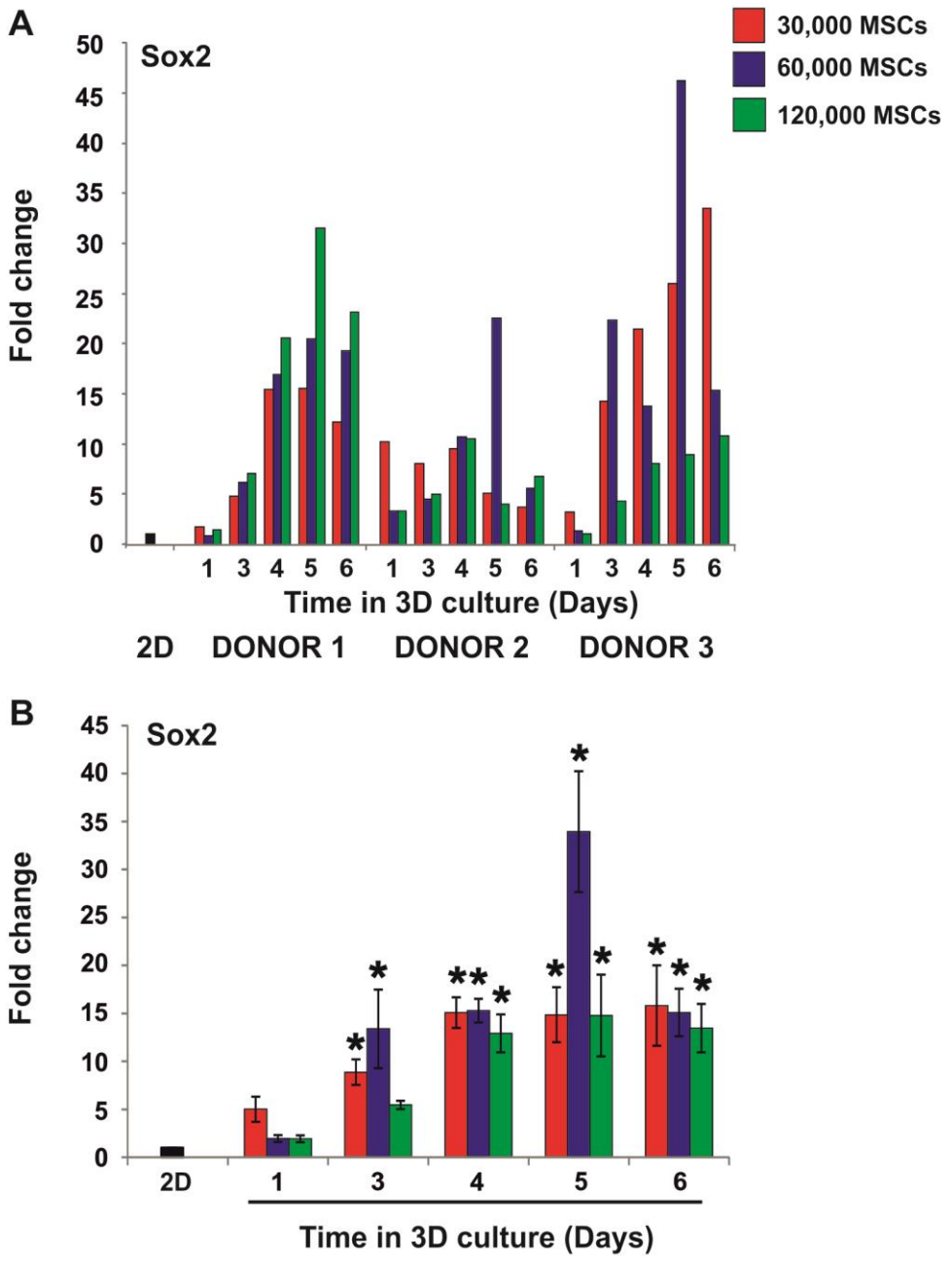

Figure 4.4.3. qPCR analysis of expression of the pluripotency factor Sox2 in MSCs over time in 3D culture

MSCs from 3 donors were cultured as 2D monolayers and 3D spheroids with initiating cell numbers of 30-, 60-, or 120,000 cells for up to 6 days in culture. cDNA samples were generated and then analysed by qPCR. A) Expression of Sox2 for each donor was normalised to expression of the housekeeping gene GAPDH and made relative to expression levels in the donor matched 2D sample. Fold changes were calculated as 2^{-ddCt}. B) Data from all 3 donors was pooled and subject to statistical analysis, mean fold changes are shown ± SEM, * $p < 0.05$. Statistical significance is relative to expression in 2D MSCs (by Kruskal Wallis test, n = 3).

Telomerase is expressed by pluripotent cells and is required for their self-renewal capacity. Telomerase activity is repressed in normal replicating somatic cells, resulting in telomere shortening and eventually leading to replicative senescence. MSCs from 3 primary donors were cultured as 2D monolayers, induced to form spheroids initiated from 60,000 cells, then maintained in culture for up to 6 days. RNA samples were isolated and analysed for expression of telomerase. 3D culture also resulted in an increase of telomerase transcript, with maximal expression on either day 3, 4 or 5, depending on donor. The highest up-regulation of telomerase expression was seen in Donor 3, with an approximately 17-fold increase at Day 3, compared to the donor matched 2D sample (Figure 4.4.4. A). The changes in telomerase expression were more varied between donors than those seen for the pluripotent transcription factors, but were still highly similar, considering the variability of MSCs from different primary donors. Pooling sample data revealed that the highest up-regulation of telomerase was observed at day 3 of 3D culture, although high variation across donors at this time point meant that statistically the only time point at which expression was significantly different to monolayer levels was day 5 (Figure 4.4.4. B). This supports the results from pluripotency factor qPCR, and highlights day 5 in 60,000 MSC spheroids as an optimal point for expression of factors associated with pluripotent cells. It should be noted here that telomerase is an enzyme, and that these qPCR results only report an increase in telomerase transcript. Functional testing would be required to see if this was accompanied by an increase in telomerase activity in the optimised 3D spheroid model.

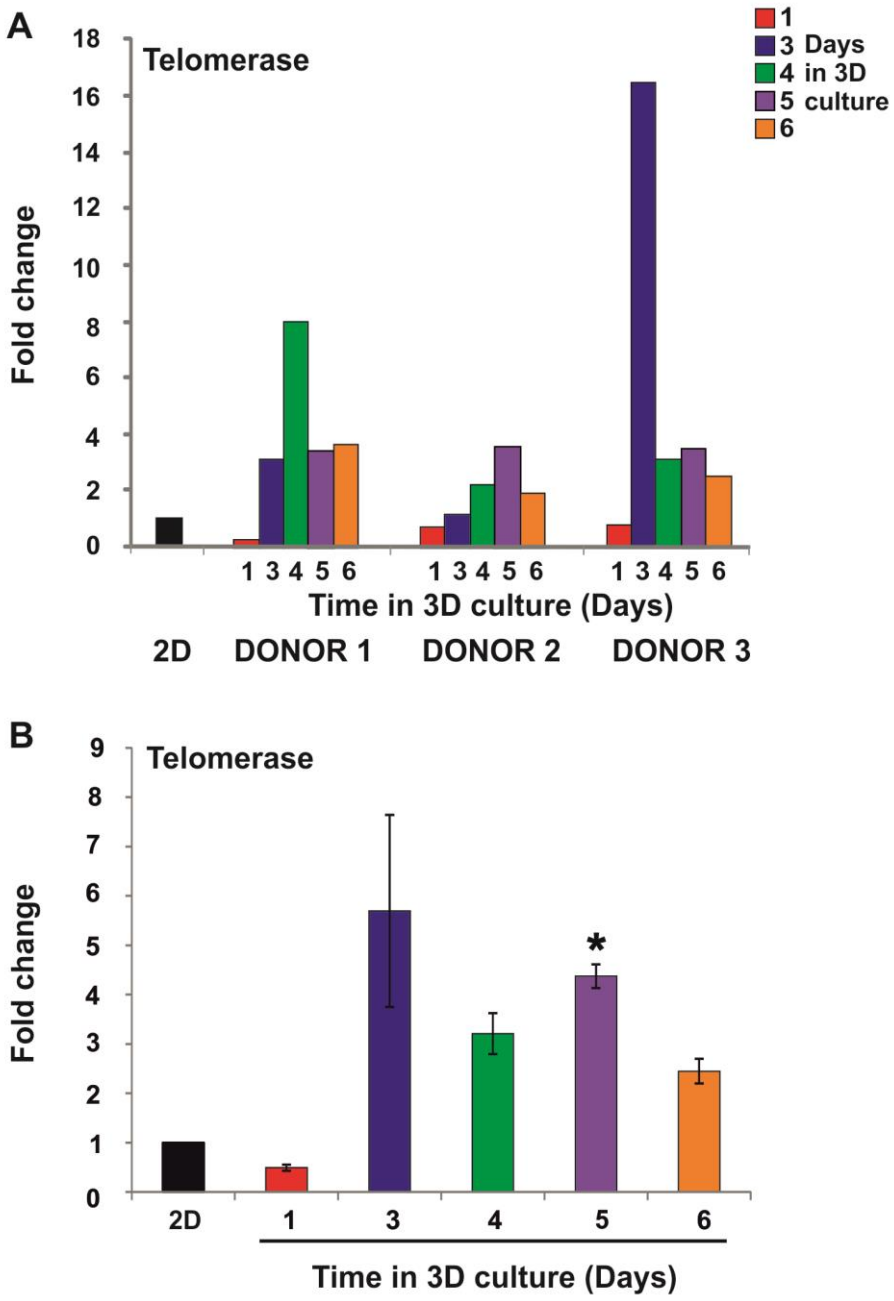

Figure 4.4.4. qPCR analysis of expression of Telomerase in MSCs over time in 3D culture

MSCs from 3 donors were cultured as 2D monolayers and 3D spheroids with an initiating cell number of 60, 000 cells for up to 6 days in culture. cDNA samples were generated and then analysed by qPCR. A) Expression of Telomerase for each donor was normalised to expression of the housekeeping gene GAPDH and made relative to expression levels in the donor matched 2D sample. Fold changes were calculated as 2^{-ddCt}. B) Data from all 3 donors was pooled and subject to statistical analysis, mean fold changes are shown ± SEM, * $p < 0.05$. Statistical significance is relative to expression in 2D MSCs (by Kruskal Wallis test, n = 3).

4.4.2 Oct4, Nanog and Sox2 proteins are not expressed at detectable levels in 2D or 3D MSCs

To examine if increases in transcript levels of pluripotency factors resulted in increased protein expression, MSCs were cultured as 60,000 MSC spheroids for 5 days. Spheroids were then snap-frozen, sectioned and stained for Oct4A and Nanog. There was no specific Oct4A or Nanog staining in 3D MSC sections (Figure 4.4.5), suggesting that protein levels of these factors were not detectable by immunocytochemistry. It was possible that a small population of cells within the spheroid had significantly up-regulated expression of pluripotency factors, and that this population would also be expressing protein at detectable levels. To ensure all cells within the spheroid were examined, 3D MSC spheroids were disaggregated to a single cell suspension, incubated with antibodies to Oct4A, Nanog and Sox2, and then analysed by flow cytometry. Donor matched 2D MSCs and 2102Eps (positive control) were also analysed using this method. 2102Eps are an embryonal carcinoma cell line, known to express pluripotency factors, and are a useful positive control for *in vitro* pluripotency assays. Oct4A, Nanog and Sox2 were all highly expressed in 2102Eps, confirming that the proteins of interest were detectable by flow cytometry (Figure 4.4.6). 3 primary MSC donors were examined using flow cytometry, and there was no detectable protein expression in any donor in either 2D or 3D samples (Figures 4.4.7 – 4.4.9). Although in all MSC donors there was a small but noticeable shift in the peak for Nanog. However, the magnitude of this shift was similar to that observed when the Nanog peak was compared to peaks for Oct4A and Sox2 in 2102Eps. As 2D MSCs have not previously been reported to express Nanog, it is possible that the Nanog antibody used in this study may bind with higher affinity than the other antibodies used. Further antibody titrations and use of an IgG control would demonstrate if the concentration of Nanog antibody used may have been resulting in a degree of non-specific binding in the samples shown. Overall, the results from flow cytometry and immunocytochemistry suggest that MSCs do not express pluripotency-associated proteins at levels comparable to 2102Eps and that protein expression is not up-regulated in 3D MSCs, despite a significant up-regulation of transcript levels of Oct4, Nanog and Sox2 under these conditions.

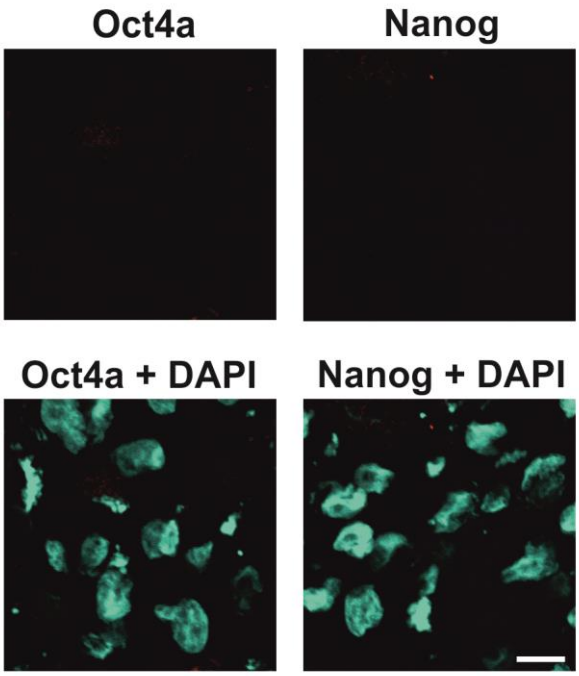

Figure 4.4.5. Staining of 3D MSC spheroid sections for the pluripotency markers Oct4a and Nanog

MSCs were cultured as 3D spheroids with an initiating cell number of 60,000 cells for 5 days in culture. Spheroids were then snap-frozen, sectioned and stained for markers of pluripotency. Samples were imaged using confocal microscopy. Oct4a (red) with DAPI (cyan) staining of 3D MSC sections (left panel). Nanog (red) with DAPI (cyan) staining of 3D MSC sections (right panel). Example images from one donor shown, scale bar = 10µm.

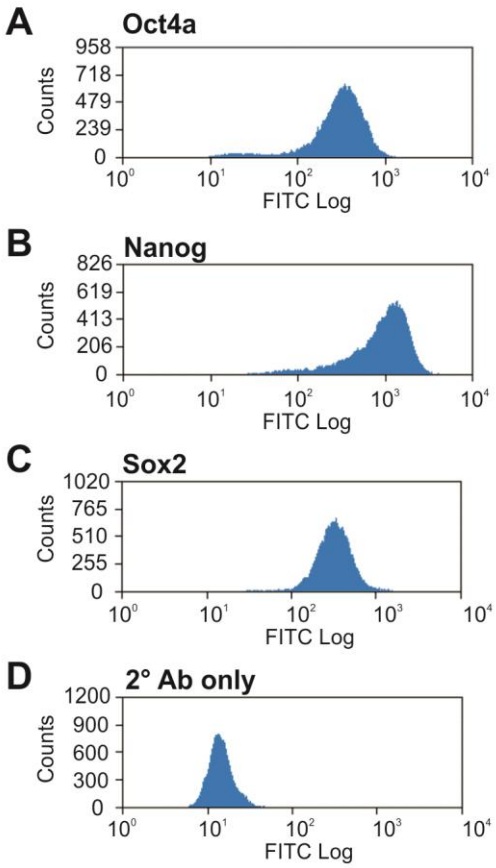

Figure 4.4.6 Flow cytometry analysis of expression of pluripotency markers in 2102Ep embryonal carcinoma cells

2102Ep cells were incubated with antibodies for Oct4a, Nanog and Sox2 in solution and analysed by flow cytometry. The histograms show marker expression of A) Oct4a, B) Nanog, C) Sox2 and D) 2º antibody only control.

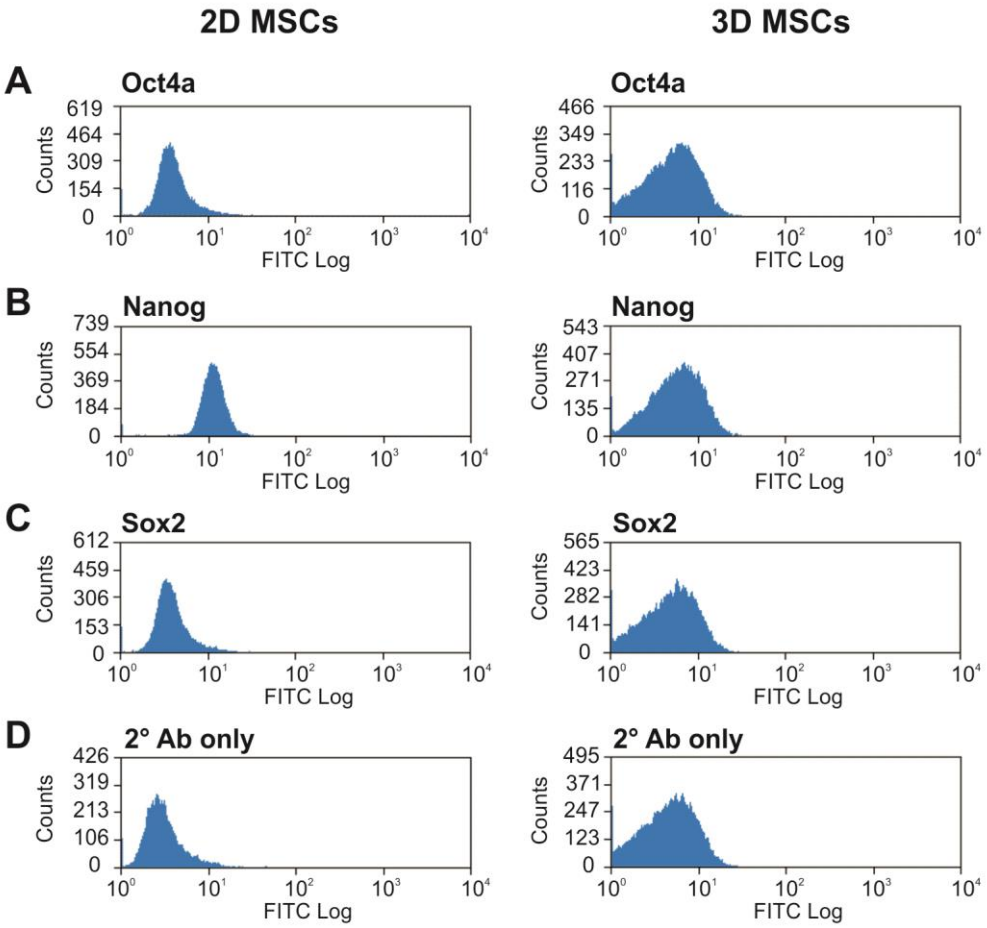

Figure 4.4.7 Flow cytometry analysis of expression of pluripotency markers in 2D and 3D MSCs (Donor 1)

2D and 3D MSCs (disaggregated to a single cell suspension) cells were incubated with antibodies for Oct4a, Nanog and Sox2 in solution and analysed by flow cytometry. The histograms show marker expression of A) Oct4a, B) Nanog, C) Sox2 and D) 2º antibody only control in 2D MSCs (left panel) and 3D MSCs (right panel).

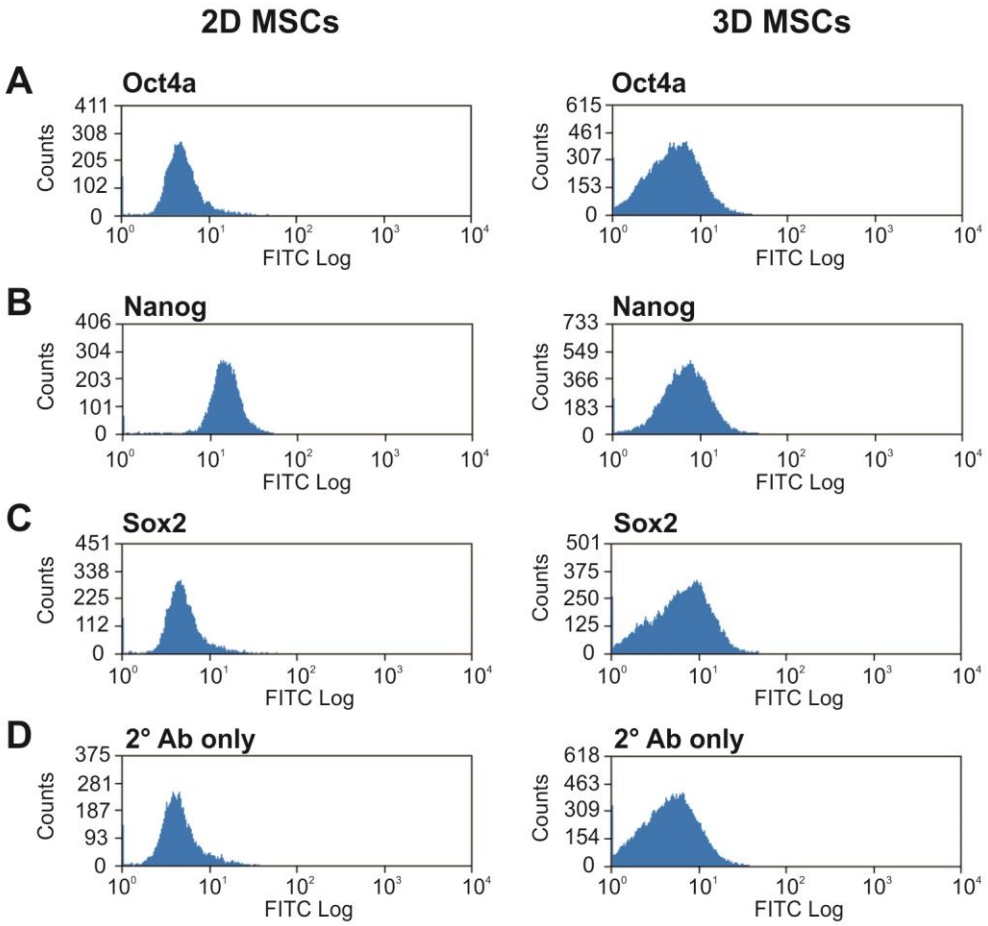

Figure 4.4.8 Flow cytometry analysis of expression of pluripotency markers in 2D and 3D MSCs (Donor 2)

2D and 3D MSCs (disaggregated to a single cell suspension) cells were incubated with antibodies for Oct4a, Nanog and Sox2 in solution and analysed by flow cytometry. The histograms show marker expression of A) Oct4a, B) Nanog, C) Sox2 and D) 2º antibody only control in 2D MSCs (left panel) and 3D MSCs (right panel).

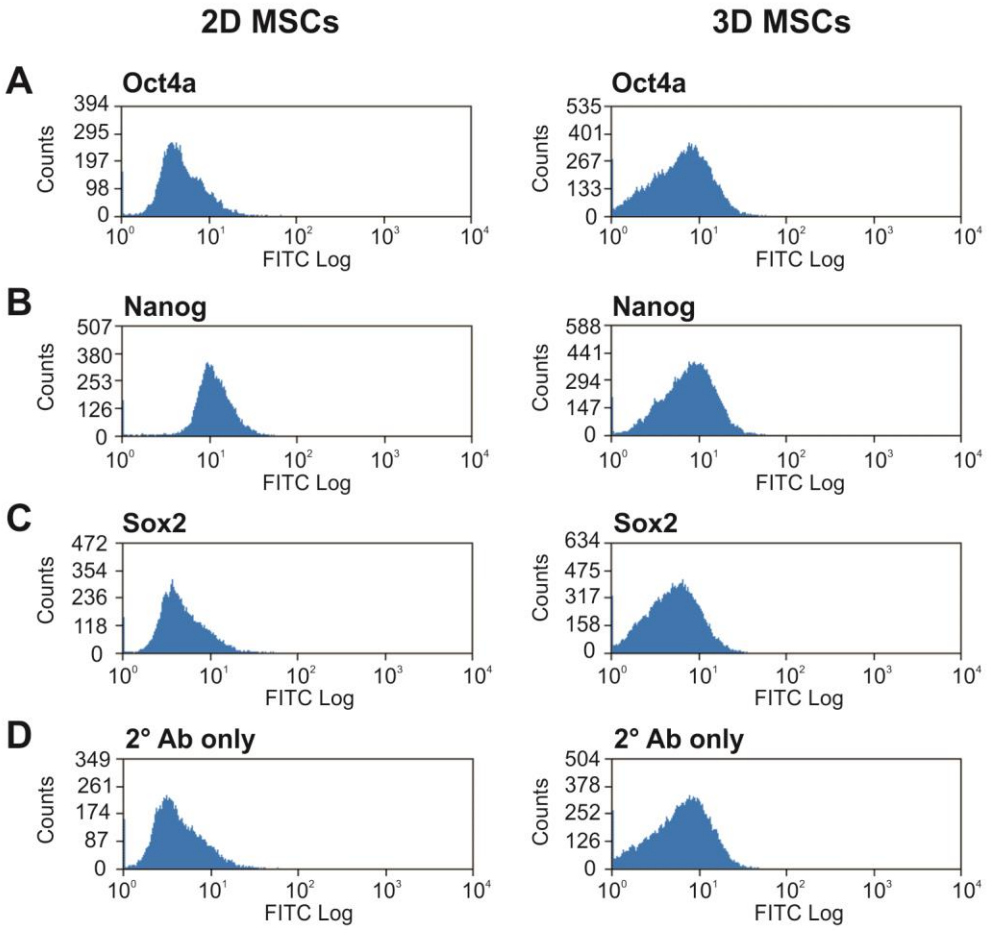

Figure 4.4.9 Flow cytometry analysis of expression of pluripotency markers in 2D and 3D MSCs (Donor 3)

2D and 3D MSCs (disaggregated to a single cell suspension) cells were incubated with antibodies for Oct4a, Nanog and Sox2 in solution and analysed by flow cytometry. The histograms show marker expression of A) Oct4a, B) Nanog, C) Sox2 and D) 2º antibody only control in 2D MSCs (left panel) and 3D MSCs (right panel).

4.4.3 Transcript levels of pluripotency factors are lower in the 3D MSC optimised model than in human ESCs

Despite enhanced expression of pluripotency factors at the transcript level in 3D MSCs, protein expression in these cells was not detected. Using RNA isolated from three different primary MSCs donors, cultured as both 2D monolayers and as 60,000 cell 3D spheroids for 5 days, transcript levels of Oct4, Nanog and Sox2 were compared directly to transcript levels in H9 human ESCs, cultured on feeders, by QPCR. As previously demonstrated, expression levels of Oct4, Nanog and Sox2 were higher in 3D MSCs than in the donor matched 2D samples. However levels in 3D MSCs remained lower than those in H9 ESCs for all genes examined. Oct4 expression was between 30 – 60 fold lower in 3D MSCs than ESCs, whilst Nanog expression was 104 – 181 fold lower, and Sox2 expression was 15 – 30 fold lower. Notably, although the expression levels of pluripotent transcription factors varied across donors, the expression of all factors in all 3D MSC samples was higher than the expression observed in all 2D samples. Oct4 expression was between 82 – 98 fold lower in 2D MSCs than ESCs, whilst Nanog expression was 665 – 3080 fold lower, and Sox2 expression was 275 – 1700 fold lower (Figure 4.4.10). So whilst the optimised 3D model results in a substantial increase in transcript levels of these factors compared to those seen in 2D MSCs, it cannot enhance expression of pluripotency factors to ESC levels. The observed increase in transcript levels in 3D MSCs does not appear sufficient to increase protein expression, which is required for the establishment and maintenance of pluripotency.

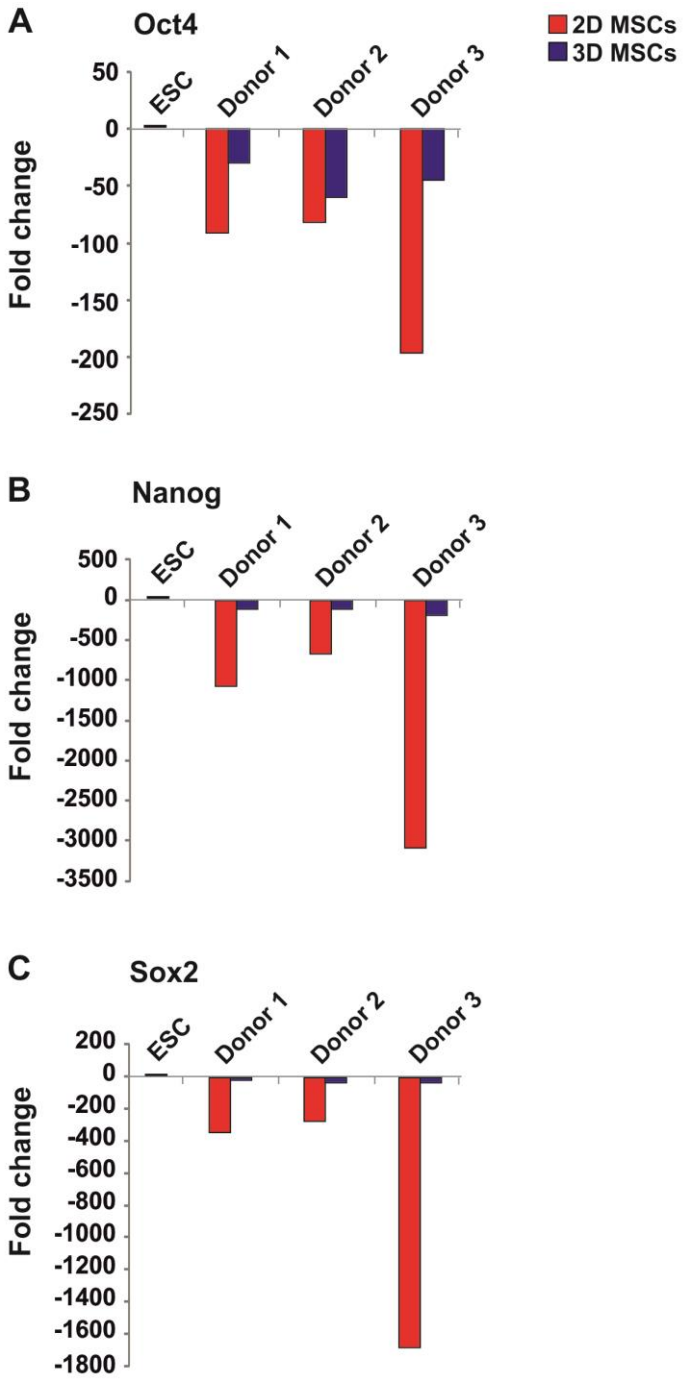

Figure 4.4.10. qPCR analysis of expression levels of pluripotent transcription factors in 2D and 3D MSCs compared to expression in human ESCs

MSCs from 3 donors were cultured as 2D monolayers and 3D spheroids with an initiating cell number of 60, 000 cells for 5 days in culture. cDNA samples were generated and then analysed by qPCR. Expression of Oct4 (A), Nanog (B) and Sox2 (C) for each donor was normalised to expression of the housekeeping gene GAPDH and made relative to expression levels in pluripotent human H9 ESCs. Fold changes were calculated as 2^{-ddCt}.

4.4.3 3D MSC spheroids form small organised tissue masses but not teratomas *in vivo*

Lack of detectable protein expression, and lower mRNA expression than ESCs suggested that although 60,000 MSCs cultured in 3D for 5 days resulted in enhanced pluripotent transcript expression, MSCs cultured in these conditions were not pluripotent. To test this, MSC spheroids initiated from 60,000 cells were cultured for 5 days, before implantation into nude mice. Donor-matched 2D MSCs were also implanted to test their *in vivo* potency, and mouse ESCs were implanted to act as a positive control for teratoma generation. After 12 weeks, tissue masses generated from the implanted cells were isolated, fixed, sectioned and examined by histological analyses. Sections of tissue masses generated from both mouse ESCs and 3D MSCs were examined by stereo microscopy. At the same magnification it was clear that mouse ESCs formed very large tissue masses, typical of teratomas, whilst the tissue masses isolated from 3D MSCs were much smaller (Figure 4.4.11. A). 2D MSCs failed to form any tissue structures. When H & E stained sections of the large tissue masses generated from mouse ESCs were examined under higher magnification, tissues from all three germ layers were clearly visible, confirming that the masses were indeed teratomas, generated from pluripotent cells (Figure 4.4.11 B). By comparison, there was no evidence of tissue from endoderm or ectoderm in the tissue masses generated by 3D MSCs, although distinct, segregated mesodermal structures including connective tissue, muscle and adipose tissue were observed, and these tissues appeared highly organised, in contrast to the typically disorganised arrangement of teratoma tissue (Figure 4.4.11. C).

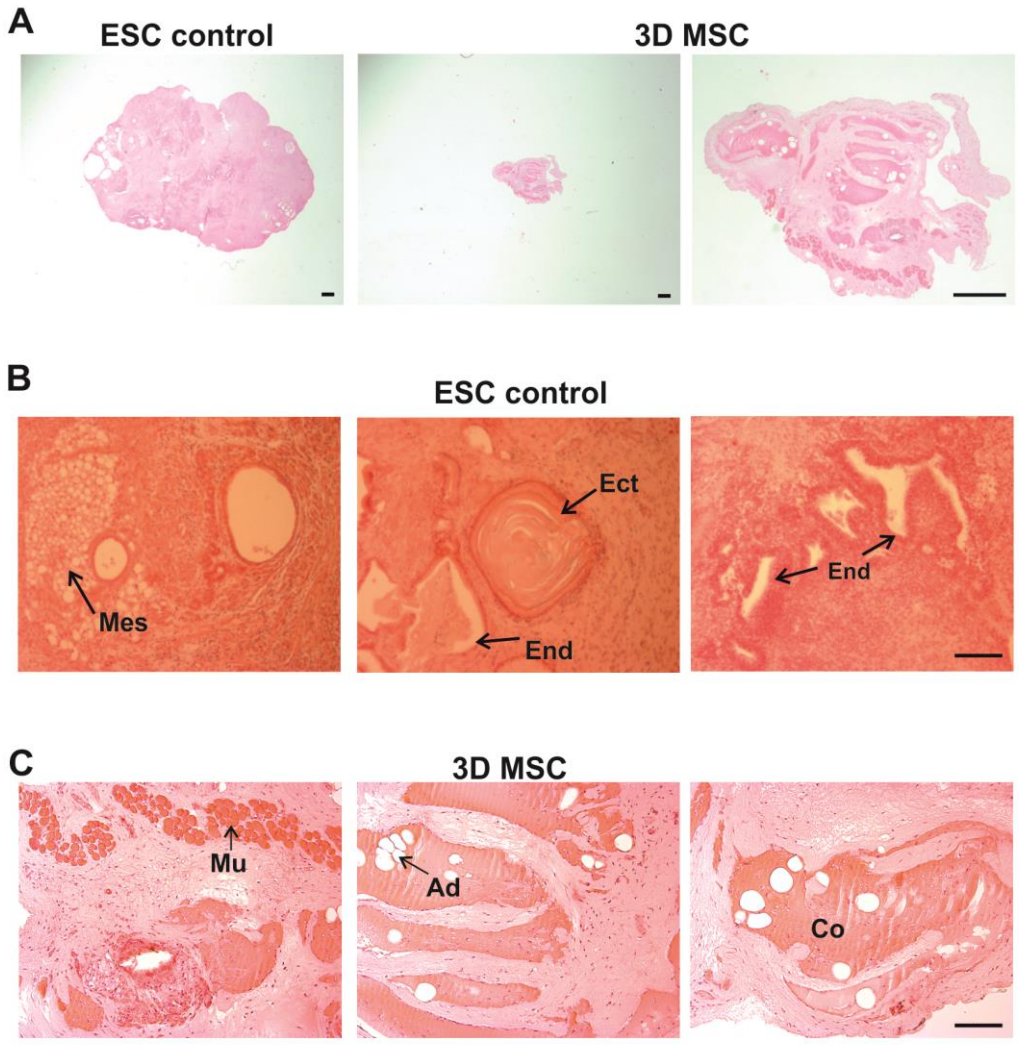

Figure 4.4.11. Histological analysis of *in vivo* tissue generation capacity following implantation into nude mice

3D MSC spheroids (initial cell number = 60’ 000 cells) were cultured in 3D conditions for 5 days before subcutaneous injection into nude mice. Mouse ESCs were also implanted as a positive control for teratoma formation. After 12 weeks tissue samples were recovered, fixed and stained with hematoxylin and eosin (H + E). A) Stereo – microscopy images of tissue masses generated by positive control mouse ESCs (left panel) and 3D MSCs (centre panel and right panel, scale bar = 500µm). B) Light microscopy images of teratomas generated by positive control mouse ESCs tissues (arrows indicate the presence of tissues from all 3 germ layers - Mes = mesoderm, Ect = ectoderm, End = endoderm; scale bar = 100µm). C) Light microscopy images of organised tissue masses generated by 3D MSCs (labels indicate tissues of mesodermal origin – Mu = muscle, Ad = adipose, Co = connective tissue; scale bar = 100µm).

4.4.4 MSCs cultured as 3D spheroids for 5 days maintain enhanced expression of reprogramming factors immediately after spheroid disaggregation

The process of reprogramming human cells to pluripotency was established in HDFs, differentiated cells which are not reported to express the pluripotency factors Oct4, Nanog and Sox2. Recent work has demonstrated that the efficiency of reprogramming to pluripotency is improved if the starting cell population endogenously express some of the factors required for reprogramming (Kim et al., 2009a; Kim et al., 2009b; Kim et al., 2008; Tsai et al., 2011; Tsai et al., 2010; Zhu et al., 2010). It was therefore possible that MSCs cultured in the optimised 3D model may reprogramme to pluripotency more efficiently than their donor-matched 2D samples. Comparative efficiencies for reprogramming to pluripotency rely on the accurate assessment of lentiviral transduction efficiencies, which then allow for the calculation of reprogramming efficiencies by counting reprogrammed colonies. 3D MSC spheroids were initiated from 60,000 cells, but it was not possible to accurately estimate the number of cells remaining after 5 days in 3D culture. Nor was it possible to assume that lentiviral particles would have access to all the cells within the spheroid equally. It was therefore necessary to adapt the system in order to make it comparable to 2D MSCs for reprogramming efficiency experiments.

MSCs from 3 different primary donors were cultured as 2D monolayers and as 3D spheroids (initiated from 60,000 cells) for 5 days in culture. On day 5, 3D spheroids were disaggregated to a single cell suspension (d-3D MSCs) using enzymatic digestion. The resulting cell suspension was re-seeded onto plastic for 5 hours, allowing attachment. At 5 hours following return to 2D culture, RNA samples were isolated and analysed for expression of the 'Yamanaka factors' (Oct4, Sox2, Klf4 and c-Myc, also known as OKSM). In order to assess the suitability of MSCs for reprogramming to pluripotency, the expression of OKSM was compared to expression levels in 2D HDFs.

In 2D MSCs the expression of Oct4 was similar or slightly higher than in HDFs. Expression of Oct4 was enhanced in 3D MSCs, with around 5-16-fold up-regulation compared to HDFs, depending on MSC donor. At 5 hours following return to 2D culture, levels in disaggregated 3D (d-3D) MSCs had fallen, but still remained above those seen in HDFs and 2D MSCs (Figure 4.4.12). A similar pattern was seen when

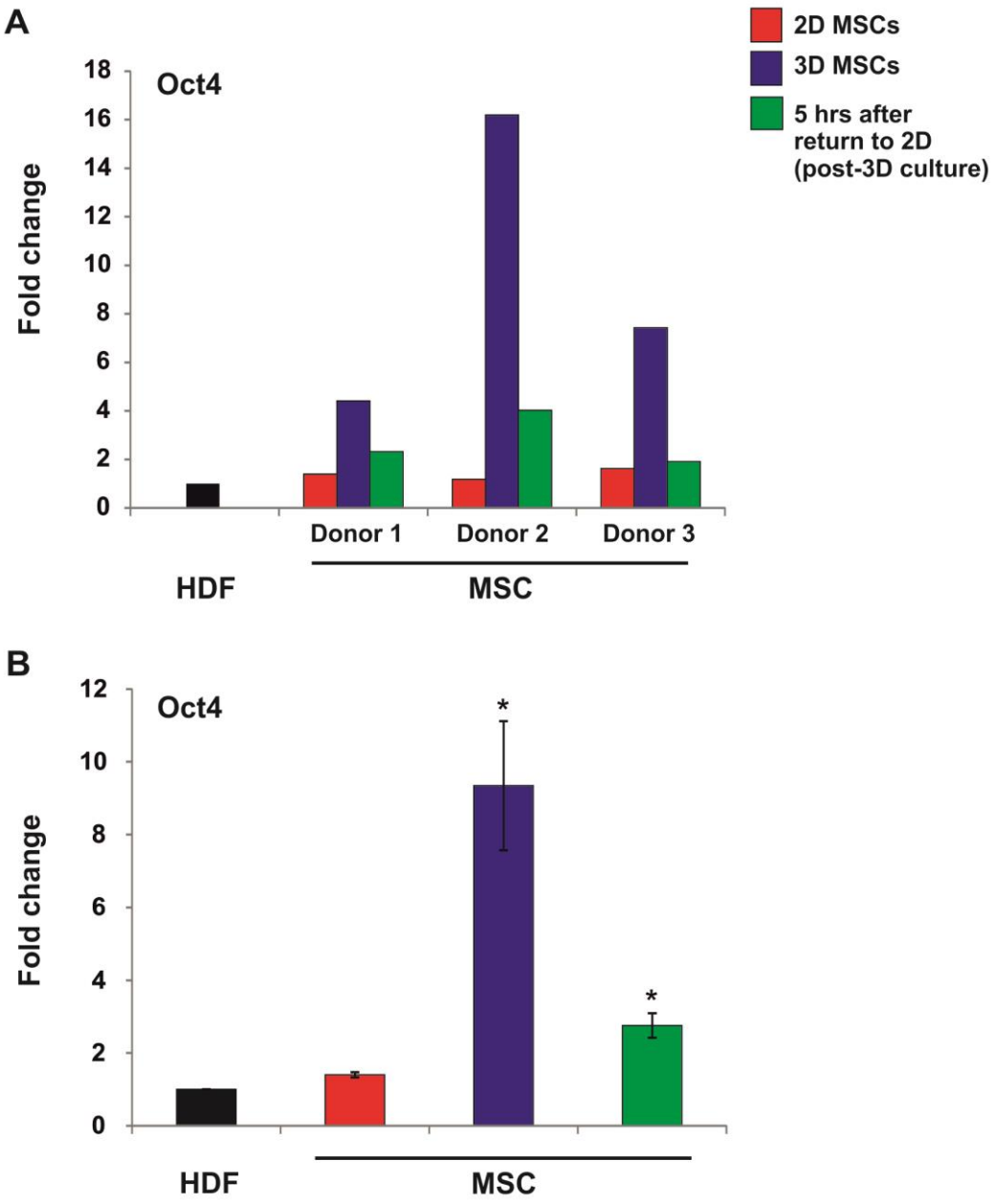

Figure 4.4.12. qPCR analysis of Oct4 expression in MSCs 5 hours after spheroid disaggregation.

MSCs from 3 donors were cultured as 2D monolayers and 3D spheroids with an initiating cell number of 60,000 cells for 5 days. After 5 days MSC spheroids were disaggregated to single cells and re-plated on tissue culture plastic for 5 hours. cDNA samples were generated and then analysed by qPCR. A) Expression of Oct4 for each donor was normalised to expression of the housekeeping gene GAPDH and made relative to expression levels in monolayer-cultured HDFs. Fold changes were calculated as 2^{-ddCt}. B) Data from all 3 donors was pooled and subject to statistical analysis, mean fold changes are shown ± SEM, * $p < 0.05$. Statistical significance is relative to expression in HDFs (by Kruskal Wallis test, n = 3).

Sox2 expression was examined. Although levels of Sox2 in 2D MSCs were lower than those seen in HDFs, the levels of Sox2 in 3D MSCs and d-3D MSCs remained higher than those in HDFs. Up-regulation of Sox2 by approximately 5-35-fold in 3D MSCs (dependent on donor) and 4-7-fold in d-3D MSCs (dependent on donor) were observed compared to levels in HDFs (Figure 4.4.13).

The expression of Klf4 was inconsistent across different MSC donors. In Donor 1, expression of Klf4 was at its lowest in 3D MSCs, although under these conditions expression remained comparable to HDFs. Expression of Klf4 in Donor 2 peaked in 3D MSCs, whilst in d-3D MSCs, expression had fallen to levels similar to those in HDFs. Donor 3 showed that 3D culture had little effect on Klf4 expression, whilst Klf4 expression peaked in d-3D MSCs after return to 2D culture. Taken together these results suggest that 3D culture does not have a consistent effect on Klf4 expression in primary MSC cultures, although they do demonstrate that across the primary donors tested and on average, Klf4 expression is higher in MSCs than HDFs, in all three culture conditions tested (Figure 4.4.14). c-Myc expression was observed to be higher in 2D and 3D MSCs than HDFs across all donors tested, although again, as with Klf4, the expression pattern of c-Myc across donors and conditions was less consistent than observed for Oct4 and Sox2. Following disaggregation, levels of c-Myc increased substantially in d-3D MSCs across all donors tested. Up-regulation of approximately 15-72-fold (dependent on donor) was observed compared to c-Myc expression in HDFs (Figure 4.4.15). Considered altogether, these results suggest that d-3D MSCs may represent a suitable cell type for reprogramming to pluripotency. Furthermore, increased endogenous expression of reprogramming factors may mean that they can be reprogrammed to pluripotency more efficiently, or with fewer factors, than their originating 2D cell populations

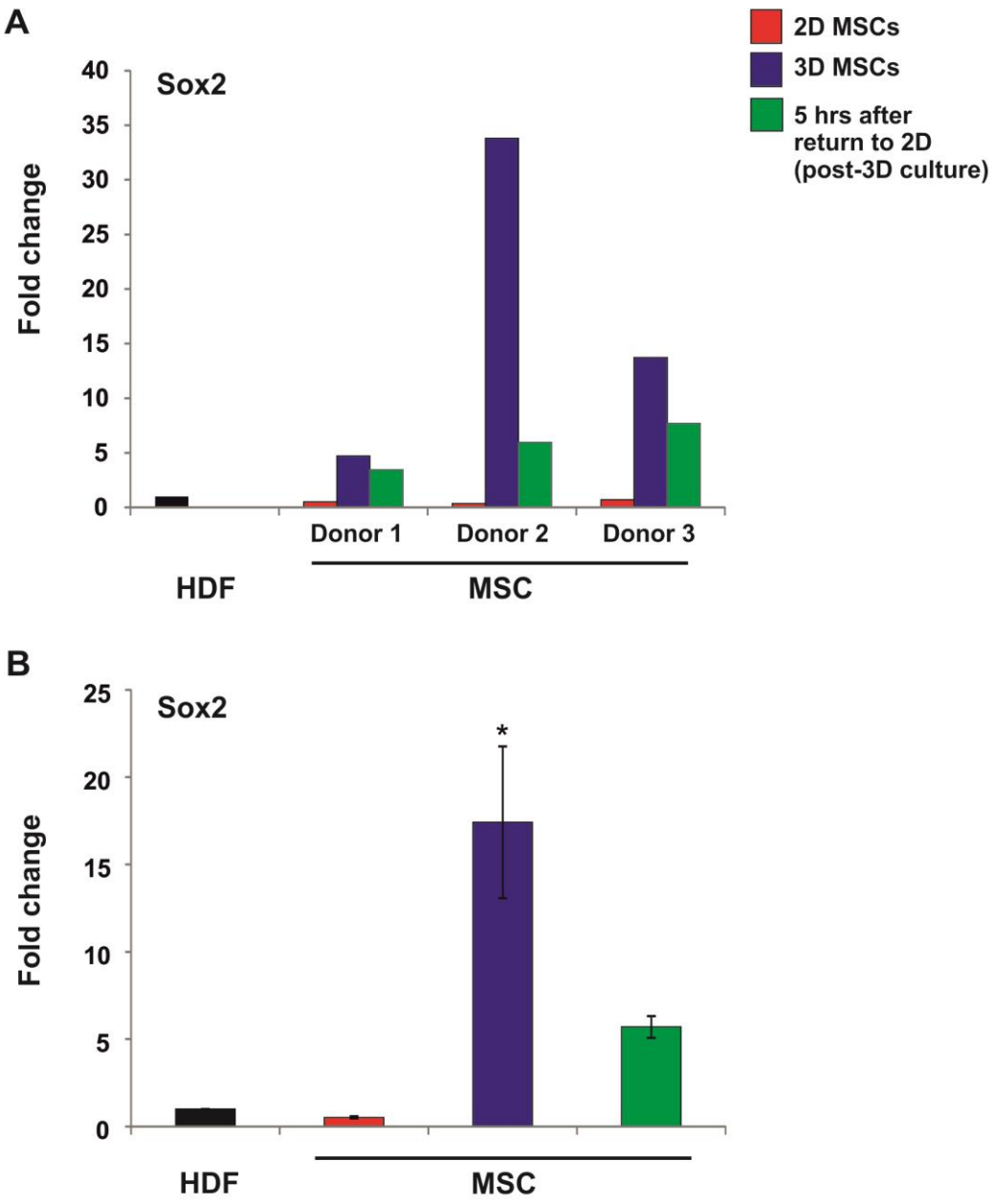

Figure 4.4.13. qPCR analysis of Sox2 expression in MSCs 5 hours after spheroid disaggregation.

MSCs from 3 donors were cultured as 2D monolayers and 3D spheroids with an initiating cell number of 60,000 cells for 5 days. After 5 days MSC spheroids were disaggregated to single cells and re-plated on tissue culture plastic for 5 hours. cDNA samples were generated and then analysed by qPCR. A) Expression of Sox2 for each donor was normalised to expression of the housekeeping gene GAPDH and made relative to expression levels in monolayer-cultured HDFs. Fold changes were calculated as 2^{-ddCt}. B) Data from all 3 donors was pooled and subject to statistical analysis, mean fold changes are shown ± SEM, * $p < 0.05$. Statistical significance is relative to expression in HDFs (by Kruskal Wallis test, n = 3).

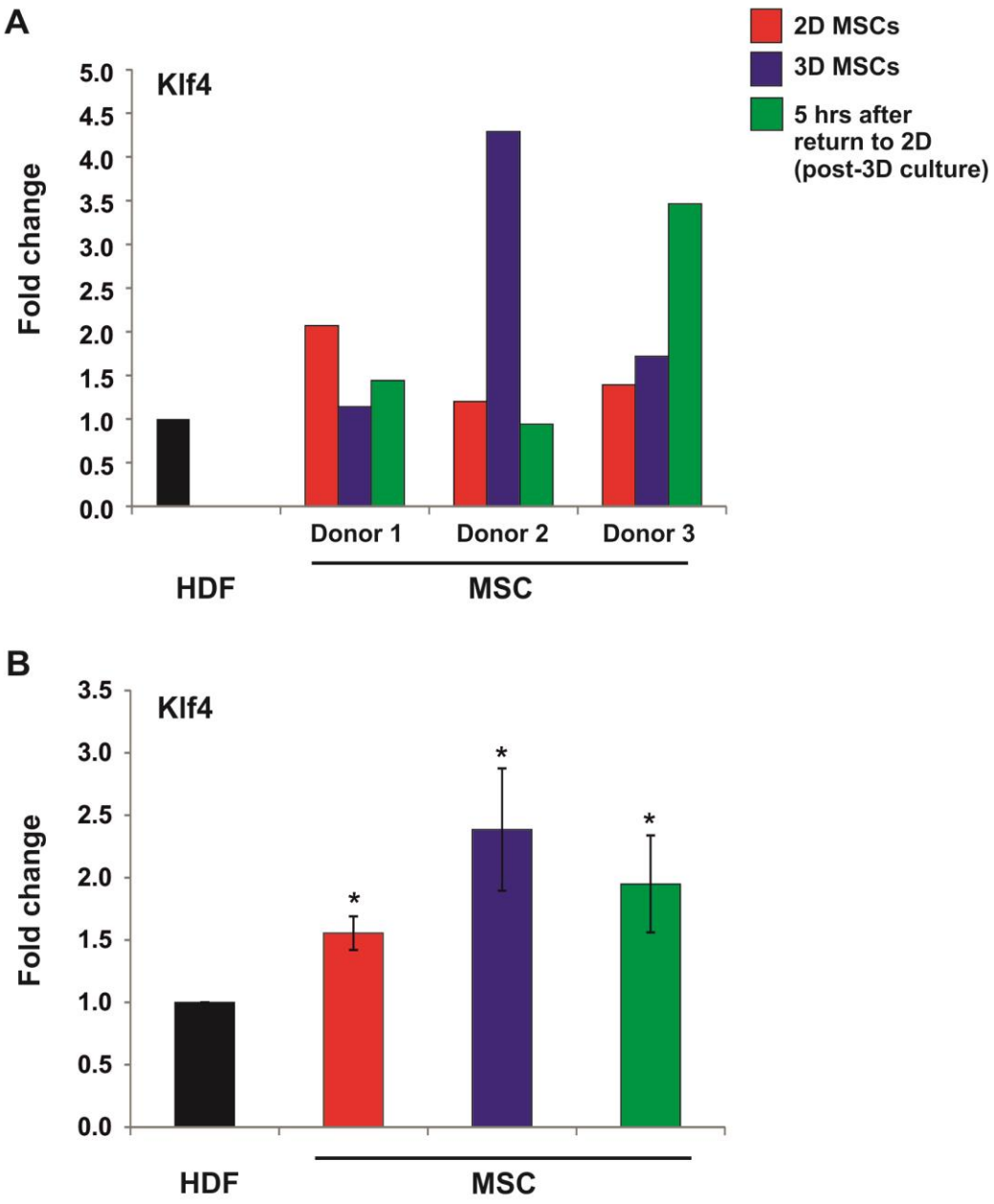

Figure 4.4.14. qPCR analysis of Klf4 expression in MSCs 5 hours after spheroid disaggregation.

MSCs from 3 donors were cultured as 2D monolayers and 3D spheroids with an initiating cell number of 60,000 cells for 5 days. After 5 days MSC spheroids were disaggregated to single cells and re-plated on tissue culture plastic for 5 hours. cDNA samples were generated and then analysed by qPCR. A) Expression of Klf4 for each donor was normalised to expression of the housekeeping gene GAPDH and made relative to expression levels in monolayer-cultured HDFs. Fold changes were calculated as 2^{-ddCt}. B) Data from all 3 donors was pooled and subject to statistical analysis, mean fold changes are shown ± SEM, * $p < 0.05$. Statistical significance is relative to expression in HDFs (by Kruskal Wallis test, n = 3).

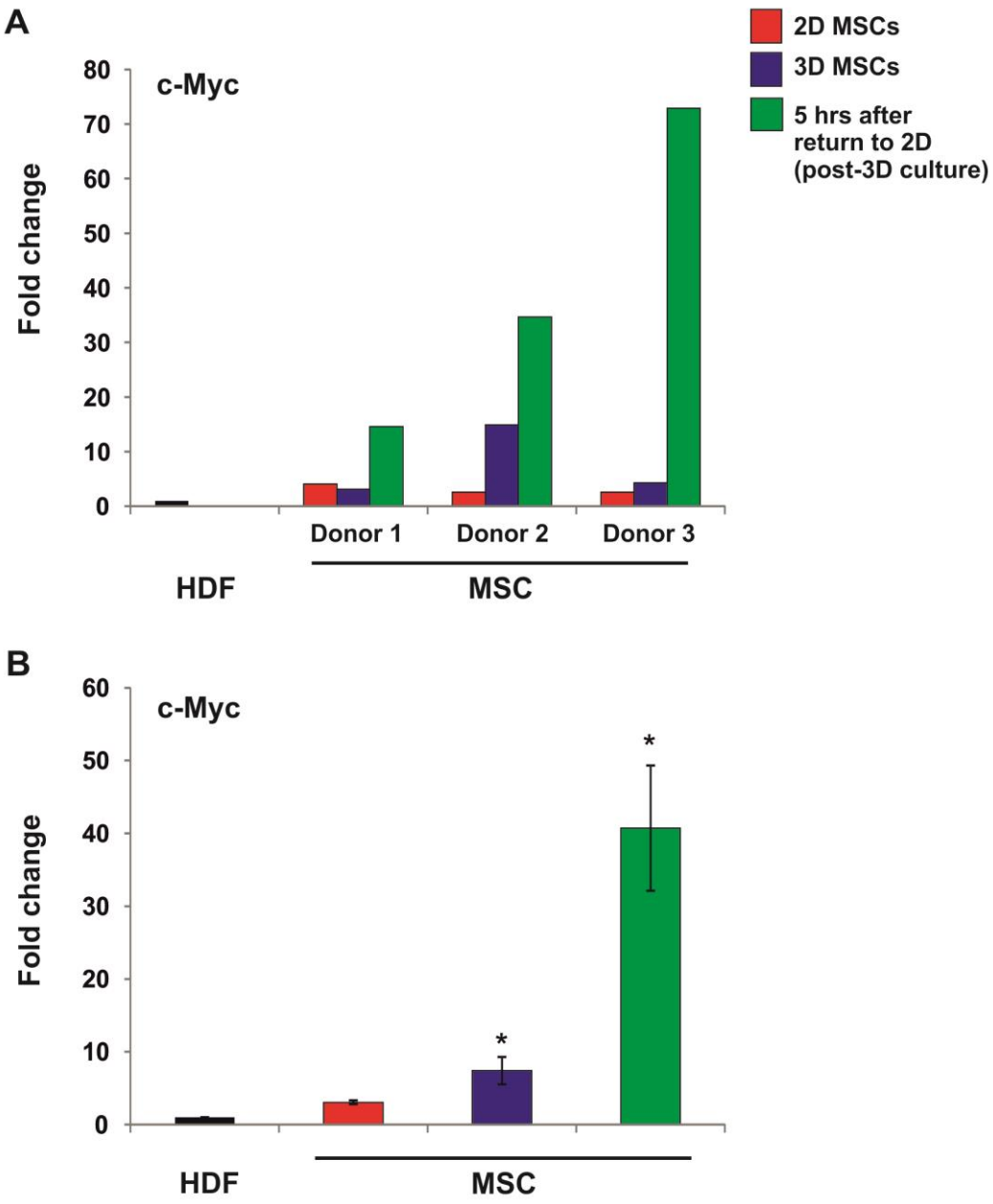

Figure 4.4.15. qPCR analysis of c-Myc expression in MSCs 5 hours after spheroid disaggregation.

MSCs from 3 donors were cultured as 2D monolayers and 3D spheroids with an initiating cell number of 60,000 cells for 5 days. After 5 days MSC spheroids were disaggregated to single cells and re-plated on tissue culture plastic for 5 hours. cDNA samples were generated and then analysed by qPCR. A) Expression of c-Myc for each donor was normalised to expression of the housekeeping gene GAPDH and made relative to expression levels in monolayer-cultured HDFs. Fold changes were calculated as 2^{-ddCt}. B) Data from all 3 donors was pooled and subject to statistical analysis, mean fold changes are shown ± SEM, * $p < 0.05$. Statistical significance is relative to expression in HDFs (by Kruskal Wallis test. n = 3).

4.4.5 The efficiency of derivation of Oct4A+ ESC-like colonies is similar in 2D MSCs and d-3D MSCs

In an attempt to derive iPSC colonies from MSCs, 3D MSCs were cultured under optimal conditions for 5 days, before disaggregation and re-seeding onto plastic (d-3D MSCs) as described above. 2D MSCs were trypsinised and re-seeded at identical densities to d-3D MSCs. MSC duplicate wells were transduced with lentiviral vectors expressing OKSM for 22 hours, before culture in MSC media for 5 days. Identical wells were also infected with lentiviral vectors expressing GFP, in order to calculate transduction efficiencies. After 5 days, lenti-GFP wells were viewed using fluorescence microscopy, and multiple images per sample were taken (n=10). The number of GFP-positive cells was counted and then used to calculate the transduction efficiency for each sample. Example (inverted) images are shown in Figure 4.4.16, and transduction efficiencies are given in Table 4.4.1. The transduction efficiencies observed in d-3D MSCs from both donors tested were considerably higher than those observed in 2D MSCs. Increased transduction efficiency may be another benefit associated with the reprogramming of d-3D MSCs, as higher transduction efficiencies mean more cells will be exposed to the reprogramming cocktail, and so more cells have a chance of undergoing reprogramming to pluripotency. At day 5 following transduction, OKSM-transduced cells were trypsinised, counted and seeded onto irradiated MEF (iMEF) feeder cells in iPSC media and observed for colony formation. At day 18 (Donor 1) and day 27 (Donor 2) following lentiviral transduction, individual wells were fixed and stained for the pluripotency markers Oct4A and Nanog. Wells were then imaged using confocal microscopy. A tile scanning method was applied, which was then used to generate a composite image of each whole well. The staining of Oct4A revealed intense immune-reactivity, so for each well, manual counting was applied to identify number of Oct4A+ colonies. This was then used with the transduction efficiencies generated from GFP-transduction, to determine the reprogramming efficiency for each sample (Table 4.4.2). The composite images are shown in Figure 4.4.17. In both donors examined, the generation of Oct4A+ colonies was slightly more efficient in 2D than d-3D MSCs, so enhanced expression of reprogramming factors at the time of transduction does not confer a reprogramming advantage on d-3D MSCs. Nor did it enhance the speed at which Oct4A+ colonies appeared in culture,

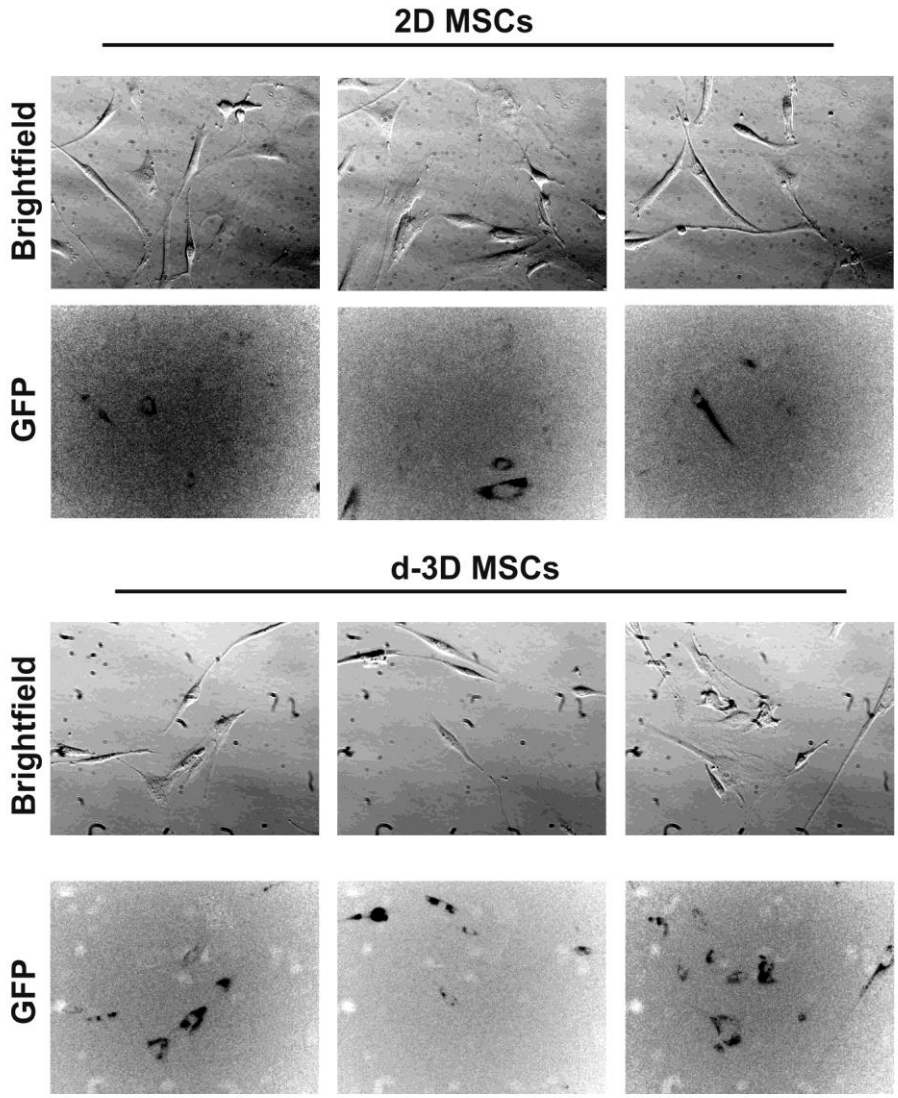

Figure 4.4.16 Analysis of lentiviral transduction efficiencies in 2D and d-3D MSCs

d-3D MSCs and 2D MSCs were incubated with GFP-lentivirus for 24 hours. After 24 hours media was exchanged for MSC expansion media, and cells were cultured for 5 days. On day 5 2D and d-3D MSCs were examined by fluorescence microscopy, and counted for GFP+ cells. Multiple bright field and inverted fluorescence (GFP) images were used to calculate transduction efficiencies from mean GFP+ cells in each sample (n = 10, example images shown, GFP images are inverted).

Table 4.4.1. Transduction efficiencies of 2D and d-3D MSCs calculated from GFP+ cell numbers

Sample ID	Total cell no.	GFP+ cell no.	Transduction efficiency
Donor 1 2D	101	38	37.6%
Donor 1 d-3D	67	51	76.1%
Donor 2 2D	72	37	51.4%
Donor 2 d-3D	56	40	71.4%

Table 4.4.2. Reprogramming efficiencies of 2D and d-3D MSCs calculated from Oct4A+ colony numbers

Sample ID	Transduction efficiency	No. of cells plated	No. of Oct4A+ colonies	Reprogramming efficency
Donor 1 2D	37.6%	20,000	65	0.86%
Donor 1 d-3D	76.1%	20,000	93	0.61%
Donor 2 2D	51.4%	20,000	18	0.18%
Donor 2 d-3D	71.4%	20,000	16	0.11%

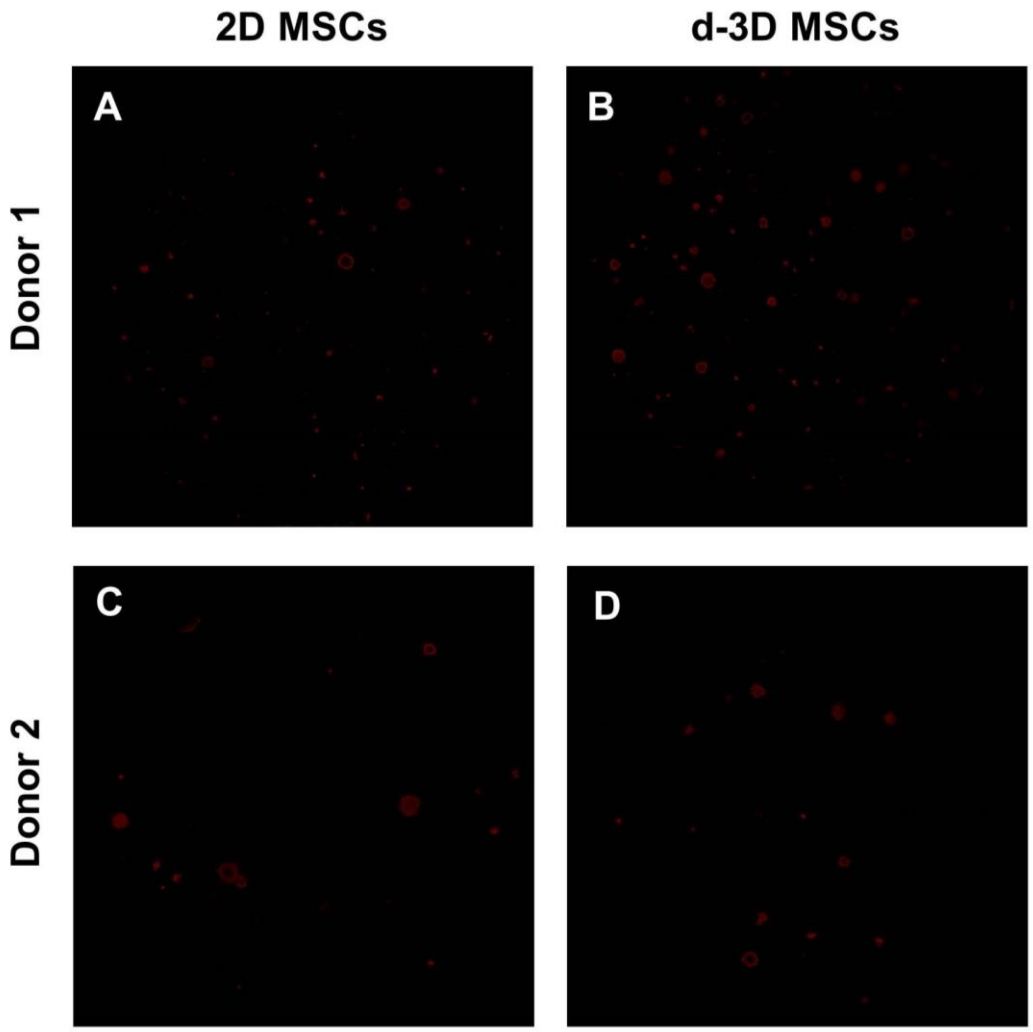

Figure 4.4.17 Analysis of the generation of Oct4a+ colonies from OKSM-transduced 2D and d-3D MSCs

d-3D MSCs and 2D MSCs were transduced with OKSM-expressing lentiviruses and cultured under standard protocols for the induction of pluripotency in 6-well plates. One well of a 6-well plate for each sample was stained with an antibody against Oct4a. Wells were examined by fluorescence microscopy, using a tile scanning method to allow quantification of absolute Oct4a+ colony numbers. Composite images of whole wells stained for Oct4a (red) for A) Donor 1 2D MSCs, B) Donor 1 d-3D MSCs, C) Donor 2 2D MSCs and D) Donor 2 d-3D MSCs.

this was donor-dependent, with samples from Donor 1 generating more colonies and much more quickly than Donor 2. Example higher magnification images of colonies generated from both 2D and d-3D MSCs, stained for Oct4A and Nanog, are shown in Figure 4.4.18.

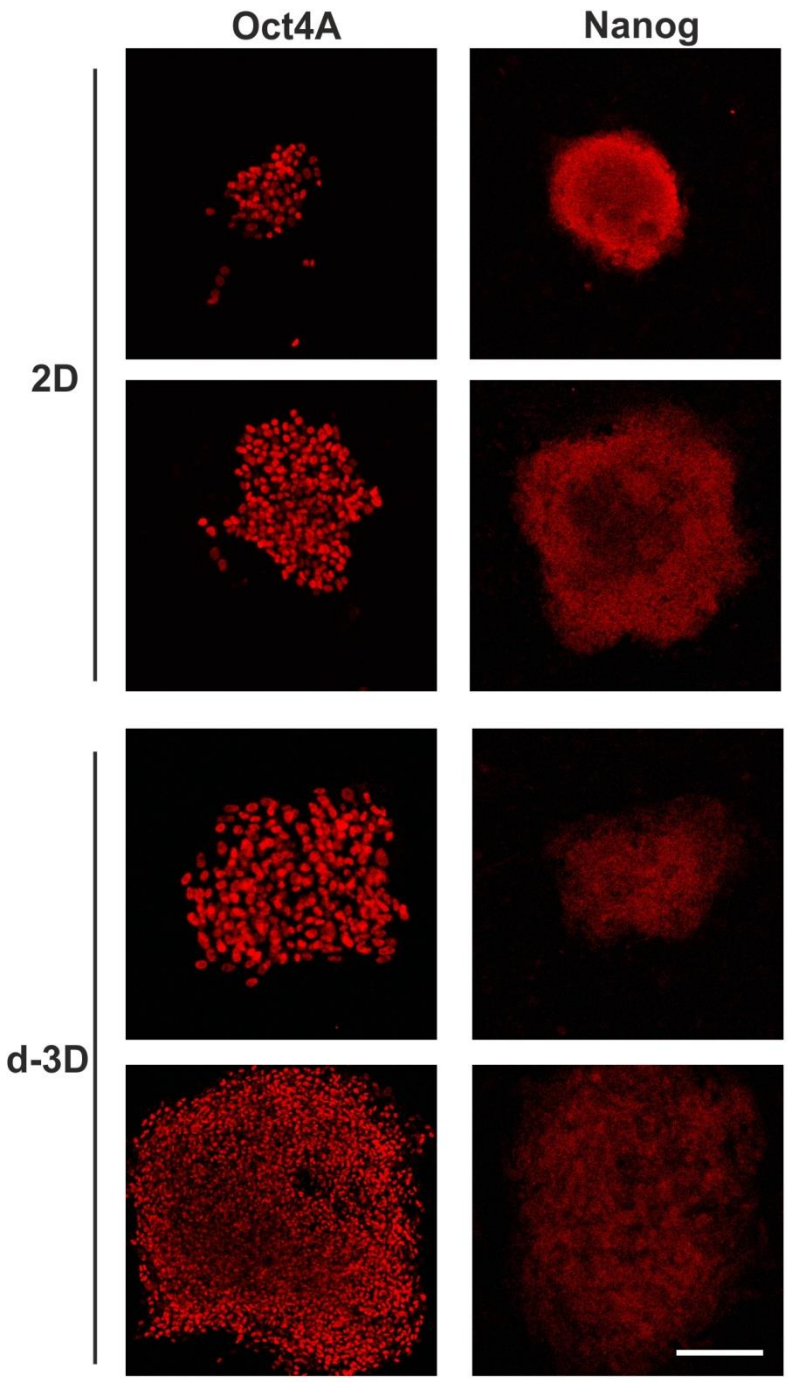

Figure 4.4.18 Assessment of Oct4a and Nanog expression in colonies generated by OKSM transduction of 2D and d-3D MSCs

Colonies generated from OKSM-transduced 2D and d-3D MSCs were stained for Oct4a and Nanog and imaged using fluorescence microscopy. Upper panels show staining of colonies generated from 2D MSCs for Oct4a (left) and Nanog (right). Lower panels show staining of colonies generated from d-3D MSCs for Oct4a (left) and Nanog (right, scale bar = 100µm).

4.4.6 Enhanced expression of pluripotency and reprogramming factors in 3D MSCs is lost within 24 - 48 hours of return to 2D culture

In order to investigate the similarity of reprogramming efficiencies in 2D and d-3D MSCs, three different primary MSC donors were cultured as described in 4.4.5, and samples taken at 5, 24 and 48 hours following return to 2D culture, to track changes in pluripotency factor expression with time in 2D culture. In these experiments, expression in d-3D MSCs at 5, 24 and 48 hours was compared to that in 2D MSCs. The expression of all pluripotency factors returned to 2D MSCs levels in d-3D MSCs. As previously observed when compared to HDF expression levels, the expression of Oct4 (Figure 4.4.19) and Sox2 (Figure 4.4.20) was highest in 3D MSCs and fell in d-3D MSCs 5 hours after return to 2D culture, whilst still remaining higher than levels in 2D MSCs. However within 24 hours of disaggregation expression levels of Oct4 reduced to 2D MSC levels (Figure 4.4.19), and a similar pattern was observed for Sox2, where between 24 and 48 hours after disaggregation, expression fell to 2D MSC levels (Figure 4.4.20). Although not one of the 'Yamanaka factors', Nanog plays a role in pluripotency maintenance, and was included in the four factor combination of reprogramming factors demonstrated to reprogramme HDFs to pluripotency by the Thompson laboratory (Yu et al., 2007). The expression pattern of Nanog was very similar to that of Oct4, with expression levels returning to those observed in 2D MSCs around 24 hours after spheroid disaggregation (Figure 4.4.21). Interestingly, the effect of returning 3D MSCs to 2D culture appeared to be detrimental to Klf4 expression in d-3D MSCs. 24 hours following disaggregation the expression of Klf4 in d-3D MSCs had actually fallen below levels observed in 2D MSCs, with only a small but donor-dependent recovery of expression 48 hours after disaggregation, and on average Klf4 levels were still significantly lower than those in 2D MSCs 48 hours after disaggregation (Figure 4.4.22). Whilst a peak in c-Myc expression was observed 5 hours after return to 2D culture, this effect was transient, with expression in d-3D MSCs returning to 2D MSCs levels within 48 hours of return to 2D culture following spheroid disaggregation (Figure 4.4.23).

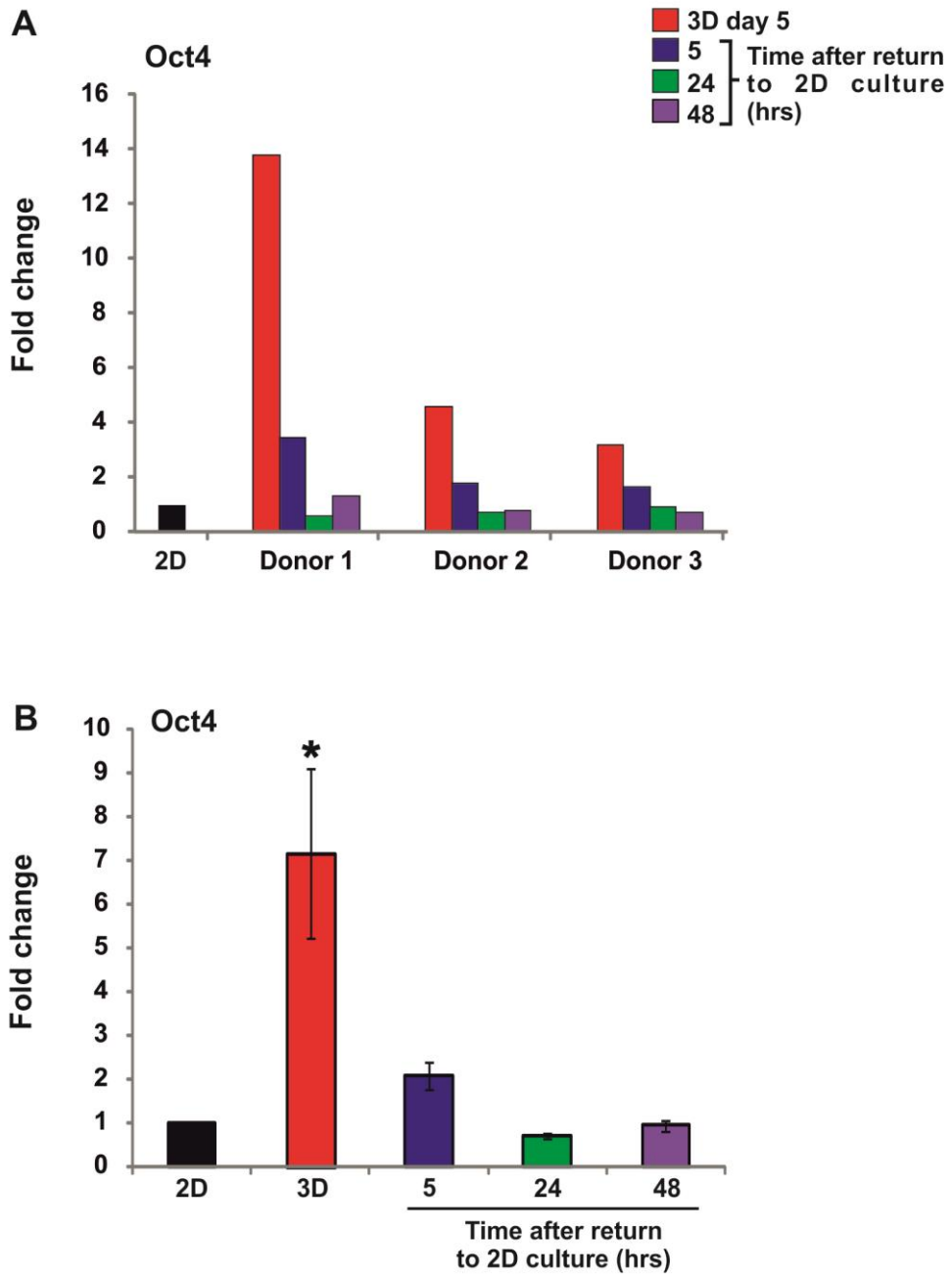

Figure 4.4.19. qPCR analysis of Oct4 expression in MSCs up to 48 hours after spheroid disaggregation.

MSCs from 3 donors were cultured as 2D monolayers and 3D spheroids with an initiating cell number of 60,000 cells for 5 days. After 5 days MSC spheroids were disaggregated to single cells and re-plated on tissue culture plastic for up to 48 hours. cDNA samples were generated and then analysed by qPCR. A) Expression of Oct4 for each donor was normalised to expression of the housekeeping gene GAPDH and made relative to expression levels in donor-matched 2D samples. Fold changes were calculated as 2^{-ddCt}. B) Data from all 3 donors was pooled and subject to statistical analysis, mean fold changes are shown ± SEM, * $p < 0.05$. Statistical significance is relative to expression in 2D MSCs (by Kruskal Wallis test, n = 3).

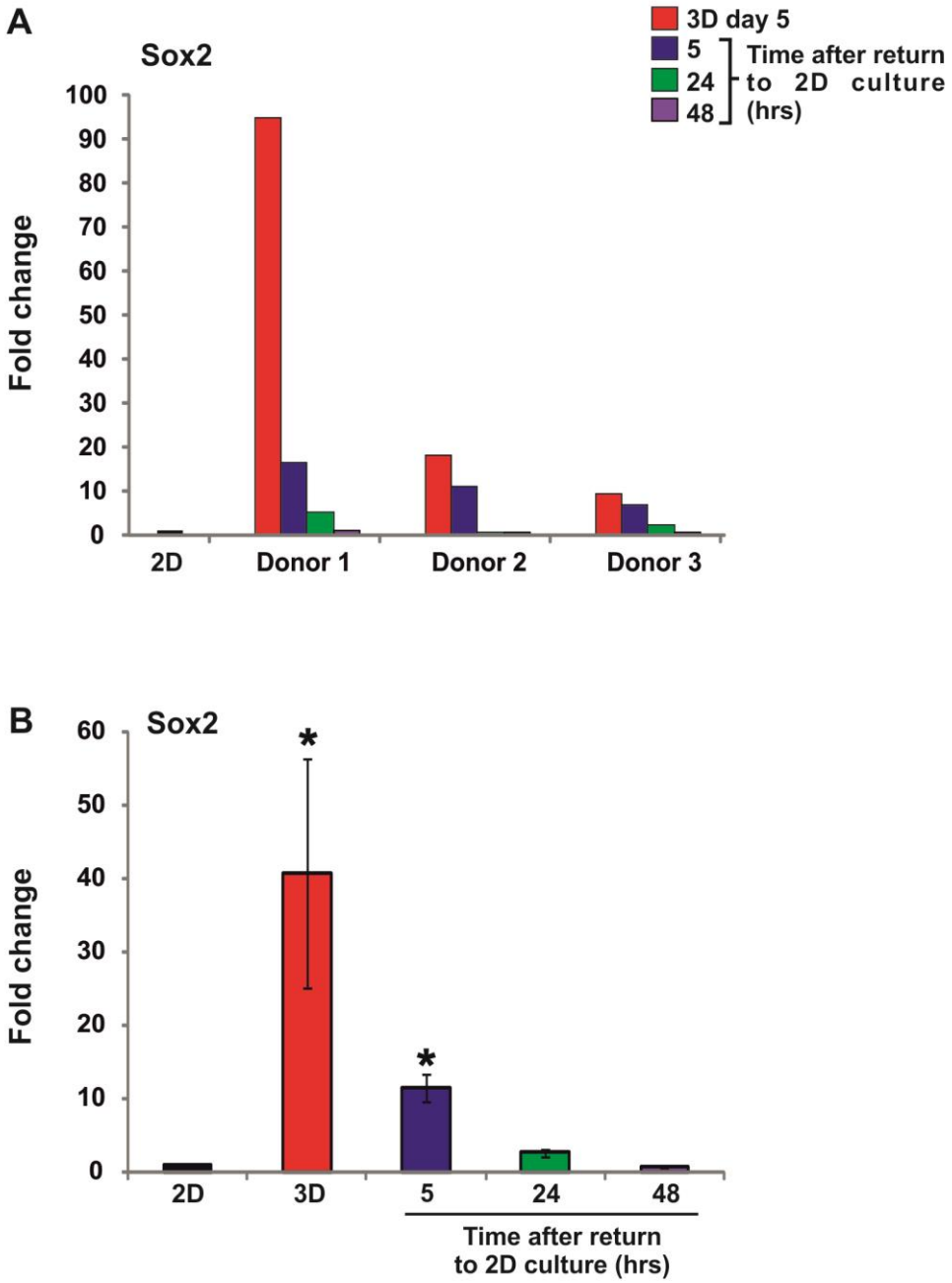

Figure 4.4.20. qPCR analysis of Sox2 expression in MSCs up to 48 hours after spheroid disaggregation.

MSCs from 3 donors were cultured as 2D monolayers and 3D spheroids with an initiating cell number of 60,000 cells for 5 days. After 5 days MSC spheroids were disaggregated to single cells and re-plated on tissue culture plastic for up to 48 hours. cDNA samples were generated and then analysed by qPCR. A) Expression of Sox2 for each donor was normalised to expression of the housekeeping gene GAPDH and made relative to expression levels in donor-matched 2D samples. Fold changes were calculated as 2^{-ddCt}. B) Data from all 3 donors was pooled and subject to statistical analysis, mean fold changes are shown ± SEM, * $p < 0.05$. Statistical significance is relative to expression in 2D MSCs (by Kruskal Wallis test, n = 3).

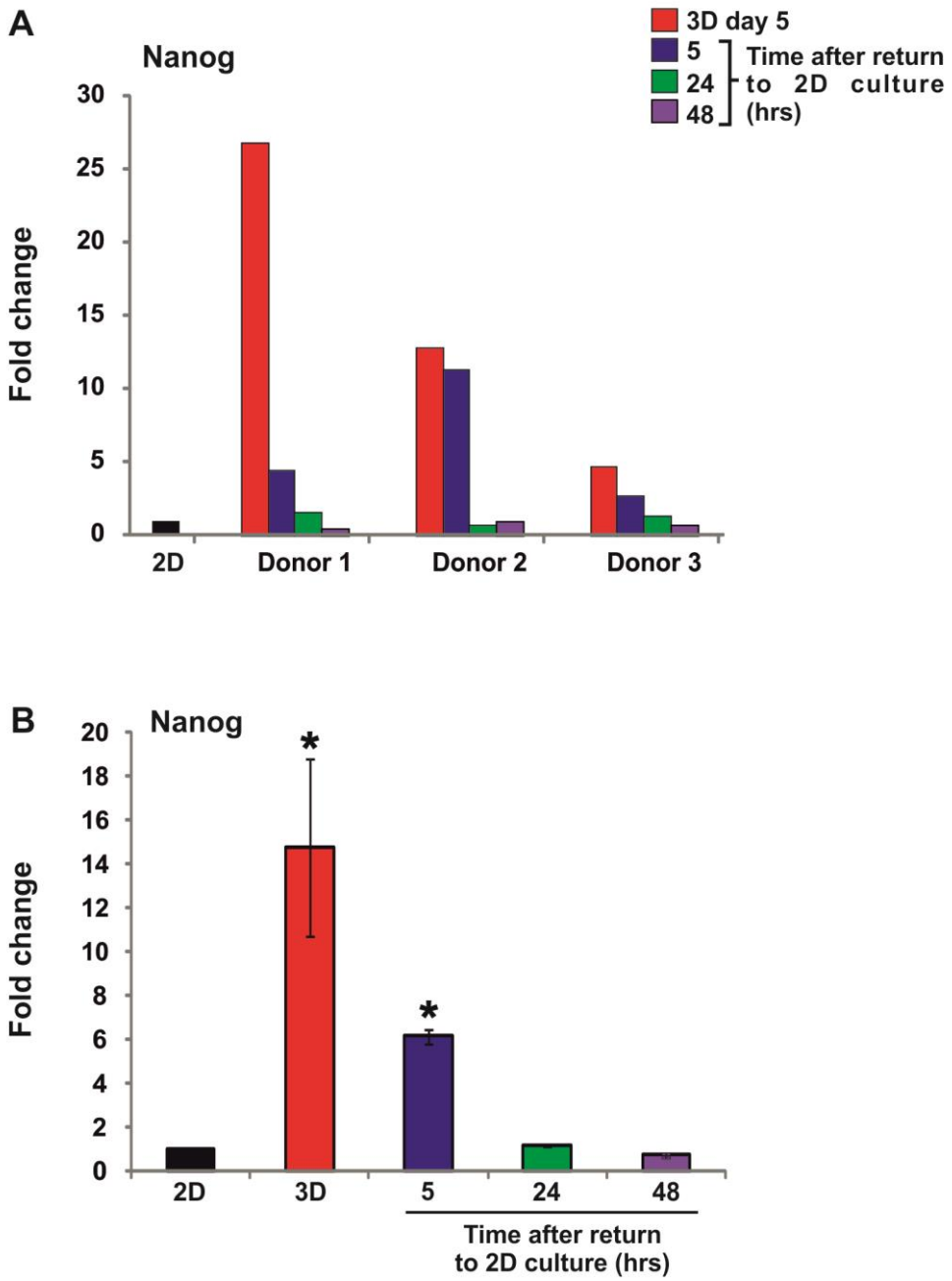

Figure 4.4.21. qPCR analysis of Nanog expression in MSCs up to 48 hours after spheroid disaggregation.

MSCs from 3 donors were cultured as 2D monolayers and 3D spheroids with an initiating cell number of 60,000 cells for 5 days. After 5 days MSC spheroids were disaggregated to single cells and re-plated on tissue culture plastic for up to 48 hours. cDNA samples were generated and then analysed by qPCR. A) Expression of Nanog for each donor was normalised to expression of the housekeeping gene GAPDH and made relative to expression levels in donor-matched 2D samples. Fold changes were calculated as 2^{-ddCt}. B) Data from all 3 donors was pooled and subject to statistical analysis, mean fold changes are shown ± SEM, * $p < 0.05$. Statistical significance is relative to expression in 2D MSCs (by Kruskal Wallis test, n = 3).

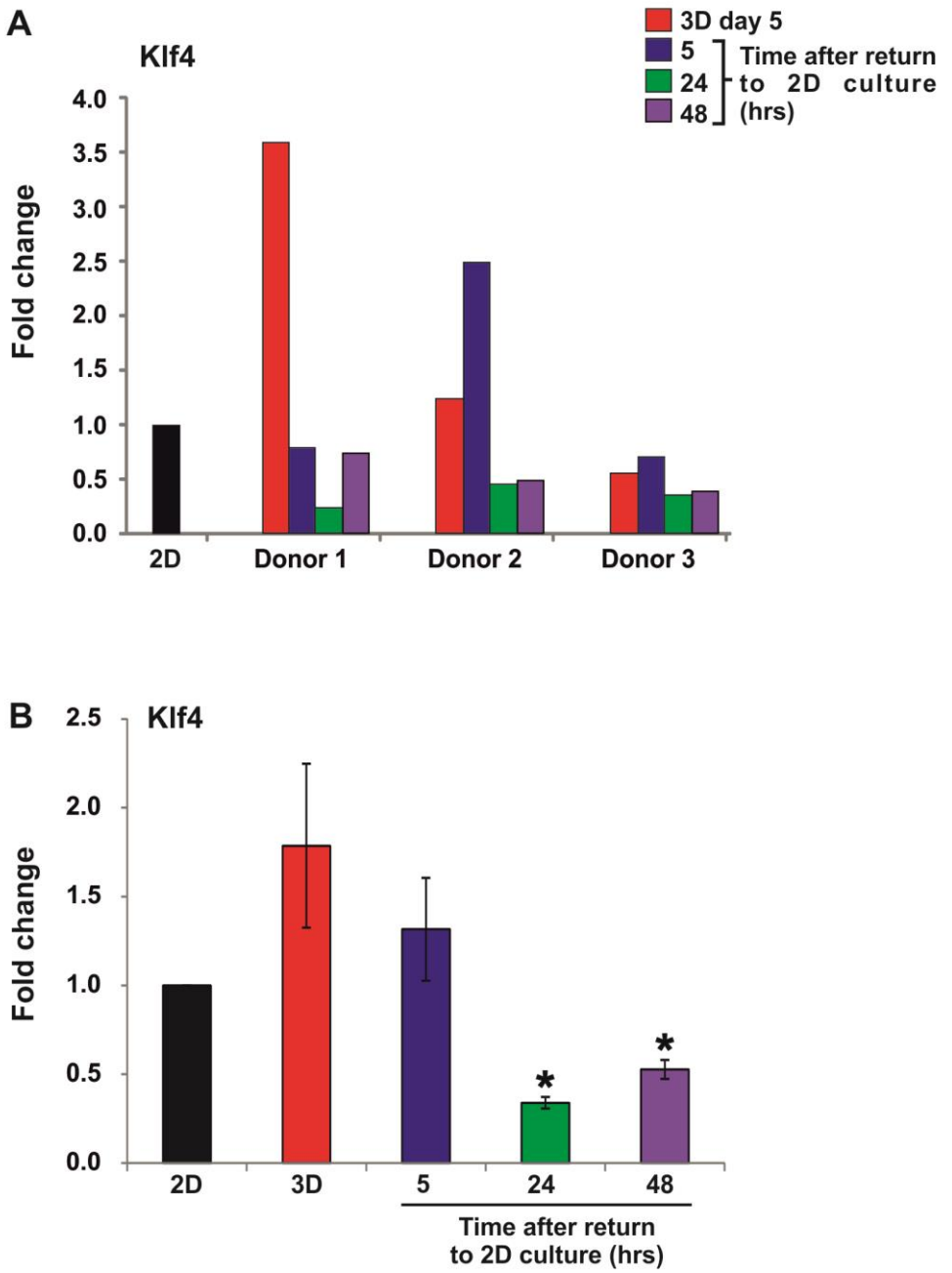

Figure 4.4.22. qPCR analysis of Klf4 expression in MSCs up to 48 hours after spheroid disaggregation.

MSCs from 3 donors were cultured as 2D monolayers and 3D spheroids with an initiating cell number of 60,000 cells for 5 days. After 5 days MSC spheroids were disaggregated to single cells and re-plated on tissue culture plastic for up to 48 hours. cDNA samples were generated and then analysed by qPCR. A) Expression of Klf4 for each donor was normalised to expression of the housekeeping gene GAPDH and made relative to expression levels in donor-matched 2D samples. Fold changes were calculated as 2^{-ddCt}. B) Data from all 3 donors was pooled and subject to statistical analysis, mean fold changes are shown ± SEM, * $p < 0.05$. Statistical significance is relative to expression in 2D MSCs (by Kruskal Wallis test, n = 3).

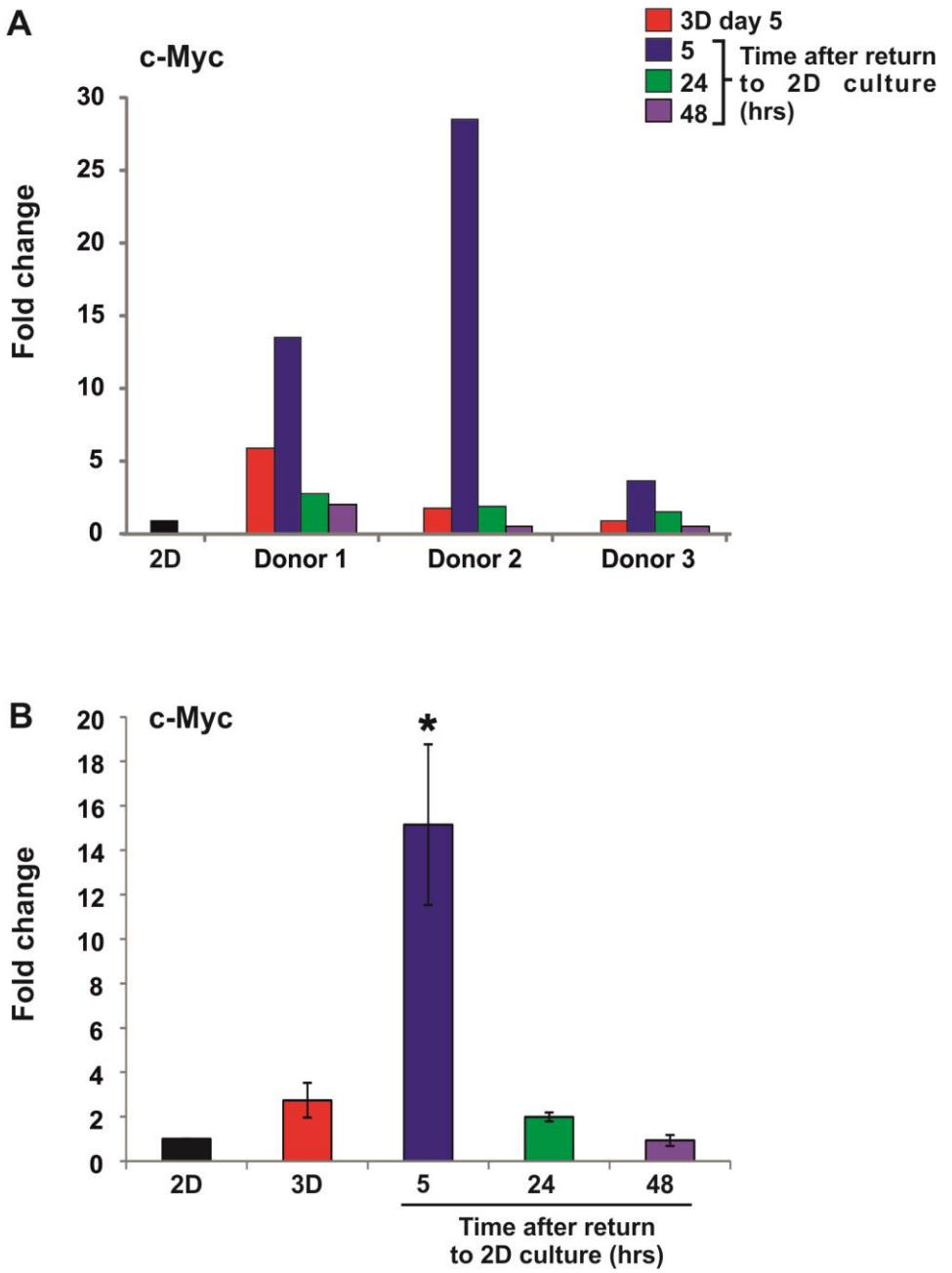

Figure 4.4.23. qPCR analysis of c-Myc expression in MSCs up to 48 hours after spheroid disaggregation.

MSCs from 3 donors were cultured as 2D monolayers and 3D spheroids with an initiating cell number of 60,000 cells for 5 days. After 5 days MSC spheroids were disaggregated to single cells and re-plated on tissue culture plastic for up to 48 hours. cDNA samples were generated and then analysed by qPCR. A) Expression of c-Myc for each donor was normalised to expression of the housekeeping gene GAPDH and made relative to expression levels in donor-matched 2D samples. Fold changes were calculated as 2^{-ddCt}. B) Data from all 3 donors was pooled and subject to statistical analysis, mean fold changes are shown ± SEM, * $p < 0.05$. Statistical significance is relative to expression in 2D MSCs (by Kruskal Wallis test, n = 3).

4.4.7 Suspension culture of d-3D MSCs maintains enhanced expression of pluripotency factors following spheroid disaggregation

Disaggregation studies demonstrated that enhanced expression of pluripotency factors in 3D MSCs was dependent on 3D culture, and that a return to adherent culture resulted in a return to 2D expression levels of these factors. In order to investigate if it was possible to expand 3D MSCs without the need to re-seed onto tissue culture plastic, MSCs were cultured as spheroids containing 60,000 cells for 5 days, before disaggregation to small cell clumps, using a more gentle method of enzymatic digestion. Semi-solid media containing 1% methyl cellulose, is a gel-like culture media, where cells are held in a static position, but do not adhere to a substrate so preventing spreading and acquisition of typical 2D MSC shape and growth behaviour. The small cell clumps generated from spheroid disaggregation (d-3D MSCs) were seeded into semi-solid media, containing either 5% FBS, or a serum-free media used for the culture of pluripotent cells. Over 7 days in culture, the d-3D MSC clusters were observed to increase in size, suggesting the cells were proliferating, and behaviour seemed similar in both media formulations (Figure 4.4.24. A). To test the colony-forming capacity over time in semi-solid media, further experiments were performed, with disaggregation to single cells/cell clumps of very few cells. For these experiments media containing 5% FBS was selected, as in the previous experiments there was no obvious differences in cell behaviour in the different media. MSCs from 2 donors were tested under these conditions, and again over 7 days demonstrated an increase in cell clump size, indicative of proliferative capacity from single cells/small cell clumps within the cultures Figure 4.4.24. B).

As discussed above, enhanced expression of pluripotency factors was lost when d-3D MSCs were re-seeded on tissue culture plastic. RNA was isolated from d-3D MSCs cultured in semi-solid media for 7 days, and expression of pluripotency factors was analysed by qPCR. Expression was normalised to GAPDH and made relative to the donor-matched 2D (adherent) sample. In both semi-solid medias tested, d-3D MSCs maintained elevated expression of Oct4, Nanog, Sox2 and telomerase, compared to expression in 2D MSCs. Oct4 expression was up-regulated around 3-6 fold (dependent on donor) in d-3D MSCs cultured in semi-solid media with 5% serum, whilst up-regulation of around 3.5 fold was observed in serum-free

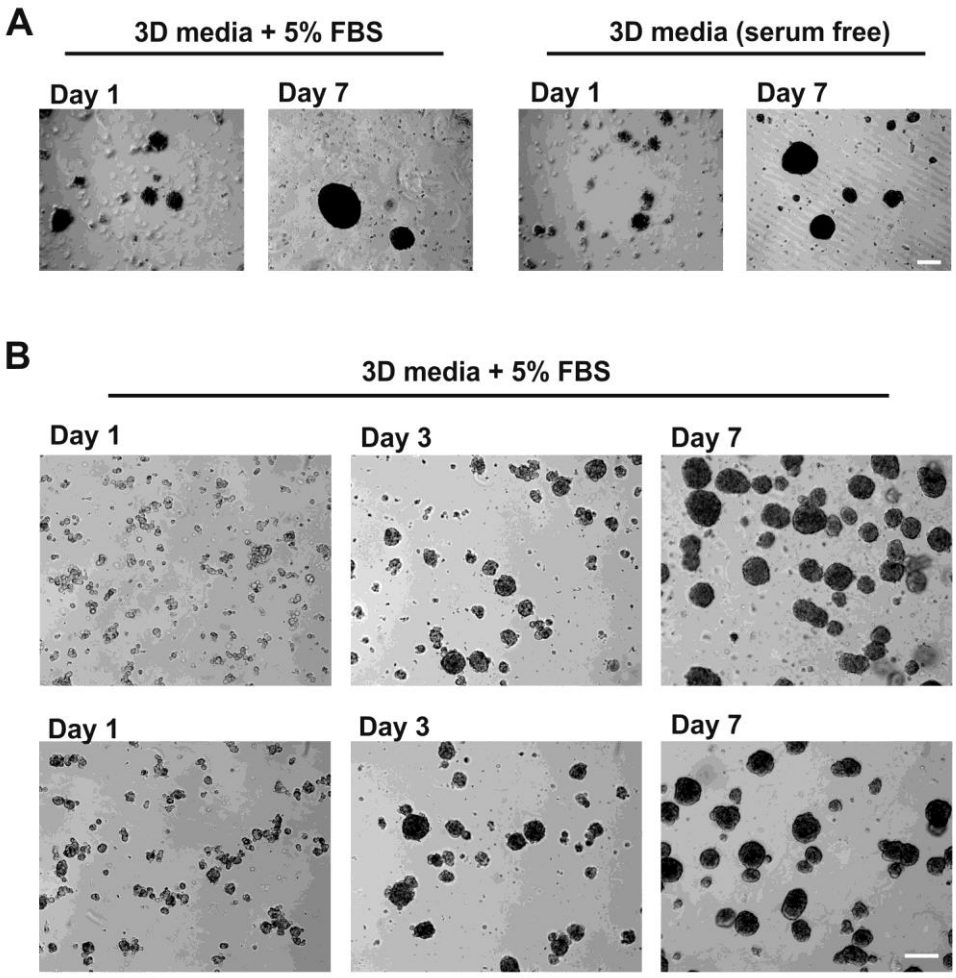

Figure 4.4.24. Analysis of MSC growth in non-adherent culture conditions following 3D spheroid disaggregation

MSC spheroids were initiated (60,000 cells per spheroid) and cultured under 3D conditions for 5 days. On day 5 spheroids were disaggregated and re-seeded as cell clumps into semi-solid media (containing 1% methyl cellulose) with 5% serum or serum-free. A) Light microscopy images of MSCs disaggregated to small cell clumps and cultured for 7 days in semi-solid media with 5% serum (left panel) or serum-free (right panel). B) Light microscopy images of MSCs from 2 donors disaggregated to single cells/very small cell clumps and cultured for 7 days in semi-solid media with 5% serum (scale bars = 100µm).

semi-solid media (Donor 1 sample was lost during recovery from media) (Figure 4.4.25. A). Similar results were observed for Nanog expression, although the up-regulation of Nanog was much more variable between donors (4-24 fold in media with 5% serum). Enhancement of Nanog expression in serum-free media was highly similar to media with serum in Donor 2 (Figure 4.4.25. B). Expression of both Sox2 and telomerase increased in both medias, although again, the expression changes between donors was highly variable. In media with 5% serum Sox2 expression was up-regulated 4-200 fold dependent on donor, whilst in Donor 2 culture in serum-free media resulted in a 250-fold increase in expression compared to 2D monolayer levels (Figure 4.4.26. A). Similarly expression of telomerase in serum free media increased around 66 fold in Donor 2, whilst up-regulation varied between 3-44 fold in media with 5% serum compared to 2D monolayer levels (Figure 4.4.26. B). This work supports the disaggregation studies with re-seeding on to plastic, and confirms that 3D non-adherent culture is required for the maintenance of a de-differentiated phenotype.

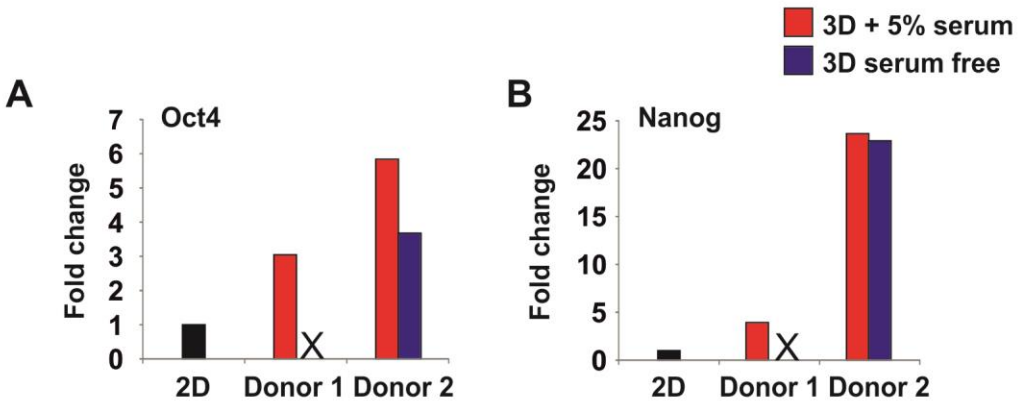

	Oct4				Nanog			
	Donor 1		Donor 2		Donor 1		Donor 2	
	Mean dCt	± *SEM*	*Mean dCt*	± *SEM*	*Mean dCt*	± *SEM*	*Mean dCt*	± *SEM*
2D	3.89	0.13	4.38	0.07	8.84	0.08	9.06	0.08
3D 5% serum	2.29	0.07	1.83	0.01	6.88	0.09	4.50	0.04
3D serum free	-	-	2.50	0.05	-	-	4.55	0.04

Figure 4.4.25. qPCR analysis of Oct4 and Nanog expression in MSCs after spheroid disaggregation and culture in semi-solid media.

MSCs from 2 donors were cultured as 2D monolayers and 3D spheroids with an initiating cell number of 60,000 cells for 5 days. After 5 days MSC spheroids were disaggregated to small cell clumps and re-seeded into semi-solid media (containing 1% methyl cellulose) with 5% serum or serum-free. cDNA samples were generated and then analysed by qPCR. A) Expression of Oct4 for each donor was normalised to expression of the housekeeping gene GAPDH and made relative to expression levels in donor-matched 2D samples. B) Expression of Nanog for each donor was normalised to expression of the housekeeping gene GAPDH and made relative to expression levels in donor-matched 2D samples, fold changes were calculated as 2^{-ddCt}. Average dCt values ± SEM for technical replicates of both genes are shown in the table.

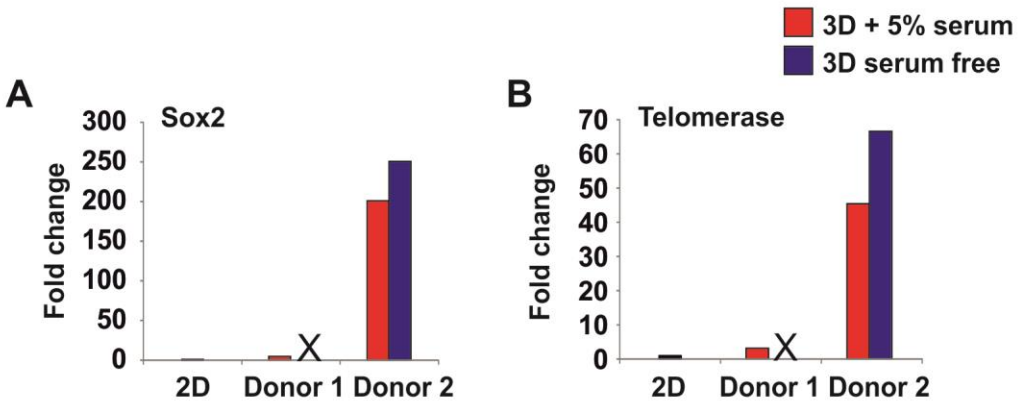

	Sox2				Telomerase			
	Donor 1		Donor 2		Donor 1		Donor 2	
	Mean dCt	± *SEM*	*Mean dCt*	± *SEM*	*Mean dCt*	± *SEM*	*Mean dCt*	± *SEM*
2D	12.05	0.13	12.14	0.96	12.10	0.20	11.44	0.06
3D 5% serum	9.78	0.17	5.06	0.04	10.49	0.42	5.96	0.12
3D serum free	-	-	4.72	0.09	-	-	5.40	0.11

Figure 4.4.26. qPCR analysis of Sox2 and Telomerase expression in MSCs after spheroid disaggregation and culture in semi-solid media.

MSCs from 2 donors were cultured as 2D monolayers and 3D spheroids with an initiating cell number of 60,000 cells for 5 days. After 5 days MSC spheroids were disaggregated to small cell clumps and re-seeded into semi-solid media (containing 1% methyl cellulose) with 5% serum or serum-free. cDNA samples were generated and then analysed by qPCR. A) Expression of Sox2 for each donor was normalised to expression of the housekeeping gene GAPDH and made relative to expression levels in donor-matched 2D samples. B) Expression of Telomerase for each donor was normalised to expression of the housekeeping gene GAPDH and made relative to expression levels in donor-matched 2D samples, fold changes were calculated as 2^{-ddCt}. Average dCt values ± SEM for technical replicates of both genes are shown in the table.

4.4.8 3D MSCs show enhanced mesodermal potency *in vivo* and express markers of early mesendoderm *in vitro*

As described above, although 3D MSCs did not form teratomas on *in vivo* implantation, they did give rise to small, organised tissue masses (Figure 4.4.11). This demonstrated an enhanced ability to form tissue *in vivo*, as 2D MSCs were without effect. Masson's trichrome staining distinguishes collagen (blue) from smooth muscle (red) on histological sections. Tissue masses from 3D MSCs showed a substantial collagen component (connective tissue - blue) and also displayed some organised blocks of muscle (red) (Figure 4.4.27. A). In contrast, teratomas from ESCs showed a reduced connective tissue component, indicated by reduced blue staining, and lacked the organised muscle blocks observed in tissue masses form 3D MSCs (Figure 4.4.27. B).

Considering the developmental origins of MSCs, and their propensity to form mesodermal-like tissues *in vivo*, expression of markers associated with early mesendoderm was examined. MSCs from two primary donors were cultured as 2D monolayers and 3D spheroids for up to 5 days in culture. The expression of all mesodermal markers examined was up-regulated in 3D versus 2D MSCs across all time points. However, maximal expression of markers did vary across time points, and there was some inter-donor variation observed. The expression of Brachyury was observed to increase in 3D culture, with maximal up-regulation of around 6-7 fold compared to 2D cultures. Donor 1 showed a peak of Brachyury expression on day 5 of 3D culture, whilst in Donor 2 the peak was on day 3 with a slight reduction in expression by day 5 (Figure 4.4.28. A). Both donors showed an increase in Goosecoid expression with time in 3D, peaking at day 5, and with a 5.5-7.5 fold increase in expression compared to the donor matched 2D sample (Figure 4.4.28. B).

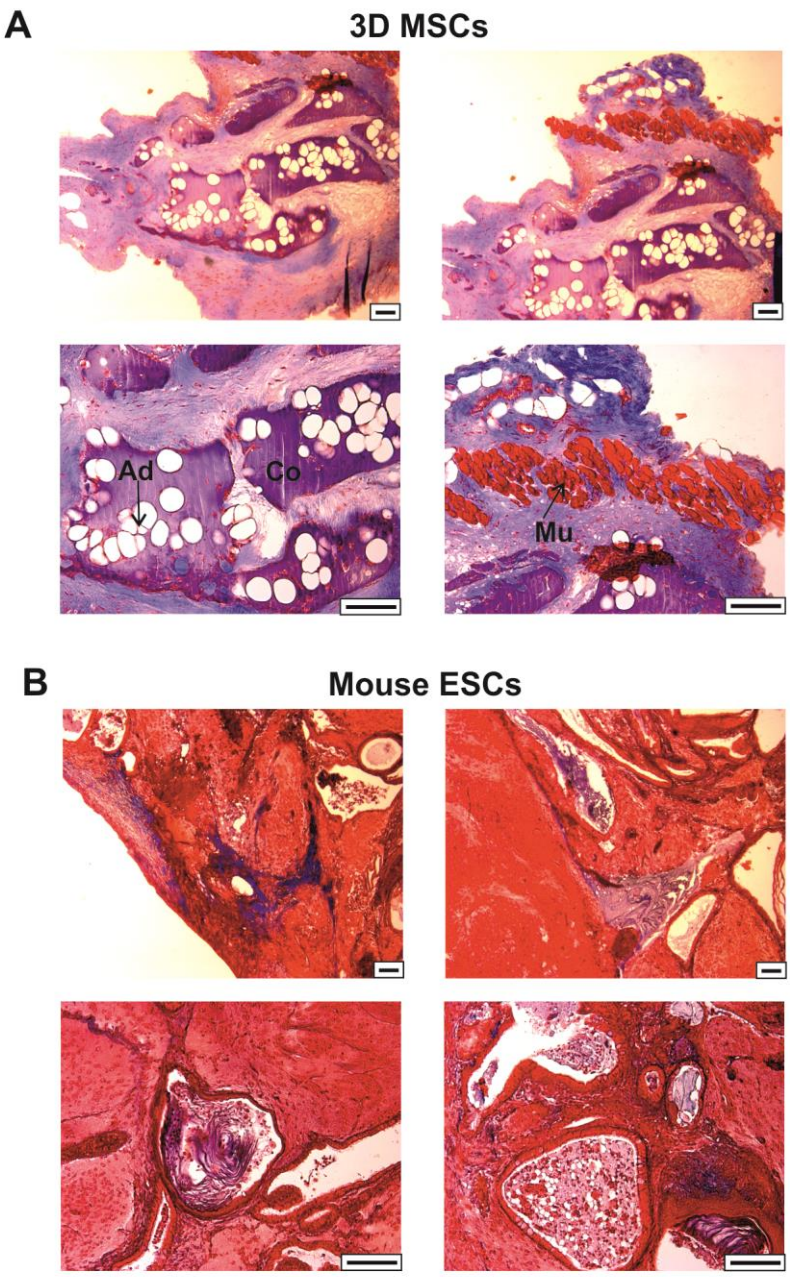

Figure 4.4.27. Histological analysis of the generation of mesoderm-derived tissue following implantation into nude mice

3D MSC spheroids (initial cell number = 60’ 000 cells) were cultured in 3D conditions for 5 days before subcutaneous injection into nude mice. Mouse ESCs were also implanted as a positive control for teratoma formation. After 12 weeks tissue samples were recovered, fixed and stained with Massons Trichome. Light microscopy images of A) tissue masses generated by 3D MSCs and B) teratomas from mouse ESC positive controls. Labels indicate tissues of mesodermal origin – Mu = muscle, Ad = adipose, Co = connective tissue; scale bar = 100µm

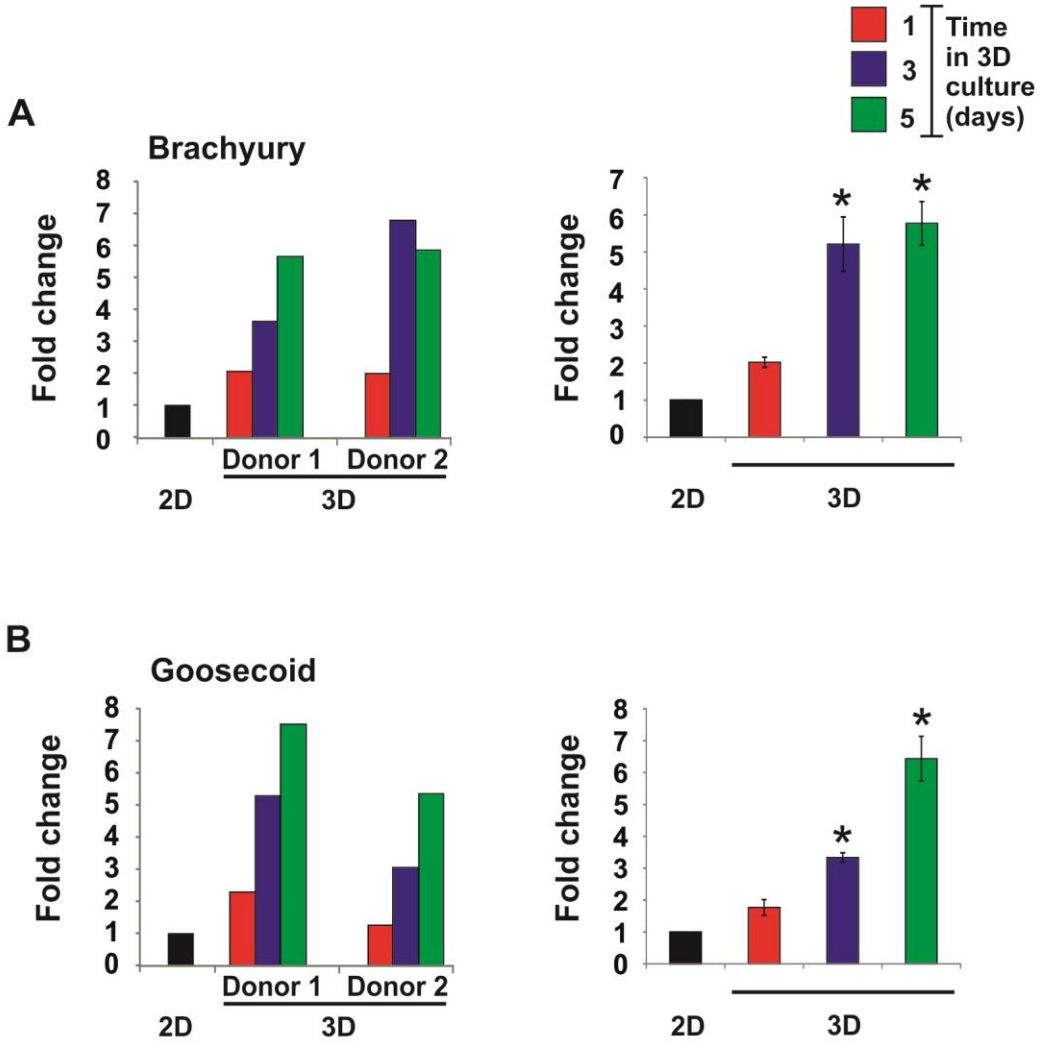

Figure 4.4.28. qPCR analysis of expression of Brachyury and Goosecoid in MSCs over time in 3D culture

MSCs from 2 donors were cultured as 2D monolayers and 3D spheroids with an initiating cell number of 60,000 cells for up to 5 days in culture. cDNA samples were generated and then analysed by qPCR. Expression of target gene for each donor was normalised to expression of the housekeeping gene GAPDH and made relative to expression levels in the donor matched 2D sample. Fold changes were calculated as 2^{-ddCt}. A) Expression of Brachyury in 2 different MSC donors (left panel), and pooled donor data (right panel). B) Expression of Goosecoid in 2 different MSC donors (left panel), and pooled donor data (right panel). Pooled donor data was subject to statistical analysis, mean fold changes are shown ± SEM, * $p < 0.05$. Statistical significance is relative to expression in 2D MSCs (by Kruskal Wallis test, n = 2).

KDR expression fell slightly on day 1 of 3D culture, but by day 3 expression of KDR had peaked in both donors, with levels 3-4.7 fold higher than in 2D MSCS. On day 5 expression of KDR had fallen in both donors, although this effect was more pronounced in Donor 2. In Donor 1 expression at days 3 and 5 was highly similar (Figure 4.4.29. A). Expression of Mixl1 increased with time in 3D culture, up to day 3, with up-regulation of between 6-11 fold, depending on donor, and compared to 2D levels. By day 5 of 3D culture the expression of Mixl1 had fallen in both donors examined, although it remained higher than observed at day 1 of 3D culture (Figure 4.4.29. B). Expression of CXCR4, a marker of haemangioblasts (blood/endothelial precursors) was highly up-regulated in 3D cultures. Although the expression pattern of CXCR4 was inconsistent across donors, both donors demonstrated prominent expression increases when cultured as 3D spheroids. Donor 1 showed increases of between 20-30 fold, whilst expression of CXCR4 increased 30-70 fold during 3D culture of Donor 2 (Figure 4.4.30).

The expression of a number of these early mesendoderm markers were also examined by immunocytochemistry, to determine if detectable protein could be identified in 3D MSCs. MSCs were cultured as 3D spheroids for 5 days, snap-frozen and cryosectioned before incubation with specific antibodies. Positive staining for Brachyury (Figure 4.4.31. A) and CXCR4 (Figure 4.4.31. C) was observed, indicating that increased transcript levels did result in the production of sufficient protein for detection by immunocytochemistry. Weak positive staining for KDR was also observed (Figure 4.4.31. B). It is possible that KDR protein expression may have been higher at day 3, as was observed for KDR transcript.

It was possible that sub-populations of cells within the 3D MSCs had undergone autophagy-driven reprogramming to different degrees due to their location within the spheroid. To investigate this, images of 3D MSC sections stained with anti-Brachyury antibody were analysed using Volocity software to identify the highest and lowest Brachyury-expressing cells. Using this technique, it was clear that for both the lowest (top panel) and highest (bottom panel) Brachyury fluorescence intensity cells, there was a relatively even distribution of cells within the section and that no obvious sub-population could be identified by low/high Brachyury expression (Figure 4.4.32).

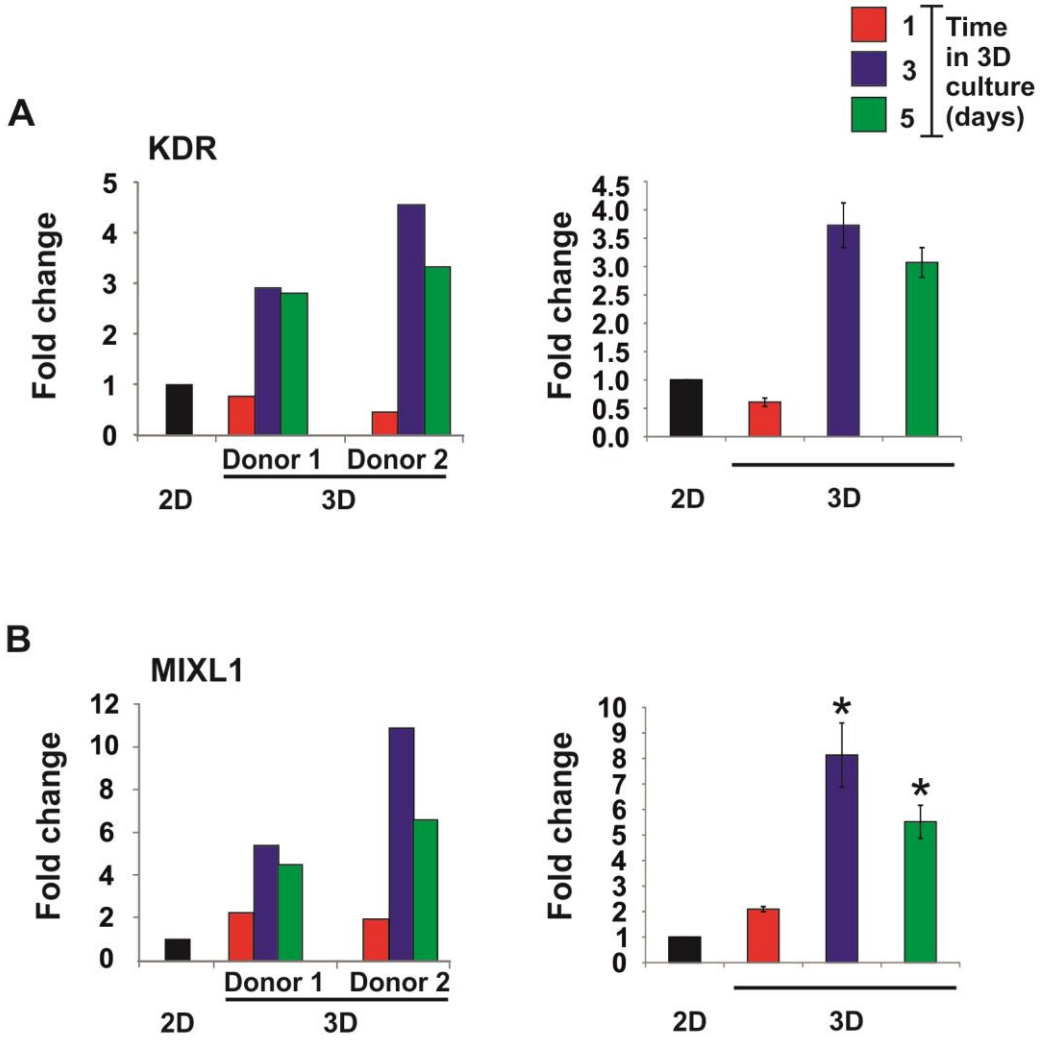

Figure 4.4.29 qPCR analysis of expression of KDR and MIXL1 in MSCs over time in 3D culture

MSCs from 2 donors were cultured as 2D monolayers and 3D spheroids with an initiating cell number of 60,000 cells for up to 5 days in culture. cDNA samples were generated and then analysed by qPCR. Expression of target gene for each donor was normalised to expression of the housekeeping gene GAPDH and made relative to expression levels in the donor matched 2D sample. Fold changes were calculated as 2^{-ddCt}. A) Expression of KDR in 2 different MSC donors (left panel), and pooled donor data (right panel). B) Expression of MIXL1 in 2 different MSC donors (left panel), and pooled donor data (right panel). Pooled donor data was subject to statistical analysis, mean fold changes are shown ± SEM, * $p < 0.05$. Statistical significance is relative to expression in 2D MSCs (by Kruskal Wallis test, n = 2).

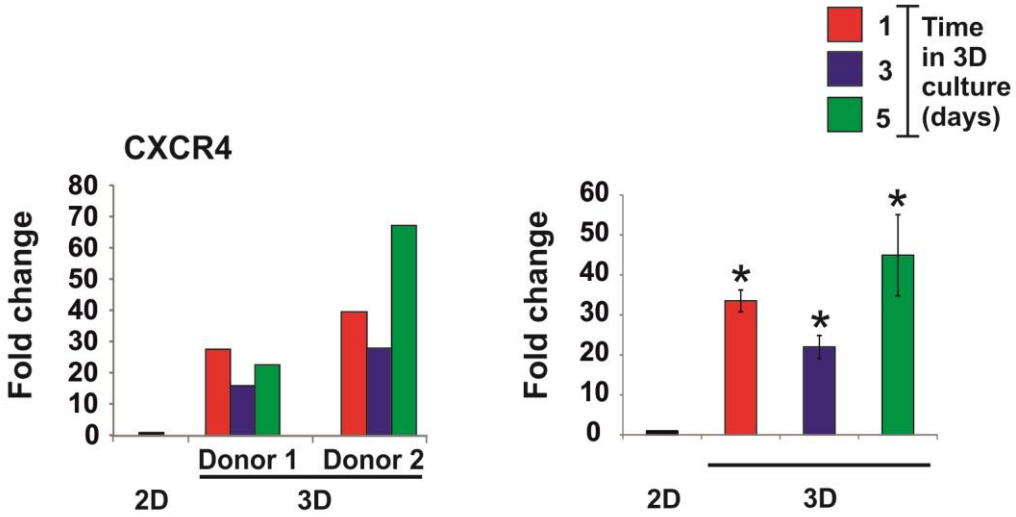

Figure 4.4.30. qPCR analysis of expression of CXCR4 in MSCs over time in 3D culture

MSCs from 2 donors were cultured as 2D monolayers and 3D spheroids with an initiating cell number of 60,000 cells for up to 5 days in culture. cDNA samples were generated and then analysed by qPCR. Expression of CXCR4 for each donor was normalised to expression of the housekeeping gene GAPDH and made relative to expression levels in the donor matched 2D sample. Fold changes were calculated as 2^{-ddCt}. Expression of CXCR4 in 2 different MSC donors (left panel), and pooled donor data (right panel). Pooled donor data was subject to statistical analysis, mean fold changes are shown ± SEM, * $p < 0.05$. Statistical significance is relative to expression in 2D MSCs (by Kruskal Wallis test, n = 2).

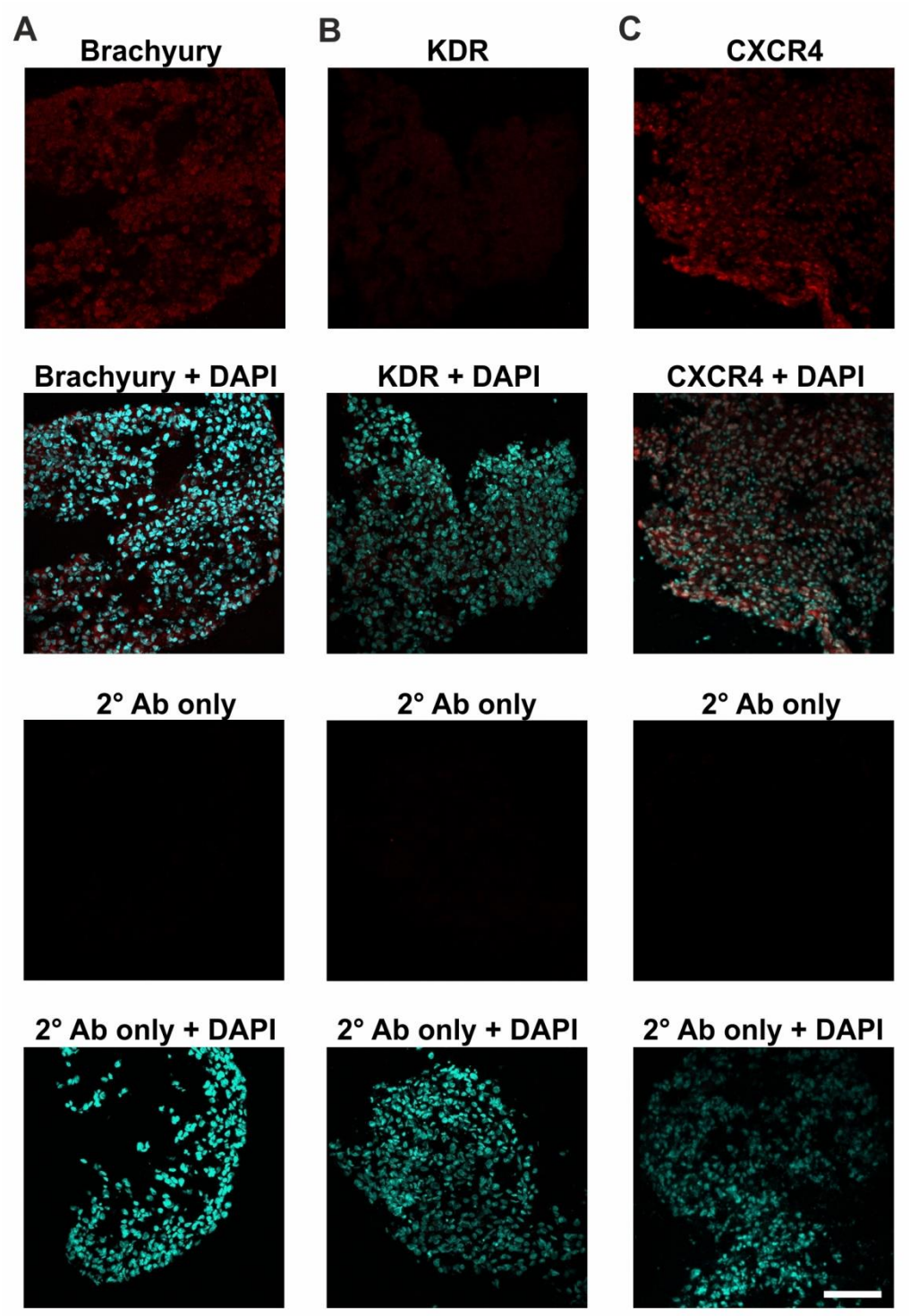

Figure 4.4.31. Staining of 3D MSC spheroid sections for early mesodermal markers

3D spheroids (60,000 MSCs) were cultured for 5 days. Spheroids were then snap-frozen, sectioned and stained for markers of early mesoderm. Samples were imaged using confocal microscopy. Red staining for Brachyury (A), KDR (B) and CXCR4 (C), with DAPI counterstain (cyan) of 3D MSC sections (upper two panels). Lower two panels show matched secondary antibody only controls (red) with DAPI (cyan). Scale bar = 100µm.

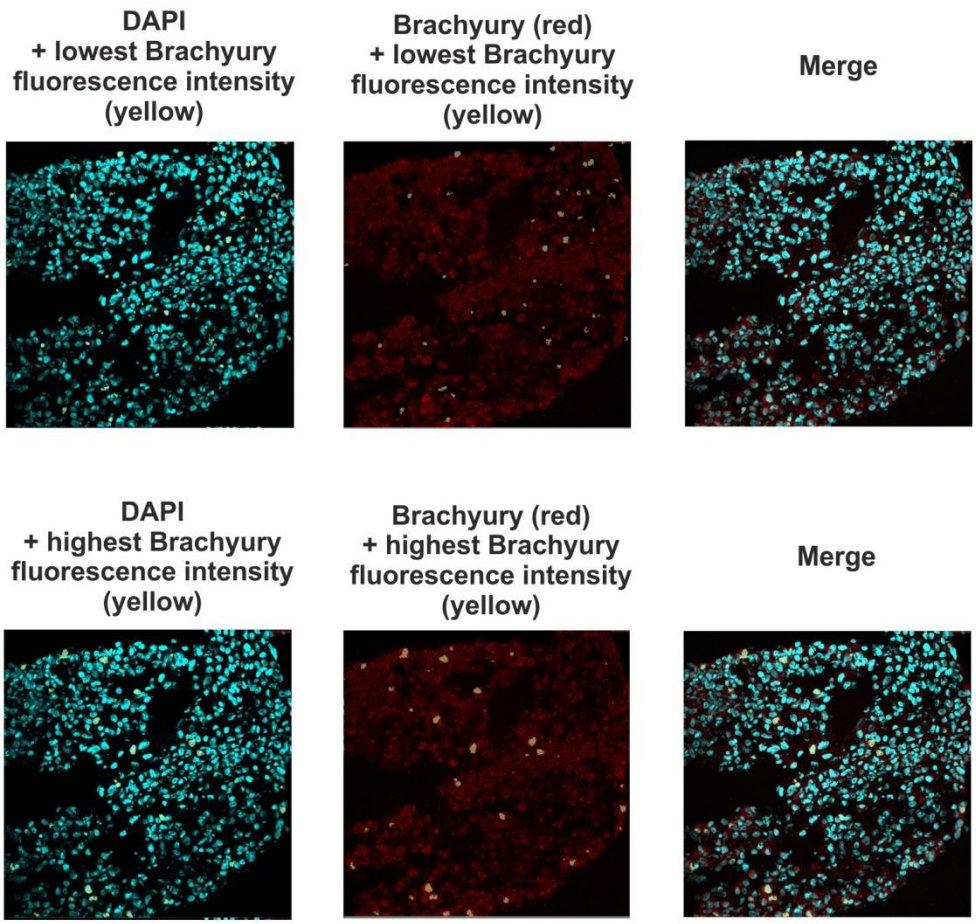

Figure 4.4.32. Analysis of the distribution of Brachyury$^+$ MSCs within the 3D spheroid structure

MSCs were cultured as 3D spheroids with an initiating cell number of 60,000 cells for 5 days in culture. Spheroids were then snap-frozen, sectioned and stained for Brachyury (red) with DAPI (cyan). Samples were imaged using confocal microscopy. The image was subject to analysis with the Velocity Software program, to identify cells expressing the lowest (top panel) and highest (bottom panel) levels of Brachyury, which were highlighted in yellow (n = 48).

CXCR4 is a marker of mesoderm and haemangioblasts (Oldershaw et al., 2010), and is expressed by early haematopoietic progenitors, acting as a marker of definitive haematopoiesis during embryogenesis (Moepps et al., 2000). CXCR4 expression was highly up-regulated in 3D MSCs. To test if enhanced expression of early mesendoderm/haemangioblast markers indicated enhanced *in vitro* haematopoietic potential in 3D MSCs, 2D and 3D MSCs were cultured for 5 days. 3D MSCs were disaggregated to a single cell suspension (d-3D MSCs), and 2D MSCs were detached from plastic and prepared as a single cell suspension. The cell suspensions were then mixed with Methocult (a semi-solid methyl cellulose-based haematopoietic induction media). After 16 days in this media, cells were examined by light microscopy to monitor the appearance of haematopoietic-like colonies. 2D monolayer MSCs remained as single cells and very few tiny cell clusters were observed. There also appeared to be increased cell debris in 2D samples, indicative of cell death (Figure 4.4.33, top panels). In contrast, colonies were observed in d-3D MSC samples, which were larger, irregular in shape, and appeared to be producing a 'halo' of smaller cells around them (Figure 4.4.33, bottom panels, arrows indicate 'budding' cells). These colonies were similar, but not typical, of the blast-like colonies of early haematopoietic progenitors seen in a standard CFU assay using CD34+ cells. Further investigation, such as isolation and analysis for CD45-positivity would confirm the haematopoietic status of the colonies derived from d-3D MSCs.

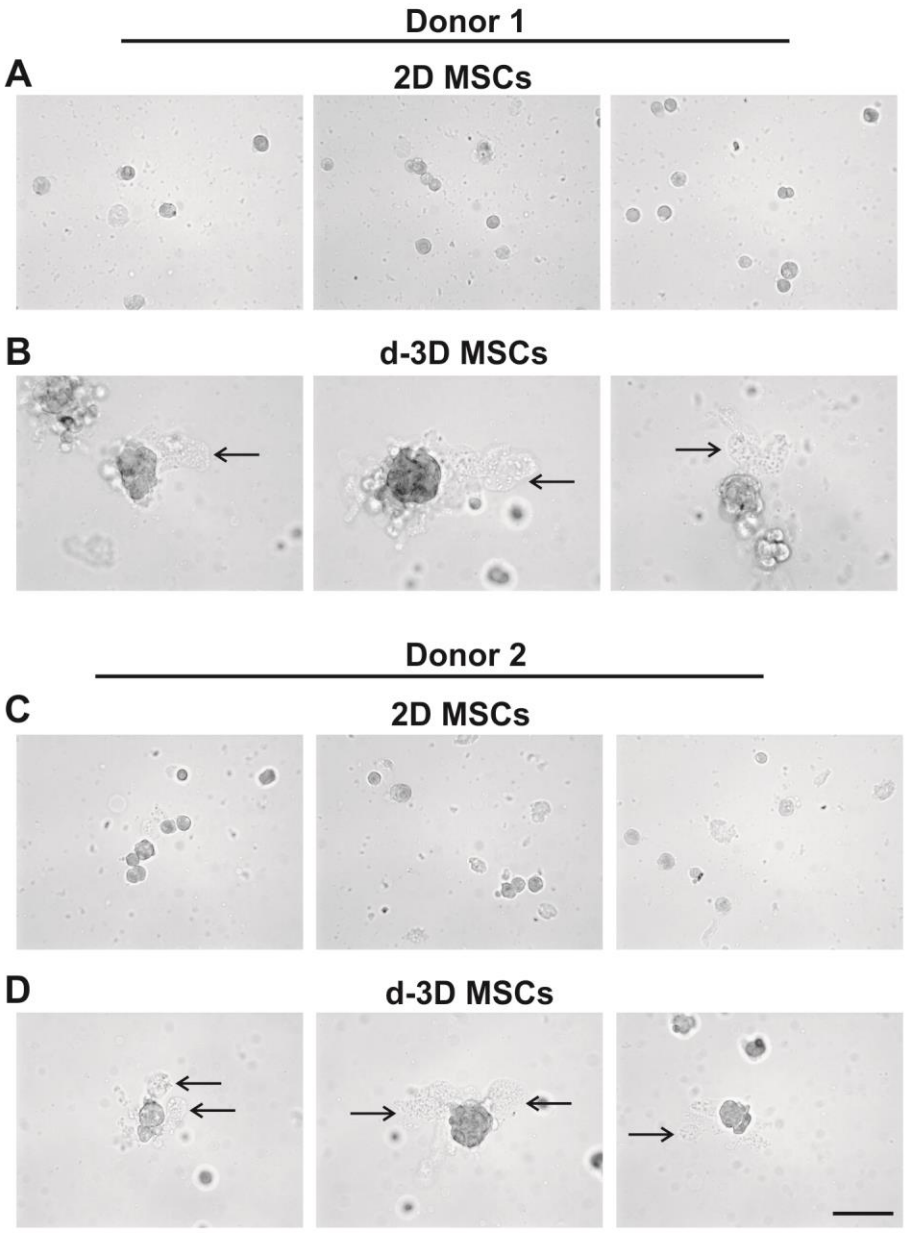

Figure 4.4.33 Assessment of MSC haematopoietic CFU ability in semi-solid induction media

3D spheroids were initiated from 60,000 MSCs and cultured for 5 days, before disaggregation to a single cell suspension. 2D and d-3D MSCs were seeded in haematopoietic induction media, and cultured for 16 days, before being analysed with brightfield microscopy for the presence of haematopoietic-like colonies. Example images from 2 different MSC donors for 2D (A, C) and d-3D (B, D) samples are shown. (Scale bar = 100μm, arrows indicate cells 'budding' from d-3D MSC colonies)

4.4.9 3D culture reverses morphological changes and growth arrest associated with replicative senescence

As described in section 3.4.3, when 3D MSCs were disaggregated and re-seeded onto tissue culture plastic, they re-adopted a typical 2D MSC morphology over 24-48 hours. However, in relation to the originating 2D MSC population, the size and morphology of d-3D MSCs was different. d-3D MSCs were smaller, and noticeably less spread out than the 2D MSCs they originated from. When 2D MSCs are maintained in culture for long periods of time, they gradually acquire morphological features of senescent cells, becoming larger, flatter and more spread out. There is also a reduction in proliferative capacity over a number of passages, although the time taken to reach cellular senescence is donor-dependent. Given that 3D MSCs express markers of a more primitive state, and d-3D MSCs appeared morphologically distinct from *in vitro* cultured MSCs, the effects of 3D culture on *in vitro*-aged MSCs was determined. 2D MSCs were cultured *in vitro* until they ceased to proliferate (Figure 4.4.34.A). At this stage, 2D MSCs had a flat, well spread morphology, typical of non-proliferative/senescent cells (Figure 4.4.34.B, left panel). These cells were then cultured under optimised 3D conditions for 5 days. Following disaggregation and re-seeding onto plastic, d-3D MSCs appeared morphologically distinct from the originating 2D MSC population, they were small, and non-spread (Figure 4.4.34.B, right panel) and had regained proliferative capacity (Figure 4.4.34.A). This suggests that optimised 3D culture conditions are sufficient to restore proliferative capacity to non-proliferative, *in vitro*-aged MSC cultures, and reverse senescence-associated cellular hypertrophy to a more primitive morphology.

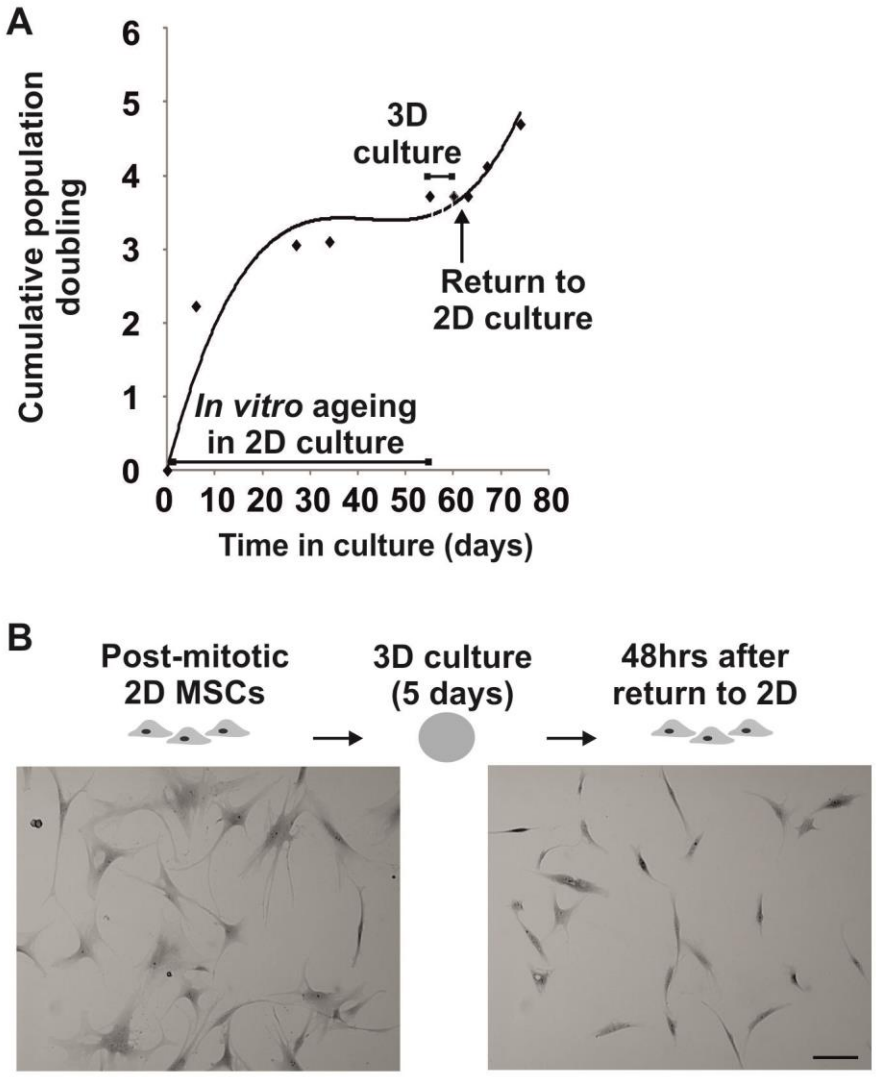

Figure 4.4.34 Analysis of morphology and proliferative capacity of senescent MSCs before and after 3D culture

2D MSCs were repeatedly passaged until a non-proliferative population was reached. Culture-aged MSCs were then used to initiate 3D spheroids (60,000 MSCs per spheroid) and cultured for 5 days, before disaggregation and re-seeding onto plastic. A) Cumulative population doublings are shown for culture-aged MSCs before and after 3D culture. B) Sample MSCs before and 48 hours after disaggregation were stained with crystal violet and imaged using brightfield microscopy (Example grayscale images are shown, scale bar = 100µm).

4.5 Discussion

The transcription factor Oct4 is expressed in the epiblast *in vivo*, and undifferentiated ESCs and ECs *in vitro* (Okamoto et al., 1990; Rosner et al., 1990). Nanog expression is also restricted to pluripotent cells (Chambers et al., 2003; Mitsui et al., 2003), whilst Sox2 is expressed throughout the epiblast and in pluripotent cells *in vitro* (Avilion et al., 2003). The expression of these factors is also up-regulated in human somatic cells, when they are reprogrammed to pluripotency by forced expression of defined factors (Takahashi et al., 2007; Yu et al., 2007). Increased expression of pluripotency factors was selected as a marker of de-differentiation/reprogramming in 3D MSCs, and used to identify optimal 3D conditions.

As demonstrated in section 3.4.1, 3D spheroid size was dependent on initial MSC seeding density and time in culture, and a wide repertoire of spheroid sizes could be generated using the conditions tested. Optimal/high expression of Oct4, Nanog and Sox2 was consistently observed across the donors examined when 60,000 MSCs were cultured in 3D for 5 days. The combined up-regulation of all 3 pluripotency factors could indicate that the level of stress imposed on 60,000 MSCs after 5 days in 3D culture, is optimal for driving an autophagy-reponse which initiates reprogramming towards pluripotency. Telomere shortening occurs during ageing in the absence of telomerase expression. This limits the proliferative capacity of normal adult cells, as when telomeres become critically short, they enter replicative senescence. Pluripotent cells, when cultured under the correct conditions have unlimited self-renewal capacity, express telomerase, and maintain telomere length through repeated passage in culture. In optimal 3D culture conditions (60,000 MSCs per spheroid), expression of telomerase was up-regulated compared to donor-matched 2D samples. This indicates that MSCs re-acquire telomerase expression, another marker of pluripotency, through culture under optimal 3D conditions. It has recently been demonstrated that during iPSC generation, activity of telomerase is restored (Takahashi et al., 2007), but also that after a few passages, iPSCs have telomeres of equivalent length to ESCs (Marion et al., 2009b). This shows that not only is expression of telomerase reactivated in iPSCs, but that it acts to lengthen and maintain telomeres in the same manner as observed in pluripotent ESCs. Increased mRNA expression of telomerase in 3D MSCs could indicate an increase in activity

during 3D culture, but this would require further validation of both telomerase activity, and telomere lengthening, to be comparable to the changes observed in factor-based reprogramming to pluripotency.

During traditional factor-based methods, partial reprogramming to pluripotency has been reported by a number of groups. In fact, the breakthrough experiments by Takahashi and Yamanaka produced cells with similar but not identical characteristics to pluripotent mouse ESCs. The Fbx15-selected iPSCs showed variable expression of endogenous pluripotency factors, at levels lower than observed in ESCs. The iPSCs generated were also unable to form viable adult chimeras, so were not equivalent of ESCs in terms of *in vivo* potency (Takahashi and Yamanaka, 2006). Similar to this, it was observed that, under optimal culture conditions (60,000 MSCs, day 5), whilst 3D MSCs up-regulated expression of all 3 pluripotency factors compared to 2D MSCs, the expression of these factors was lower than in H9 ESCs, in all MSC donors examined. Furthermore, there was no detectable Oct4A, Nanog or Sox2 protein expression in 3D MSCs, and they did not form teratomas when implanted into immunocompromised mice. Taken together these results suggest that 3D MSCs cultured under optimal conditions increase mRNA expression for factors associated with pluripotency, but that this is not associated with increased protein expression. Expression levels remain below levels observed in ESCs, and 3D MSCs are not pluripotent *in vivo*, as they are unable to form teratomas. Notably low endogenous expression of pluripotency factors (Lin et al., 2009) and absence of teratoma formation (Mikkelsen et al., 2008) have both been observed in cells partially reprogrammed with factor-based methods, and further treatment was required to induce full reprogramming to pluripotency. It was previously demonstrated in the lab that 3D MSCs are quiescent, and do not express the proliferation marker Ki67 (Elen Bray, unpublished observations). Ruiz and colleagues demonstrated that proliferation was required during reprogramming to pluripotency, and that cell cycle inhibition resulted in an absence of reprogrammed cells. Furthermore, it was demonstrated that increased proliferation increased the number of reprogrammed cells generated, rather than affecting reprogramming kinetics, which suggested that proliferation at the individual cell level is a requirement for reprogramming to pluripotency (Ruiz et al., 2011). Given that 3D

MSCs are quiescent, lack of the necessary cell proliferation could explain why they do not appear to undergo full reprogramming to pluripotency under 3D conditions.

As 3D MSCs are not pluripotent, but up-regulate expression of pluripotency factors, they were considered a potentially good source of cells for efficient factor-based reprogramming techniques. To allow for comparable experiments, 3D MSCs were disaggregated and re-seeded onto plastic (d-3D MSCs). After 5 hours, expression levels of OKSM were examined, and compared to both 2D MSCs and HDFs, which are commonly used for reprogramming. Expression levels of Oct4, Sox2 and c-Myc were higher in d-3D MSCs than HDFs and 2D MSCs, whilst on average this was also the case for Klf4, although Klf4 expression was not consistently regulated by 3D culture of MSCs. NSCs (Kim et al., 2009a; Kim et al., 2009b; Kim et al., 2008), dermal papilla cells (Tsai et al., 2011; Tsai et al., 2010) and keratinocytes (Zhu et al., 2010) all express some of the reprogramming factors at levels higher than in HDFs, and have been reprogrammed to pluripotency with increased efficiency and fewer factors. This suggested that when transduced at 5 hours post-disaggregation, 3D MSCs may be reprogrammed more efficiently than their donor matched 2D samples.

In fact, reprogramming efficiencies were higher in 2D MSCs in both donors examined, although the differences between culture conditions were relatively minor. Whilst iPSC-like colonies generated from 2D and d-3D MSCs stained for both Oct4A and Nanog, they were difficult to maintain in culture with serial passaging. Further experiments revealed that whilst at 5 hours post-disaggregation d-3D MSCs expressed OKSM at higher levels that 2D MSCs, by 24-48 hours, these levels had dropped, and were equivalent of 2D MSC expression. The optimal recommended treatment time with lentiviral vectors used was 20-24 hours, so even during this time 3D MSCs had lost the increased expression of pluripotency factors, which was hypothesised to enhance factor based reprogramming. Given the similar efficiencies achieved in both 2D and 3D MSC reprogramming, it is likely that the cells were highly similar at the time when lentiviral integration occurred. It is also probable that considering the difficulties associated with colony expansion, which is common in partially reprogrammed cells (Shi et al., 2008; Silva et al., 2008), that the colonies generated in these experiments represented partially reprogrammed, rather than true pluripotent iPSCs.

Potential technical difficulties associated with lentiviral reprogramming of 3D MSCs in suspension culture lead to the use of d-3D MSCs in the reprogramming experiments described above, but clearly any reprogramming advantage that 3D culture may confer onto 3D MSCs is lost on re-plating to tissue culture plastic. Loss of enhanced expression of Oct4, Nanog and Sox2 in d-3D MSCs clearly demonstrates that this up-regulation is dependent on 3D non-adherent culture conditions. The hypothesis suggests that cell stress, imposed on cells through varied nutrient and oxygen availability in 3D culture, is sufficient to drive reprogramming towards pluripotency. On return to tissue culture plastic 3D MSCs re-adopt typical adherent MSC morphology and behaviour in the presence of plentiful nutrients and oxygen. It would therefore seem sensible that in the absence of conditions which confer a de-differentiated state onto MSCs, the hallmarks of reprogramming would be lost, as is indeed the case for d-3D MSCs. It was demonstrated that disaggregation of 3D MSCs to both small cell clumps, and single cells, before seeding in a suspension culture in supportive semi-solid media, yielded cell colonies which increased in size with time in culture. d-3D MSCs proliferated to a similar extent in both media tested. One media consisted of DMEM supplemented with 5% FBS, to confer a level of nutrient deprivation onto cells, whilst the other media was serum-free iPSC maintenance media, which should help in the maintenance of undifferentiated cells, as it is devoid of factors in serum which can induce differentiation. QPCR revealed that in 2 different MSC donors, the expression of Oct4, Nanog, Sox2 and telomerase was higher in d-3D MSCs, cultured in semi-solid conditions for 7 days, than in 2D MSCs. This indicates that enhanced expression of pluripotency factors is maintained in d-3D MSCs well beyond the 5 hour window of enhanced expression observed when d-3D MSCs are re-seeded onto plastic. Clearly, return to 2D culture conditions is responsible for loss of pluripotency markers, and maintenance of MSCs in a 3D environment drives continued expression of pluripotency factors. As mentioned above, proliferation is required for reprogramming to pluripotency (Ruiz et al., 2011). It may be that releasing 3D MSCs from their quiescent state, whilst culturing them in an environment which supports the maintenance of a de-differentiated state is sufficient to sustain enhanced expression of pluripotency factors.

The teratoma assays also demonstrated that 3D MSCs, when freed from the constraints of plastic-adherent culture, had increased mesodermal potency compared to 2D MSCs. 2D MSCs were unable to form any tissues *in vivo,* whilst 3D MSCs formed small, highly organised masses composed of tissues of mesodermal origin. The absence of teratomas, but formation of mesodermal tissues from 3D MSCs suggests that these cells are more potent than 2D MSCs, but not pluripotent. Formation of mesoderm *in vivo* suggests that 3D MSCs may have de-differentiated to early primitive mesodermal stem cells, with the capacity to form mesodermally-derived tissue, which 2D MSCs were unable to form. The presence of tissue masses also demonstrates the proliferative potential of 3D MSCs when exposed to exogenous cues, and this proliferative capacity was also demonstrated *in vitro,* when d-3D MSCs proliferated whilst maintaining pluripotency factor expression after dissagregation appeared to release them from their quiescent state. This lineage-restricted de-differentiation rather than full reprogramming to pluripotency may actually improve the potential of 3D MSCs for therapeutic applications. Recently an increasing focus has been placed on 'direct reprogramming,' which is the reprogramming of one cell type to another, without passage through pluripotency. This method would be considered preferable in the generation of cells for therapeutic application, as it effectively circumvents pluripotency and associated teratoma risk. Functional neurons (Vierbuchen et al., 2010), hepatocytes (Huang et al., 2011) and cardiomyocytes (Ieda et al., 2010) have all been generated from mouse fibroblasts by direct reprogramming, and human fibroblasts have been directly reprogrammed to haematopoietic progenitors and mature cell types (Szabo et al., 2010). Furthermore factor-based direct reprogramming has been demonstrated *in vivo,* when β-cells were reprogrammed to mature exocrine cells of the pancreas, a cell type which, like β-cells, arise from pancreatic endoderm (Zhou et al., 2008). These studies clearly demonstrate that forced expression of factors associated with a particular cell fate can directly reprogramme fibroblast and other cell types to that fate, without the need for passage through pluripotency. In the proposed model, it would appear that 3D conditions initiate a de-differentiation programme, that is associated with increased expression of pluripotency factors, but which halts before reaching pluripotency, resulting in MSCs which have adopted a lineage-restricted post-pluripotent state. Oldershaw and colleagues demonstrated directed differentiation of human ESCs to chondrocytes, through a series of stepwise differentiation events which mimicked *in*

vivo development (Oldershaw et al., 2010). In fact, the mesendoderm/mesoderm markers expressed by MSCs during 3D culture bore a striking resemblance to the stage-specific markers proposed in this paper. Stage 1 was defined as primitive streak/mesendoderm and was characterised by expression of factors including Brachyury, Goosecoid and MIXL1, whilst Stage 2, defined as mesoderm was characterised by expression of Brachyury, KDR and CXCR4. However qPCR actually showed that at Stage 1, high expression of Oct4, Nanog, Sox2, Brachyury and Goosecoid was observed, whilst maximal expression of KDR and MIXL1 was observed at Stage 2 (Oldershaw et al., 2010). 3D MSCs expressed high/maximal levels of Oct4, Nanog and Sox2, along with Brachyury and Goosecoid at day 5 of 3D culture, suggesting a similarity to the primitive streak/mesendoderm cells described by Oldershaw and colleagues. Most strikingly, expression of KDR and MIXL1 was highest at day 3 in 3D MSCs, and at Stage 2 (mesoderm cells) in this publication. This suggests that 3D MSCs undergo de-differentiation in a manner that passes through stages similar to those observed when ESCs are differentiated in a stage-specific manner, thought to represent the normal developmental process. Taken together these results indicate that the de-differentiation initiated by 3D culture could represent a stage-specific reversal of normal developmental progression, and that 3D MSCs at day 5 share similarities with cells of the primitive streak/mesendoderm. Expression of markers of mesendoderm was not restricted to mRNA, as Brachyury protein was detectable by immunofluorescence at day 5 of 3D culture. KDR protein was weakly detected at this time point, though it could be speculated that expression would have been stronger if day 3 samples had been examined. This would also have provided further evidence for the theory of step-wise de-differentiation, from the starting population of MSCs, though mesoderm to primitive streak/mesendoderm at day 5 of 3D culture. Interestingly it appeared that the distribution of Brachyury+ cells was uniform throughout the 3D structure, so a small highly expressing population was not responsible for the observed up-regulation of Brachyury mRNA. In fact, based on Brachyury expression, approximately 70% of cells were positive for Brachyury staining (using Volocity software, calculated as a percentage of DAPI+ nuclei). This indicates that 3D culture is highly efficient at inducing Brachyury expression in 3D MSCs at day 5. Strong expression of the mesoderm/haemangioblast marker CXCR4 was also observed in 3D MSCs, along with an enhanced ability to form blast-like colonies when

disaggregated and re-seeded in haematopoietic induction media, suggestive of a functional enhancement of potency in 3D compared to 2D MSCs. Along with this ability to drive de-differentiation in cycling cells, 3D culture also appeared to reverse the effects of culture-induced cell senescence in MSCs. Cellular ageing is associated with the accumulation of damaging protein aggregates and mutated mitochondria, which are thought to contribute to the phenotype of aged cells. Indeed, age-associated neurodegeneration is caused by these damaging protein aggregates, and recently compounds which drive cytoplasmic clearance (including autophagy stimulators) have been found to reverse some of the effects of protein accumulation (Ravikumar et al., 2004; Rubinsztein, 2006; Rubinsztein et al., 2011). Autophagy stimulators are also associated with increased longevity (Eisenberg et al., 2009; Harrison et al., 2009; Morselli et al., 2009), and autophagy inhibition results in cellular degeneration which mimics that observed in physiological ageing (Harris and Rubinsztein, 2012; Rubinsztein et al., 2011). This suggests that reversal of replicative senescence in MSCs could indeed be induced by an enhanced autophagy response, stimulated by 3D culture conditions.

The results presented in this chapter suggest that 3D culture drives de-differentiation of 3D MSCs, characterised by enhanced/maximal expression of markers of pluripotency/primitive streak/mesendoderm. 3D MSCs do not reach full pluripotency, which could indicate a reduced teratoma risk when compared to pluripotent, teratoma-initiating cells. Instead 3D culture appears to drive a highly efficient lineage-restricted de-differentiation to a population of mesendoderm-like cells with enhanced potency *in vitro* and *in vivo*, although the mechanism driving this de-differentiation is unknown. 3D culture is key, as return to tissue culture plastic results in loss of de-differentiated characteristics, which supports the initial hypothesis that de-differentiation would be induced by autophagy, driven by nutrient deprivation in 3D conditions. Cytoplasmic clearance has been demonstrated to reverse age-associated defects in studies of neurodegeneration, and 3D culture reversed replicative senescence in culture aged MSCs. Although stimulation of autophagy and metabolic remodelling are mainly considered in the context of full reprogramming to pluripotency, it is possible that in lineage-restricted reprogramming, these processes could also play a role. If one considers reprogramming to pluripotency as a progressive reversal of the developmental

process, rather than a simple ‘switch’ from one cell type to another, with no intermediates in between, then it makes sense that cells would passage through de-differentiation and a number of increasingly primitive cell fates before reaching pluripotency. In this scenario, the principles of cytoplasmic clearance and metabolic restructuring would also play a role in lineage restricted de-differentiation, as well as in reprogramming to full pluripotency. Chapter 5 will attempt to confirm the mechanism driving de-differentiation in 3D MSCs by investigating autophagy markers, to determine an active autophagic response in MSCs under 3D culture conditions. It will also examine the metabolic profile of 3D MSCs to investigate if, in 3D MSCs, autophagy is driving cytoplasmic clearance and metabolic remodelling to a more primitive state.

Chapter 5: Mechanisms driving enhanced potency in 3D MSCs

5.1 Introduction

As previously described, the metabotype of pluripotent stem cells is distinct from that of differentiated cells, and during reprogramming to pluripotency, there is a requirement for metabolic remodelling. A number of hallmarks of metabolic reprogramming have been observed during factor-based reprogramming. These include a decrease in oxygen consumption and an increase in lactate production compared to the originating cell population. iPSC colonies derived from MEFs with 4 factors (OKSM) had highly similar oxygen consumption, cellular lactate levels and lactate efflux to ESCs, and these levels were significantly different to those of the parent MEFs (Folmes et al., 2011). Differential expression of components of the oxidative phosphorylation complexes I and II were also observed under these reprogramming conditions, with down-regulation of these components in iPSCs compared to expression in parental MEFs. Under TEM examination, tubular cristae rich mitochondrial networks were observed in MEFs, whilst in iPSCs, mitochondria were small, primitive and cristae-poor, occupying a perinuclear location, highly similar to mitochondria in ESCs. iPSCs also showed an increased nuclear to cytoplasmic ratio, another hallmark of pluripotent cells (Folmes et al., 2011).

Autophagy is a physiological mechanism, which recycles organelles and cytoplasmic contents, to aid cell survival in response to nutrient starvation. Breakdown and recycling of the components of an autophagosome relies on fusion with a lysosome, which contains degradative enzymes. Genes encoding lysosome proteins are expressed in a co-ordinated fashion, and this expression is regulated by the master regulator of lysosomal biogenesis transcription factor EB (TFEB) (Sardiello et al., 2009). TFEB is a member of the microphthalmia–transcription factor E (MiT/TFE) subfamily of basic helix-loop-helix (bHLH) transcription factors. In analyses of mechanisms that drive lysosome biogenesis it was observed that many lysosomal genes contained a common motif, situated close to the transcriptional start site. This motif was a palindromic 10bp GTCACGTGAC motif, which is similar to sequences known to be bound by MiT/TFE family members. When all human genes with at

least two of these motifs within 200bp of the transcriptional start site were identified, this group was found to be strongly enriched for genes associated with lysosome biogenesis and function. This suggested that this element regulated the expression of many lysosomal genes, and lead to the naming of the motif as a Coordinated Lysosome Expression and Regulation (CLEAR) element. Chromatin immunoprecipitation showed that TFEB was able to bind to CLEAR elements in lysosomal genes, and mRNA levels of such genes increased upon TFEB over-expression. TFEB over-expression also resulted in increased lysosome numbers. The lysosomal-associated membrane protein LAMP1 is a major component of lysosomal membranes, and LAMP1 expression is regulated by TFEB (Sardiello et al., 2009). Increased expression of LAMP1 can act as a marker of increased lysosome numbers, whilst another marker can be used to indicate an increase in autophagosome formation. The microtubule-associated protein I light chain 3 (LC3) is a homologue of the yeast protein Atg8, which is essential for autophagy, and is thought to play a role in autophagosome formation. LC3 exists in two forms, LC3 I is cytoplasmic, whilst LC3 II is incorporated into autophagosome membranes. Short term serum and amino acid depletion is sufficient to drive an increase in LC3 II levels, so this can act as a marker of a starvation-driven enhanced autophagic response (Kabeya et al., 2003). It was recently demonstrated that TFEB regulates not only lysosomal but also autophagy genes, coordinating the regulation of these closely linked cellular clearance mechanisms. Overexpression of TFEB resulted in an increase in autophagosomes, and enhanced autophagic flux (the rate at which autophagosomes are delivered to lysosomes). There was also an increase in expression of autophagy related genes. In contrast, autophagy genes were down-regulated after TFEB silencing, even under starvation. Furthermore the autophagy marker LC3 II also decreased under starvation conditions when TFEB was depleted, indicating a requirement for TFEB for a functional autophagy response after nutrient depletion (Settembre et al., 2011). The work in this chapter will utilise these well-defined markers of autophagy and metabolic remodelling to investigate the hypothesis that 3D culture regulates autophagy to drive cytoplasmic and metabolic remodelling in MSCs. Autophagy is a physiological response to cell stress, and if 3D culture does stimulate autophagy to drive cytoplasmic clearance as a survival mechanism, then this should be observed in cell types other than MSCs. However, the tolerance of nutrient deprivation in 3D culture is likely to be cell-type specific, so it may be

necessary to optimise conditions for any cell type cultured in 3D. To investigate this theory, I will also attempt to establish optimal 3D culture conditions for human dermal fibroblasts. HDFs have been reprogrammed to pluripotency using traditional factor based methods (Yu et al., 2007), so are amenable to the induction of de-differentiation through forced expression of pluripotency factors. Here I will investigate if optimal 3D culture conditions alone are sufficient to drive enhanced expression of pluripotency factors in HDFs, in the absence of exogenous factors.

5.2 Aims

The general aim of the work presented in this chapter is to analyse the metabolic status and autophagy response in 3D MSCs.

More specifically, the objectives are to:

- Examine the expression of markers of autophagy in 3D MSCs
- Assess the metabolic status and identify evidence of metabolic remodelling in 3D MSCs
- Investigate if optimised 3D culture conditions are sufficient to drive enhanced pluripotency factor expression in other cell types

5.3 Methods

5.3.1 Transmission electron microscopy

3D spheroids were seeded with initiating cell numbers of 60,000 MSCs and cultured for up to 5 days as described in 2.2.1.5. For general analysis of autophagy-induced ultrastructural changes, samples were isolated on days 1 and 5; for more detailed analysis of mitochondria, samples were isolated on day 5. All samples were fixed as described in 2.2.4.1. Samples were stained as described in 2.2.4.2 or for high contrast mitochondrial imaging, staining was as described in 2.2.4.3. All samples were then prepared and imaged as described in 2.2.4.4.

5.3.2 Quantitative real time polymerase chain reaction

2D MSCs were cultured as described in 2.2.1.3. 3D spheroids were seeded with initiating cell numbers of 60,000 MSCs and cultured for up to 5 days as described in 2.2.1.5. Samples were isolated every day of 3D culture for analysis of TFEB expression. For qPCR of rapamycin-treated cells, 3D spheroids were initiated from 60,000 MSCs, and maintained in culture for 5 days as described in 2.2.1.5. Medium was refreshed daily. For treated samples, 3D MSC medium was supplemented with 0.3nM rapamycin; 3D MSC medium alone was used for control samples. 2D HDF monolayers were cultured as described in 2.2.1.4, and 3D HDFs were cultured as described in 2.2.1.6 for 5 days, with samples isolated daily. RNA was isolated from all 2D and 3D samples before cDNA was generated and analysed by qPCR as described in 2.2.5. Primer sequences for TFEB were as follows (5'-3'):

forward primer: CCAGAAGCGAGAGCTCACAGA;
reverse primer: TGTGATTGTCTTTCTTCTGCCG

5.3.3 Promoter analysis for TFEB binding sites

A promoter search was performed using the Gene Name Input option of MatInspector software. Searches were performed for human Oct4, Nanog and Sox2.

5.3.4 Protein isolation and quantification

Monolayer MSCs were trypsinised, centrifuged and re-suspended in RIPA buffer (Thermo Scientific) containing 0.5% protease inhibitor cocktail set III (Calbiochem) and 100μM Na_3VO_4 (Sigma). 3D MSC spheroids were homogenized in RIPA buffer as above. Protein quantification was performed using the BCA Protein Assay Kit (Thermo Scientific). Absorbance was measured at 570nm, then protein concentrations were calculated from a standard curve generated from standard samples of known concentrations.

5.3.5 Western blot analysis

For LAMP1 immunoblotting, 20μg of total protein was loaded onto a 10% SDS polyacrylamide gel, electrophoresed at 180V, and then wet transferred to a nitrocellulose membrane and probed with an anti-LAMP1 antibody. For LC3 immunoblotting, 20μg of total protein was loaded onto a 15% SDS polyacrylamide gel, which following electrophoresis at 180V, was wet transferred to a PVDF membrane and probed with an anti-LC3 antibody. Detection was performed by enhanced chemiluminescence (ECL) following manufacturer's instructions (Promega) and intensities quantified using Image J analysis software. Antibody details are given in Table 5.3.1.

Table 5.3.1 Antibodies used in Western Blot

Antibody	Host	Dilution	Supplier	Cat. no.
Anti-LAMP1	Mouse	1:1000	Developmental Studies Hybridoma Bank	H4A3
Anti-LC3	Mouse	1:200	Nanotools	0231-100
Anti-GAPDH	Mouse	1:2000	GeneTex	GTX28245
Anti-Mouse IgG (HRP conjugate)	Goat	1:2000	Santa Cruz Biotechnology	sc-2005

5.3.6 Transcriptomics analyses

2D MSC were cultured as described in 2.2.1.3. 3D spheroids were initiated from 60,000 MSCs and maintained in culture for 5 days as described in 2.2.1.5. For global gene expression analyses, duplicate RNA samples from two primary MSC donors were generated as described in 2.2.5.1 and 2.2.5.2. RNA quality was assessed using the Agilent 2100 Bioanalyzer, both samples had RNA integrity numbers of 9.8 or greater. 150ng RNA per sample was then spiked with control RNA, and labelled with Cy-3. 600ng Cy3-labelled RNA per sample was then hybridized onto an Agilent SurePrint G3 Human Gene Expression 8x60K v2 Microarray. Arrays were scanned using an Agilent DNA Microarray Scanner (G2565CA) with SureScan High-Resolution Technology. Data was analysed using Genespring version 12.1 software (Agilent technologies). Pathway analysis was performed on lists of genes differentially expressed in response to 3D culture conditions, using the pathway analysis tool within Genespring v12.1 software.

5.3.7 Metabolic measurements

3D spheroids were seeded with initiating cell numbers of 60,000 MSCs and cultured for up to 5 days as described in 2.2.1.5. Oxygen consumption by 3D MSCs was measured using the BD Biosciences Oxygen Biosensor System (OBS). Briefly, every day for 5 days, two MSC spheroids were cultured in triplicate wells of the OBS plates in 50µl of culture medium, alongside blank wells containing medium alone. Cells were maintained at 37^{o}C on 5% CO_2 in air for the duration of the assays. Kinetic measurements were taken every 20 seconds for 30 minutes. Raw fluorescence data was corrected against a pre-blank reading and converted to oxygen concentration in accordance with manufacturer's guidelines. The OBS 96-well plates contain a proprietary fluorescent compound immobilized to the bottom of each well which is quenched in the presence of oxygen. Aerobically respiring cells reduce the concentration of oxygen dissolved in the media, which means there is a reduction in fluorescence quenching and an increase in fluorescence intensity. The oxygen consumption rate (OCR) was calculated as the gradient of change in oxygen concentration over time in nmol/spheroid/hr. At the end of oxygen assays, the medium was collected and lactate release into the medium was determined by using enzyme linked fluorescent assays. Briefly, sample media were added to an assay

mixture and incubated at 25ºC for 30 minutes. The assay mixture contained lactate dehydrogenase (40 IU ml^{-1}) in a glycine hydrazine buffer, pH 9.4. Changes in fluorescence due to NAD^+ reduction were proportional to lactate concentration in the culture medium, which was calculated using a standard curve. Results were analysed for statistical significance using a T-test (n=3).

5.4 Results

5.4.1 Enhanced autophagy in 3D MSCs

I hypothesised that cell stress triggered by 3D culture would be sufficient to induce autophagy in 3D MSCs, and that the cytoplasmic clearance and restructuring which cells undergo during an autophagic response, could drive de-differentiation to a more primitive state.

As TFEB is the master regulator of lysosomal biogenesis, and also regulates the expression of many autophagy genes the effects of 3D culture on TFEB expression were determined. MSCs from two different primary donors were cultured as 2D monolayers and 3D spheroids for up to 5 days. RNA samples were isolated and samples analysed for TFEB expression by qPCR. In both donors examined, expression of TFEB increased during 3D culture. By day 1 of 3D culture, up-regulation of almost 3-fold was observed, relative to the donor-matched 2D sample. This up-regulation continued to day 2, where expression in 3D MSCs was just over 5-fold higher than in 2D MSCs. In both donors there was a small decrease in expression of TFEB on day 3, before expression increased again on day 4 and was maintained to day 5 around 4.5-5.5 fold higher than 2D MSCs depending on donor (Figure 5.4.1. A). Pooling donor data showed significantly enhanced expression on days 2-5 of 3D culture, relative to 2D MSCs (Figure 5.4.1. B). TFEB regulates expression of lysosomal/autophagy genes through binding the Coordinated Lysosomal Expression and Regulation (CLEAR) consensus sequence. Multiple CLEAR elements can be found close to the transcriptional start sites of genes regulated by TFEB. A promoter search using MatInspector identified a CLEAR element immediately upstream of the human Sox2 transcriptional start site (Figure 5.4.2). However, no functional validation of this binding site was performed in this study. CLEAR elements were not identified in Oct4 or Nanog promoters.

Lysosomal-associated membrane protein 1 (LAMP1) is a lysosome membrane protein, and an increase in LAMP1 is associated with an increase in lysosome numbers, which can indicate enhanced autophagy. To assess the effects of 3D culture on LAMP1 levels, MSCs were cultured as 2D monolayers and 3D spheroids for up to 5 days. Protein samples were isolated and analysed for LAMP1 expression by

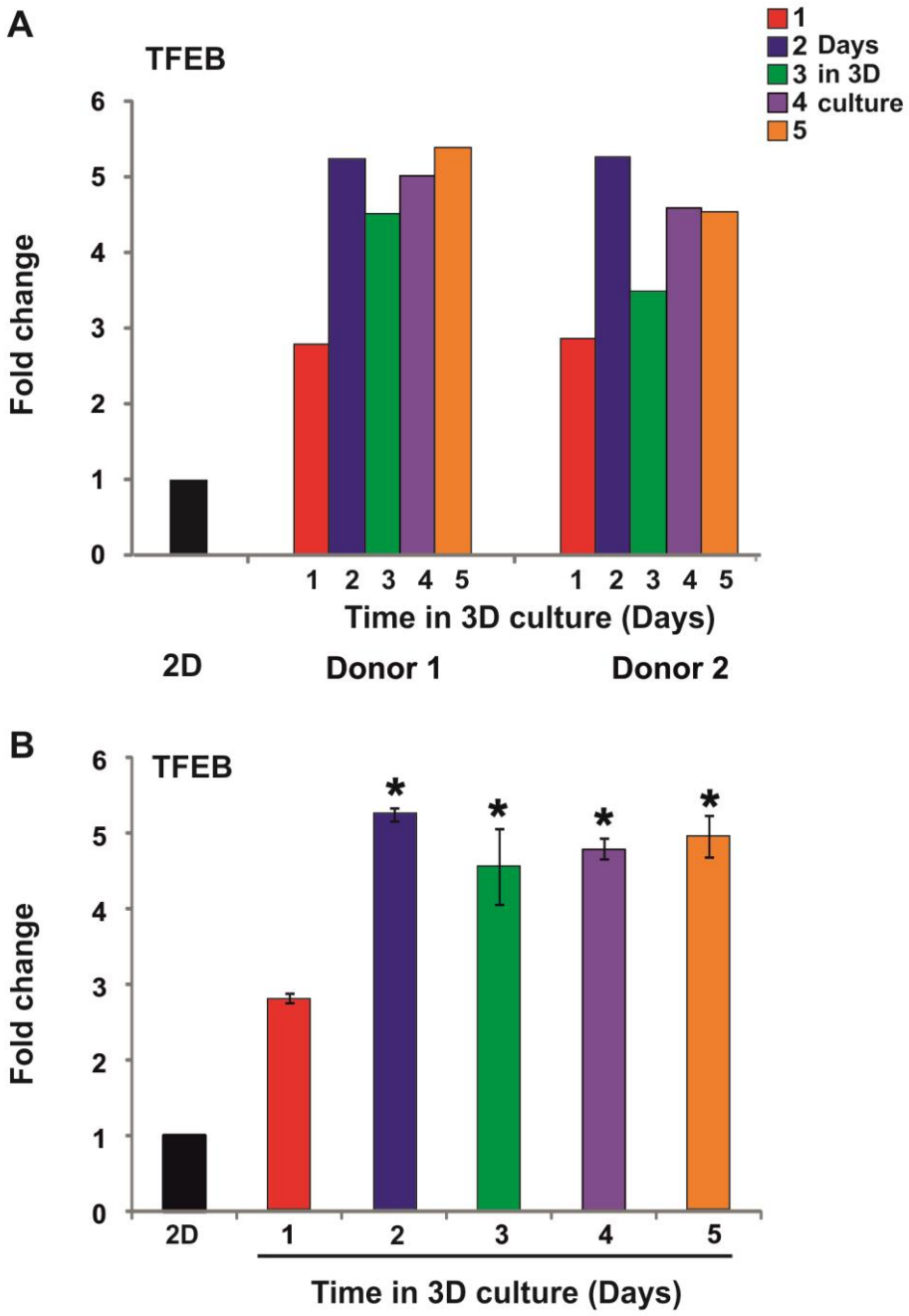

Figure 5.4.1. qPCR analysis of expression of the lysosome and autophagy regulator TFEB in MSCs over time in 3D culture

MSCs from 2 donors were cultured as 2D monolayers and 3D spheroids with an initiating cell number of 60,000 cells for up to 5 days in culture. cDNA samples were generated and then analysed by qPCR. A) Expression of TFEB for each donor was normalised to expression of the housekeeping gene GAPDH and made relative to expression levels in the donor matched 2D sample. Fold changes were calculated as 2^{-ddCt}. B) Data from both donors was pooled and subject to statistical analysis, mean fold changes are shown ± SEM, * $p< 0.05$. Statistical significance is relative to expression in 2D MSCs (by Kruskal Wallis test, n = 2).

Figure 5.4.2. Identification of a TFEB binding site in the promoter region of the Sox2 gene

A promoter search using MatInspector identified a sequence, which matches that of known TFEB binding sites, at the transcriptional start site of the human Sox2 gene.

Western blot. In the two primary MSC donors examined, expression of LAMP1 increased in 3D culture. A small increase was observed by day 1, and expression had increased further by day 5 of 3D culture (Figure 5.4.3). To examine if 3D culture-induced autophagy was reversed when 3D MSCs were returned to 2D culture, further studies were performed. MSCs were cultured as 2D monolayers and 3D spheroids for 5 days in culture. On day 5 of 3D culture, 3D MSC spheroids were disaggregated to single cells (d-3D MSCs) and re-seeded onto tissue culture plastic. d-3D MSCs were maintained in 2D culture for up to 7 days. When these samples were analysed for LAMP1 expression, it was again observed that LAMP1 expression increased during 3D culture. Maximal expression was observed on 3D day 5. Following return to 2D culture, the levels of LAMP1 reduced in both primary donors examined. Four days after return to 2D culture, levels of LAMP1 in d-3D MSCs were lower than observed in the donor matched 2D sample. There was a small recovery towards 2D levels in d-3D MSCs 7 days after return to 2D culture (Figure 5.4.4). These results suggest that enhanced expression of LAMP1 in MSCs is induced by 3D culture, and that return to 2D culture is sufficient to reverse the observed increase in LAMP1 expression.

Microtubule-associated protein 1 light chain 3 (LC3) exists in two forms; LC3 I is cytoplasmic, whilst the lipidated form, LC3 II is associated exclusively with autophagosome membranes. Reduction of LC3 I and increase in LC3 II indicate an increase of autophagosome numbers. To assess the effects of 3D culture on LC3 levels, MSCs were cultured as 2D monolayers and 3D spheroids for up to 5 days. Protein samples were isolated and analysed for LC3 expression by Western blot. By day 5 of 3D culture, there was near total loss of LC3 I, in both primary MSC donors examined, indicating that at this point LC3 existed almost exclusively in its autophagosome-incorporated form (Figure 5.4.5).

Examination of 3D MSCs over time in culture using TEM revealed the presence of few cytoplasmic vesicular structures at day 1 of 3D culture (Figure 5.4.6, A-B). In contrast, by day 5, many typical autophagic structures were observed in the cytoplasm of 3D MSCs. These included double-membrane bound vesicles, and contained presumptive degraded cytoplasmic contents (Figure 5.4.6, C-F)

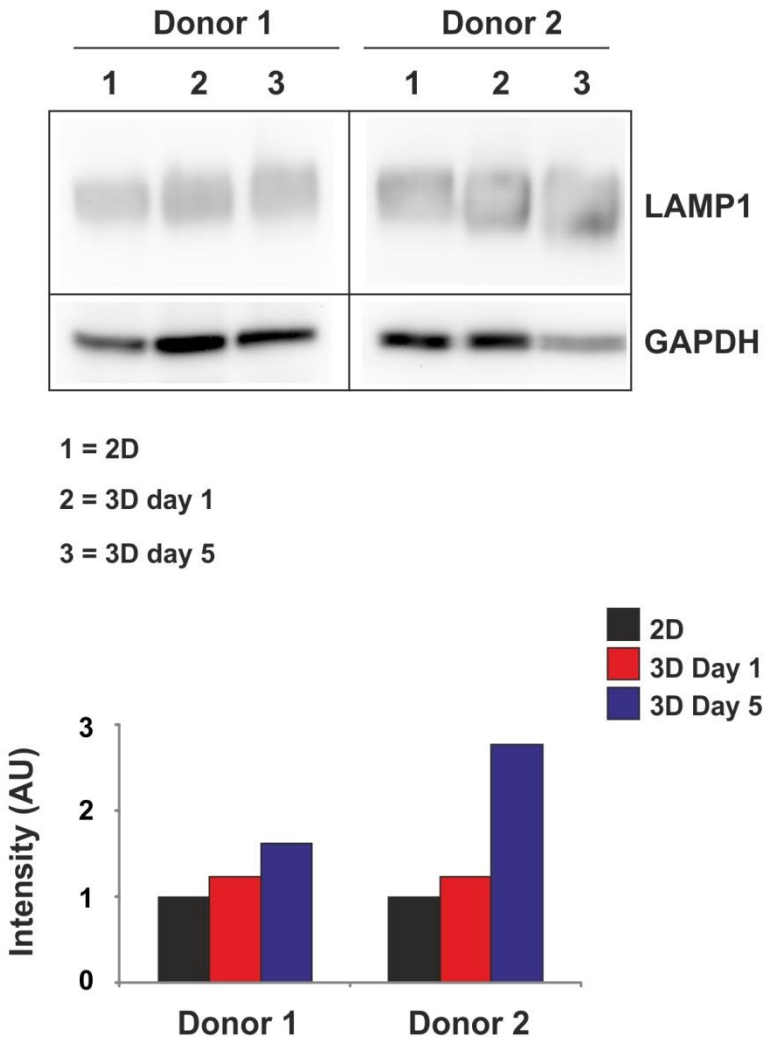

Figure 5.4.3. Analysis of the expression of the lysosomal membrane protein LAMP1 in MSCs over time in 3D culture

MSCs from 2 donors were cultured as 2D monolayers and 3D spheroids with an initiating cell number of 60,000 cells for up to 5 days in culture. Total protein was isolated from each sample and analysed by Western blot. The membrane was probed against anti-LAMP1 and anti-GAPDH, which was used as a loading control. Densitometry was performed using ImageJ, normalised to GAPDH and made relative to levels in 2D MSCs, displayed on the bar chart as relative normalised intensity.

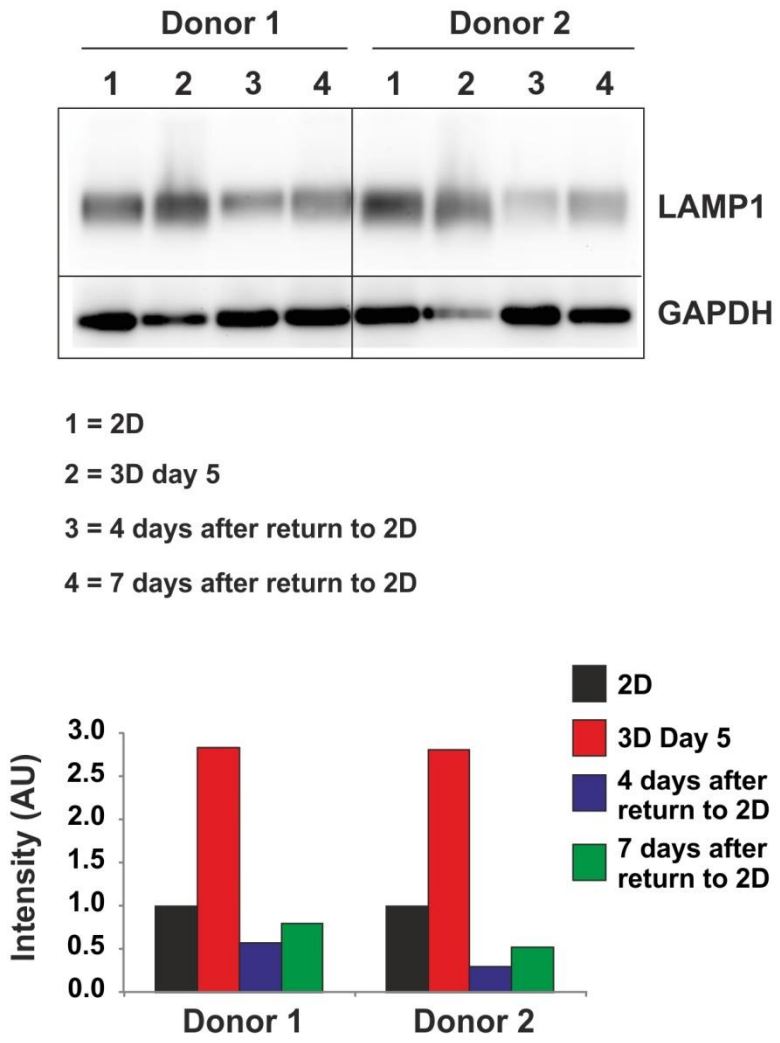

Figure 5.4.4. Analysis of the expression of the lysosomal membrane protein LAMP1 in MSCs following disaggregation of 3D spheroids and return to 2D culture

MSCs from 2 donors were cultured as 2D monolayers and 3D spheroids with an initiating cell number of 60,000 cells for up to 5 days in culture. On day 5 spheroids were disaggregated to a single cell suspension and re-seeded onto tissue culture plastic for up to 7 days. Total protein was isolated from each sample and analysed by Western blot. The membrane was probed against anti-LAMP1 and anti-GAPDH, which was used as a loading control. Densitometry was performed using ImageJ, normalised to GAPDH and made relative to levels in 2D MSCs, displayed on the bar chart as relative normalised intensity.

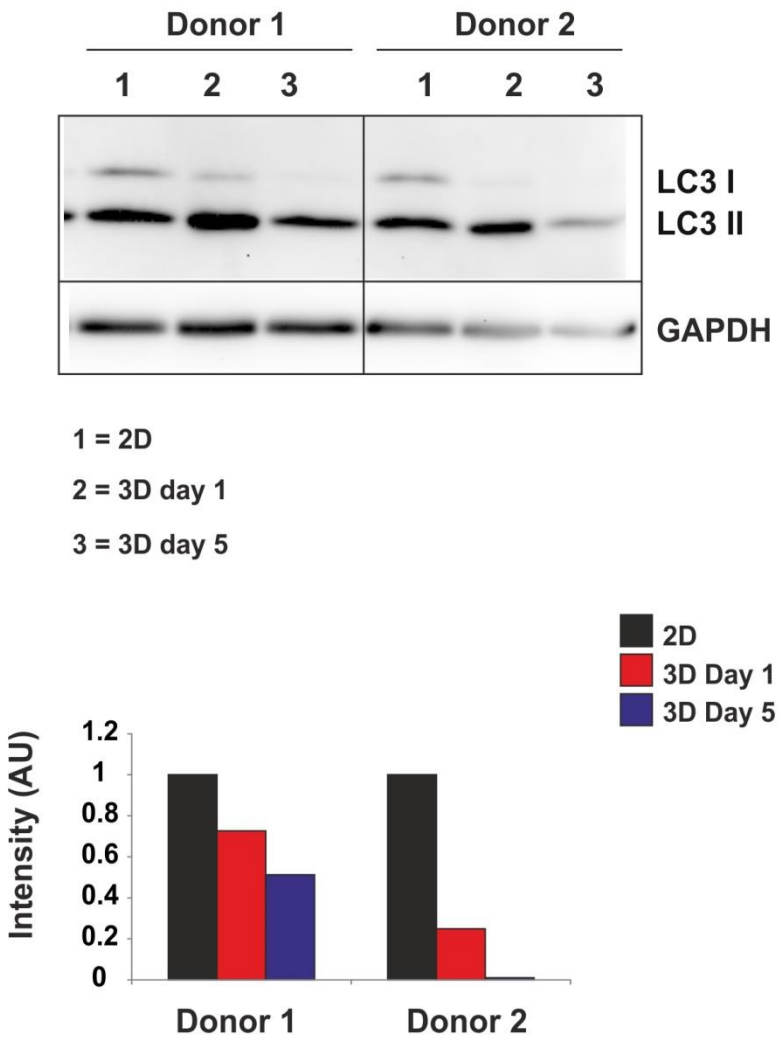

Figure 5.4.5. Analysis of the expression of the autophagy marker LC3 in MSCs over time in 3D culture

MSCs from 2 donors were cultured as 2D monolayers and 3D spheroids with an initiating cell number of 60,000 cells for up to 5 days in culture. Total protein was isolated from each sample and analysed by Western blot. The membrane was probed against anti-LC3 and anti-GAPDH, which was used as a loading control. Densitometry to evaluate loss of cytoplasmic LC3 I was performed using ImageJ, normalised to GAPDH and made relative to levels in 2D MSCs, displayed on the bar chart as relative normalised intensity.

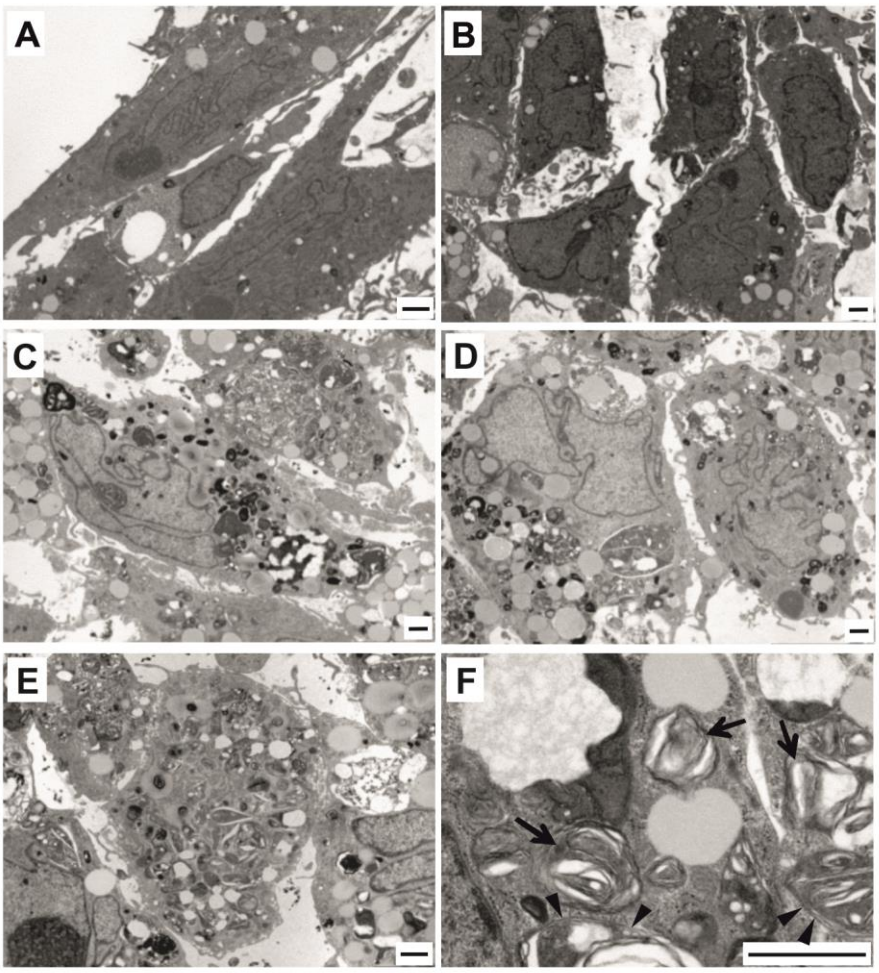

Figure 5.4.6. TEM analysis of 3D MSCs for the presence of cytoplasmic markers of enhanced autophagy

3D spheroids were initiated from 60,000 MSCs and maintained in culture for up to 5 days. On days 1 and 5, spheroids were fixed, stained and sectioned for TEM analysis. Sections were then examined for the presence of markers of enhanced autophagy. Example images are shown of 3D MSCs at day 1 (A-B) and day 5 (C-F). Scale bars = 1µm, arrows indicate typical autophagasomes, arrow heads indicate autophagic vesicles which appear to be bound by double membranes.

5.4.2 Donor-dependent enhancement of pluripotency factor expression in 3D MSCs treated with rapamycin

Rapamycin is a known autophagy stimulator, acting through inhibition of the mTOR complex (itself an autophagy inhibitor). To investigate if pharmacological enhancement of autophagy was sufficient to drive further increased expression of pluripotency factors in 3D MSCs, MSCs were cultured as 2D monolayers and 3D spheroids for up to 5 days in culture. 3D spheroids were grown in the presence and absence of 0.3nm rapamycin. Cultures were fed daily and samples harvested each day for 5 days. Samples were analysed by qPCR for expression of Oct4, Nanog and Sox2. Notably the 2 primary MSC donors examined responded differently to treatment. In Donor 1, by day 5 of 3D culture, expression of all 3 pluripotency factors examined was over two times higher in rapamycin-treated versus control samples. Clearly in this donor, rapamycin stimulated an increase in pluripotency factor expression. In contrast, donor 2 showed little or no change in pluripotency factor expression with rapamycin treatment (Figures 5.4.7. - 5.4.9). These results highlight the donor-dependent nature of increased pluripotency factor expression in response to pharmacological inhibition of autophagy. Given the contradicting responses to rapamycin treatment in these two primary donors, there is little to be gained from pooling data at this stage. Further analysis of more donors would indicate if there is a common response to rapamycin treatment in 3D MSCs, or if this response is donor-dependent and highly variable across a greater range of samples.

5.4.3 Metabolic differences are observed in MSCs cultured as 3D spheroids

Enhanced autophagy in 3D MSCs may be driving cytoplasmic and organelle remodelling. Mitophagy is a form of autophagy, which recycles mitochondria and remodels the mitochondrial network. Transcriptomics analyses were performed on 2 primary MSC donors, cultured under 2D and optimised 3D conditions. Gene ontology analysis was used to identify the pathways in which many related genes were differentially expressed. Figure 5.4.10 shows the top 25 differentially expressed pathways in 3D versus 2D MSCs, included in this list were a number of pathways related to autophagy and oxidative metabolism. The electron transport chain and oxidative phosphorylation pathways were ranked first and third in this list. 67 of the genes assigned to the electron transport chain by gene ontology analysis were

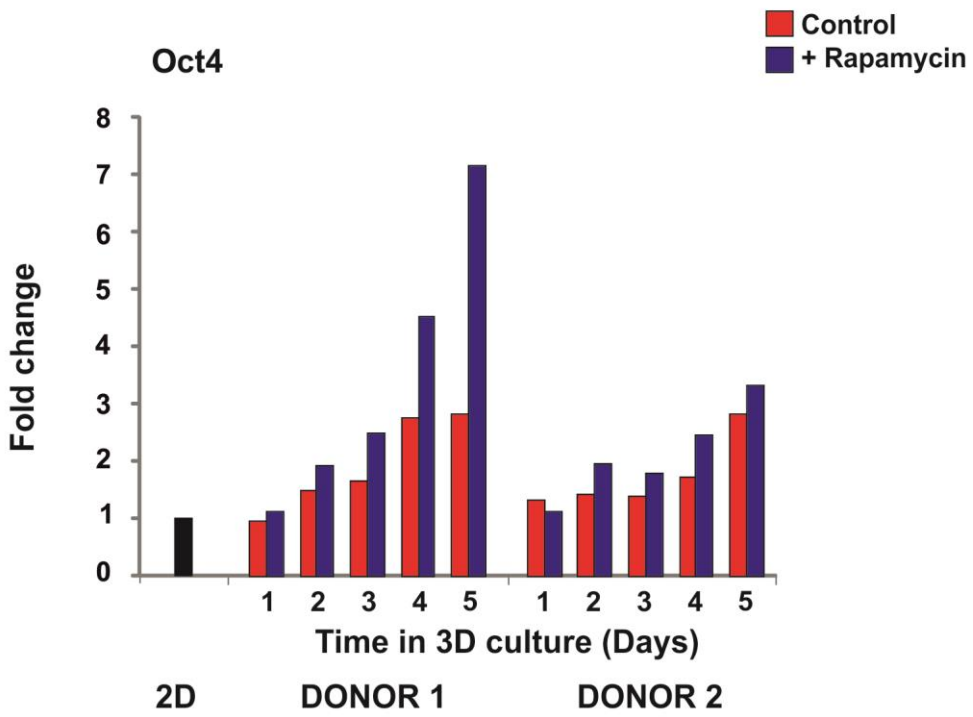

	Donor 1				Donor 2			
	Control		+ rapamycin		Control		+ rapamycin	
	Mean dCt	± *SEM*	*Mean dCt*	± *SEM*	*Mean dCt*	± *SEM*	*Mean dCt*	± *SEM*
2D	4.68	0.25	-	-	4.99	0.01	-	-
3D Day 1	4.28	0.08	4.51	0.10	5.08	0.11	4.82	0.03
3D Day 2	4.18	0.07	3.71	0.03	4.41	0.08	4.06	0.13
3D Day 3	4.20	0.02	3.85	0.04	4.26	0.08	3.67	0.08
3D Day 4	3.90	0.15	3.39	0.08	3.53	0.05	2.81	0.08
3D Day 5	3.20	0.13	2.95	0.04	3.49	0.04	2.15	0.03

Figure 5.4.7. qPCR analysis of expression of Oct4 in 3D MSCs treated with the autophagy stimulator rapamycin

MSCs from 2 donors were cultured as 2D monolayers and 3D spheroids with an initiating cell number of 60,000 cells for up to 5 days in culture. Media was refreshed daily with 3D MSC media (control samples) or 3D MSC media supplemented with 0.3nM rapamycin. 3D MSCs were isolated every day for 5 days, before cDNA samples were generated and then analysed by qPCR. Expression of target gene for each donor was normalised to expression of the housekeeping gene GAPDH and made relative to expression levels in the donor matched 2D sample. Fold changes were calculated as 2^{-ddCt}. Expression of Oct4 in 2 different MSC donors in both control and treated samples is shown. Average dCt values ± SEM for technical replicates are shown in the table.

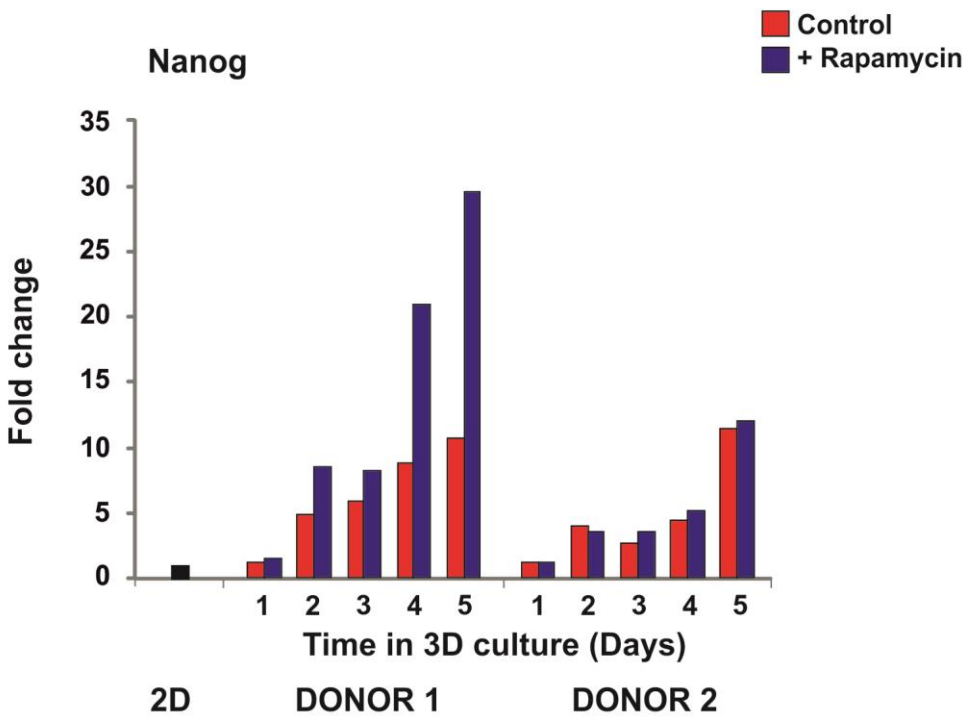

	Donor 1				Donor 2			
	Control		+ rapamycin		Control		+ rapamycin	
	Mean dCt	± *SEM*	*Mean dCt*	± *SEM*	*Mean dCt*	± *SEM*	*Mean dCt*	± *SEM*
2D	8.70	0.22	-	-	8.79	0.14	-	-
3D Day 1	8.47	0.02	8.53	0.15	8.56	0.06	8.39	0.23
3D Day 2	6.77	0.18	6.94	0.07	6.53	0.14	5.73	0.04
3D Day 3	7.34	0.11	6.91	0.18	6.26	0.09	5.77	0.03
3D Day 4	6.62	0.07	6.36	0.11	5.68	0.06	4.41	0.05
3D Day 5	5.21	0.12	5.13	0.12	5.38	0.03	3.92	0.11

Figure 5.4.8. qPCR analysis of expression of Nanog in 3D MSCs treated with the autophagy stimulator rapamycin

MSCs from 2 donors were cultured as 2D monolayers and 3D spheroids with an initiating cell number of 60,000 cells for up to 5 days in culture. Media was refreshed daily with 3D MSC media (control samples) or 3D MSC media supplemented with 0.3nM rapamycin. 3D MSCs were isolated every day for 5 days, before cDNA samples were generated and then analysed by qPCR. Expression of target gene for each donor was normalised to expression of the housekeeping gene GAPDH and made relative to expression levels in the donor matched 2D sample. Fold changes were calculated as 2^{-ddCt}. Expression of Nanog in 2 different MSC donors in both control and treated samples is shown. Average dCt values ± SEM for technical replicates are shown in the table.

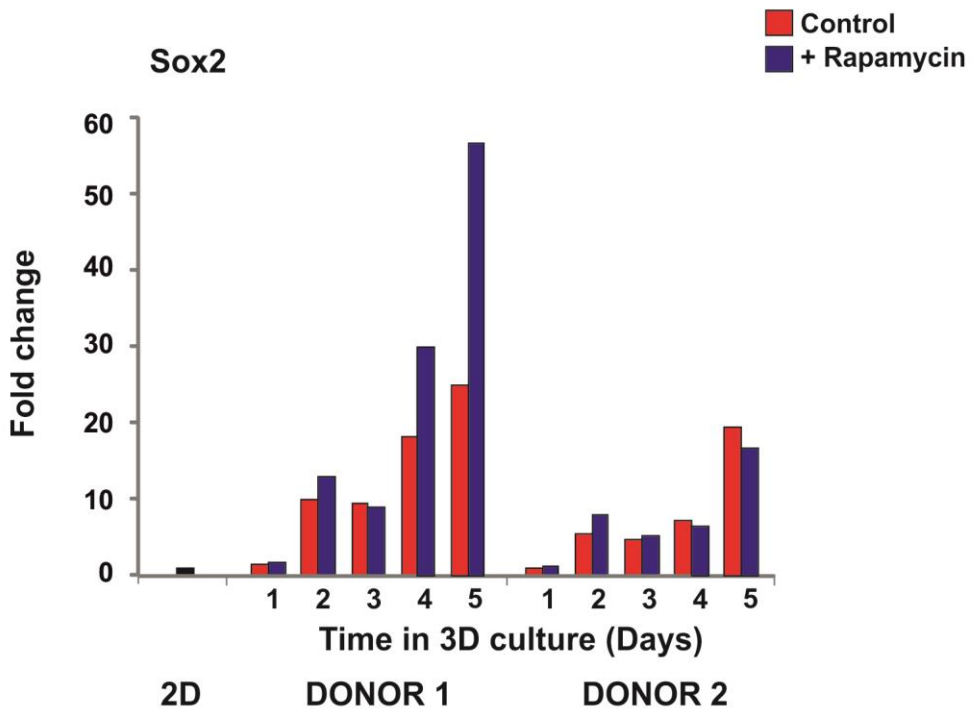

	Donor 1				Donor 2			
	Control		+ rapamycin		Control		+ rapamycin	
	Mean dCt	± *SEM*	*Mean dCt*	± *SEM*	*Mean dCt*	± *SEM*	*Mean dCt*	± *SEM*
2D	9.78	0.04	-	-	9.91	0.29	-	-
3D Day 1	9.95	0.10	9.71	0.00	9.66	0.02	9.20	0.06
3D Day 2	7.36	0.06	6.79	0.13	6.61	0.08	6.23	0.06
3D Day 3	7.53	0.05	7.41	0.07	6.66	0.02	6.74	0.11
3D Day 4	6.92	0.05	7.12	0.13	5.73	0.06	5.33	0.02
3D Day 5	5.50	0.05	5.73	0.10	5.27	0.04	4.09	0.09

Figure 5.4.9. qPCR analysis of expression of Sox2 in 3D MSCs treated with the autophagy stimulator rapamycin

MSCs from 2 donors were cultured as 2D monolayers and 3D spheroids with an initiating cell number of 60,000 cells for up to 5 days in culture. Media was refreshed daily with 3D MSC media (control samples) or 3D MSC media supplemented with 0.3nM rapamycin. 3D MSCs were isolated every day for 5 days, before cDNA samples were generated and then analysed by qPCR. Expression of target gene for each donor was normalised to expression of the housekeeping gene GAPDH and made relative to expression levels in the donor matched 2D sample. Fold changes were calculated as 2^{-ddCt}. Expression of Sox2 in 2 different MSC donors in both control and treated samples is shown. Average dCt values ± SEM for technical replicates are shown in the table.

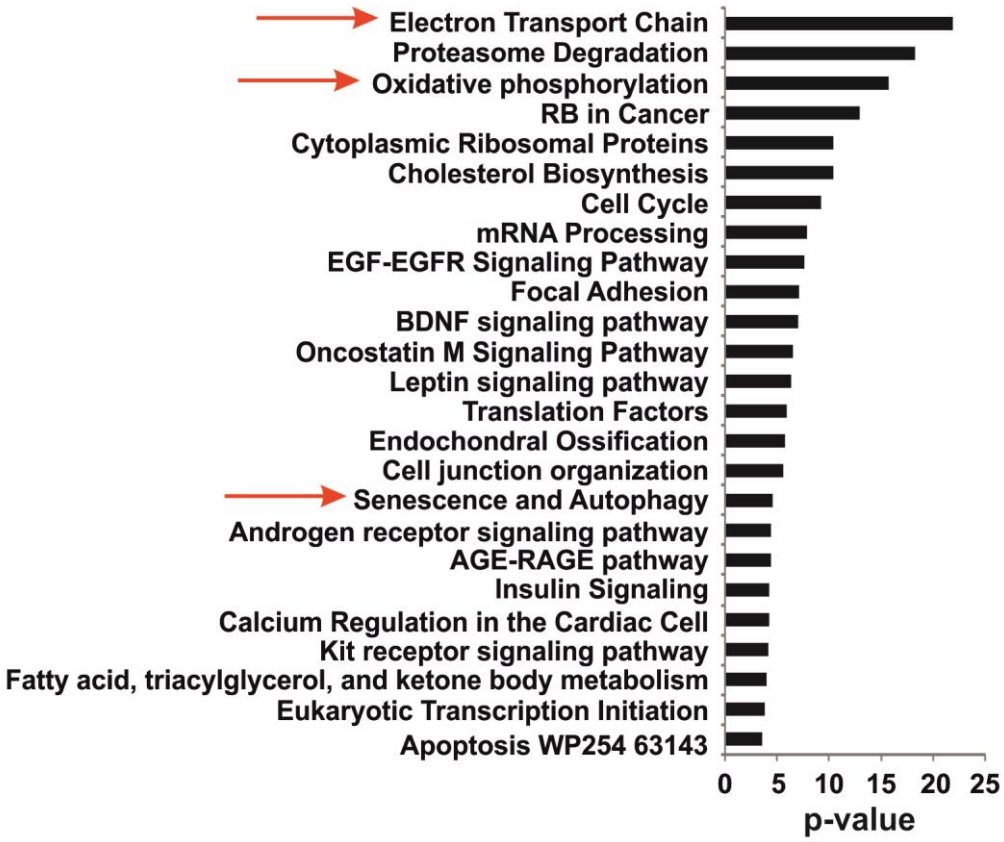

Figure 5.4.10 Agilent array analysis of the top 25 differentially expressed pathways in 3D vs 2D MSCs

MSCs from 4 different donors were cultured as 2D monolayers and 3D spheroids (60,000 MSCs for 5 days). Samples were then subject to transcriptomics analyses, which identified differentially expressed pathways between 2D and 3D samples. The top 25 differentially expressed pathways are shown (arrows highlight pathways related to metabolism and autophagy).

significantly differentially expressed in 3D versus 2D MSCs, and out of these, 66 were down-regulated in 3D (Figure 5.4.11 and Table 5.4.1). Similarly, 42 genes assigned to oxidative phosphorylation by pathway analysis were differentially expressed, and of these 41 were down-regulated in 3D MSCs (Figure 5.4.11 and Table 5.4.2). Supportive of a reduction in oxidative phosphorylation, analysis of oxygen consumption rates (OCR) demonstrated that oxygen consumption reduced with time in optimised 3D conditions. By day 5 of 3D culture OCR had reduced 17.5-fold compared to consumption on day 1. This difference was statistically significant (Figure 5.4.12.A). Under identical culture conditions, 3D MSCs also maintained efflux of lactate into the culture medium, indicating sustained lactate production throughout 3D culture (Figure 5.4.12.B). Another feature of pluripotent ESCs is a distinct cytotype, characterised by few, immature, rounded mitochondria. TEM examination of 3D MSCs revealed the presence of small, rounded mitochondria, typical of those seen in ESCs, after 5 days cultured under optimal 3D conditions (Figure 5.4.13).

5.4.4 Expression of pluripotency factors identifies optimal 3D conditions for HDFs

If autophagy induction by cell stress in 3D culture is responsible for the changes observed in MSCs, it should be possible to induce similar changes in other cell types, and this phenomenon should not be specific to MSCs. To investigate if the optimised 3D model could enhance expression of pluripotency factors in other cell types, HDF monolayer cultures were grown to confluence on tissue culture plastic, before seeding as 3D spheroids, initiated from 60,000 cells and maintained in 3D culture for 5 days. RNA samples were isolated and examined for expression of pluripotency factors by qPCR. In 3D HDFs expression of Oct4 remained unchanged, whilst there was a significant reduction in expression of Nanog relative to expression in 2D HDFs. There was however a significant increase of around 100-fold of Sox2 expression compared to 2D levels (Figure 5.4.14). Although expression of Sox2 was enhanced by the optimised 3D model, it appeared that 3D culture had no/negative effects on the expression of other pluripotent transcription factors, so the conditions optimised for MSCs were not sufficient to induce enhanced expression of all three pluripotency factors in HDFs. If this mechanism relies on a precise scaling of cell

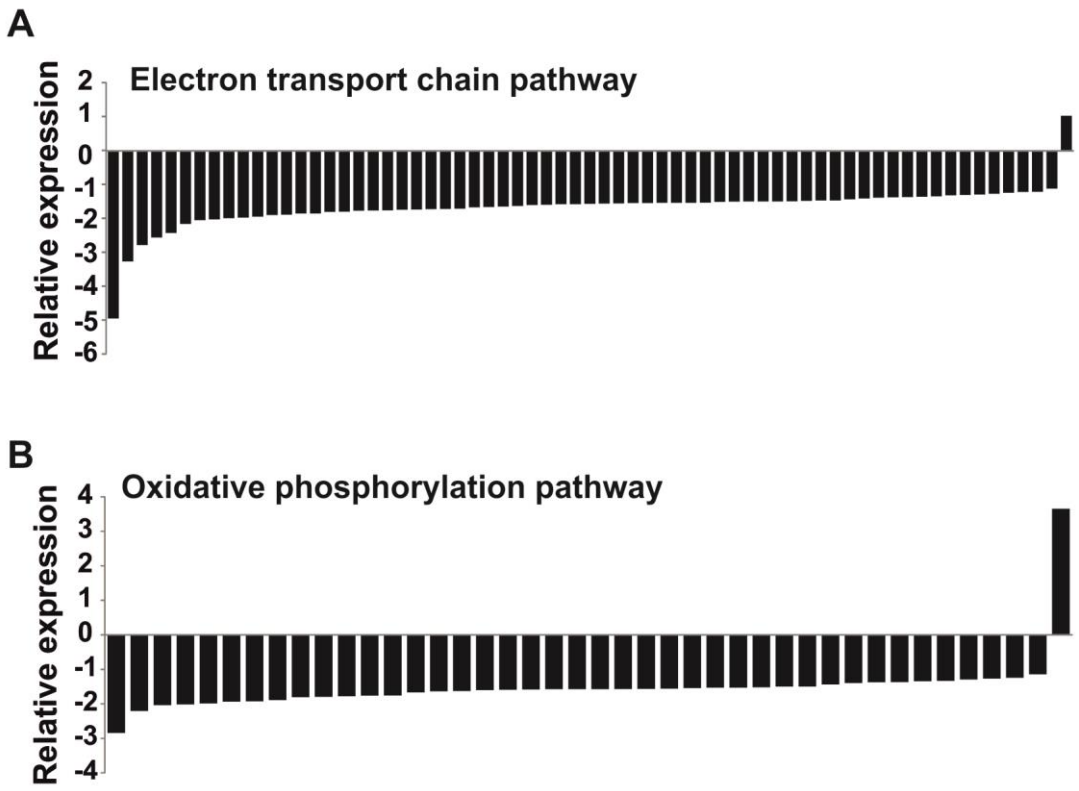

Figure 5.4.11. Agilent array analysis of expression of genes assigned to the electron transport chain and oxidative phosphorylation pathways in 3D vs 2D MSCs

Transcritomics analyses identified the electron transport chain (A) and oxidative phosphorylation (B) amongst the most differentially expressed pathways in 3D MSCs. Relative expression of genes assigned to these pathways is shown in 3D versus 2D MSCs. Gene lists and fold changes are shown in Tables 5.4.1 and 5.4.2.

Table 5.4.1 Fold change expression of genes assigned to the electron transport chain pathway (using Genespring v12.1) in 3D MSCs vs 2D MSCs.

Gene name	Fold change	Gene name	Fold change
ND4L	-5.05674	NDUFA8	-1.5948
SLC25A4	-3.34134	ATP5B	-1.58734
ATP5G1	-2.84382	NDUFB10	-1.57776
COX7A1	-2.61804	NDUFA9	-1.575
ATPIF1	-2.48431	NDUFAB1	-1.57454
NDUFS8	-2.20634	ATP5S	-1.57138
SLC25A5	-2.09295	NDUFS4	-1.56911
COX8A	-2.07	ATP5G3	-1.5637
NDUFB7	-2.03715	ATP5L	-1.54443
NDUFB2	-2.01686	COX6B1	-1.53532
ATP5J2	-1.98975	ATP5G2	-1.53316
NDUFA4	-1.93893	ATP5O	-1.53188
NDUFA7	-1.93	COX7B	-1.52843
COX5A	-1.89533	NDUFA6	-1.52465
ATP5F1	-1.89167	COX7C	-1.51127
UCRC	-1.84434	NDUFB5	-1.50213
DAP13	-1.84087	NDUFA2	-1.49991
ATP5D	-1.8098	COX5B	-1.4669
UQCRFS1	-1.80153	ATP5J	-1.438
NDUFS6	-1.79843	SURF1	-1.41699
ATP5H	-1.77936	NDUFA1	-1.40509
NDUFB3	-1.77505	NDUFS5	-1.39763
NDUFC1	-1.76233	SCO1	-1.3874
ATP5A1	-1.75855	ATP5E	-1.37441
COX6A1	-1.75063	NDUFS1	-1.34605
QP-C	-1.70969	NDUFB9	-1.33539
ATP5C1	-1.69572	UQCRB	-1.3215
SDHB	-1.68605	NDUFC2	-1.2961
NDUFA3	-1.66852	NDUFS3	-1.26757
NDUFB6	-1.63827	NDUFS7	-1.2454
NDUFB1	-1.62896	UQCRC1	-1.23871
SDHC	-1.6136	NDUFA10	-1.1436
UQCRH	-1.61309	COX11	1.054393
NDUFB8	-1.60262		

Table 5.4.2 Fold change expression of genes assigned to the mitochondrial oxidative phosphorylation pathway (using Genespring v12.1) in 3D vs 2D MSCs.

Gene name	Fold change	Gene name	Fold change
ATP5G1	-2.84382	FASN2A	-1.57454
NDUFS8	-2.20634	ATP5S	-1.57138
B18	-2.03715	AQDQ	-1.56911
NDUFB2	-2.01686	ATP5G3	-1.5637
ATP5J2	-1.98975	ATP5L	-1.54443
NDUFA4	-1.93893	ATP5G2	-1.53316
B14.5a	-1.93	ATP5O	-1.53188
ATP5F1	-1.89167	B14	-1.52465
ATP5D	-1.8098	CI-SGDH	-1.50213
NDUFS6	-1.79843	NDUFA2	-1.49991
ATP5H	-1.77936	ATP5J	-1.438
KFYI	-1.76233	NDUFS5	-1.39763
ATP5A1	-1.75855	ATP5E	-1.37441
B9	-1.66852	ATP6AP1	-1.37354
B17	-1.63827	CI-75Kd	-1.34605
CI-SGDH	-1.62896	B22	-1.33539
ASHI	-1.60262	B14.5b	-1.2961
NDUFA8	-1.5948	NDUFS3	-1.26757
ATP5B	-1.58734	NDUFS7	-1.2454
NDUFB10	-1.57776	CI-42KD	-1.1436
NDUFA9	-1.575	NUOMS	3.654102

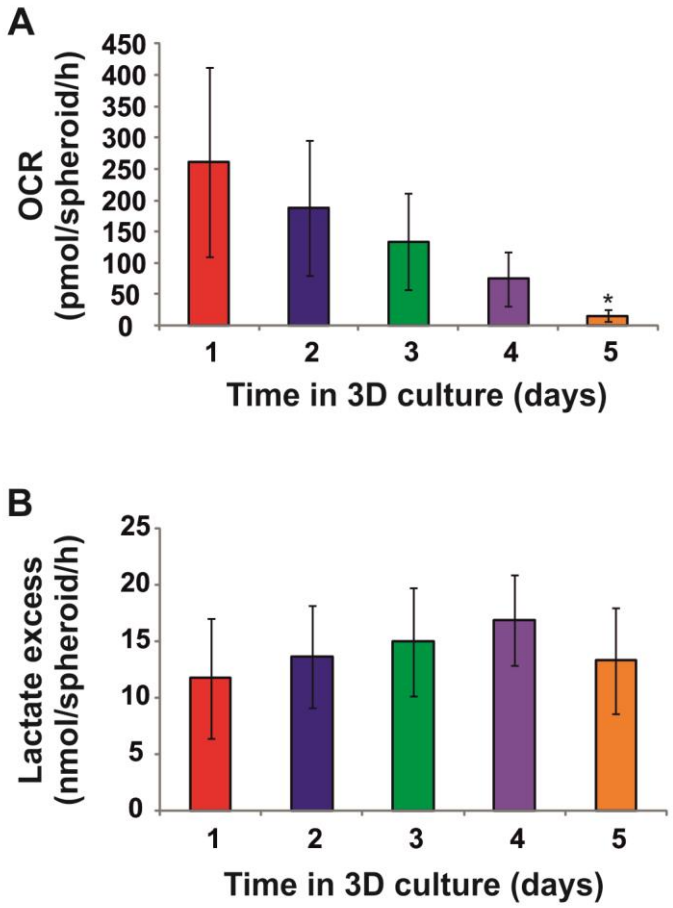

Figure 5.4.12. Analysis of oxygen consumption rates and lactate production in 3D MSCs over time in 3D culture

3D spheroids were initiated from 60,000 MSCs and maintained in culture for up to 5 days. Every day a measure of oxygen consumption rate (A) and lactate production (B) was taken. Mean values are shown, ± SEM, * $p < 0.05$. Statistical significance is relative to expression in 3D MSCs at day 1 (by T-test, $n = 3$).

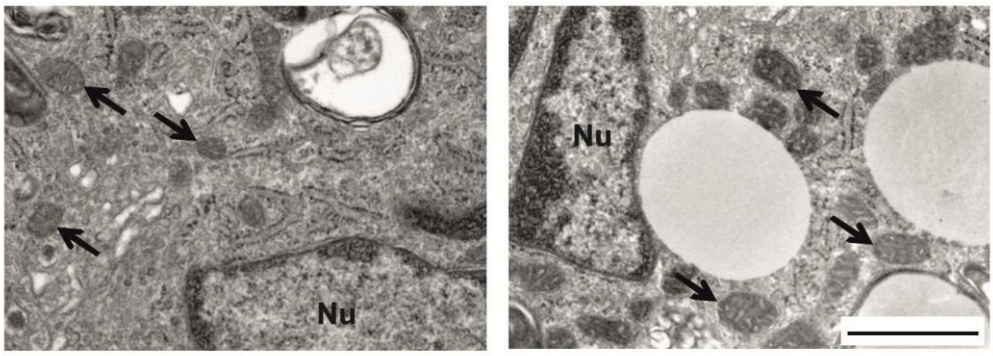

Figure 5.4.13. TEM analysis of 3D MSCs for evidence of mitochondrial remodelling

3D spheroids were initiated from 60,000 MSCs and maintained in culture for 5 days. On day 5, spheroids were fixed, stained and sectioned for TEM analysis. Sections were then examined for the presence of pluripotent stem cell-like mitochondria. Arrows indicate small, rounded mitochondria, typical of those seen in primitive cell types (scale bar = 1µm).

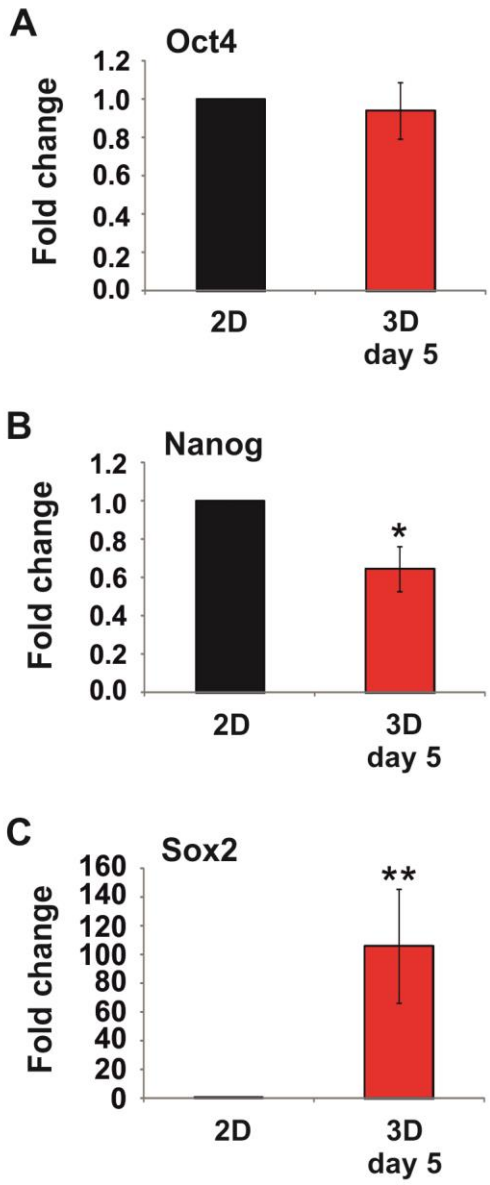

Figure 5.4.14. qPCR analysis of expression of pluripotency factors in HDFs cultured under optimised 3D conditions

HDFs were cultured as 2D monolayers and 3D spheroids (initiating cell number – 60,000 cells per spheroid) for 5 days in culture. RNA samples from three biological replicates were isolated and analysed for expression of Oct4, Nanog and Sox2. In all samples expression was normalised to expression of the housekeeping gene GAPDH and made relative to expression in 2D monolayers. Expression of A) Oct4, B) Nanog and C) Sox2 in 60,000 HDF 3D spheroids after 5 days in 3D culture compared to expression in HDF 2D monolayers. Data was pooled and subject to statistical analysis, mean fold changes are shown ± SEM, * $p < 0.05$, ** $p < 0.01$. Statistical significance is relative to expression in 2D HDFs (by T-test, n = 3).

stress to stimulate autophagy and drive pluripotency factor expression, different cells may require slightly modified conditions to achieve optimal autophagy induction. To investigate whether this was the case, 3D HDF spheroids initiated from 30-, 60-, or 120,000 cells were cultured for up to 5 days. RNA samples were isolated and analysed for expression of Oct4, Nanog and Sox2. Strikingly it again appeared that an optimal time point could be identified by maximal expression of Oct4, Nanog and Sox2. When spheroids initiated from 30,000 HDFs were cultured for 4 days, there was a peak in the expression of Oct4, around 3 fold higher than expression observed in 2D HDFs (Figure 5.4.15). This pattern was also observed for Nanog expression. At day 4 of 3D culture, spheroids initiated from 30'000 HDFs showed around a 3.8 fold increase compared to 2D HDFs (Figure 5.4.16). Notably day 4 of 3D culture also showed a peak of Sox2 expression, with around a 37 fold up-regulation compared to 2D levels, in spheroids initiated from 30,000 HDFs (Figure 5.4.17). These results provide evidence that increased expression of pluripotency factors during 3D culture is not an MSC-specific phenomena, and that optimal culture conditions to stimulate this up-regulation can be identified in other cell types. Further investigation would be necessary to confirm if similar changes in metabolism and autophagy markers also occur in the HDF optimised model.

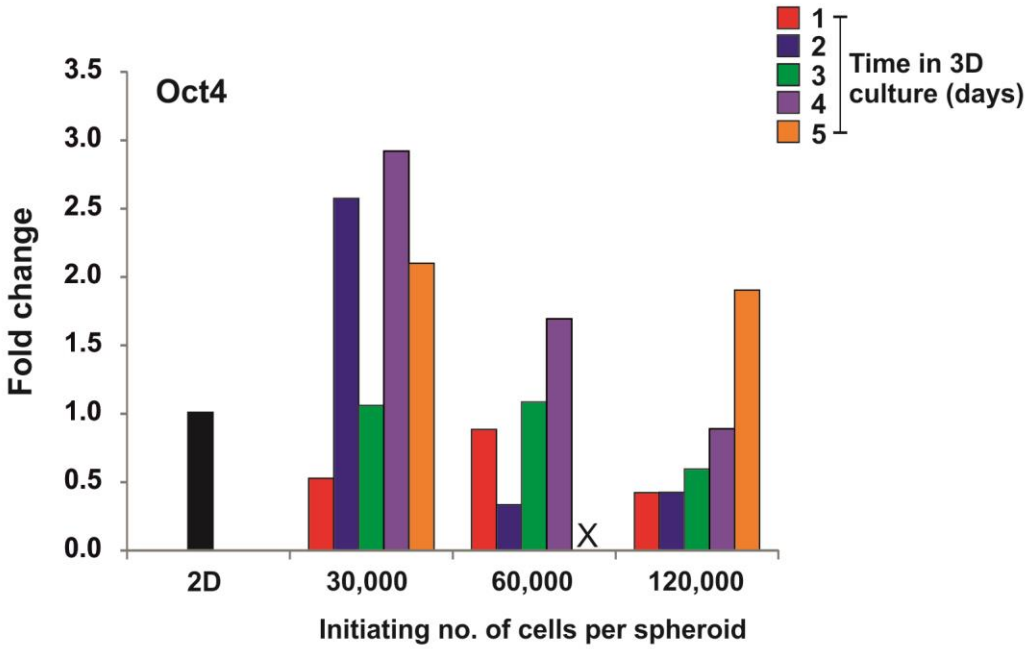

	Initiating number of cells per spheroid					
	30'000		60'000		120'000	
	Mean dCt	± *SEM*	*Mean dCt*	± *SEM*	*Mean dCt*	± *SEM*
2D	5.44	0.61	-	-	-	-
3D Day 1	6.37	0.02	5.64	0.20	6.69	0.04
3D Day 2	4.12	0.24	7.02	0.06	6.76	0.36
3D Day 3	5.40	0.26	5.33	0.11	6.20	0.08
3D Day 4	3.94	0.26	4.69	0.08	5.66	0.27
3D Day 5	4.38	0.04	-	-	4.53	0.14

Figure 5.4.15. qPCR analysis of expression of the pluripotency factor Oct4 in HDFs over time in 3D culture

HDFs were cultured as 2D monolayers and 3D spheroids with initiating cell numbers of 30-, 60-, or 120,000 cells for up to 5 days in culture. cDNA samples were generated and then analysed by qPCR. Expression of Oct4 was normalised to expression of the housekeeping gene GAPDH and made relative to expression levels in the 2D sample. Fold changes were calculated as 2^{-ddCt}. Average dCt values ± SEM for technical replicates are shown in the table.

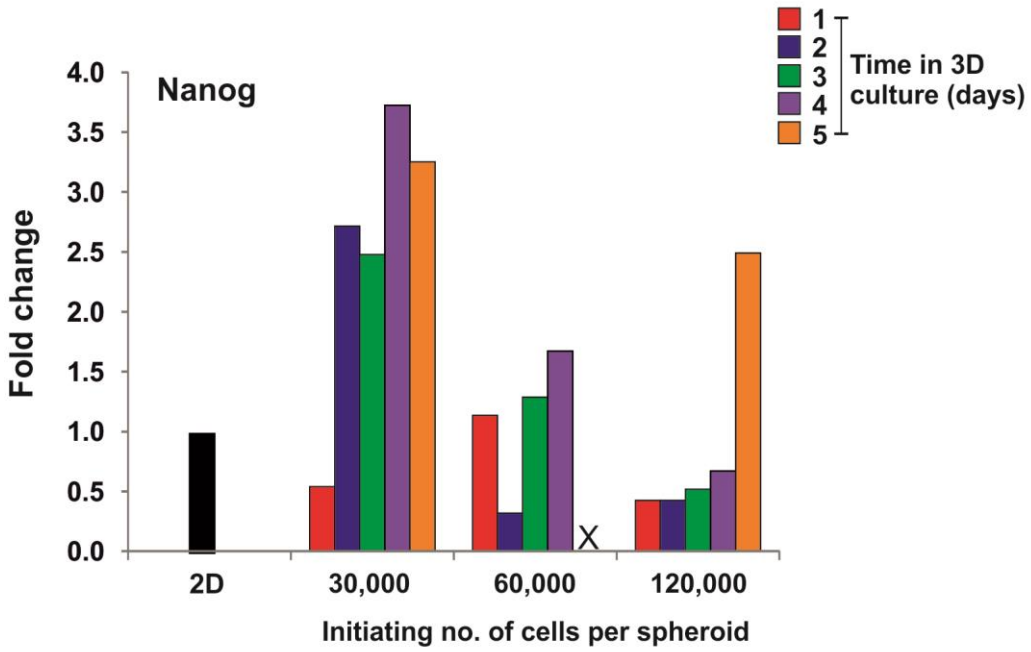

	Initiating number of cells per spheroid					
	30'000		60'000		120'000	
	Mean dCt	± *SEM*	*Mean dCt*	± *SEM*	*Mean dCt*	± *SEM*
2D	13.25	0.21	-	-	-	-
3D Day 1	14.19	0.26	13.08	0.09	14.48	0.03
3D Day 2	11.82	0.12	14.94	0.23	14.50	0.11
3D Day 3	12.29	0.68	13.03	0.46	14.28	0.34
3D Day 4	11.37	0.13	12.52	0.13	13.83	0.08
3D Day 5	11.60	0.27	-	-	11.97	0.24

Figure 5.4.16. qPCR analysis of expression of the pluripotency factor Nanog in HDFs over time in 3D culture

HDFs were cultured as 2D monolayers and 3D spheroids with initiating cell numbers of 30-, 60-, or 120,000 cells for up to 5 days in culture. cDNA samples were generated and then analysed by qPCR. Expression of Nanog was normalised to expression of the housekeeping gene GAPDH and made relative to expression levels in the 2D sample. Fold changes were calculated as 2^{-ddCt}. Average dCt values ± SEM for technical replicates are shown in the table.

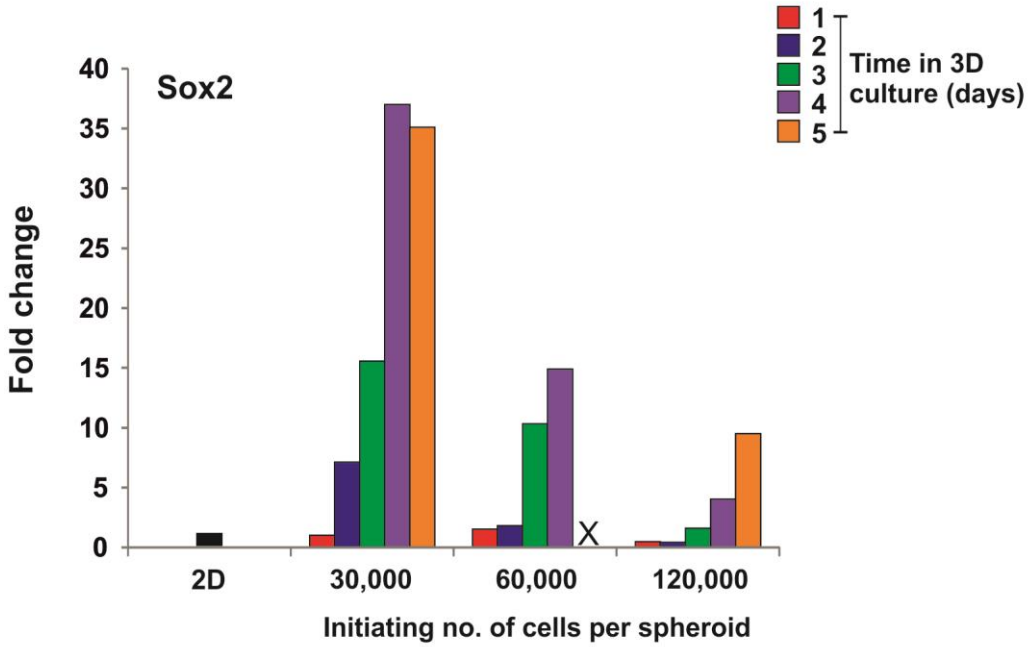

	Initiating number of cells per spheroid					
	30'000		60'000		120'000	
	Mean dCt	± *SEM*	*Mean dCt*	± *SEM*	*Mean dCt*	± *SEM*
2D	8.80	0.13	-	-	-	-
3D Day 1	8.79	0.16	8.21	0.11	9.80	0.02
3D Day 2	5.97	0.08	7.95	0.13	10.01	0.19
3D Day 3	4.85	0.10	5.45	0.17	8.13	0.13
3D Day 4	3.59	0.05	4.91	0.06	6.79	0.03
3D Day 5	3.67	0.08	-	-	5.55	0.05

Figure 5.4.17. qPCR analysis of expression of the pluripotency factor Sox2 in HDFs over time in 3D culture

HDFs were cultured as 2D monolayers and 3D spheroids with initiating cell numbers of 30-, 60-, or 120,000 cells for up to 5 days in culture. cDNA samples were generated and then analysed by qPCR. Expression of Sox2 was normalised to expression of the housekeeping gene GAPDH and made relative to expression levels in the 2D sample. Fold changes were calculated as 2^{-ddCt}. Average dCt values ± SEM for technical replicates are shown in the table.

5.5 Discussion

The results presented in this chapter confirm enhanced autophagy in MSCs cultured as 3D spheroids. There is also evidence that 3D culture drives metabolic remodelling in 3D MSCs. Transcriptomics analyses highlighted the senescence and autophagy pathway as one of the top 25 differentially expressed pathways in 3D versus 2D MSCs. Autophagy and lysosomal biogenesis are regulated by the master transcriptional regulator TFEB (Sardiello et al., 2009; Settembre et al., 2011). TFEB expression was up-regulated early (day 1) in 3D culture, and reached maximal up-regulation by day 2. High expression of TFEB was then maintained throughout 3D culture. It has recently been demonstrated that TFEB is itself regulated by the nutrient sensor and autophagy inhibitor mTORC1, so showing a direct link between nutrient availability and TFEB activity. Under nutrient-rich conditions, mTORC1 acts to phosphorylate and inactivate proteins required for the initiation of autophagy, so inhibiting an autophagic response. In contrast, nutrient deprivation leads to the inactivation of mTORC1, and induction of autophagy (Martina et al., 2012). mTORC1 also regulates TFEB localisation through phosphorylation of both serine 142 (Settembre et al., 2012) and serine 211 (Martina et al., 2012; Settembre et al., 2012). When nutrients are plentiful, TFEB is phosphorylated by mTORC1, and through interactions with a member of the 14-3-3 family of proteins, is maintained in the cytosol (Martina et al., 2012). However during nutrient deprivation, mTORC1 is inactivated, TFEB is not phosphorylated, and translocates to the nucleus, where it regulates the expression of lysosome and autophagy genes (Martina et al., 2012; Settembre et al., 2012). Although the localisation of TFEB was not tracked during 3D culture, strong, sustained up-regulation of TFEB expression was observed in 3D MSCs. Nuclear translocation in fact occurs before TFEB up-regulation in response to nutrient starvation. Nuclear translocation of TFEB was observed very quickly after elimination of nutrients from the media, whilst increase in TFEB expression occurred several hours later (Settembre et al., 2013). Exogenous over-expression of TFEB could also positively regulate endogenous TFEB expression, suggesting the presence of a positive auto-regulatory loop, in which nuclear translocation of TFEB-induced TFEB up-regulation in response to starvation (Settembre et al., 2013). The presence of an auto-regulatory loop is supportive of the results seen in 3D MSCs, where there was progressive up-regulation of TFEB expression from day 1 of 3D

culture. It is likely that TFEB nuclear translocation would have been observed prior to the up-regulation of TFEB mRNA. Using TEM, many typical autophagic structures were observed in the cytoplasm of day 5 3D MSCs, including vesicles with presumptive degraded cytoplasmic contents and double-membrane bound structures. This coincided with an increase in the lysosome marker LAMP1 during 3D culture, indicating an increase in lysosome numbers. This increase was dependent on 3D culture, as expression returned to 2D levels after 3D MSCs were disaggregated and re-plated onto plastic. The recovery of 'normal' LAMP1 levels after return to 2D conditions provides strong evidence that the observed increase in lysosomes is driven by 3D culture conditions, supporting the hypothesis that 3D culture induces an autophagic response. Conversion of LC3 I to LC3 II is a marker of an increase in autophagosome abundance (Kabeya et al., 2003). In 3D MSCs, by day 5 of 3D culture, there is almost complete loss of cytoplasmic LC3 I, indicating that by this stage virtually all LC3 exists in its autophagosome-incorporated form. This indicates a highly active autophagy response in MSCs by day 5 of 3D culture. This also supports the sustained expression of TFEB through to day 5. TFEB is required to activate the expression of many autophagy genes, so would be expressed throughout an autophagic response. A number of compounds which act to enhance autophagy have been demonstrated to increase reprogramming efficiency, including rapamycin, PP242 and spermidine (Chen et al., 2011). Using Oct4, Nanog and Sox2 expression as a readout of de-differentiation, the effect of rapamycin treatment on 3D MSCs was examined. The response to rapamycin was donor-dependent in the MSC donors examined. One donor up-regulated pluripotency factor expression during 3D culture in response to rapamycin, whilst the other donor did not. It may be that Donor 2 was unresponsive to rapamycin at this concentration. It is also possible that whilst in this donor, pluripotency factors were not up-regulated, other markers of de-differentiation, such as early mesendoderm markers may have been enhanced by rapamycin treatment. Furthermore, it has been demonstrated that rapamycin is a partial mTORC1 inhibitor, as some phosphorylation of mTORC1 substrates has been observed during rapamycin treatment (Settembre et al., 2012). It is possible that in Donor 2, the level of rapamycin treatment was insufficient to entirely inactivate mTORC1, so some level of autophagy inhibitory activity may have remained even during treatment. Alternatively, in this donor, 3D conditions alone may have achieved mTORC1 inhibition through nutrient starvation, so no further enhancement

of the autophagy response (and pluripotency factor expression) was stimulated through pharmacological intervention. The results presented here confirm an active autophagy response, which is stimulated early in 3D culture, is 3D culture-dependent, and is reversed when 3D MSCs are re-plated onto tissue culture plastic.

Transcriptomics analyses also highlighted the electron transport chain and oxidative phosphorylation as the first and third most differentially expressed pathways in 3D versus 2D MSCs. 66/67 and 41/42 significantly differentially expressed genes were down-regulated in 3D compared to 2D MSCs respectively. This is similar to the down-regulation of electron transport chain genes when cells undergo reprogramming to pluripotency (Folmes et al., 2011). Indeed, the observed down-regulation of these pathways suggests that by day 5 of 3D culture, MSCs have a markedly reduced reliance on oxidative metabolism. This was further supported by the observation that oxygen consumption reduced progressively over time in 3D culture, and 3D MSCs maintained lactate production throughout 3D culture, both hallmarks of a shift to an anerobic metabolism, which was again observed when MEFs underwent reprogramming to pluripotency (Folmes et al., 2011). It was previously demonstrated that there is no detectable HIF1α staining in 3D MSCs, suggesting that 3D culture does not generate a hypoxic environment (Elen Bray, unpublished observations). Strikingly, this would indicate that the shift to an anerobic metabolism is not driven by hypoxia in 3D MSCs, and anaerobic metabolism in the presence of plentiful oxygen is a hallmark of pluripotent cells (Zhang et al., 2012). Another feature of ESCs is a distinct mitochondrial profile, consisting of few small, simple, perinuclear mitochondria, whilst differentiated cells have a cytoplasmic network of tubular cristae-rich mitochondria, which can support the oxidative metabolism in these cells (Varum et al., 2011). The mitochondria in 3D MSCs were highly similar to mitochondria observed in ESCs, with a small, rounded morphology. The presence of a reduced mitochondrial network could explain the metabolic shift observed in 3D MSCs, as it would result in a decrease in overall oxidative capacity, and an increased reliance on anaerobic metabolism. Altogether, these results confirm that during 3D culture, MSCs undergo metabolic remodelling, and that by day 5 of 3D culture, resemble pluripotent cells in both metabolism and mitochondrial phenotype.

Finally, the robustness of the hypothesis was tested using HDFs. If de-differentiation is driven by the induction of autophagy alone, then this mechanism should be applicable to other cell types, not just MSCs, which may be more amenable to reprogramming and de-differentiation due to their multipotent developmental state. Whilst MSC-optimised 3D conditions only stimulated the enhanced expression of Sox2 in HDFs, it was observed that when 30,000 HDFs were cultured in 3D for 4 days, there was maximal up-regulation of Oct4, Nanog and Sox2. Further study would be required to investigate the metabolic status of these cells, and also to provide evidence of a functional autophagy response. However, this does suggest that with optimisation, 3D culture can be used to drive expression of pluripotency factors in cells other than MSCs.

Much of the research in reprogramming to pluripotency has focused on the need for somatic cells to re-adopt an ESC-like gene expression and epigenetic profile, as these factors are thought to underlie the mechanisms of pluripotency maintenance, and often the need for metabolic remodelling had been overlooked. However, more recently, the importance of metabolic reprogramming has been acknowledged. Indeed, it has been demonstrated that factors which enhance glycolysis can increase reprogramming efficiency (Panopoulos et al., 2012), whilst blocking glycolysis inhibited reprogramming to pluripotency (Folmes et al., 2011; Panopoulos et al., 2012). Furthermore, inhibition of mitochondrial fission, through the use of a compound which drives the production of mitochondrial net-like structures, significantly reduced the formation of iPSC colonies in MEFs. Early treatment was sufficient to inhibit iPSC formation, suggesting that the remodelling of the mitochondrial network was a necessary early event in the reprogramming process (Vazquez-Martin et al., 2012).

Although in this case, I observe lineage-restricted de-differentiation rather than reprogramming to pluripotency, the underlying principles of metabolic remodelling would still apply. The evidence presented here indicates that metabolic remodelling occurs, not only during factor-based reprogramming to pluripotency, but also in culture-driven de-differentiation. This would suggest that cytoplasmic clearance and resetting of the metabolism is a fundamental requirement when cells undergo de-differentiation. It makes sense that if differentiation involves the development of an

increasingly complex metabolism and cytotype, then forced de-differentiation would require the reversal of this process, to a simplistic, primitive metabolism and cytotype. Although the precise mechanism which facilitates metabolic remodelling remains unknown, in separate studies, it has been demonstrated that a functional autophagy response is required early during factor-based reprogramming to pluripotency (Wang et al., 2013). Autophagy is an effective cytoplasmic clearance mechanism, which clears cytoplasmic contents including mitochondria, during cell stress (Klionsky and Emr, 2000). The hypothesis of this work stated that a scaled autophagic response would be sufficient to drive de-differentiation in MSCs cultured under optimised 3D conditions. An autophagy response was observed early in 3D culture, whilst the metabolic remodelling appeared progressive over the culture period, which would support the idea that autophagy is the mechanism by which cytoplasmic clearance occurs. A diminished oxidative capacity due to the reduced mitochondrial network would then necessitate a shift to an anaerobic metabolism. Strikingly, a promoter search revealed the presence of a TFEB binding site directly upstream of the Sox2 promoter. Although this would require functional validation, it does provide a potential direct link between mechanisms driving enhanced autophagy and pluripotency factor expression. Although no such site was observed in the Oct4 or Nanog promoters, Sox2 is known to bind both Oct4 and Nanog and positively regulate their expression (Boyer et al., 2005). Taken together, these results suggest that nutrient deprivation could stimulate autophagy, and that autophagy, through cytoplasmic clearance, could drive metabolic remodelling, whilst autophagy related expression of TFEB could initiate expression of pluripotency factors via a Sox2-mediated positive auto-regulatory feedback loop, in MSCs cultured in our optimised 3D model.

Chapter 6: Discussion

Heterogeneity is common in un-sorted MSCs isolated from bone-marrow. Although enhanced expression of pluripotency/mesendoderm-associated genes is highly similar across different MSC donors, the response to rapamycin was notably different in the 2 donors examined, demonstrating that it is always necessary to perform experiments in as many primary donors as possible. It is therefore most important to consider the results presented here in that context. One must be careful to ensure that they do not overestimate the extent to which the behaviours observed in a small number of donors are representative of MSC behaviours across a large population. That said, results such as those presented here, which show similar cell behaviour across MSCs isolated from a number of donors can be used as an indicator of MSC behaviour, and form the basis for more extensive study in further donors. The use of primary cells in this way also ensures that one is forced to consider variations in cell behaviour, which may be overlooked when using biological replicates of a single cell line, where you could expect behaviour to be much more homogeneous.

Since the first derivation of iPSCs from mouse somatic cells in 2006 (Takahashi and Yamanaka, 2006), our knowledge of reprogramming has grown. The generation of human iPSCs using distinct factor combinations (Takahashi et al., 2007; Yu et al., 2007) has been followed by a range of technical refinements, including removal of the oncogene c-Myc to reduce tumour incidence in offspring (Nakagawa et al., 2008; Wernig et al., 2008), along with the use of epigenetic compounds (Huangfu et al., 2008a; Huangfu et al., 2008b; Mikkelsen et al., 2008; Shi et al., 2008) and diverse cell types aimed at improving the efficiency of reprogramming to pluripotency (Kim et al., 2009b; Kim et al., 2008; Tsai et al., 2011; Tsai et al., 2010). The process of direct reprogramming has also been developed, based on the principles of factor based reprogramming, whereby exogenous expression of factors associated with a particular lineage can drive reprogramming towards that cell fate in other somatic cell types. Of particular note, the process of direct reprogramming switches one cell type from another, without passage through a pluripotent state. This effectively circumvents the associated teratoma risk of induced pluripotency, so is of particular relevance to therapeutic applications, as a safer way to generate patient-specific cells

(Huang et al., 2011; Ieda et al., 2010; Szabo et al., 2010; Vierbuchen et al., 2010). Recent work has highlighted the need for metabolic transition during the reprogramming process. As well as a resetting of the transcriptome and epigenome, the metabotype of differentiated cells also requires resetting to the pluripotent state. Pluripotent ESCs have a simple cytotype, characterised by the presence of very few, immature mitochondria, with a rounded, cristae-poor morphology, which are observed in a perinuclear location. The limited oxidative capacity of ESCs means they rely on glycolysis (anaerobic metabolism) to meet their energy needs, even under normoxic conditions. In contrast, differentiated cells generally respire aerobically, unless they are exposed to a hypoxic environment, and contain a cytoplasmic network of tubular, cristae rich mitochondria (Varum et al., 2011). It has been demonstrated that a glycolytic shift is required for successful reprogramming to pluripotency (Folmes et al., 2011; Panopoulos et al., 2012), although the exact mechanism of this shift, and the mechanism which facilitates mitochondrial remodelling has not been identified. However, if we consider differentiation as the acquisition of increased cellular and cytoplasmic complexity, then clearly the process of reprogramming or de-differentiation, which is essentially the reversal of differentiation, would require mechanisms to reduce cytoplasmic/metabolic complexity and to reinstate the less complex cytotype of pluripotent cells. Autophagy is known to recycle cytoplasmic contents, including mitochondria, during a cell stress response (Klionsky and Emr, 2000). Separately it has been demonstrated that a functional autophagy response is also required for reprogramming to pluripotency, and that exogenous Sox2 expression can actually trigger a transient autophagy response (Wang et al., 2013). Longevity-promoting drugs such as rapamycin and spermidine have been shown to enhance the efficiency of reprogramming to pluripotency (Chen et al., 2011), although both these drugs are known autophagy inducers, so it may be that they act through their ability to induce autophagy to enhance the reprogramming process. As of yet though, there seems to be little connection between autophagy and metabolic remodelling in reprogramming/de-differentiation. The work presented in this thesis investigated the hypothesis that the requirement for a functional autophagy response and metabolic remodelling during de-differentiation are in fact closely linked, and that autophagy could be the mechanism by which cytoplasmic clearance is facilitated. Previous work in the laboratory showed that when 3D MSCs are cultured as spheroids, they

up-regulate expression of Oct4, Nanog and Sox2. It was assumed that oxygen and nutrient gradient across the spheroid structure must be providing optimal conditions for MSC potency, although the precise mechanisms driving enhanced pluripotency factor expression remained unknown (Elen Bray, unpublished observations). In this study I hypothesised that controlled induction of autophagy by nutrient deprivation, was the mechanism driving de-differentiation in 3D MSCs. The variation of initial cell seeding number and culture time enabled the generation of a wide range of spheroid sizes, and associated variation in nutrient deprivation. It was hypothesised that under optimal conditions, cell stress alone, in the absence of exogenous factors, would be sufficient to induce an optimal autophagic response, resulting in widespread cytoplasmic clearance and metabolic remodelling to drive de-differentiation.

Under optimal 3D conditions, enhanced pluripotency factor expression was observed, along with evidence of active autophagy, including high expression of TFEB, the master regulator of autophagy and lysosomal biogenesis. TFEB can positively regulate its own expression, and the activity of TFEB is positively regulated by the nutrient sensor (and autophagy inhibitor) mTORC1 during nutrient deprivation (Settembre et al., 2012). Coinciding with maximal expression of pluripotency markers, there was maximal reduction in OCR, reduced mitochondrial complexity, and decreased expression of genes linked to oxidative metabolism under optimal 3D culture conditions. Although a direct link between autophagy and metabolic remodelling in 3D MSCs was not demonstrated, autophagy was activated early in 3D culture, whilst reduced oxygen consumption was a gradual process, so it is possible that mitochondrial clearance through sustained autophagy was responsible for the observed shift to an anaerobic metabolism. Though it was not functionally validated during this study, the presence of a TFEB binding site was identified in the promoter of Sox2. This binding site was optimally positioned directly upstream of the transcriptional start site, and if functional, provides a direct link between nutrient deprivation, autophagy and increased pluripotency factor expression. TFEB, activated by the nutrient sensor mTORC1 during nutrient deprivation in 3D culture conditions, could translocate to the nucleus, and establish a positive feedback loop to maintain autophagy in the presence of nutrient deprivation. As well as regulating its own expression and that of lysosome and autophagy genes,

TFEB could also up-regulate expression of Sox2, by binding to the CLEAR element in the Sox2 promoter. Expression of Sox2 could then positively regulate the expression of itself, along with Oct4 and Nanog. Indeed stimulation of autophagy through rapamycin treatment could increase expression of pluripotency factors in some primary MSCs cultured in 3D, although this was donor-dependent. At the same time, cytoplasmic clearance by autophagy, driven by sustained nutrient deprivation during 3D culture, could result in mitochondrial remodelling and a reduced mitochondrial network. This would in turn result in a reduced oxidative capacity, and an increased reliance on anaerobic metabolism.

The processes occurring during reprogramming to pluripotency *in vitro* are not dissimilar to those which are required for tissue regeneration *in vivo*. During tissue regeneration, there is widespread reorganisation of the cytoplasmic compartment. Studies of zebrafish caudal fin regeneration have demonstrated a requirement for functional autophagy following fin amputation (Varga et al., 2013). Autophagy is also known to play a key role in early embryogenesis, during pre-implantation mammalian development. Embryos showed reduced protein synthesis and failed to develop beyond the 4-8 cell stage in the absence of functional autophagy. It is suggested that this is likely due to the failure to degrade maternally-derived proteins, which would provide metabolites and amino acids for zygotic protein production and normal development, as pre-implantation mammalian embryos develop in the absence of an extracellular nutrient store (Tsukamoto et al., 2008). 3D MSCs had enhanced capacity to generate tissue *in vivo*, possibly fuelled by increased autophagy and the provision of sufficient metabolites and amino acids for tissue generation. The regeneration of the caudal fin also requires de-differentiation of differentiated cells in the area of the amputation. It was observed that when autophagy was impaired, these cells showed reduced proliferative capacity, increased cell death, and differentiation defects, leading to failure of fin regeneration. Autophagy clearly plays a fundamental role in driving tissue de-differentiation through cytoplasmic clearance, and promotes cell survival and proliferation following cell stress (Varga et al., 2013). 3D culture restored proliferation in culture-aged MSCs, and reversed senescence-associated hypertrophy. After non-proliferative MSCs were cultured as 3D spheroids, they re-entered active cell cycling following disaggregation onto tissue culture plastic. The resultant cells were also notably smaller and less spread than the

originating 2D cell population, suggestive of re-organisation and reduction of the cytoplasmic compartment during 3D culture. Aging in cells is associated with increased mTOR activity (Chen et al., 2009) and presumably impaired autophagy. Reduced self-renewal capacity and poor haematopoietic reconstitution are both features of aged HSCs. Restoration of self-renewal and *in vivo* haematopoietic regenerative capacity were observed in HSCs following treatment with rapamycin (Chen et al., 2009). Autophagy stimulation through cellular rejuvenation is the likely mechanism for these observations, and this supports our observation that culture-aged MSCs are rejuvenated by 3D culture-driven autophagy.

3D MSCs did not form teratomas *in vivo*, instead they gave rise to highly organised tissue of mesodermal origin, showing enhanced *in vivo* potency compared to their originating 2D cell population, which could not form any tissue on implantation into nude mice. d-3D MSCs were also responsive to *in vitro* haematopoietic induction, forming non-typical blast-like colonies in a haematopoietic colony assay. This clearly demonstrated enhanced *in vitro* potency, as 2D MSCs were unresponsive to such induction. Haematopoietic lineages arise from early mesoderm, branching off before the specification of MSCs (Oldershaw et al., 2010), which suggests that 3D MSCs have de-differentiated sufficiently far to regain their haematopoietic potential. The absence of teratoma formation by 3D MSCs suggests they are in a post-pluripotent state. Supportive of this, although mRNA levels of Oct4, Nanog and Sox2 are up-regulated under optimal 3D conditions, these levels remain lower than expression levels in human ESCs, and pluripotency factor protein expression is variable or undetectable in 3D MSCs.

It is interesting to observe expression of pluripotency factors, albeit at the transcript level, in the absence of pluripotency. However, the recent establishment of mouse EpiSCs from post-implantation blastocysts should perhaps change the way we traditionally view pluripotency. It has long been known that mouse and human ESCs are distinct in their requirements for cell signalling to maintain their pluripotent state, with mouse ESCs requiring LIF (Nichols et al., 1990; Smith et al., 1988), whilst human ESCs rely on FGF/Activin/Nodal signalling to maintain pluripotency (James et al., 2005; Vallier et al., 2005). Mouse EpiSCs in fact closely resemble human ESCs in their signalling requirements, and are also less potent than mouse ESCs, as

they are not capable of germline contribution (Brons et al., 2007; Tesar et al., 2007). Some groups have shown that mouse EpiSCs can revert to ESCs, through the use of stringent cell culture conditions (Bao et al., 2009), suggesting that EpiSCs represent a slightly later developmental state than ESCs. It has even been observed that some EpiSC lines, although capable of teratoma formation, so technically pluripotent, express the mesendoderm markers Brachyury and Goosecoid, alongside the pluripotency markers Oct4, Nanog and Sox2. It was noted that expression of these mesendodermal markers made EpiSCs refractory to culture-based reprogramming to ESCs, whilst the most easily reprogrammed EpiSCs were those which only expressed pluripotency markers (Bernemann et al., 2011). This again suggests another element of complexity to the definition of pluripotency, as this study alone highlighted 3 distinct developmental states, all pluripotent by teratoma assay, but subtly distinct in their gene expression profile and differentiation potential *in vitro*. Strikingly, co-expression of pluripotency factors with markers of mesendoderm was observed in 3D MSCs, and given the similarity to their gene expression profile, one could speculate that 3D MSCs represent a developmental state 'downstream' of the EpiSCs which co-express pluripotency and mesendoderm markers. 3D MSCs remain distinctly post-pluripotent, but have undergone de-differentiation to a primitive mesendoderm state, capable of enhanced lineage-restricted differentiation, and marked by characteristics of a primitive developmental state, including gene expression, metabotype and mitochondrial profile.

The concept of cell stress as a driving mechanism for de- differentiation/ reprogramming has been highlighted by 2 recent high profile publications (Obokata et al., 2014a; Obokata et al., 2014b). Obokata and colleagues claimed that simple exposure to sub-lethal cell stress (acidic pH) was sufficient to drive reprogramming to pluripotency in neonatal mouse cells (Obokata et al., 2014b). A 30 minute incubation at pH 5.4-5.8 induced Oct4-GFP expression in CD45+ haematopoietic cells, which by day 7 after acid exposure showed extensive demethylation of the Oct4 and Nanog promoters and were capable of teratoma formation and chimera contribution. This process was named stimulus-triggered acquisition of pluripotency (STAP), and the resultant cells were referred to as STAP cells. Although there were notable differences between STAP cells and ESCs, such as the lack of proliferative capacity of STAP cells in LIF-supplemented media, this work suggested that simple,

non-physiological sub-lethal cell stress was sufficient to drive de-differentiation to a fully reprogrammed state. The authors raised the question of *in vivo* induction of pluripotency by cell stress, and how this might be regulated to prevent teratoma formation in tissues frequently exposed to acidic pH, such as the oesophageal mucosa (Obokata et al., 2014b). However, no mechanism was identified in this study, and since publication, questions have been raised about the reproducibility of the method. Whilst I am unable to comment on the reproducibility or the validity of the results presented in the publications by Obokata and colleagues, I believe that the work presented in this thesis may offer support to the theory of sub-lethal stress induced de-differentiation. It would appear that in MSCs, sub-lethal cell stress (in this case nutrient deprivation) is sufficient to drive de-differentiation. Strikingly, some of the observations made by Obokata and colleagues are not dissimilar to those seen in 3D MSCs. It was noted that STAP cells were observed to decrease in size prior to Oct4-GFP expression (Obokata et al., 2014b), possibly reflective of active autophagy and cytoplasmic recycling in response to cell stress. It was also observed that by day 3, between one third and one half of cells had been lost through apoptotic cell death (Obokata et al., 2014b), perhaps representative of autophagy scaled in favour of apoptosis in these cells. Cells strongly expressed Oct4-GFP and other pluripotency markers at day 7, but at day 3 expressed mesodermal markers such as KDR, indicating a progressive passage to pluripotency (Obokata et al., 2014b), similar to the progressive de-differentiation process proposed for 3D MSCs. Many questions remain regarding the research into STAP cells, but the theory behind their generation is in part supported here by evidence that sub-lethal cell stress (although distinct from that applied to generate STAP cells) can drive de-differentiation in MSCs cultured under optimal 3D conditions.

In this study ‘optimal conditions’ are defined as the point when maximal expression of pluripotency and mesendoderm markers and maximal evidence of metabolic shift is observed. This most likely represents the point where autophagy is finely balanced between its pro-survival/anti-apoptotic and its pro-apoptotic effects, the threshold point between sub-lethal and lethal cell stress. It is proposed that autophagy may play a role in hormesis, the phenomenon by which pre-conditioning of cells by exposure to sub-lethal stress confers resistance when cells are later exposed to the same stress at a level which would normally prove lethal (Rubinsztein et al., 2011).

As previously discussed, autophagy has also been demonstrated to have fundamental roles in reprogramming to pluripotency (Wang et al., 2013) and tissue regeneration (Varga et al., 2013). The work presented in this thesis provides a mechanism to help interpret the recent body of work linking cell-stress and autophagy to de-differentiation and reprogramming. It demonstrates that an intrinsic mechanism, driven by controlled sub-lethal cell stress precisely scales the autophagy response in favour of optimal cytoplasmic clearance and cell survival in MSCs cultured as 3D spheroids. In these conditions cells undergo lineage-restricted reprogramming, avoiding pluripotency and teratoma formation, and giving rise to a primitive cell population with enhanced tissue forming capacity *in vivo* (Figure 6.1). It could be considered that the process of STAP, through uncontrolled cell stress, drives inappropriate reprogramming to a pluripotent, teratoma initiating state, whilst in contrast, the model presented here could reflect a physiologically-relevant capacity for lineage-restricted de-differentiation and tissue formation in response to controlled cell stress.

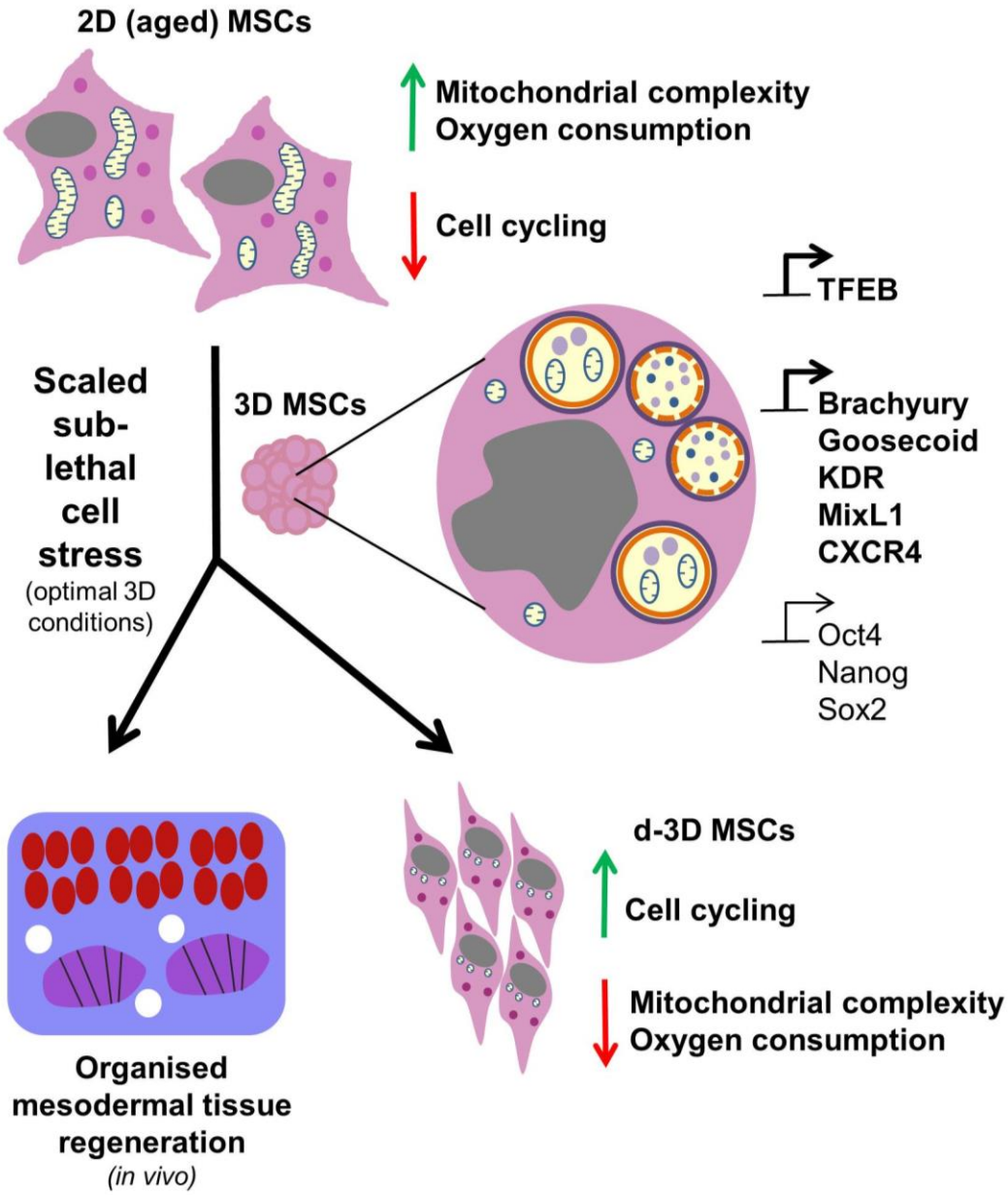

Figure 6.1. Schematic summarising the data presented in this thesis and showing the proposed mechanism of de-differentiation and cellular rejuvenation in 3D MSCs

2D MSCs are characterised by increased mitochondrial network complexity, aerobic metabolism and decreased cell cycling with time in culture. Optimal 3D culture conditions precisely scale sub-lethal cell stress, driving enhanced autophagy, cytoplasmic remodelling, a metabolic shift to anerobic metabolism and expression of markers of mesendodermal and pluripotent cells. This results in increased cell cycling and reversal of cellular hypertrophy *in vitro*, and enhanced mesodermal tissue regeneration *in vivo*.

List of abbreviations

2i	2 compounds which maintain ESCs in an undifferentiated state when used in combination
3i	3 compounds which maintain ESCs in an undifferentiated state when used in combination
5' AZA	5' azacytidine
BMP	Bone morphogenetic protein
CLEAR	Coordinated Lysosome Expression and Regulation
DIA	differentiation inhibitory activity
d-3D MSCs	Disaggregated 3D MSCs
Dox	doxycycline
DMEM	Dulbecco's Modified Eagle Medium
EC	embryonal carcinoma
ESCs	embryonic stem cells
EpiSCs	Epiblast stem cells
ERK	Extracellular signal-regulated kinase
FGF	Fibroblast growth factor
FGF4	Fibroblast growth factor 4
GSK3β	Glycogen synthase kinase 3 beta
GFP	Grren fluorescent protein
H3K79me3	Histone 3 dimethylated at lysine 36
H3K27me3	Histone 3 trimethylated at lysine 27
H3K36me3	Histone 3 trimethylated at lysine 36
H3K4me3	Histone 3 trimethylated at lysine 4
H3K36me2	Histone 3 trimethylated at lysine 80
H3K9me3	Histone 3 trimethylated at lysine 9

H4K20me3	Histone 4 trimethylated at lysine 20
HDAC	Histone deacetylase
HDFs	Human dermal fibroblasts
HUVECs	Human umbilical vein endothelial cells
IVF	In vitro fertilisation
iPSCs	induced pluripotent stem cells
ICM	inner cell mass
iMEF	Irradiated mouse embryonic fibroblasts
lenti-GFP	Lentiviral particles constitutively expressing green fluorescent protein
LIF	Leukaemia inhibitory factor
mTOR	mammalian target of rapamycin
MTORC1	mammalian target of rapamycin complex 1
MSCs	Mesenchymal stem cell/multipotent stromal cells
MAPK	Mitogen-activated protein kinase
MEK	Mitogen-activated protein kinase kinase (often referred to as MAPKK)
MEFs	mouse embryonic fibroblasts
3D MSCs	MSCs cultured as 3D spheroids
2D MSCs	MSCs cultured as adherent monolayers
NSCs	Neural stem cells
NuRD	Nucleosome remodelling and histone deacetylation
O	Oct4 (in the context of single factor reprogramming)
OM	Oct4 and c-Myc
OK	Oct4 and Klf4
OS	Oct4 and Sox2

OKS	Oct4, Klf4 and Sox2
OKSM	Oct4, Klf4, Sox2 and c-Myc
OSNL	Oct4, Sox2, Nanog and Lin28
OCR	Oxygen consumption rate
PcG	Polycomb group
PRC	Polycomb repressive complex
RNAi	RNA interference
SCID	Severe combined immunodeficient
shRNA	Short hairpin RNA
siRNA	Short interfering RNA
SSEA	Stage specific embryonic antigen
STAP	Stimulus triggered acquisition of pluripotency
TGFβ	Transforming growth factor beta
TEM	Transmission electron microscopy
VPA	Valproic acid

References

Andrews, P.W. (2002). From teratocarcinomas to embryonic stem cells. Philosophical transactions of the Royal Society of London Series B, Biological sciences *357*, 405-417.

Avilion, A.A., Nicolis, S.K., Pevny, L.H., Perez, L., Vivian, N., and Lovell-Badge, R. (2003). Multipotent cell lineages in early mouse development depend on SOX2 function. Genes & development *17*, 126-140.

Azuara, V., Perry, P., Sauer, S., Spivakov, M., Jorgensen, H.F., John, R.M., Gouti, M., Casanova, M., Warnes, G., Merkenschlager, M., *et al.* (2006). Chromatin signatures of pluripotent cell lines. Nat Cell Biol *8*, 532-U189.

Bao, S., Tang, F., Li, X., Hayashi, K., Gillich, A., Lao, K., and Surani, M.A. (2009). Epigenetic reversion of post-implantation epiblast to pluripotent embryonic stem cells. Nature *461*, 1292-1295.

Beddington, R.S.P., and Robertson, E.J. (1999). Axis development and early asymmetry in mammals. Cell *96*, 195-209.

Bernemann, C., Greber, B., Ko, K., Sterneckert, J., Han, D.W., Arauzo-Bravo, M.J., and Scholer, H.R. (2011). Distinct developmental ground states of epiblast stem cell lines determine different pluripotency features. Stem cells *29*, 1496-1503.

Bernstein, B.E., Mikkelsen, T.S., Xie, X., Kamal, M., Huebert, D.J., Cuff, J., Fry, B., Meissner, A., Wernig, M., Plath, K., *et al.* (2006). A bivalent chromatin structure marks key developmental genes in embryonic stem cells. Cell *125*, 315-326.

Boyer, L.A., Lee, T.I., Cole, M.F., Johnstone, S.E., Levine, S.S., Zucker, J.P., Guenther, M.G., Kumar, R.M., Murray, H.L., Jenner, R.G., *et al.* (2005). Core transcriptional regulatory circuitry in human embryonic stem cells. Cell *122*, 947-956.

Boyer, L.A., Plath, K., Zeitlinger, J., Brambrink, T., Medeiros, L.A., Lee, T.I., Levine, S.S., Wernig, M., Tajonar, A., Ray, M.K., *et al.* (2006). Polycomb complexes repress developmental regulators in murine embryonic stem cells. Nature *441*, 349-353.

Brons, I.G., Smithers, L.E., Trotter, M.W., Rugg-Gunn, P., Sun, B., Chuva de Sousa Lopes, S.M., Howlett, S.K., Clarkson, A., Ahrlund-Richter, L., Pedersen, R.A., *et al.* (2007). Derivation of pluripotent epiblast stem cells from mammalian embryos. Nature *448*, 191-195.

Chambers, I., Colby, D., and Robertson, M. (2003). Functional Expression Cloning of Nanog, a Pluripotency Sustaining Factor in Embryonic Stem Cells. Cell *113*, 643-655.

Chen, C., Liu, Y., Liu, Y., and Zheng, P. (2009). mTOR regulation and therapeutic rejuvenation of aging hematopoietic stem cells. Science signaling *2*, ra75.

Chen, T.T., Shen, L., Yu, J., Wan, H.J., Guo, A., Chen, J.K., Long, Y., Zhao, J., and Pei, G. (2011). Rapamycin and other longevity-promoting compounds enhance the generation of mouse induced pluripotent stem cells. Aging Cell *10*, 908-911.

Constantinescu, D., Gray, H.L., Sammak, P.J., Schatten, G.P., and Csoka, A.B. (2006). Lamin A/C expression is a marker of mouse and human embryonic stem cell differentiation. Stem cells *24*, 177-185.

Cowan, C.A., Atienza, J., Melton, D.A., and Eggan, K. (2005). Nuclear reprogramming of somatic cells after fusion with human embryonic stem cells. Science *309*, 1369-1373.

Dechat, T., Pfleghaar, K., Sengupta, K., Shimi, T., Shumaker, D.K., Solimando, L., and Goldman, R.D. (2008). Nuclear lamins: major factors in the structural organization and function of the nucleus and chromatin. Genes & development *22*, 832-853.

Dreesen, O., Chojnowski, A., Ong, P.F., Zhao, T.Y., Common, J.E., Lunny, D., Lane, E.B., Lee, S.J., Vardy, L.A., Stewart, C.L., *et al.* (2013). Lamin B1 fluctuations have differential effects on cellular proliferation and senescence. The Journal of cell biology *200*, 605-617.

Efroni, S., Duttagupta, R., Cheng, J., Dehghani, H., Hoeppner, D.J., Dash, C., Bazett-Jones, D.P., Le Grice, S., McKay, R.D., Buetow, K.H., *et al.* (2008). Global transcription in pluripotent embryonic stem cells. Cell stem cell *2*, 437-447.

Eisenberg, T., Knauer, H., Schauer, A., Buttner, S., Ruckenstuhl, C., Carmona-Gutierrez, D., Ring, J., Schroeder, S., Magnes, C., Antonacci, L., *et al.* (2009). Induction of autophagy by spermidine promotes longevity. Nat Cell Biol *11*, 1305-1314.

Evans, M.J., and Kaufman, M.H. (1981). ESTABLISHMENT IN CULTURE OF PLURIPOTENTIAL CELLS FROM MOUSE EMBRYOS. Nature *292*, 154-156.

Folmes, C.D., Nelson, T.J., Martinez-Fernandez, A., Arrell, D.K., Lindor, J.Z., Dzeja, P.P., Ikeda, Y., Perez-Terzic, C., and Terzic, A. (2011). Somatic oxidative bioenergetics transitions into pluripotency-dependent glycolysis to facilitate nuclear reprogramming. Cell metabolism *14*, 264-271.

Freund, A., Laberge, R.M., Demaria, M., and Campisi, J. (2012). Lamin B1 loss is a senescence-associated biomarker. Molecular biology of the cell *23*, 2066-2075.

Frith, J.E., Thomson, B., and Genever, P.G. (2010). Dynamic Three-Dimensional Culture Methods Enhance Mesenchymal Stem Cell Properties and Increase Therapeutic Potential. Tissue Eng Part C-Methods *16*, 735-749.

Gurdon, J.B. (1962). DEVELOPMENTAL CAPACITY OF NUCLEI TAKEN FROM INTESTINAL EPITHELIUM CELLS OF FEEDING TADPOLES. Journal of Embryology and Experimental Morphology *10*, 622-&.

Harris, H., and Rubinsztein, D.C. (2012). Control of autophagy as a therapy for neurodegenerative disease. Nature reviews Neurology *8*, 108-117.

Harrison, D.E., Strong, R., Sharp, Z.D., Nelson, J.F., Astle, C.M., Flurkey, K., Nadon, N.L., Wilkinson, J.E., Frenkel, K., Carter, C.S., *et al.* (2009). Rapamycin fed late in life extends lifespan in genetically heterogeneous mice. Nature *460*, 392-395.

Hong, H., Takahashi, K., Ichisaka, T., Aoi, T., Kanagawa, O., Nakagawa, M., Okita, K., and Yamanaka, S. (2009). Suppression of induced pluripotent stem cell generation by the p53-p21 pathway. Nature *460*, 1132-1135.

Huang, P.Y., He, Z.Y., Ji, S.Y., Sun, H.W., Xiang, D., Liu, C.C., Hu, Y.P., Wang, X., and Hui, L.J. (2011). Induction of functional hepatocyte-like cells from mouse fibroblasts by defined factors. Nature *475*, 386-U142.

Huangfu, D., Maehr, R., Guo, W., Eijkelenboom, A., Snitow, M., Chen, A.E., and Melton, D.A. (2008a). Induction of pluripotent stem cells by defined factors is greatly improved by small-molecule compounds. Nature biotechnology *26*, 795-797.

Huangfu, D., Osafune, K., Maehr, R., Guo, W., Eijkelenboom, A., Chen, S., Muhlestein, W., and Melton, D.A. (2008b). Induction of pluripotent stem cells from primary human fibroblasts with only Oct4 and Sox2. Nature biotechnology *26*, 1269-1275.

Ichida, J.K., Blanchard, J., Lam, K., Son, E.Y., Chung, J.E., Egli, D., Loh, K.M., Carter, A.C., Di Giorgio, F.P., Koszka, K., *et al.* (2009). A small-molecule inhibitor of tgf-Beta signaling replaces sox2 in reprogramming by inducing nanog. Cell stem cell *5*, 491-503.

Ieda, M., Fu, J.D., Delgado-Olguin, P., Vedantham, V., Hayashi, Y., Bruneau, B.G., and Srivastava, D. (2010). Direct Reprogramming of Fibroblasts into Functional Cardiomyocytes by Defined Factors. Cell *142*, 375-386.

James, D., Levine, A.J., Besser, D., and Hemmati-Brivanlou, A. (2005). TGFbeta/activin/nodal signaling is necessary for the maintenance of pluripotency in human embryonic stem cells. Development *132*, 1273-1282.

Kabeya, Y., Mizushima, N., Ueno, T., Yamamoto, A., Kirisako, T., Noda, T., Kominami, E., Ohsumi, Y., and Yoshimori, T. (2003). LC3, a mammalian homolog of yeast Apg8p, is localized in autophagosome membranes after processing (vol 19, pg 5720, 2000). Embo J *22*, 4577-4577.

Kawamura, T., Suzuki, J., Wang, Y.V., Menendez, S., Morera, L.B., Raya, A., Wahl, G.M., and Izpisua Belmonte, J.C. (2009). Linking the p53 tumour suppressor pathway to somatic cell reprogramming. Nature *460*, 1140-1144.

Kidder, B.L., Palmer, S., and Knott, J.G. (2009). SWI/SNF-Brg1 regulates self-renewal and occupies core pluripotency-related genes in embryonic stem cells. Stem cells *27*, 317-328.

Kim, J.B., Greber, B., Arauzo-Bravo, M.J., Meyer, J., Park, K.I., Zaehres, H., and Scholer, H.R. (2009a). Direct reprogramming of human neural stem cells by OCT4. Nature *461*, 649-643.

Kim, J.B., Sebastiano, V., Wu, G., Arauzo-Bravo, M.J., Sasse, P., Gentile, L., Ko, K., Ruau, D., Ehrich, M., van den Boom, D., *et al.* (2009b). Oct4-induced pluripotency in adult neural stem cells. Cell *136*, 411-419.

Kim, J.B., Zaehres, H., Wu, G., Gentile, L., Ko, K., Sebastiano, V., Arauzo-Bravo, M.J., Ruau, D., Han, D.W., Zenke, M., *et al.* (2008). Pluripotent stem cells induced from adult neural stem cells by reprogramming with two factors. Nature *454*, 646-650.

Kim, K., Doi, A., Wen, B., Ng, K., Zhao, R., Cahan, P., Kim, J., Aryee, M.J., Ji, H., Ehrlich, L.I., *et al.* (2010). Epigenetic memory in induced pluripotent stem cells. Nature *467*, 285-290.

Kim, Y., Sharov, A.A., McDole, K., Cheng, M., Hao, H., Fan, C.M., Gaiano, N., Ko, M.S., and Zheng, Y. (2011). Mouse B-type lamins are required for proper organogenesis but not by embryonic stem cells. Science *334*, 1706-1710.

Klionsky, D.J., and Emr, S.D. (2000). Cell biology - Autophagy as a regulated pathway of cellular degradation. Science *290*, 1717-1721.

Kouzarides, T. (2007). Chromatin modifications and their function. Cell *128*, 693-705.

Lee, T.I., Jenner, R.G., Boyer, L.A., Guenther, M.G., Levine, S.S., Kumar, R.M., Chevalier, B., Johnstone, S.E., Cole, M.F., Isono, K., *et al.* (2006). Control of developmental regulators by Polycomb in human embryonic stem cells. Cell *125*, 301-313.

Lin, T.X., Ambasudhan, R., Yuan, X., Li, W.L., Hilcove, S., Abujarour, R., Lin, X.Y., Hahm, H.S., Hao, E., Hayek, A., *et al.* (2009). A chemical platform for improved induction of human iPSCs. Nat Methods *6*, 805-U824.

Lister, R., Pelizzola, M., Kida, Y.S., Hawkins, R.D., Nery, J.R., Hon, G., Antosiewicz-Bourget, J., O'Malley, R., Castanon, R., Klugman, S., *et al.* (2011). Hotspots of aberrant epigenomic reprogramming in human induced pluripotent stem cells. Nature *471*, 68-73.

Loh, Y.H., Zhang, W., Chen, X., George, J., and Ng, H.H. (2007). Jmjd1a and Jmjd2c histone H3 Lys 9 demethylases regulate self-renewal in embryonic stem cells. Genes & development *21*, 2545-2557.

Maherali, N., and Hochedlinger, K. (2009). Tgfbeta signal inhibition cooperates in the induction of iPSCs and replaces Sox2 and cMyc. Current biology : CB *19*, 1718-1723.

Maherali, N., Sridharan, R., Xie, W., Utikal, J., Eminli, S., Arnold, K., Stadtfeld, M., Yachechko, R., Tchieu, J., Jaenisch, R., *et al.* (2007). Directly reprogrammed fibroblasts show global epigenetic remodeling and widespread tissue contribution. Cell stem cell *1*, 55-70.

Marion, R.M., Strati, K., Li, H., Murga, M., Blanco, R., Ortega, S., Fernandez-Capetillo, O., Serrano, M., and Blasco, M.A. (2009a). A p53-mediated DNA damage

response limits reprogramming to ensure iPS cell genomic integrity. Nature *460*, 1149-1153.

Marion, R.M., Strati, K., Li, H., Tejera, A., Schoeftner, S., Ortega, S., Serrano, M., and Blasco, M.A. (2009b). Telomeres acquire embryonic stem cell characteristics in induced pluripotent stem cells. Cell stem cell *4*, 141-154.

Martin, G.R. (1981). ISOLATION OF A PLURIPOTENT CELL-LINE FROM EARLY MOUSE EMBRYOS CULTURED IN MEDIUM CONDITIONED BY TERATOCARCINOMA STEM-CELLS. Proceedings of the National Academy of Sciences of the United States of America-Biological Sciences *78*, 7634-7638.

Martin, G.R., and Evans, M.J. (1975). DIFFERENTIATION OF CLONAL LINES OF TERATOCARCINOMA CELLS - FORMATION OF EMBRYOID BODIES INVITRO. Proc Natl Acad Sci U S A *72*, 1441-1445.

Martina, J.A., Chen, Y., Gucek, M., and Puertollano, R. (2012). MTORC1 functions as a transcriptional regulator of autophagy by preventing nuclear transport of TFEB. Autophagy *8*, 903-914.

Meshorer, E., Yellajoshula, D., George, E., Scambler, P.J., Brown, D.T., and Misteli, T. (2006). Hyperdynamic plasticity of chromatin proteins in pluripotent embryonic stem cells. Developmental cell *10*, 105-116.

Mikkelsen, T.S., Hanna, J., Zhang, X., Ku, M., Wernig, M., Schorderet, P., Bernstein, B.E., Jaenisch, R., Lander, E.S., and Meissner, A. (2008). Dissecting direct reprogramming through integrative genomic analysis. Nature *454*, 49-55.

Mitsui, K., Tokuzawa, Y., Itoh, H., Segawa, K., Murakami, M., Takahashi, K., Maruyama, M., Maeda, M., and Yamanaka, S. (2003). The homeoprotein Nanog is required for maintenance of pluripotency in mouse epiblast and ES cells. Cell *113*, 631-642.

Moepps, B., Braun, M., Knopfle, K., Dillinger, K., Knochel, W., and Gierschik, P. (2000). Characterization of a Xenopus laevis CXC chemokine receptor 4:

implications for hematopoietic cell development in the vertebrate embryo. Eur J Immunol *30*, 2924-2934.

Morselli, E., Galluzzi, L., Kepp, O., Criollo, A., Maiuri, M.C., Tavernarakis, N., Madeo, F., and Kroemer, G. (2009). Autophagy mediates pharmacological lifespan extension by spermidine and resveratrol. Aging-US *1*, 961-970.

Nakagawa, M., Koyanagi, M., Tanabe, K., Takahashi, K., Ichisaka, T., Aoi, T., Okita, K., Mochiduki, Y., Takizawa, N., and Yamanaka, S. (2008). Generation of induced pluripotent stem cells without Myc from mouse and human fibroblasts. Nature biotechnology *26*, 101-106.

Nichols, J., Evans, E.P., and Smith, A.G. (1990). ESTABLISHMENT OF GERM-LINE-COMPETENT EMBRYONIC STEM (ES) CELLS USING DIFFERENTIATION INHIBITING ACTIVITY. Development *110*, 1341-1348.

Nichols, J., Zevnik, B., Anastassiadis, K., Niwa, H., Klewe-Nebenius, D., Chambers, I., Scholer, H., and Smith, A. (1998). Formation of pluripotent stem cells in the mammalian embryo depends on the POU transcription factor Oct4. Cell *95*, 379-391.

Niwa, H., Miyazaki, J., and Smith, A.G. (2000). Quantitative expression of Oct-3/4 defines differentiation, dedifferentiation or self-renewal of ES cells. Nature Genet *24*, 372-376.

Obokata, H., Sasai, Y., Niwa, H., Kadota, M., Andrabi, M., Takata, N., Tokoro, M., Terashita, Y., Yonemura, S., Vacanti, C.A., *et al.* (2014a). Bidirectional developmental potential in reprogrammed cells with acquired pluripotency. Nature *505*, 676-680.

Obokata, H., Wakayama, T., Sasai, Y., Kojima, K., Vacanti, M.P., Niwa, H., Yamato, M., and Vacanti, C.A. (2014b). Stimulus-triggered fate conversion of somatic cells into pluripotency. Nature *505*, 641-647.

Okamoto, K., Okazawa, H., Okuda, A., Sakai, M., Muramatsu, M., and Hamada, H. (1990). A NOVEL OCTAMER BINDING TRANSCRIPTION FACTOR IS

DIFFERENTIALLY EXPRESSED IN MOUSE EMBRYONIC-CELLS. Cell *60*, 461-472.

Okita, K., Ichisaka, T., and Yamanaka, S. (2007). Generation of germline-competent induced pluripotent stem cells. Nature *448*, 313-317.

Oldershaw, R.A., Baxter, M.A., Lowe, E.T., Bates, N., Grady, L.M., Soncin, F., Brison, D.R., Hardingham, T.E., and Kimber, S.J. (2010). Directed differentiation of human embryonic stem cells toward chondrocytes. Nature biotechnology *28*, 1187-1194.

Pajerowski, J.D., Dahl, K.N., Zhong, F.L., Sammak, P.J., and Discher, D.E. (2007). Physical plasticity of the nucleus in stem cell differentiation. Proc Natl Acad Sci U S A *104*, 15619-15624.

Panopoulos, A.D., Yanes, O., Ruiz, S., Kida, Y.S., Diep, D., Tautenhahn, R., Herrerias, A., Batchelder, E.M., Plongthongkum, N., Lutz, M., *et al.* (2012). The metabolome of induced pluripotent stem cells reveals metabolic changes occurring in somatic cell reprogramming. Cell research *22*, 168-177.

Pittenger, M.F. (1999). Multilineage Potential of Adult Human Mesenchymal Stem Cells. Science *284*, 143-147.

Rais, Y., Zviran, A., Geula, S., Gafni, O., Chomsky, E., Viukov, S., Mansour, A.A., Caspi, I., Krupalnik, V., Zerbib, M., *et al.* (2013). Deterministic direct reprogramming of somatic cells to pluripotency. Nature *502*, 65-70.

Ravikumar, B., Vacher, C., Berger, Z., Davies, J.E., Luo, S., Oroz, L.G., Scaravilli, F., Easton, D.F., Duden, R., O'Kane, C.J., *et al.* (2004). Inhibition of mTOR induces autophagy and reduces toxicity of polyglutamine expansions in fly and mouse models of Huntington disease. Nat Genet *36*, 585-595.

Reubinoff, B.E., Pera, M.F., Fong, C.Y., Trounson, A., and Bongso, A. (2000). Embryonic stem cell lines from human blastocysts: somatic differentiation in vitro. Nature biotechnology *18*, 399-404.

Rosner, M.H., Vigano, M.A., Ozato, K., Timmons, P.M., Poirier, F., Rigby, P.W.J., and Staudt, L.M. (1990). A POU-DOMAIN TRANSCRIPTION FACTOR IN EARLY STEM-CELLS AND GERM-CELLS OF THE MAMMALIAN EMBRYO. Nature *345*, 686-692.

Rubinsztein, D.C. (2006). The roles of intracellular protein-degradation pathways in neurodegeneration. Nature *443*, 780-786.

Rubinsztein, D.C., Marino, G., and Kroemer, G. (2011). Autophagy and aging. Cell *146*, 682-695.

Ruiz, S., Panopoulos, A.D., Herrerias, A., Bissig, K.D., Lutz, M., Berggren, W.T., Verma, I.M., and Izpisua Belmonte, J.C. (2011). A high proliferation rate is required for cell reprogramming and maintenance of human embryonic stem cell identity. Current biology : CB *21*, 45-52.

Sardiello, M., Palmieri, M., di Ronza, A., Medina, D.L., Valenza, M., Gennarino, V.A., Di Malta, C., Donaudy, F., Embrione, V., Polishchuk, R.S., *et al.* (2009). A gene network regulating lysosomal biogenesis and function. Science *325*, 473-477.

Sehgal, P., Chaturvedi, P., Kumaran, R.I., Kumar, S., and Parnaik, V.K. (2013). Lamin A/C haploinsufficiency modulates the differentiation potential of mouse embryonic stem cells. PloS one *8*, e57891.

Settembre, C., De Cegli, R., Mansueto, G., Saha, P.K., Vetrini, F., Visvikis, O., Huynh, T., Carissimo, A., Palmer, D., Klisch, T.J., *et al.* (2013). TFEB controls cellular lipid metabolism through a starvation-induced autoregulatory loop. Nat Cell Biol *15*, 647-658.

Settembre, C., Di Malta, C., Polito, V.A., Garcia Arencibia, M., Vetrini, F., Erdin, S., Erdin, S.U., Huynh, T., Medina, D., Colella, P., *et al.* (2011). TFEB links autophagy to lysosomal biogenesis. Science *332*, 1429-1433.

Settembre, C., Zoncu, R., Medina, D.L., Vetrini, F., Erdin, S., Erdin, S., Huynh, T., Ferron, M., Karsenty, G., Vellard, M.C., *et al.* (2012). A lysosome-to-nucleus

signalling mechanism senses and regulates the lysosome via mTOR and TFEB. The EMBO journal *31*, 1095-1108.

Shi, Y., Do, J.T., Desponts, C., Hahm, H.S., Scholer, H.R., and Ding, S. (2008). A combined chemical and genetic approach for the generation of induced pluripotent stem cells. Cell stem cell *2*, 525-528.

Shimi, T., Butin-Israeli, V., Adam, S.A., Hamanaka, R.B., Goldman, A.E., Lucas, C.A., Shumaker, D.K., Kosak, S.T., Chandel, N.S., and Goldman, R.D. (2011). The role of nuclear lamin B1 in cell proliferation and senescence. Genes & development *25*, 2579-2593.

Silva, J., Barrandon, O., Nichols, J., Kawaguchi, J., Theunissen, T.W., and Smith, A. (2008). Promotion of reprogramming to ground state pluripotency by signal inhibition. PLoS biology *6*, e253.

Smith, A.G., Heath, J.K., Donaldson, D.D., Wong, G.G., Moreau, J., Stahl, M., and Rogers, D. (1988). INHIBITION OF PLURIPOTENTIAL EMBRYONIC STEM-CELL DIFFERENTIATION BY PURIFIED POLYPEPTIDES. Nature *336*, 688-690.

Szabo, E., Rampalli, S., Risueno, R.M., Schnerch, A., Mitchell, R., Fiebig-Comyn, A., Levadoux-Martin, M., and Bhatia, M. (2010). Direct conversion of human fibroblasts to multilineage blood progenitors. Nature *468*, 521-526.

Tada, M., Takahama, Y., Abe, K., Nakatsuji, N., and Tada, T. (2001). Nuclear reprogramming of somatic cells by in vitro hybridization with ES cells. Curr Biol *11*, 1553-1558.

Takahashi, K., Tanabe, K., Ohnuki, M., Narita, M., Ichisaka, T., Tomoda, K., and Yamanaka, S. (2007). Induction of pluripotent stem cells from adult human fibroblasts by defined factors. Cell *131*, 861-872.

Takahashi, K., and Yamanaka, S. (2006). Induction of pluripotent stem cells from mouse embryonic and adult fibroblast cultures by defined factors. Cell *126*, 663-676.

Tesar, P.J., Chenoweth, J.G., Brook, F.A., Davies, T.J., Evans, E.P., Mack, D.L., Gardner, R.L., and McKay, R.D. (2007). New cell lines from mouse epiblast share defining features with human embryonic stem cells. Nature *448*, 196-199.

Thomson, J.A. (1998). Embryonic stem cell lines derived from human blastocysts (vol 282, pg 1147, 1998). Science *282*, 1827-1827.

Thomson, J.A., Kalishman, J., Golos, T.G., Durning, M., Harris, C.P., Becker, R.A., and Hearn, J.P. (1995). ISOLATION OF A PRIMATE EMBRYONIC STEM-CELL LINE. Proc Natl Acad Sci U S A *92*, 7844-7848.

Tsai, S.Y., Bouwman, B.A., Ang, Y.S., Kim, S.J., Lee, D.F., Lemischka, I.R., and Rendl, M. (2011). Single Transcription Factor Reprogramming of Hair Follicle Dermal Papilla Cells to Induced Pluripotent Stem Cells. Stem cells *29*, 964-971.

Tsai, S.Y., Clavel, C., Kim, S., Ang, Y.S., Grisanti, L., Lee, D.F., Kelley, K., and Rendl, M. (2010). Oct4 and klf4 reprogram dermal papilla cells into induced pluripotent stem cells. Stem cells *28*, 221-228.

Tsukamoto, S., Kuma, A., Murakami, M., Kishi, C., Yamamoto, A., and Mizushima, N. (2008). Autophagy is essential for preimplantation development of mouse embryos. Science *321*, 117-120.

Vallier, L., Alexander, M., and Pedersen, R.A. (2005). Activin/Nodal and FGF pathways cooperate to maintain pluripotency of human embryonic stem cells. J Cell Sci *118*, 4495-4509.

Varga, M., Sass, M., Papp, D., Takacs-Vellai, K., Kobolak, J., Dinnyes, A., Klionsky, D.J., and Vellai, T. (2013). Autophagy is required for zebrafish caudal fin regeneration. Cell death and differentiation.

Varum, S., Rodrigues, A.S., Moura, M.B., Momcilovic, O., Easley, C.A.t., Ramalho-Santos, J., Van Houten, B., and Schatten, G. (2011). Energy metabolism in human pluripotent stem cells and their differentiated counterparts. PloS one *6*, e20914.

Vazquez-Martin, A., Cufi, S., Corominas-Faja, B., Oliveras-Ferraros, C., Vellon, L., and Menendez, J.A. (2012). Mitochondrial fusion by pharmacological manipulation impedes somatic cell reprogramming to pluripotency: New insight into the role of mitophagy in cell stemness. Aging-US *4*, 393-401.

Vierbuchen, T., Ostermeier, A., Pang, Z.P., Kokubu, Y., Sudhof, T.C., and Wernig, M. (2010). Direct conversion of fibroblasts to functional neurons by defined factors. Nature *463*, 1035-U1050.

Wagers, A.J., and Weissman, I.L. (2004). Plasticity of adult stem cells. Cell *116*, 639-648.

Wang, S., Xia, P., Ye, B., Huang, G., Liu, J., and Fan, Z. (2013). Transient Activation of Autophagy via Sox2-Mediated Suppression of mTOR Is an Important Early Step in Reprogramming to Pluripotency. Cell stem cell *13*, 617-625.

Wernig, M., Meissner, A., Cassady, J.P., and Jaenisch, R. (2008). c-Myc is dispensable for direct reprogramming of mouse fibroblasts. Cell stem cell *2*, 10-12.

Wernig, M., Meissner, A., Foreman, R., Brambrink, T., Ku, M., Hochedlinger, K., Bernstein, B.E., and Jaenisch, R. (2007). In vitro reprogramming of fibroblasts into a pluripotent ES-cell-like state. Nature *448*, 318-324.

Wilmut, I., Schnieke, A.E., McWhir, J., Kind, A.J., and Campbell, K.H.S. (1997). Viable offspring derived from fetal and adult mammalian cells (vol 385, pg 810, 1997). Nature *386*, 200-200.

Yamanaka, S. (2012). Induced pluripotent stem cells: past, present, and future. Cell stem cell *10*, 678-684.

Yang, S.H., Chang, S.Y., Yin, L., Tu, Y., Hu, Y., Yoshinaga, Y., de Jong, P.J., Fong, L.G., and Young, S.G. (2011). An absence of both lamin B1 and lamin B2 in keratinocytes has no effect on cell proliferation or the development of skin and hair. Human molecular genetics *20*, 3537-3544.

Ying, Q.L., Wray, J., Nichols, J., Batlle-Morera, L., Doble, B., Woodgett, J., Cohen, P., and Smith, A. (2008). The ground state of embryonic stem cell self-renewal. Nature *453*, 519-523.

Yu, J., Vodyanik, M.A., Smuga-Otto, K., Antosiewicz-Bourget, J., Frane, J.L., Tian, S., Nie, J., Jonsdottir, G.A., Ruotti, V., Stewart, R., *et al.* (2007). Induced pluripotent stem cell lines derived from human somatic cells. Science *318*, 1917-1920.

Zhang, J., Nuebel, E., Daley, G.Q., Koehler, C.M., and Teitell, M.A. (2012). Metabolic regulation in pluripotent stem cells during reprogramming and self-renewal. Cell stem cell *11*, 589-595.

Zhou, Q., Brown, J., Kanarek, A., Rajagopal, J., and Melton, D.A. (2008). In vivo reprogramming of adult pancreatic exocrine cells to beta-cells. Nature *455*, 627-632.

Zhu, S., Li, W., Zhou, H., Wei, W., Ambasudhan, R., Lin, T., Kim, J., Zhang, K., and Ding, S. (2010). Reprogramming of human primary somatic cells by OCT4 and chemical compounds. Cell stem cell *7*, 651-655.